American Journal of Fluid Dynamics 2022, 12(1): 16-119
DOI: 10.5923/j.ajfd.20221201.02

Bubbly Two-Phase Flow: III- Applications

Hassan Abdulmouti

Department of Mechanical Engineering Division, Sharjah Men's College, Higher Colleges of Technology, Sharjah, UAE

Abstract Multi-phase flows appear in numerous forms in Nature. They can be found in sediment-laden flows in rivers, in underflows associated with volcanic eruptions, in turbidity currents, in the bubbly wake of ships, in many engineering fields as materials, mechanical, and in liquid-vapor mixtures in nuclear reactors, waste treatment, gas mixing and resolution, heat and mass transfer among many others. Multiphase flows, the simultaneous flow of more than one phase, encompasses a vast field, a host of different technological contexts, a wide spectrum of different scales, a broad range of engineering disciplines, and a multitude of different analytical approaches. Basic aspects of the flow in a bubble plume were addressed by many researchers. Furthermore, multiphase flow occurs in many facets of chemical engineering, e.g., distillation, absorption, evaporation, condensation, solvent extraction. It is particularly prevalent and important in hydrocarbon production and refining, minerals transport, power generation as well as in many environmental applications. Bubble plume, which is a typical form of bubble flow, has received considerable attention in the last four decades and has recently become a very important topic of research due to its large and wide range of application value and its effect on many processes the efficiency of many devices. The motivation for studying bubble plumes is evident, from the fact that these plumes are encountered in a variety of engineering problems. In the past 40 years, the range of its application prompted scholars to do experiments and numerical research about this phenomenon. The bubble plume is known as one of the transport phenomena able to drive large-scale convection due to the buoyancy of the bubbles. The flow in the vicinity of a free surface induced by a bubble plume is utilized as an effective way to control surface floating substances on lakes, oceans, as well as in various kinds of reactors and industrial processes handling a free surface. The surface flows generated by bubble plumes are considered key phenomena in many kinds of processes in modern industries. In our two earlier papers (Bubbly Two-Phase Flow: Part I- Characteristics, Structures, Behaviors and Flow Patterns and Bubbly Two-Phase Flow: Part II- Characteristics and Parameters) the major finding of the previous research of bubbly two-phase flow characteristics, structures, behaviors and flow patterns were demonstrated, reviewed and summarized. Moreover, some important models and techniques to measure the two-phase bubbly flow parameters such as bubble motion, flow regime, bubble shape which play a considerable role in many engineering applications were elucidated. Furthermore, our earlier papers also demonstrated, reviewed, and summarized the major finding of the previous research of the techniques and the important models for the measurement of the dominated two-phase bubbly flow/ bubble plume parameters such as gas flow rate bubble size, bubble velocity, and void fraction which are considered important and play an important role in operational safety, process control and reliability of continuum processes of many engineering applications. Beyond that, the turbulent bubbly flow structure was explained in detail. The motivation of the present work (part 3) which is extended to parts 1 and 2 is the dement to demonstrate, review, and summarize the major finding of previous research of the following points: 1) The differences of surface flow generation mechanisms among single-phase liquid jet, single-phase buoyant plume, and bubble plume. 2) The study of bubble plumes, their properties, characteristics, features, and their effects on the applications. 3) The important applications of bubbly flow and gas-liquid two-phase flow especially on bubble plumes and their associated surface flow since they can contribute to improvements in various directions including the conventional oil fence (function, problems, oil accidents on seas and oceans). The techniques of gas injection have been widely utilized in many engineering fields. The surface flows generated by bubble plumes are considered key phenomena in many kinds of processes in modern industries. It is utilized as an effective way to control surface floating substances on lakes, oceans, as well as in various kinds of reactors and industrial processes handling a free surface. 4) Summary of the above applications as a table of industrial processes that employ bubbly flow, a table of the environmental and naval engineering applications of bubbly flow, and a table of the applications: aerospace, biomedical, electrical, and mechanical.

Keywords Bubble Plume, Multiphase Flow, Bubbly Flow, Bubble, Buoyant Flow, Surface Flow, Free-Surface, Wave, and Oil Fence

* Corresponding author:
habdulmouti@hct.ac.ae (Hassan Abdulmouti)
Received: Jun. 5, 2022; Accepted: Jun. 25, 2022; Published: Jun. 29, 2022
Published online at http://journal.sapub.org/ajfd

1. Introduction

A two-phase flow which is an important topic in fluid dynamics is one of the most common flows in nature as well as in many applications; it covers gas-solid, liquid-liquid, solid-liquid, and gas-liquid flows. Among these, the gas-liquid flows can be encountered in a wide variety of industrial applications including boilers, distillation towers, chemical reactors, oil pipelines, nuclear reactors. A two-phase flow can be found in numerous fields in engineering, e.g., aerospace, biomedical, chemical, electrical, environmental, mechanical, nuclear, and naval engineering. There is an enormous variation in applications, e.g., rocket engines, contamination spreading, multiphase mixture transport, cavitation, sonoluminescence, ink-jet printing, particle transport in blood, crystallization, multiphase cooling, fluidized beds, drying of gases, air entrainment in oceans/rivers, and anti-icing fluids. The number of papers on multiphase flow in the field of fluid dynamics is huge and still growing. The diversity of flow types makes a general description almost impossible. This makes fundamental research necessary. Especially, controlled experiments are needed for a better physical understanding and as test cases for numerical and theoretical work. The subject of multiphase flows encompasses a vast field, a host of different technological contexts, a wide spectrum of different scales, a broad range of engineering disciplines, and a multitude of different analytical approaches. The term multiphase flow is used to refer to any fluid flow consisting of more than one phase or component. Consequently, the flows have some level of phase or component separation at a scale well above the molecular level. This still leaves a massive spectrum of different multiphase flows. One could classify them according to the state of the different phases or components and therefore refer to gas/solid's flows, liquid/solid flows or gas/particle flows or bubbly flows, and so on; many texts exist that limit their attention in this way. Some treatises are defined in terms of a specific type of fluid flow and deal with low Reynolds number suspension flows, dusty gas dynamics, and so on. Others focus attention on a specific application such as slurry flows, cavitating flows, aerosols, debris flows, and so on. The basic fluid mechanical phenomena were identified to illustrate those phenomena with examples from a broad range of applications and types of flow. Multi-phase flows appear in numerous forms in Nature. They can be found in sediment-laden flows in rivers, in underflows associated with volcanic eruptions, in turbidity currents, in the bubbly wake of ships, and liquid-vapor mixtures in nuclear reactors, among many others. Basic aspects of the flow in a bubble plume, which is a simple paradigm of multiphase flow that appears in many situations: They can be used as breakwaters, as destratification devices, and as containment for oil spills; they are also encountered in oil-well blowouts and nuclear devices. Parenthetically, it is valuable to reflect on the diverse and ubiquitous challenges of multiphase flow. Virtually every processing technology must deal with the multiphase flow, from cavitating pumps and turbines to electrophotographic processes to papermaking to the pellet form of almost all raw plastics. The amount of granular material, coal, grain, ore, etc. that is transported every year is enormous, and, at many stages, that material is required to flow. The ability to predict the fluid flow behavior of these processes is central to the efficiency and effectiveness of those processes. For example, the effective flow of toner is a major factor in the quality and speed of electrophotographic printers. Multiphase flows are also a ubiquitous feature of our environment whether one considers rain, snow, fog, avalanches, mudslides, sediment transport, debris flows, and countless other natural phenomena to say nothing of what happens beyond our planet. Very critical biological and medical flows are also multiphase, from blood flow to semen to the bends to lithotripsy to laser surgery cavitation and so on. No single list can adequately illustrate the diversity and ubiquity; consequently, any attempt at a comprehensive treatment of multiphase flows is flawed unless it focuses on common phenomenological themes and avoids the temptation to digress into lists of observations. Two-phase flows with phase change occur in many engineering systems. Of specific interest are two applications involving a wide range of length and time scales: (a) bubbly turbulent flows in the ship boundary layers for drag reduction and (b) hydrodynamics of cavitation. These problems share common physical mechanisms of mass, momentum, and energy exchange across the interface between the two phases. Furthermore, multiphase flow, the simultaneous flow of more than one phase, occurs in many facets of chemical engineering, e.g., distillation, absorption, evaporation, condensation, solvent extraction. The possible combinations of phases are gas/liquid; gas/solid; liquid/solid; the simultaneous flow of two immiscible liquids and gas/liquid/solids. The first four can be termed two-phase flow. The last, more complex case can be found in some catalytic reactors. Hydrocarbon production can involve the flow of gas, oil, water, and solids emerging from the reservoir. A complication of these flows is that the phases can be dispersed unevenly about the pipe cross-section and axially. This has important implications for the flow particularly the pressure drop/ flow rate/geometry relationships which are central to designers. It also has an import for the separation of the phases. The phase disposition can be especially complex in the case of gas/liquid and liquid/liquid flows. The extremely deformable nature of the interface leads to a large number of possible configurations. Even with gas/solids and liquid/solid flows, there can be systematic variations of the temporal and spatial concentration of the dispersed solids. It is because of these factors that workers in the field have used the concept of flow patterns as general descriptions of the disposition of the phases. Flow patterns, methods are outlined below, for gas/liquid (Dong, F. et. al. 2003, Hassan 2002, 2003, 2006 and 2011, Hassan and Tamer 2006, Abdulmouti, et. al. 2000, Hassan et. al. 1997, 1998, 1999- No. 1, 1999- No. 2 and 2001, Hassan and Esam, 2013, Christopher 2005, A.W.G. de Vries 2001, E. Shams et. al. 2010, B.J. Azzopardi 2012, Fabian et. al. 2004).

Over the last decades, Bubble plumes (Buoyant plumes produced by a source of bubbles in a liquid medium) are observed and have had several applications in various engineering disciplines and fields, e.g. in industrial, materials, chemical, mechanical, civil, and environmental engineering applications such as chemical plants, nuclear power plants, naval, chemical reactions, waste treatment, gas mixing and resolution, heat and mass transfer, aeronautical and astronautical systems, biochemical reactors as well as distillation plants, etc. Furthermore, bubble plumes, which are a special case of bubbly flows, have great application value in projects, such as alleviating the damage of waves to building structure, preventing the invasion of brine with air bubble curtain in the estuary, controlling the stratification structure of reservoirs and lakes to improve water quality, preventing channel and harbor from being frozen, enhancing oxygen for aquatic growth and so on. Most especially in recent years, with the large-scale exploitation of oil and gas under the sea, the oil-gas blowout causes serious pollution to the sea, and bubble plumes can be used to control the pollution area. Above all has greatly stimulated the research on bubble plumes to widen their applied range. Therefore, the bubble plume has been a key issue in the current research field of fluid mechanics. Moreover, bubble plumes have received considerable attention in the last four decades due to their large range of applications. For example, they have been proposed as a means of containing surface-floating substances, such as oil from large oil spills in rivers and estuaries; they have been employed to augment convective heat and mass transfer rates in various applications; they have been used as pneumatic breakwaters; they have been utilized for preventing icing in navigational waterways, to prevent surface ice formation in harbors and to damp sea waves in harbors. One area of application that has received a great deal of recent attention is the use of bubble plumes as a desertification device, in the mixing of very hot or toxic liquids and the desertification of lakes and reservoirs, inducing mixing while introducing dissolved oxygen for improving water quality in lakes and reservoirs. Besides, one of the reasons for the study of bubbly flows is their wide applications ranging from hydraulic engineering to high energy physics experiments. In particular, the researcher is interested in a recent application of bubbly fluids in the mitigation of cavitation damages in the Spallation Neutron Source (SNS) (Riemer et al. 2002). Another important motivation is to connect the microscopic behavior of individual bubbles to the macroscopic behavior of the mixed medium that one directly observes.

On the other hand, bubbly flows are encountered in many fields of engineering, pertaining to different spatial scales. At a small scale, they are found for instance in metallurgy in the gas stirring of ladles and nuclear devices. Because of the numerous industrial applications, the problem of injection of gas from below has been widely studied, even though most of the studies have been carried out on the large-scale phenomena which determine the mixing properties. A lot of experimental data are available on this subject; they can be classified into Aqueous experiments (where the liquid is water) and non-Aqueous experiments (where the liquid is normally a molten metal). At an extremely large scale, they take place in induced events of carbon dioxide sequestration, by which this compound is “injected” into deep seas. In industry, bubble plumes are also used with two objectives: enhancing mass transfer and mixing. As a mixing technique, the use of bubbles is attractive because it is very simple and cheap to operate. The most common applications of bubble-driven mixing are encountered in the delicate mixing of pharmaceutical and food products. Whereas bubbly flows are central to many industrial processes. Heat transfer through boiling is the preferred mode in most power plants and bubble-driven circulation systems are used in metal processing operations such as steelmaking, ladle metallurgy, and the secondary refining of aluminum and copper. Similarly, many natural processes involve bubbles. Bubbles play a major role in the interactions of the oceans with the atmosphere, for example, both air bubbles near a free surface and cavitation bubbles are of major importance for the detection of submarines in naval applications. Bubbly flows are frequently encountered in chemical engineering. Much research on the hydrodynamics of these flows has been performed. Nevertheless, our understanding of the complex features found, for instance in a bubble column is limited. During the last decade, CFD as a research tool has opened the possibility to perform detailed studies on the behavior of bubble columns. Also, the bubble plume experiment has drawn quite some attention. At the environmental scale, air-bubble systems have been used extensively and for a variety of purposes, the application range is vast: bubble plumes have been used as barriers against saltwater intrusion in rivers and locks and as barriers to contain density intrusions or oil spills or for stopping the spreading of oil spills on the water surface, as breakwaters and for reduction of underwater explosion waves and agitation and mixing operations in process industries and to protect installations from shock waves produced by underwater explosions and as silt curtains. However, the technique may also be used for destratification purposes and water quality control management of lakes and, reservoirs in which case the characteristics of the air-bubble plume are of more interest than the induced horizontal flow in the surface layer and to mix stratified fluid layers, to reaerate lakes. With increasing, subsea activities plumes have acquired increased importance from a risk assessment point of view. It becomes imperative to obtain knowledge about the implications of a rupture, or even breakage, of a subsea pipeline. Thus, in the case of an underwater blowout of inflammable gas, the following points are very important in studying the plumes:

- The concentration of gas at the free surface.
- The extension of the area covered by gas at the free surface.
- The rising time of the gas.

In sanitary engineering, bubble plumes are usually employed for aeration purposes in water and wastewater treatment plants. Additionally, arrays of bubble diffusers are used in reservoirs aimed at storing combined sewer overflows, to avoid the occurrence of anaerobic conditions. The bubble plume also contributes to improving the following processes:

a- The prevention of seawater pollution by heavy oil leakage from tankers. Moreover, the development of the technology to prevent the diffusion of the leaked oil or oil generated from oil sources in the sea.
b- The prevention of diffusion of organic or harmful substances on the sea surface, lake surfaces, and river surfaces, and the forced collection of them using the surface flow.
c- The prevention of freezing over the surfaces of seas and lakes in the winter season.
d- Damping of waves propagating on the sea, lakes, and rivers.
e- Accumulation of the surface slag in the metal refining process.
f- The reduction of surfactants in chemical reaction processes. Beyond that, the removal of oxide films or floating impurities from the surface of the chemical reactors to maintain the performance of reactions.
g- Prevention of surface sloshing in furnaces. Beyond that, the removal of oxide films or floating impurities from the surface of the metal refining furnaces to maintain their performance.

Flows induced by a bubble plume are utilized in the above industrial processes where the main features of this kind of flow are:

(1) A large-scale circulation of the liquid phase can be generated in natural circulation systems like lakes, agitation tanks, etc.
(2) Strong rising flows can be induced by the pumping effect as in air-lifting pumps.
(3) High-speed surface flows may be developed at the free surface, by which the density and the transportation of the surface floating substances can be controlled.
(4) High turbulence energy can be produced in the two-phase region due to the strong local interaction between individual bubbles and the surrounding liquid flow (Hassan, 2012, 2013 and 2014, Murai et. al. 2001, Abdel Aal et. al. 1966, Goosens and Smith 1975, Al Tawell and Landau 1977, Chesters et. al. 1980, Bankovic et. al. 1984, Sun and Faeth 1986 a, b, Szekely et. al. 1988, Gross and Kuhlman 1992, Bulson 1968, Cheng Wen et al. 2008, Schladow 1992, Riemer et al. 2002, Lapin and LuKbbert 1994, Devanathan et. al. 1995, Delnoij et. al. 1997, Becker et al., 1994, Becker et al., 1999, Sokolichin and Eigenberger 1994, Klas and John 1970, Kristian and Iver 2008 and Fabian 2004).

Bubble plume has become a very important topic of research recently due to their wide applications, and its effect on many processes, and the efficiency of many devices. In the past 30 years, the range of its application prompted scholars to do experiments about this phenomenon. Most of these experiments were focusing on determining time-averaged velocities in small and big tanks. Some scaling relations were proposed to the bubble plume available applications. The focus was on the vertical direction in vassals and later including the radial or the horizontal one. Also, the procedure to analyze how to plumes interact, and the velocity distribution and turbulence aspect in tanks were attractive and interesting points to be studied. As a result, the motivation for studying bubble plumes is evident, from the fact that these plumes are encountered in a variety of engineering problems. Hence, by applying the bubble plume, the above processes are expected to be improved.

In our two earlier papers (Hassan 2014): Bubbly Two-Phase Flow: Part I- Characteristics, Structures, Behaviors and Flow Patterns and Bubbly Two-Phase Flow: Part II- Characteristics and Parameters) the major finding of the previous research of bubbly two-phase flow characteristics, structures, behaviors, and flow patterns were demonstrated, reviewed, and summarized. Moreover, some important models and techniques to measure the two-phase bubbly flow parameters such as bubble motion, flow regime, bubble shape which play a considerable role in many engineering applications were elucidated. Moreover, our earlier papers also demonstrated, reviewed, and summarized the major finding of the previous research of the techniques and the important models for the measurement of the dominated two-phase bubbly flow/ bubble plume parameters such as gas flow rate bubble size, bubble velocity, and void fraction which are considered important and play an important role in operational safety, process control and reliability of continuum processes of many engineering applications. Furthermore, the turbulent bubbly flow structure was explained in detail.

The motivation of the present work (part 3) which is extended for parts 1 and 2 is the dement to demonstrate, review, and summarize the major finding of previous research of the following points:

1) The differences of surface flow generation mechanisms among single-phase liquid jet, single-phase buoyant plume, and bubble plume.
2) The study of bubble plumes, their properties, characteristics, features, and their effects on the applications.
3) The important applications of bubbly flow and gas-liquid two-phase flow especially on bubble plumes and their associated surface flow since they can contribute to improvements in various directions including the conventional oil fence (function, problems, oil accidents on seas and oceans). The

techniques of gas injection have been widely utilized in many engineering fields. The surface flows generated by bubble plumes are considered key phenomena in many kinds of processes in modern industries. It is utilized as an effective way to control surface floating substances on lakes, oceans, as well as in various kinds of reactors and industrial processes handling a free surface. These applications were summarized in 3 tables as follows: table 1 is a list of industrial processes that employ bubbly flow, and Table 2 lists the environmental and naval engineering applications of bubbly flow, while Table 3 illustrates the applications: aerospace, biomedical, electrical, and mechanical.

Table 1. Industrial, chemical, and nuclear applications of bubbly flow

Unit operation	Applications	References	Description (how does it work)	Remarks
Bubble column reactors	Oxidation of ethylene, cumene, butane toluene, and xylene; chlorination of aliphatic and aromatic hydrocarbons; isobutene hydration; carbonylation of methanol. multiphase mixture transport,	Deckwer 1985, Jacobsen 2008, W. Bai et. al. 2010	The bubble column reactors represent contactors in which a gas or a mixture of gases is distributed in the liquid at the column bottom by an appropriate distributor and moves upwards in the form of bubbles causing intense mixing of the liquid phase. Bubble columns are intensively utilized as multiphase contactors and reactors	Small scale Bubble column reactors are often used because of their simple construction, low operating cost, and excellent heat transfer characteristics at immersed surfaces The bubble columns offer numerous advantages: good heat and mass transfer characteristics, no moving parts, reduced wear and tear, higher catalyst durability, ease of operation, and low operating and maintenance costs. One of the main disadvantages of bubble column reactors is significant back-mixing, which can affect product conversion.
Bubble slurry reactors	Liquefaction of solid fuels	Saxena et al. 1988		Medium scale at high pressure pipes.
	Fischer-Tropsch synthesis	Krishna and Sie 2000		Small scale
Froth flotation cells	Mineral separation flotation cells	Finch and Dobby 1991, Pal and Masliyah 1989, R. B. H. Tan et. al. 2000	The dispersion of gases through submerged orifices, slots, or holes is an efficient and commonly used method of creating a large interfacial area per unit volume in process equipment such as distillation columns, absorption towers, flotation cells, aerated stirred tanks, biological wastewater treatment systems, and metallurgical smelters.	Initially was used on a large scale then due to new technology fame decreases. In many industrial gas-liquid operations, the continuous phase is caused to flow normally across the emerging gas at the orifices either by bulk liquid motion tangential to the orifice or by the motion of the orifices as in gas-sparged impellers or rotary spargers. Bubble formation under such conditions of liquid crossflow is known to produce smaller bubbles when compared with formation under stagnant or quiescent liquid conditions. Another advantage of cross-flowing liquids is that the detached bubbles tend to be swept away from the region of the orifice, thereby reducing the likelihood of coalescence.
Foam fractionatio	A destratification system, Artificial destratification is	Stevenson et. al. 2008, Schladow 1992, and	bubble plumes produced by air diffuser systems have been widely used for	Large scale The main advantages of this

n Bubble plumes	practiced avoiding further deterioration of water quality, and water quality control management of lakes and, reservoirs, controlling the stratification structure of reservoirs and lakes to improve water quality, Water purification water quality may deteriorate significantly due to algal blooms in the upper layer and anoxic conditions in the bottom layer when reservoirs are eutrophic. Air diffuser systems are employed in many sources water reservoirs	1993, Sahoo and Luketina 2005, Yum et al. 2005, Sung et. al. 2010, Kreshimir and Hienz 1994	destratification and/or to add oxygen to the bottom layer without causing destratification to improve water quality. Water bodies, such as lakes and reservoirs, experience seasonal temperature stratification with warmer water at the surface and colder water at the bottom. Temperature stratification is strongest during the late summer months because of the high incidence of solar radiation. This energy input warms the surface of the reservoir, causing large thermal gradients in the water body. The thermal gradients impede circulation and internal mixing and restrict the transport of oxygen from the surface layers to the bottom. Therefore, the cold water (hypolimnion) deep in the reservoir becomes isolated from the warmer surface water (epilimnion). Biochemical processes in the reservoir water and at the reservoir bottom use oxygen. Because oxygen is not transported to the hypolimnion from the epilimnion, low oxygen concentrations, or even anaerobic conditions are created at these lower depths. Under anaerobic conditions, water quality suffers because of trace metal dissolution, nutrient release that stimulates eutrophication, production of hydrogen sulfide gas, and a lowering of the pH	approach are economic efficiency and technical soundness. Destratification, as its name implies, has the objective of disrupting thermal stratification to allow natural processes to improve the quality of the lake. The induced mixing and circulation acts to cool the epilimnion and warm the hypolimnion, resulting in a more uniform temperature profile throughout the water column. Destratification of a lake or reservoir eliminates or minimizes the undesirable anaerobic conditions of the lower layers by mixing the hypolimnion and epilimnion and exposing the water to the surface where oxygen absorption occurs. A destratification system operates by adding energy to the water body through an artificial means to destratify the lake or reservoir. Depending upon its specific character, usually, a destratification system results in the cyclical mixing of the water column. The induced circulation brings the cooler, oxygen-deficient bottom water to the surface where reaeration occurs. The warmer, oxygen-rich surface waters are entrained and displaced to the lower depths causing an increase in the temperature and dissolved oxygen content of the bottom water.
Two-phase pipe flow	Oil transportation, oil and gas extraction and transportation Air-sea gas transfer oil and/or natural gas transport	Szilas 1975, Schladow, 1992 J. W. A. De Swart and R. Krishna, (1995), K. A. Shollenberger, et. el., (1997), B. Eisenberg, et. el., 1994	High turbulence energy can be produced in the two-phase region due to the strong local interaction between individual bubbles and the surrounding liquid flow	Large scale due to requirement of oil transportation
Heat exchangers two-phase flow occurs through the concentric circular annulus	Nuclear cooling systems micro cooler nuclear-engineering devices, such as outputs from vessel cores and pipes passing through cooling systems. multiphase cooling, different cooling passages	Poullikkas 2003, Schladow, 1992 Sadatomi et al., 1982; Caetano, 1984; Kelessidis and Dukler, 1989; Hasan and Kabir, 1992; Caetano et al., 1992; Das et al., 1999; Sun et al., 2004 Dissanayake, A., Gros, J. and Socolofsky, S., 2018.	The heat from the reactor is first transferred to the water. Due to a large amount of heat transferred, the water turns to steam. The steam is then transferred via a pump to a heat exchanger. The steam is used to move a turbine, which generates an electric current. In multiphase cooling, two or more cooling stages occur where compressors and other equipment are also installed. It is required at high preference to control the flow of gases to provide better cooling. Hence bubble plume phenomenon occurred here to monitor control the surface flow to provide better cooling.	Medium scale Multistage cooling process based on the bubble plume mechanism.

Mass transfer units	Fluid aeration; bioreactors	Enes 2010	The oxygen mass transfer from air to liquid takes place by rotating the double impellers. In the same field for aeration, operation condition, and power consumption.	Small scale
Gas-bubble injection techniques and Bubble plume	Enhancing mass transfer, mixing, and water purification. Augment convective heat and mass transfer rates in various applications, promoting heat and mass transfer Natural convection heat transfer along with a heated plate that is widely seen in a variety of heat exchangers such as solar water heaters. The heat transfer enhancement for the natural convections provides high efficiency to the heat exchangers. Heat Transfer applications in Vertical Plates.	Hassan 2003, 2013, 2014, Duplat 2017, Kenji et. al. 2007, Schladow, 1992, Donnelly, B., et. al. (2008), Xiaobo et.al. 2006	Heat or mass transfer around an evaporating drop or condensing vapor bubble is a complex issue due to the interplay between the substrate properties, diffusion- and convection-driven mass transfer, and Marangoni effects, to mention but a few. To disentangle these mechanisms, we focus here mainly on the convective mass transfer contribution in an isothermal mass transfer problem. Gas-bubble injection techniques enhance the heat transfer for the natural convection of liquid along with a heated vertical plate. Bubble flow enhances the normal laminate flow. It is used to increase the flow rate. As the flow rate increases the rate of exchange of heat also increases. Enhanced mass transfer associated with bubble plumes is widely observed and exploited in engineering applications, with water purification using ozone bubble plumes being one of them. The plume mass transfer efficiency is one of the key parameters in practice as it is desirable to achieve high mass transfer efficiency when an expensive gas such as ozone is used	A large-scale (phenomena) circulation of the liquid phase can be generated in natural circulation systems
Bubble plume	Wastewater treatment, Chemical, petrochemical, and metallurgical industries	M Gresch 2011, Atila et. al. 2002, W. Bai et. al. 2010	The presence of heavy metals in residual water is commonly observed as a product of mining and metallurgical works; if these waters are discharged directly this will cause a major environmental problem; therefore, it is necessary to treat these waters to remove impurities to acceptable levels to avoid any damage to the environment.	The use of bubbles is attractive because it is very simple and cheap to operate
bubble-driven mixing	The delicate mixing of pharmaceutical and food products, Food and pharmaceutical industry Use for the mixing application Mixing of pharmaceutical products and food mixing.	Hassan 2003, 2013, 2014, 2019. Asiagbe, K. S., et. al. (2017).		the large-scale phenomena. Bubble plume creates a surface flow with an appropriate magnitude of velocity for kicking applications
Bubble plume	Well-bores for the exploration and extraction of oil and natural gas, solvent extraction	Hasan and Kabir, 1992, Caetano et al., 1992, Das et al., 1999, Sun et al., 2004		
Bubble plume: Strong rising flows can be induced by the pumping effect	mitigation of cavitation damages in the Spallation Neutron Source (SNS) cavitation, and cavitating pumps, mitigation of cavitation damages in the Spallation Neutron Source (SNS), pumping effect	M Gresch 2011, Hussain and Siegel 1976	The cavitation damage derives from pressure waves caused by the beam energy deposition. Vapor bubbles form when low to negative pressures occur in the mercury near the stainless-steel target window due to wave interaction with the structure. The collapse of these bubbles can focus wave energy on small liquid jets that erode the window surface. The compressibility of the mercury can be enhanced to reduce the amplitude of the pressure wave caused by the beam energy deposition. Bubble	The use of bubbles is attractive because it is very simple and cheap to operate. Cavitation is a severe effect that breaks the metal surface and causes damage. As bubble plumes reduce the mitigation of cavitation damage. Hence, it's a god phenomenon in SNS.

			plumes are used to accelerate the transferring of mass and then also the mixing of mass. When cavitation occurred a bubble plume replaces that cavity with mass quickly as it accelerates it. Hence, it causes the mitigation of damages with cavitation in SNS.	
Bubble-driven circulation systems	Heat and mass transfer through boiling is the preferred mode in most power plants boiling heat transfer	J. W. A. De Swart and R. Krishna, (1995), K. A. Shollenberger, et. el., (1997)., B. Eisenberg, et. el., (1994)		
Bubble-driven circulation systems	Metal processing operations such as steelmaking, ladle metallurgy, or metallurgy in the gas stirring of ladles or gas stirred melt ladles which are commonplace. and nuclear devices, and the secondary refining of aluminum and copper, Accumulation of the surface slag in the metal refining process. The upward movement of inert gas into a bath provokes a large agitation in the molten metal, resulting in the chemical and thermal homogenization of the mixture, as well as in an acceleration of the absorption of harmful non-metallic inclusions into an overlaying slag.	Atila et. al. 2002	The liquid metal homogenization can indistinctly be performed by a single gas plume, by a combination of geometrically arranged plumes, or by a curtain of bubbles. The degree of agitation – and consequently the flow properties provided by rising bubbles of inert gas in the liquid metal medium must hence be determined to achieve minimum mixing times and maximum recoveries of alloy additions at optimum flow rates.	simplicity of installation
Bubble plume	Agitation and mixing operations in process industries	Hassan 2003, 2013, 2014, 2021	A large-scale circulation of the liquid phase can be generated in natural circulation systems	the large-scale phenomena
bubbly flows	Powder dispersion, solid blending, and gas dispersion into liquid	Luewisutthichat et. al. 1997, P. Tirto et. al. 2001, X. Tu and C. Trägårdh 2002		where the resulting product quality and productivity are highly dependent on the mixing process
Bubble plume	Underwater blowout of inflammable gas	Hassan 2003, 2013, 2014, 2020		
Bubbly flows/ Bubble plume	power generation, thermal and nuclear power generation, and nuclear power plants Chemical reactors, biochemical reactors, nuclear reactors, Mixing in Nuclear Reactors. stirred reactors microreactor and nuclear devices. The reduction of surfactants in chemical reaction processes and the removal of oxide films or floating impurities from the surface of the chemical reactors to maintain the performance of reactions. control surface floating substances in various kinds of reactors	Leitch and Baines 1983, Kreutzer, et. al. 2005, Takashi and Koichi 2007, Arnold et al., 1997, Walsche and de Cachard 2000, Marco 2005, Schladow, 1992, Asiagbe, K. S., et. al. 2017	bubbly flows in nuclear power plants can be found in the so-called pressure suppression pools of Boiling Water Reactors (BWR) In passive cooling systems of such reactors, decay heat removal may be achieved by venting steam mixed with non-condensable gases into the suppression pool to reduce the pressure in the reactor system. (Walsche and de Cachard 2000) and (Marco 2005) investigated these venting phenomena. In their example, they provided a better important understanding of the condensation and the mixing phenomena controlling the effectiveness of such suppression pools, to avoid incomplete steam condensation and stratified conditions in the pool which lead to higher pressures and possibly to an over-design of the containment building	High-speed surface flows may be developed at the free surface Simplicity of installation Bubble column reactors are often used because of their simple construction, low operating cost, and excellent heat transfer characteristics at immersed surfaces

	handling a free surface. Solidified materials or impurities, as well as the stabilization of the interface motion. a means of containing surface-floating substances, such as oil from large oil spills in rivers and estuaries the removal of oxide films or floating impurities from the surface of the metal refining furnaces to maintain their performance hydrocarbon production and refining, petroleum refining		Bubble flow is used in nuclear reactors for mixing as well as separating some components from another based on the size of particles.	
Bubble plume	Prevention of surface sloshing in furnaces, In the metallurgical furnaces where the liquid metal or slag is heated from the top and hence is stratified, metallurgical smelters	Baines and Leitch 1992 R. B. H. Tan et. al. 2000	High-speed surface flows may be developed at the free surface	Simplicity of installation
Bubble plume	gas mixing, and resolution Bubbly flows encompass a vast domain of natural and artificial flow conditions. They are encountered, for instance, in the surroundings of surface ships' hulls	Hassan 2003, 2013, 2014, 2020, Carrica et al., 1998	A large-scale circulation of the liquid phase can be generated in natural circulation systems	the large-scale phenomena
Bubble plume	distillation, distillation plants, distillation towers, distillation columns, absorption, absorption towers evaporation, condensation, Liquid weeping effect	R. B. H. Tan et. al. 2000, Wenxing and Tan 2000, Sundar and Tan, 1999, McCann and Prince 1969, Kupferberg and Jameson 1970, Jameson and Kupferberg, 1967, Miyahara and Takahashi 1984, Antoniadis, Mantzavinos, and Stamatoudis 1992	It is well-known that weeping occurs, most readily, at low-vapor flow rates, corresponding to the 'bubbling' regime	Liquid weeping remains a significant problem for the operation of distillation and absorption processes involving sieve trays. Hydraulically, weeping can affect the liquid hold-up on the tray deck and can influence the tray pressure drop and other wet-tray hydraulic characteristics. In terms of process performance, weeping results in a bypassing of gas-liquid contact, and thereby contributes to decreased tray efficiencies.
bubbly flow	Plunging liquid jets have also been demonstrated as an efficient gas-liquid contacting device. For example, oceans absorb atmospheric gases including human-generated CO_2 emissions by plunging breaking water waves. The same mechanism of air entrainment is responsible for the formation of long bubbly wakes behind naval ships by breaking bow waves. This bubbly flow alters flow hydrodynamics around the ship and produces unintended acoustic and	Bin (1993), Chanson et al., 2006, Moraga et al., 2008. J. W. A. De Swart and R. Krishna, (1995), K. A. Shollenberger, et. el., (1997)., B. Eisenberg, et. el., (1994)	Plunging jet-based systems are in use as chemical or biological reactors. A liquid jet plunging in a pool of liquid entrains gas at the gas-liquid interface. Entrained gas is dispersed in a liquid pool in the form of bubbles. This simple phenomenon of gas entrainment is widely observed in nature and bears great industrial significance.	

	optical signatures. Ship hydrodynamics			
Bubble columns	minerals transport and applied to minerals separation flotation columns	Bennett et. al. 1999		
Surface flow induced by bubble plume	Control surface floating substances in various kinds of industrial processes handling a free surface	Hassan 2003, 2013, 2014, 2020, Schladow, 1992	High-speed surface flows may be developed at the free surface	Simplicity of installation
two-phase flow occurs through the concentric circular annulus	Boilers, natural circulation boilers, oil pipelines gas-liquid pipeline reactors, and process vaporizers double pipe heat exchangers rise of steam in boiler tubes	Sadatomi et al., 1982; Caetano, 1984; Kelessidis and Dukler, 1989; Hasan and Kabir, 1992; Caetano et al., 1992; Das et al., 1999; Sun et al., 2004, R. B. H. Tan et. al. 2000	In many industrial gas-liquid operations, the continuous phase is caused to flow normally across the emerging gas at the orifices either by bulk liquid motion tangential to the orifice or by the motion of the orifices as in gas-sparged impellers or rotary spargers. Bubble formation under such conditions of liquid crossflow is known to produce smaller bubbles when compared with formation under stagnant or quiescent liquid conditions.	It is a complicated flow pattern Another advantage of cross-flowing liquids is that the detached bubbles tend to be swept away from the region of the orifice, thereby reducing the likelihood of coalescence.
Slug (or Taylor) flow two-phase flow	various gas lift devices air-lift reactors The flow of immiscible fluids in porous media, and monolithic and microchemical multiphase reactors	Sadatomi et al., 1982; Caetano, 1984; Kelessidis and Dukler, 1989; Hasan and Kabir, 1992; Caetano et al., 1992; Das et al., 1999; Sun et al., 2004 Kreutzer et al. 2005 Taylor 1949	occurs through the concentric circular annulus	
multifluid systems including gas injection techniques	Combustion cleaning high-pressure evaporators	A. Bankovic, et. al. (1984), S. Hara, et. al. (1984), and N. A. Hussain and B. S. Narang, (1984)	(which is the most popular model in the field of bubble dynamics)	
Bubbly flow	Full lift hypolimnetic aerators	McQueen and Lean, 1986, Lorenzen and Fast 1977, Burris et al., 2002, Vickie 2008.	Full-lift hypolimnetic aerators typically consist of 1) a vertical riser tube, 2) a diffuser inside the bottom of the riser tube, 3) an air-water separation chamber at the top of the riser, and 4) one or two return pipes, called downcomers. Compressed air is delivered to the aerator and bubbles freely from the diffuser. This creates a positively buoyant gas-water mixture that ascends the riser. At the top of the riser, some of the bubbles are released to the atmosphere, although some may be entrained in the water that enters the downcomers. The oxygenated water flows through the downcomers and is returned to the hypolimnion. One of the earliest attempts to design airlift aerators, developed by Lorenzen and Fast [1977], consists of determining approximate specifications for the compressor. The design airflow rate is based on the hypolimnetic oxygen depletion rate and the induced water flow rate through the aeration device.	
Bubbly flow	The Speece Cone,	Vickie 2008, McGinnis and Little, 1998, Speece et al., 1973, Thomas et al., 1994	The Speece Cone developed by Dr. Richard Speece was originally known as a downflow bubble contact system. The system consists of a source of oxygen gas, a conical bubble contact chamber, a submersible pump, and a diffuser that	

			disperses highly oxygenated water into the hypolimnion. Ambient water and oxygen gas bubbles are introduced at the top of the cone. As water flows down the cone, the velocity decreases because the cross-sectional area of the cone increases. The system is designed so that the downward velocity of the water is sufficient to overcome the rise velocity of the bubbles at all levels. The applied water flow rate and slope of the cone walls control the water velocity and, therefore, the time available for gas transfer.	
Bubble plume	Linear Bubble Plume Model for Hypolimnetic Oxygenation	McGinnis et al. 2001, Wuest et al. 1992, Asaeda and Imberger, 1993; Brevik and Killie, 1996; Brevik and Kluge, 1999; Cederwall and Ditmars, 1970; Ditmars and Cederwall, 1974; Fannelop and Sjoen, 1980; Johansen, 2000; Kobus, 1968; McDougall, 1978; Milgram, 1983; Rayyan and Speece, 1977; Sahoo and Luketina, 2003; Schladow, 1992; Speece and Rayyan, 1973; Tsang, 1990; Zheng et al., 2002	bubble plume diffusers are one of the primary types of hypolimnetic oxygenation devices. Two areal diffuser geometries are typically installed, circular and linear. A bubble plume model to predict oxygen transfer from linear diffusers was presented by McGinnis et al. [2001], based on the model for a circular diffuser developed earlier by Wuest et al. [1992]. While several models for point-source or circular bubble plumes have been proposed.	
Bubble plume	Coupled Bubble-Plume/Reservoir Models for Hypolimnetic Oxygenation	McGinnis et al., 2004, Arega and Lee, 2005; Beutel, 2003; Hondzo, 1998; Josiam and Stefan, 1999; Lorke et al., 2003; Mackenthun and Stefan, 1998, Vickie 2008	While bubble plumes are successful at adding oxygen, the added energy may induce large-scale hypolimnetic mixing. An unconfined bubble plume is in intimate contact with the ambient water column and is strongly influenced by the local density profile. Plume-induced mixing changes the thermal structure of the reservoir, and plume performance depends strongly on the vertical density gradient, establishing a feedback loop that continually changes plume behavior. Mixing may partially erode the thermocline and subsequently lead to warming of the hypolimnion and even premature destratification of the reservoir. Higher hypolimnetic temperatures and plume-induced mixing may also be responsible for increased sediment oxygen uptake (SOU).	Because the sediment is the largest sink of oxygen in most lakes and reservoirs, the effect of plume-induced mixing must be included to avoid serious under-sizing of oxygenation systems. The specific plume-induced mixing mechanisms should be identified and incorporated in a coupled bubble-plume/reservoir model for successful design and operation
Bubble plume	Bubble Pump	Susan 2001	Contrary to conventional dual and triple pressure absorption refrigeration cycles, a single pressure absorption cycle does not require mechanical work to pump fluid from the absorber to the higher-pressure generator. However, the single pressure cycle does require a mechanism to lift the fluid from the generator to the absorber against gravity and friction. A bubble pump, or vapor-lift pump, is used for this task because it requires only thermal energy input as the driving force, which is the same as that required to drive the	

			absorption cycle. In a bubble pump, heat addition creates vapor, thereby increasing the buoyancy of the fluid causing it to rise through a vertical tube under two-phase flow conditions. Airlift pumps have been used for decades in the oil industry that run on the same principles, however, instead of bubbles forming from the phase change involved with boiling the liquid, the air is injected into the flow, creating the same buoyancy effect.	
Bubble plume	Air-Lift Pumps	Clark and Dabolt 1986, Stepanoff 1929, Pickert 1932, Nicklin 1963, White and Beardmore 1962 and Zukoski 1966	Air-Lift pumps run on the same principles as vapor-lift pumps except that air is injected to increase the buoyancy of the fluid instead of bubbles forming from liquid vaporization. Although air-lift pumps have a wide variety of possible applications, most studies have been concerned with dewatering mines or raising oil from dead wells. More recently, the importance of airlifts in moving liquids at nuclear fuel reprocessing plants has been realized, requiring more accurate design equations.	

Table 2. Environmental and naval engineering applications of bubbly flow

Unit operation	Applications	References	Description (how does it work)	Remarks
Bubble plume	Desertification device, in the mixing of very hot or toxic liquids, and the desertification of lakes and reservoirs, inducing mixing while introducing dissolved oxygen for improving water quality in lakes and reservoirs	Hassan 2003, 2013, 2014, 2019	A large-scale circulation of the liquid phase can be generated in natural circulation systems	the large-scale phenomena
Bubble plume induced surface flow	Interactions of the oceans with the atmosphere for example, both air bubbles near a free surface and cavitation bubbles are of major importance for the detection of submarines in naval applications	Hassan 2003, 2013, 2014	High-speed surface flows may be developed at the free surface	Simplicity of installation
Bubble plume induced surface flow	Barriers against saltwater intrusion in rivers and locks and as barriers to contain density intrusions or oil spills or for stopping the spreading of oil spills on the water surface. Application in environmental protection such as oil removal from water bodies. Bubble flow is used for many water cleaning applications The bubbles stick to the oil substances or droplets and cause them to move and float on the surface of the water which makes the froth layer which can easily be removed	Hassan 2003, 2013, 2014, 2019, Hoult 1969, Schladow, 1992, University of Cambridge: Ceb.cam.ac.uk. 2021.	High-speed surface flows may be developed at the free surface	Simplicity of installation
Bubble plume induced	Protect installations from shock waves produced by	Hassan 2003, 2013, 2014, 2017	High-speed surface flows may be developed at the free surface	

surface flow:	underwater explosions and as silt curtains			
Bubble plume induced surface flow:	Reservoirs and mix stratified fluid layers, to reaerate lakes.	Hassan 2003, 2013, 2014, 2018	A large-scale circulation of the liquid phase can be generated in natural circulation systems	
Bubble plume induced surface flow	The implications of a rupture, or even breakage, of a subsea pipeline.	Hassan 2003, 2013, 2014, 2020		
A surface jet produced by a bubble plume: High-speed surface flows may be developed at the free surface	The propagation of pressure waves Breakwaters and for reduction of underwater explosion waves, pneumatic breakwaters; utilized for preventing icing in navigational waterways, to prevent surface ice formation in harbors, and to damp sea waves in harbors. inhibit surface ice formation by bringing bottom water to the surface	Taylor 1955, Hassan 2003, 2013, 2014, 2019, Baines and Leitch 1992, Asaeda and Imberger 1993, Jones 1972, McDougall 1978, Schladow, 1992, Phu D. Tran 2011, Campbell and Pitcher 1958	Gas bubbles may be released at high points in liquid lines after rapid pressure reduction. This may happen in a force main when the sudden stoppage of a pump occurs either during normal operation or because of an emergency condition such as power failure. This may also happen in a long gravity main owing to the closure of a valve located near the upstream end of the main. The presence of gas bubbles in liquids, even in minute quantities, has important effects on the propagation of pressure waves in closed conduit flow. The combination of high compressibility of the gas phase and large inertia of the liquid phase yields a very low acoustic velocity for the two-phase mixture, which may be much lower than the acoustic velocity of the gas phase alone	The simplicity of installation, the surface flow in the direction against the waves can break them
Bubble plume induced surface flow	oil refineries, oil barriers (oil fences) The prevention of seawater pollution by heavy oil leakage from tankers. Wave damping effect, damping of waves propagating on the sea, lakes, and rivers alleviating the damage of waves to the building structure,	Hassan 2002, 2003, 2006, 2011, 2012, 2013, 2014, 2018, 2021, Hassan and Tamer 2006, Abdulmouti, et. al. 2000, Hassan et. al. 1997, 1998, 1999-No. 1, 1999- No. 2 and 2001, Hassan and Esam, 2013, Shoichi et. al. 1984, Shoichi et. al. 1985, and Hassan et. al 1998, Fabregat Tomàs, et. al. 2016.	In case of accidents of tankers and seaside oil refineries, oil barriers (oil fences) are usually set on the water surface to prevent spilled oil from spreading. It is well known that seas and oceans are exposed to pollution by oil leakages. Many accidents have happened in many areas of the world. These incidents are the motivation for the development of a new bubbling jet flow type employing the bubble plume to support the function of an oil fence, as one of the most important applications of a bubble plume. The most important functions of the oil fence are as follows: a) to encircle an area of water surface over which oil has leaked and then to limit the polluted area. b) to encircle a special area like a power plant, factory, or station in the sea and protect them by keeping oil far away from these areas. A conventional oil fence is sufficient when sea waves are weak but fails when wave amplitude becomes large. In this case, the oil will concentrate near the inside border of the oil fence and then will leak beyond it, either by passing over or under the oil fence. it is considered possible to use the bubble plume as an effective way to control the density and transportation of surface-floating substances since the plume can generate a strong and wide surface flow over the bubble generation system. Moreover, it is expected to be an effective tool to support the function of an oil fence, and able to damp the wave motion especially for high values of	Bubble plume is used as an application for alleviating the damage of waves of the building structure. And for wave damping. A large-scale circulation of the liquid phase can be generated in natural circulation systems The building structures can be damaged due to waves. To alleviate the damage of waves to the structure of the building bubble plume is used. Bubble plume induced the surface flow to deal with that. The control of this can be done with a bubble plume

			current velocity, wave height, and wind velocity. The bubble plume decreases the intensity of the wave motion and restrains the waves passing over an oil fence body	
Bubble plume induced surface flow	Prevent the diffusion of the leaked oil or oil generated from oil sources in the sea.	Hassan 2003, 2013, 2014, 2021, Hoult 1969, Shoichi et. al. 1982		
Bubble plume induced surface flow	The prevention of diffusion of organic or harmful substances on the sea surface, lake surfaces, and river surfaces, and the forced collection of them using the surface flow.	Hassan 2003, 2013, 2014, 2020	High-speed surface flows may be developed at the free surface	Simplicity of installation
Bubble plume induced surface flow:	The prevention of freezing over the surfaces of seas and lakes in the winter season.	Baines 1959, 1961, and 1983	A large-scale circulation of the liquid phase can be generated in natural circulation systems	The prevention of clean surface rivers or lakes from freezing over in general
Bubble plume induced surface flow	contamination spreading, containing and controlling surface floating substances such as oil from large oil spills in rivers and estuaries, lakes, oceans, or containment for oil spills air entrainment in oceans/rivers, and contain oil slicks on water surfaces, and protect from underwater explosion damage	Jones 1972, Hoult 1969, Hassan 2003, 2013, 2014, 2020, 2021, Asaeda and Imberger 1993, Jones 1972, McDougall 1978, Liro et al. 1991, and Caulfield 1996, Schladow, 1992	bubble curtains for contaminant A large-scale circulation of the liquid phase can be generated in natural circulation systems	Simplicity of installation
Bubble plume induced surface flow	anti-icing fluids preventing channel and harbor from being frozen,	Hassan 2003, 2013, 2014, 2020		
bubble jets /Bubble plume induced surface flow	mixing processes in density stratification to the design of air bubble diffusers for lake/reservoir destratification and aeration, destratification in lakes and prevention of ice formation in harbors, reaeration in lakes and reservoirs, bubble barriers for shockwave protection from underwater explosions, and oil well blow-outs	Asaeda and Imberger 1993; Lemckert and Imberger 1993; McGinnis et al. 2004; Schladow 1993, Imberger and Patterson 1990, Mortimer 1941, 1942, Jones 1972, McDougall 1978, Liro et al. 1991, and Caulfield 1996	A large-scale circulation of the liquid phase can be generated in natural circulation systems Density stratification of lakes and water storage. When its duration is sufficiently long, oxygen depletion resulting from biochemical and biological demand can occur in the hypolimnetic waters that have become isolated from the water surface. The immediate consequences of this are varied and can include the formation of iron and manganese compounds in solution and suspension, and widespread fish kills	
Bubble Plume	encountered in oil-well blowouts,	Topham 1974, Mcdougall 1978, Boufadel, M. and Socolofsky, S., 2021.	Oil well blowouts deal with the gases and plumes. Bubbles are generated in it, the flow of these bubbles and gases is directed and controlled with the process of bubble plume. with the large-scale exploitation of oil and gas under the sea, the oil-gas blowout causes serious pollution to the sea, during an underwater oil-well blow-out, a plume of bubbles, oil droplets, and seawater develop; the extent of the damage to marine life depends on whether all the oil rises to the surface or spreads out horizontally at some intermediate depth. bubble plumes used in the context of	bubble plumes can be used to control the pollution area The bubble plume process deals with the flow of gases from oil blowouts.

			rectifying an oil-well blowout. Characteristically a lot of gas is emitted with the oil, and a plume develops due to the presence of bubbles formed by this gas. The extent of damage caused by an oil-well blowout was strongly dependent on whether all the oil rises straight to the surface or some of it spreads out horizontally at some intermediate depth.	
two-phase plumes	induced events of carbon dioxide sequestration, by which this compound is "injected" into deep seas. in the proposed deep ocean sequestration of carbon dioxide to help mitigate potential global climate change planning of deep-sea CO2 sequestration	Liro et al. 1991, and Caulfield 1996 Crounse et al. 2007; Socolofsky et al. 2008		At an extremely large scale
Bubble plume induced surface flow: A large-scale circulation of the liquid phase can be generated in natural circulation systems	Drinking water treatment, lakes, reservoirs Destratification devices/purposes the destratification of reservoirs by mixing the lower-level water with the surface water. Denser water is lifted upward where the turbulence generated by the bubbles produces mixing with the lighter water. Thermal stratification during summer may result in lowered dissolved oxygen levels below the thermocline of lakes and reservoirs.	Baines and Leitch 1992, Dong et. al. 2009, S. Geoffrey 1993, Schladow, 1992, Wang, Ruo-Qian et. al. 2016, Beutel and Horne, 1999, Ga¨chter and Mu¨ller, 2003, Cooke et al., 1993, Wu et al., 2003, Wuest et al., 1992, McGinnis and Little, 1998, Burris et al., 2002	Destratification induced by bubble plumes to reduce evaporation from open impoundments is a technique that is practically in use. Bubble plume is induced to use as a destratification device to reduce the evaporation process from the impoundment. Excess phosphorous loading in lakes and reservoirs increases the content of organic matter, which, through decomposition, increases oxygen demand. Many eutrophic lakes do not contain sufficient hypolimnetic dissolved oxygen (DO) to meet this demand during the stratified season and become anoxic before the advent of deepwater convection in winter. As a result, anoxic products such as methane, hydrogen sulfide, ammonia, iron, manganese, and phosphorus are formed, these conditions cause environmental and drinking water treatment problems, which vary depending on the water use. For drinking water sources, water depletion of DO may lead to taste and odor problems, increased treatment costs, and increased formation of disinfection by-products. For cold-water fisheries, low hypolimnetic DO stresses or eradicates fish populations, and eggs deposited in anoxic sediments may not develop. Hypoxia itself has been shown to be an endocrine disruptor and negatively impacts fish reproduction. Anoxic reservoir releases also negatively impact downstream water quality. Preventing the occurrence of anoxia in the hypolimnion may be achieved with oxygenating bubble plumes or other oxygenation systems such as the Speece Cone or airlift aerator	in which case the characteristics of the air-bubble plume are of more interest than the induced horizontal flow in the surface layer The use of bubble plumes as a destratification device, inducing mixing while introducing dissolved oxygen for improving water quality in lakes and reservoirs Destratification devices are examples of the bubble plume effect and can be used.
arrays of bubble diffusers	used in reservoirs aimed at storing combined sewer overflows to avoid the	Hassan, 2012, 2013 and 2014, Murai et. al. 2001, Abdel Aal et. al.		

	occurrence of anaerobic conditions	1966		
bubble plumes	keeping swimming areas free from slow-moving objects such as sea nettles	Marks and Cargo 1974		

Table 3. Other applications: aerospace, biomedical, electrical, and mechanical

Unit operation	Applications	References	Description (how does it work)	Remarks
Bubble plume	rocket engines,	Moran, Robert P., and Houston, Janice D. 2011.	Rocket engine works on the repulsive phenomena of gases. Gases flow can be controlled with the help of a bubble plume. Hence, bubble plume increases the flow of gases. Therefore, rocket engine starts moving upward towards the sky.	Bubble plume is such a phenomenon that can be used in a rocket engine to provide great acceleration and velocity to the rocket.
Bubble plume induced surface flow	sonoluminescence	American, S., 2021. Scientific American	Sonoluminescence is the emission of short bursts of light from imploding bubbles in a liquid when excited by sound. Imploding bubbles deal with the bubble plume phenomenon, therefore bubble plumes can be used in sonoluminescence. The bubbles produced by ultrasound in water (sonoluminescence) reach extremely high temperatures and pressures for brief periods	There is a huge impact of bubble plume induced surface flow on sonoluminescence
Bubble plume induced surface flow	ink-jet printing, electrophotographic processes	J. W. A. De Swart and R. Krishna, (1995), K. A. Shollenberger, et. el., (1997)., B. Eisenberg, et. el., (1994)]. Jeff Tyson 2021. Dougherty, E., 1991.	Bubble plume is one of the effective ways of surface floating. In inkjet printing, the bubble plume is for the inkjet printer to float the ink to the paper. Hence, bubble plume induced surface flow is generated in the inkjet printing service. The control of toner in the electrophotographic printer is very important to obtain better quality. Along with the toner, speed is another factor that enhances the quality. Hence, bubble plume is a phenomenon that controls the process of electrophotographic, by controlling the speed and quantity of tonner.	Inkjet printing is an application of bubble plume. the effective flow of toner is a major factor in the quality and speed of electrophotographic printers which control through a bubble plume.
Bubble plume induced surface flow	particle transport in blood, laser surgery cavitation medical settings and medical ultrasound imaging	Rocheleau, J., 2021, Lim, Kang Yuan et. el. 2010. J. W. A. De Swart and R. Krishna, (1995), K. A. Shollenberger, et. el., (1997)., B. Eisenberg, et. el., (1994)	Bubble plume is the source that enhances the transportation of particles at a fast rate. When the particle is moving, low pressure developed which pushes the particle to move. Hence, it induced the surface flow of the particle in the transportation. Lithotripsy deals with laser surgery where control of the laser is very mandatory which contains bubble plume.	The movement of the particle through blood is a critical portion and a bubble plume induces the surface flow which enhances the movement. All kinds of blood flow from semen to the bends to lithotripsy
Bubble plume induced surface flow	crystallization,	Boudreau, A., 2016.	Crystallization is the process of atoms or molecules arranging into a well-defined, rigid crystal lattice to minimize their energetic state. The smallest entity of crystal lattice is called a unit cell, which can accept atoms or molecules to grow a macroscopic crystal. In crystallization, it is important to maintain the size of the unit cell, which can be controlled with a bubble plume.	Bubble plumes control and maintain the size of the crystal in the crystallization process.
Bubble plume induced surface flow	fluidized beds,	W. Warsito, L.-S. Fan, 2005,	Fluidized beds are reactors that have sand or similar medium and jets of air that are injected vertically from the bottom of the bed. Fluidized beds include a jet of air which is injected vertically from the reactor, the flow of air or the jet of air controlled by bubble plume, the jet occurred as concerned with the bubble plume, hence fluidized beds is an example of bubble plume.	The fluidized bed is an example of a bubble plume which deals with the flow of air jet.

Bubble plume induced surface flow	drying of gases, polymer polymerization	Emerson, S. and Bushinsky, S., 2016. The role of bubbles during air ‐ sea gas exchange. *Journal of Geophysical Research: Oceans*, 121(6), pp.4360-4376.	Gases dryings deal with the removal of moisture from the gases. Adsorption Zeolites, silica gels, or activated aluminum powder. Condensation Cooling with the injection of hydrates inhibitors (glycols or methanol), Membranes Based on elastomer or glassy polymers. Chemical method hygroscopic salts -usually metal chlorides (CaCL2 and others.) are used for the drying process. It is mandatory to use these substances in a sufficient quantity. A bubble plume is used to control gases flow and the surface flow to dry the gases to a sufficient amount.	Bubble Plume control the process and drying of gases is an example of that.
Bubble plume induced surface flow	turbines	Robert S. Bernard, Robert S. Maier, Henry T. Falvey, A simple computational model for bubble plumes, Applied Mathematical Modelling, Volume 24, Issue 3, 2000, Pages 215-233, ISSN 0307-904X,	Turbines works when high speed fluid flows through them. Most of the time turbine uses gas for its operation. Hence the flow control is very important as an increase in velocity reduces the pressure and there is a chance of cavitation. A bubble plume is used to control that process and avoid cavitation which may damage the surface of turbine blades.	Proper flow through the turbine with optimized velocity and pressure is very important which can be obtained through a bubble plume.
Bubble plume induced surface flow	Papermaking,	Dissanayake, A., et. al., 2021.	The papermaking industry deals with the process involve water treatment. It is important to control the quantity of water and other gases in papermaking. Bubble Plume provides control in the papermaking industry.	Providing control of the water in paper making industry is an important aspect that is utilized through bubble plume for better optimization.
Bubble plume induced surface flow	pellet form of almost all raw plastics	Sreedhar, N., 2021.	Pillet formation is mandatory before the formation of the actual project. Pillets are made in circular or rectangular form. For plastic, the treatment is mandatory to deform the process according to the required shape. These processes include bubble plumes which enhance production and control productivity.	
Bubble plume induced surface flow	preventing the invasion of brine with air bubble curtain in the estuary	Nader, M., Kermani, M. and Barani, G., 2021.	Brine is the solution of water and sodium chloride. The invasion of brine and air contains the control of air bubbles through bubble plumes.	A bubble plume is used to control the air bubble in the invasion of brine.
bubble columns	aeration tanks, aerated stirred tanks, aeration purposes in water and wastewater treatment plants, biological wastewater treatment systems biological fermentation, polymer polymerization aeronautical and astronautical systems	R. B. H. Tan et. al. 2000 A. M. Leitch and W. D. Baines, (1989), and Y. Y. Sheng and G. A. Irons, (1992)		because of their simple construction and ease of operation, bubble columns are widely used
air bubbles	The air lubrication method, which reduces the resistance of the hull by using air bubbles, The Mitsubishi Air Lubrication System (MALS) was the first air lubrication system in the world to be applied to a newly built ship and resulted in a substantial reduction in the ship's resistance.	Kodama et al. 2000, Makoto et. al 2011	The development of energy-saving ships has been greatly anticipated by the shipping industry as a countermeasure against the surging prices of raw materials, including oil, arising from the economic growth of developing countries, and environmental issues such as CO2 emission regulations for international shipping operations	the method is expected to result in prominent energy-saving effects.

2. The Difference of Surface Flow Generation Mechanism

Surface flows generated by bubble plumes are considered a key phenomenon in many processes in bioreactors, chemical plants, modern industrial technologies, such as metal refinement, and future-type nuclear power plants, in addition to the many applications of bubble plumes mentioned above. These processes, which are expected to be improved by applying the bubble plume, require the control of both concentration and transportation of surface-floating substances, i.e., solidified materials or impurities, as well as the stabilization of the interface motion itself in order to guarantee their designed performances. Hence, the flow in the vicinity of a free surface induced by a bubble plume was utilized as an effective way to control surface floating substances on lakes, rivers, seas, oceans, as well as in various kinds of reactors and industrial processes handling a free surface.

However, the main reason for surface flows induced by bubble plumes to be utilized in so many fields mentioned above is the simplicity of installation. However, from the fluid mechanical point of view, it is important to focus on the advantages of the bubble plume compared to various other types of jet flows. As an example, Fig. 1 shows schematic figures of three types of jet flows:

1) Single-phase liquid jet flow (water jet flow).
2) Single-phase buoyant jet flow.
3) Bubble plume induced flow.

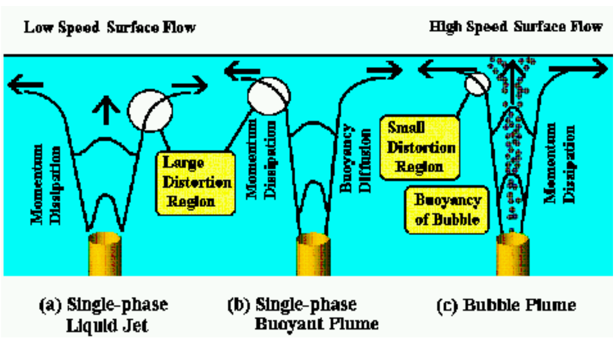

Figure 1. Different surface flow generation mechanisms

Bubble plumes and water jets are widely used to promote circulation and turbulent mixing in aeration tanks, mixing chambers, reservoirs, lakes, and other water bodies. While bubble plumes entrain the surrounding liquid mainly due to buoyancy, water jets induce the entrainment mainly due to momentum.

1) In the case of the single-phase liquid jet flow (water jet flow), the maximum velocity in the jet decreases monotonically due to turbulent momentum diffusion so that the width of the jet expands near the surface. The resultant thick layer surface flow has a slow velocity.
2) In the case of a single-phase buoyant jet flow, the maximum velocity peak is flattened by the buoyancy effect. However, the buoyancy is dissipated due to turbulent mixing near the free surface so that no thin high-speed surface flow occurs.
3) On the contrary, the bubble plume keeps its initial buoyancy even close to the surface since bubbles do not diffuse immediately (it is called an immiscible buoyant jet). Furthermore, an individual bubble has motion characteristics different from the surrounding liquid, therefore, the buoyancy distribution does not simply diffuse. The resultant surface flow is thinner and faster than in the first two cases. Hence, the surface flow is rather effective in the case of the bubble plume compared to the first two flows because the distortion point occurs near the surface (Hassan 2002, 2003, 2013, 2014, 2018, 2019 and2020, Hassan and Tamer 2006, Abdulmouti, et. al. 2000, Hassan et. al. 1997, 1998, 1999- No. 1, 1999- No. 2, 2001, Hassan and Esam, 2013, Abramovich 1963, Rajaratnam 1976; Socolofsky 2001, Soga and Rehmann 2004, Sheng and Irons 1992, Iguchi et. al. 1991, Tomiyama et. al. 1994, 1997, 1998, 2001 and 2002).

3. The Study of Bubble Plumes, Their Properties, Characteristics, Features, and Their Effects on the Applications

Over the last decades, buoyant plumes driven by a source of gas bubbles have had several applications. They have been used with varying degrees of success. For instance, the following systems using bubble plumes were discussed in several kinds of literature. (Taylor 1955) explained how bubble-breakwaters were operated employing a surface jet produced by a bubble plume. He also demonstrated theoretically that the surface flow in the direction against the waves can break them. (Baines 1959, 1961, and 1983) mentioned that the prevention of clean surface rivers or lakes from freezing over is possible using a bubble plume. (Baines and Leitch 1992) found that lines of bubble plumes have been used successfully to inhibit surface ice formation by bringing bottom water to the surface. They explained also that the most extensive application at that time was the destratification of reservoirs by mixing the lower-level water with the surface water. Denser water is lifted upward where the turbulence generated by the bubbles produces mixing with the lighter water. There is a similar process in metallurgical furnaces where the liquid metal or slag is heated from the top and hence is stratified. (Jones 1972) explained that bubble plumes can also contain oil slicks on water surfaces and protect from underwater explosion damage. (Marks and Cargo 1974) reported that bubble plumes were also useful for keeping swimming areas free from slow-moving objects such as sea nettles. Oil is very harmful to marine life, and it is very difficult to clean the ocean from it (Hoult 1969). Besides, during an underwater oil-well blow-out, a plume of bubbles, oil droplets, and seawater develop; the extent of the damage to marine life depends on whether all the oil rises to the surface or spreads out horizontally at some intermediate depth. Hence, another interest in bubble plumes arises in the context of rectifying an oil-well blowout. Characteristically a lot of gas is emitted with the oil, and a plume develops due to the presence of bubbles formed by this gas (Topham 1974). (Mcdougall 1978) explained that the extent of damage caused by an oil-well blowout was strongly dependent on whether all the oil rises straight to the surface or some of it spreads out horizontally at some intermediate depth. (Kobus 1968 and McDougall 1978) made analytical studies on the vertical rising flow using experimental constants. (Shoichi et. al. 1982) measured two-dimensional surface flows velocity profiles using hot wires as a basic tool for studying the prevention of oil diffusion with the help of a bubble plume (Hassan and Monsif 2020, Hassan 2019, 2021, 2022).

A bubble plume is one of the typical bubbly flows observed in aeration tanks, natural circulation boilers, in the above-mentioned disciplines, as well as in metal refining furnaces. For designing these devices experimental research of this kind of flow has been performed previously:

(a) (Hussain and Siegel 1976) reported the relationship between the gas flow rate and the liquid flux induced by large gas bubbles studying the pumping effect.

(b) (Leitch and Baines 1989) described the generation and restriction of turbulence due to bubbles and measured the liquid volume flux, which was induced in a tank by a weak bubble plume.

(c) (Alam and Arakeri 1993), (Iguchi et al. 1997) investigated the microscopic flow structure of a plane bubble plume and observed a sinuous instability for small bubble concentrations.

(d) (Fannelop et al 1991, Hussain and Narang 1984, Hassan 2002, 2003, 2006, 2011, 2012, 2013, Hassan and Tamer 2006, Abdulmouti, et. al. 2000, Hassan et. al. 1997, 1998, 1999- No. 1, 1999- No. 2 and 2001, Hassan and Esam, 2013, Murai et. al. 2000) reported the availability of surface flow induced by a bubble plume.

(e) Later on, (Hassan 2002, 2003, 2006, 2011, 2012, 2013, 2014, 2015, 2016, 2017 and 2018, Hassan and Tamer 2006, Abdulmouti, et. al. 2000, Hassan et. al. 1997, 1998, 1999- No. 1, 1999- No. 2 and 2001, Hassan and Esam, 2013) addressed details studies on the following research subjects:

1- The detailed flow structure and the global flow pattern of bubbly two-phase flows. And the fluid dynamic characteristics of a bubble plume, especially focusing on the technique for generating and using a strong and high-speed surface flows at a free surface by using a bubble plume to improve the applications of the bubble plume and to collect surface-floating substances, especially an oil layer during large oil-leakage accidents to protect naval systems, rivers, and lakes. Here is a summary of their results on these topics:

A- There are two large circulation flow regions of liquid near the bubble plume (at the right and the left side of the bubble plume).

B- The local liquid flow pattern around the bubble plume depends on the gas flow rate. It is recognized that as the gas flow rate increases, the magnitude of velocity increases, and the effective area of the bubble plume (the width of the surface flow) expands in the horizontal direction.

C- Inside the bubble plume and near the free surface, the velocity of the two-phase flow is higher while it is slower in other regions. Hence, high-speed two-phase flow is maintained and further accelerated along the vertical axis, and it produces large entrainment flow in the lower region. This is because of the buoyancy of bubbles. Hence, the generation of this high-speed flow is considered the main contribution to induce a strong surface flow. If a vertically rising liquid jet is applied to induce the surface flow instead of the bubble plume, the high-speed upward flow is not maintained near the free surface due to the turbulent momentum dissipation and the lack of buoyancy inside the jet, and in this case, the power efficiency is considerably less due to the dissipation of momentum under the free surface.

D- The spacing of the streamlines becomes the smallest at the free surface. Moreover, near the free surface, the liquid flow in the horizontal direction is maintained over long distances. Hence, the maximum velocity in the horizontal direction is observed to be near the free surface. This means that the horizontal velocity is fastest on the free surface since there is no shear stress acting on the free surface. This is also one of the reasons why such a wide and thin surface flow is generated by the bubble plume.

E- The highest kinetic energy is generated at a long distance (far up) inside the bubble plume and in the vicinity of the free surface. This observation confirms the fact that the bubble plume can indeed generate a strong and wide surface flow over the bubble generation system.

F- The results of the whole flow field structure obtained by the PIV measurement show a good analogy with those obtained by the numerical prediction.

2- Separation of bubbles and tracer particles by processing the original images, by using image processing software to measure the velocity distribution of both gas and liquid phases in a bubble plume. In addition, to get information and knowledge of the relative velocity which is important to study the response of bubbles and that of the ambient (surrounding liquid). Since a simultaneous measurement of the velocities of both bubbles and liquid demands a separation of bubble images and tracer images in the same frame. This step was very important to study and clarify the flow pattern for both bubble motion and particle motion (liquid).

3- The fundamental characteristics (fundamental features) of the surface flow generation mechanism induced by the bubble plume, despite the complexity and irregularity (respectively nonlinearity) of the surface flow behavior near a free surface due to the strong dynamic interaction between the bubble and vortex motion. Moreover, a detailed discussion concerning the actual surface flow generation process, which depends on the gas flow rate, the bubble size, and the internal two-phase flow structure of the bubble plume in the vicinity of the surface. Furthermore, the dependence of the surface flow speed on the bubble's injection condition. Hence, it made room for more improvement toward higher efficiency in generating the surface flow. Their results showed that the maximum surface velocity increases with the gas flow rate at a power index of around 0.25 to 0.45. The increase of the surface flow velocity responds to the increase of liquid volume flux pumped by the bubbles. Moreover, the power index of the bubble diameter for the surface flow velocity ranges from -0.75 to -0.25. Their results indicated that the smaller the bubbles the faster the induced surface flow velocity. Moreover, the local fluctuation velocity increases with increasing gas flow rate. It concentrates, however, in the bubble plume region and closes to the end wall. The fluctuations calm down in the region where the surface flow is fast. This inverse relationship is considered as one of the factors stabilizing a high speed and thin surface flow and it elucidates the reason why the surface flow is maintained over long distances. Moreover, their results indicated also that when a bubble plume reaches the free surface, the liquid phase flow changes its orientation rapidly from the vertical to the horizontal direction in the vicinity of the free surface. Therefore, the rapid distortion of the liquid phase results just in a layer under the free surface. Moreover, high vorticity distribution, high shear strain rate, and high shear stress rate are generated by the surface flow. These phenomena appear in the layer under the free surface. Therefore, it can be said that the initial surface flow is rapidly generated in this layer. This is qualitatively different from (not found in) the case of a single-phase liquid jet flows whose speed is equivalent to the bubble plume. Hence, a surface flow is more effectively generated utilizing bubbles than by a liquid jet flow because the distortion point appears in the vicinity of the surface. On the other hand, the width of the upward flow induced by the bubble plume is larger than the thickness of the surface flow.

4- The transportation effect of surface floating substances due to a bubble plume is qualitatively confirmed by flow visualization using floating particles. As a result, it is confirmed that when the bubble plume is utilized, surface floating substances (which are the floating particles in their experiments) do not reach and/or do not stick on the oil fence (which is the cylinder in their experiments). Furthermore, the waves become extinct and damped. This is because the elliptical fluid motion of the wave vanishes due to the appearance of the strong surface flow induced by the bubble buoyancy close to the cylinder. Beyond that, the decrease of the average local density and the turbulence generation due to the inclusion of bubbles are important factors, which reduce the local kinematic energy of the wave near the cylinder. Moreover, the combination of the cylinder and the bubble plume gives us the highest safety for the prevention of these surface floating substances from crossing the cylinder position. Hence, the surface flow induced by the bubble plume is quite useful to control the surface floating substances and the bubble plume can stop the spreading of the surface floating substance.

5- Several experiments with many different situations were carried out to identify the effect of a bubble plume. The efficient effect of wave damping due to the bubble plume-generated surface flow is confirmed. It becomes especially remarkable for waves with short wavelengths. The following conclusions can be drawn and summarized:

A- The bubble plume reveals a remarkable effect on wave damping due to the surface flow (which depends on the bubble generation condition). It is a very effective tool to decrease the wave parameters and extinct the wave motion on the free surface.

B- The wave damping effect is much greater for the bubbling case than for the non-bubbling case. The effect of the wave damping with bubbles is 3.3 to 8.8 times greater than without bubbles.

C- In the case of using the bubble plume as an oil fence application, the effect of the bubble plume is much larger than that in the case of using only a conventional oil fence. The present results confirm that the bubble plume is very useful and workers on the coast expect to work with more ease.

6- The characteristics of a bubble and its parameters were calculated by applying image processing after carrying out flow visualization for different sections of bubble regions to find the links and interdependencies between them. The bubble motion depends on the gas flow rate, the bubble size or mean bubble diameter, the bubble velocity along the bubble plume, the void fraction, the distance between the bubble generator and the free surface which is equivalent to the water height in the tank and the internal two-phase flow structure of the bubble plume. It was confirmed that the flow structure is sensitively modulated by the gas flow rate and bubble size. The main results can be summarized as follows:

a- As the gas volume flow rates increase the mean (average) bubble diameter and bubble velocity increase. Moreover, the void friction increases with the gas flow rate at a power index of around 0.8 to 1.0.

Where the void fraction (α) is calculated

by using the equation ($\alpha = Q_g / A \times V_b$) (1)

b- The bubble size increases as the water height in the tank increase.

c- The bubble velocity increases as the water height in the tank increases, and the magnitude of bubble velocity increases along the bubble plume. Moreover, it is also recognized that the bubble velocity magnitude in the middle region is almost 1.5 times the bubble velocity magnitude over the bubble generator. Moreover, the bubble velocity magnitude under the free surface is almost twice the bubble velocity magnitude over the bubble generator.

d- The width area of the bubble plume on the surface (the area which contains bubbles on the free surface "the width of the surface flow" in the horizontal direction) increases approximately proportional to the square root of the gas flow rate.

e- Inside the bubble plume and near the free surface, the bubble velocity and hence the velocity of the two-phase flow is higher while it is slower in other regions. Hence, the generation of this high-speed flow is considered the main contribution to induce a strong surface flow.

7- The detailed structure of the surface flow generation process induced by a bubble plume is investigated by using flow visualization and image processing including the PIV measurements. The measurement of the averaged surface flow velocity is introduced in detail, and the two-dimensional behavior is measured. The flow structure is sensitively modulated by the bubble generation conditions (gas flow rate and bubble size). These experimental results and the numerical results that were obtained by (Murai et. al. 1999 and 2001, Ohno et. al. 1998 and Hassan 2015) show good analogy and the main results can be summarized as follows:

a- The velocity of the surface flow induced by the bubble plume in the vicinity of the free surface is larger and stronger than that in other regions. Moreover, the surface flow is particularly rapidly generated in the vicinity of the free surface. The maximum surface velocity increases with the gas flow rate at a power index of around 0.25 to 0.50. The increase of the surface flow velocity responds to the increase of liquid volume flux pumped by the bubbles. Moreover, the power index of the bubble diameter for the maximum surface flow velocity ranges from -0.75 to -0.25. Hence, the surface flow velocity increases with the gas flow rate. Also, it is remarkably enhanced when smaller bubbles are generated. The results indicate that the smaller the bubbles the faster the induced surface flow velocity.

b- The width of the upward flow induced by the bubble plume is larger than the thickness of the surface flow.

c- The highest kinetic energy is generated in the center of the bubble plume and in the surface flow area where the flow changes its orientation from the vertical into the horizontal direction. This implies that the surface flow induces the largest kinetic energy. This observation confirms the fact that the bubble plume can generate a strong and wide surface flow over the bubble generation system.

d- High vorticity distribution, high shear strain rate, and high shear stress rate are generated by the surface flow, which is induced by the bubble plume, and these phenomena appear in a layer under the free surface. In this layer, the liquid flow rapidly changes its orientation from the vertical to the horizontal direction. Therefore, it can be said that the initial surface flow is rapidly generated in this layer. Hence, the rapid distortion of the liquid phase results in just under the free surface. This is qualitatively different from (not found so clearly in) the case of a single-phase liquid jet flows whose speed is equivalent to the bubble plume. These results indicate that a surface flow is more effectively generated using bubbles than by a liquid jet flow because the distortion point appears in the vicinity of the surface. On the other hand, the surface flow is not induced widely in case that the free surface is covered by a solid film.

8- The detailed structure of the surface flow generation process induced by a bubble plume is investigated by numerical simulation depending on the Eulerian-Lagrangian model. The measurement of the averaged surface flow velocity is introduced in detail, and the two-dimensional behavior is measured. The flow structure is sensitively modulated by the bubble generation conditions (gas flow rate and bubble size). The experimental results that were obtained by using flow visualization and image processing including the PIV measurements (Hassan 2013 and 2014) and the numerical results show good analogy and the main results can be summarized as follows:

a- The velocity of the surface flow induced by the bubble plume in the vicinity of the free surface is larger and stronger than that in other regions. Moreover, the surface flow is particularly rapidly generated in the vicinity of the free surface. The maximum surface velocity increases with the gas flow rate at a power index of around 0.25 to 0.50. The increase of the surface flow velocity responds to the increase of liquid volume flux pumped by the bubbles. Moreover, the power index of the bubble diameter for the maximum surface flow velocity ranges from -0.75 to -0.25. Hence, the surface flow velocity increases with the gas flow rate. Also, it is remarkably enhanced when smaller bubbles are generated. The results indicate that the smaller the bubbles the faster the induced surface flow velocity.

b- The highest kinetic energy is generated in the center of the bubble plume and in the surface flow area where the flow changes its orientation from the vertical into the horizontal direction. This implies that the surface flow induces the largest kinetic energy. This observation confirms the fact that the bubble plume can generate a strong and wide surface flow over the bubble generation system.

c- High vorticity distribution, high shear strain rate, and high shear stress rate are generated by the surface flow, which is induced by the bubble plume, and these phenomena appear in a layer under the free surface. In this layer, the liquid flow rapidly changes its orientation from the vertical to the horizontal direction. Therefore, it can be said that the initial surface flow is rapidly generated in this layer. Therefore, the rapid distortion of the liquid phase results in just under the free surface. This is qualitatively different from (not found so clearly in) the case of a single-phase liquid jet flow whose speed is equivalent to the bubble plume. These results indicate that a surface flow is more effectively generated employing bubbles than by a liquid jet flow because the distortion point appears in the vicinity of the surface. On the other hand, the surface flow is not induced widely in case that the free surface is covered by a solid film.

9- Flow visualization of the bubble plume in two immiscible stratified fluids is carried out to improve the applicability of the bubble plume as an oil fence. The bubble-driven flow in a thermal stratification induces a circulation that is elucidated by using PIV measurements. The covering effect of the oil layer on the free surface and the convection due to the bubble plume are investigated by using image processing, PIV measurements, and path lines measurements. The experimental results and the numerical results that were obtained by our earlier paper (Murai et. al. 2000 and 2001 and Hassan 2015) show good analogy and the main results can be summarized as follows:

a- The flow structure is sensitively modulated by the gas flow rate and bubble size.

b- The velocity of the surface flow induced by the bubble plume in the vicinity of the oil-water interface is larger and stronger than that inside the oil layer. Moreover, the surface flow is particularly rapidly generated in the vicinity of the oil-water interface.

c- The highest kinetic energy is generated at a far distance inside the bubble plume and in the vicinity of the oil-water interface. This observation confirms the idea that the bubble plume can indeed generate a strong and wide surface flow over the bubble generation system.

d- The oil layer is easily broken by bubbles, especially with high void fraction and small bubble size, and high gas flow rates.

Figure 2 shows sample of the recorded images of their study of the flow field for the cases: (a) γ=0 and for case-4 of the experimental conditions, (b) γ=0.1 and for case-3 of the experimental conditions and (c) γ=0.3 and for case-1 of the experimental conditions respectively. While Figure 3 illustrates the path lines of the flow pattern.

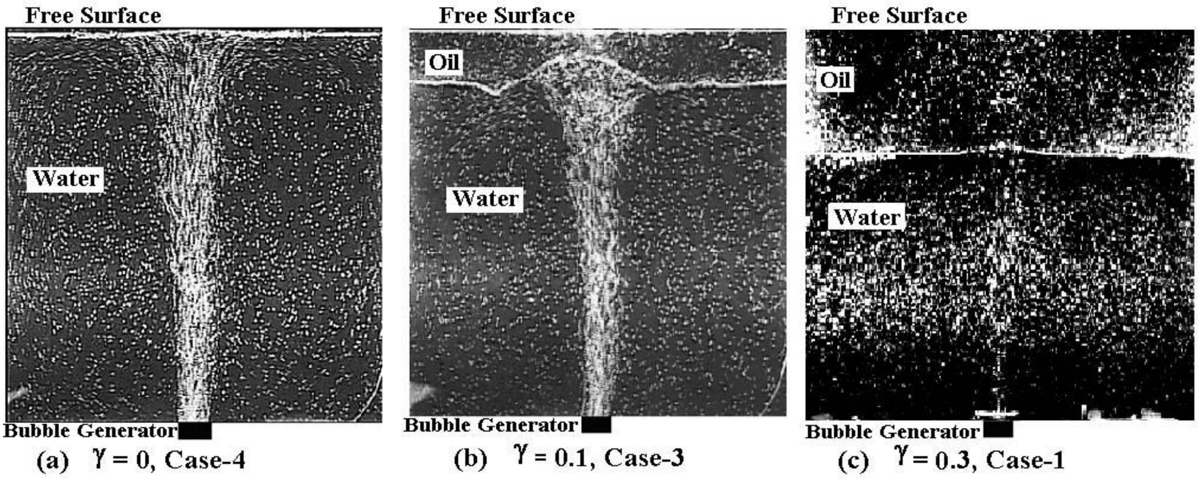

Figure 2. Sample of recorded images

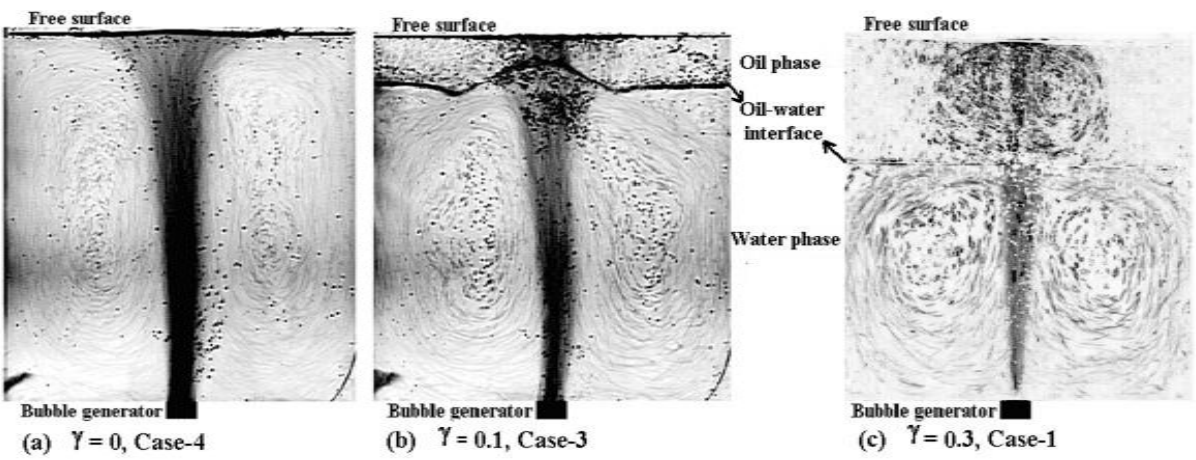

Figure 3. The path lines of the flow pattern

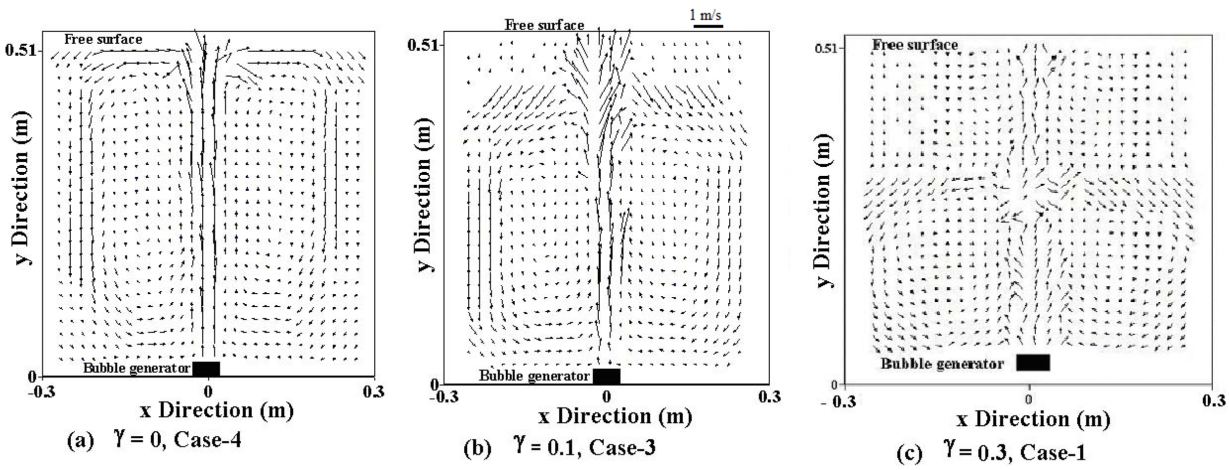

Figure 4. The time averaged velocity vector map of the flow pattern

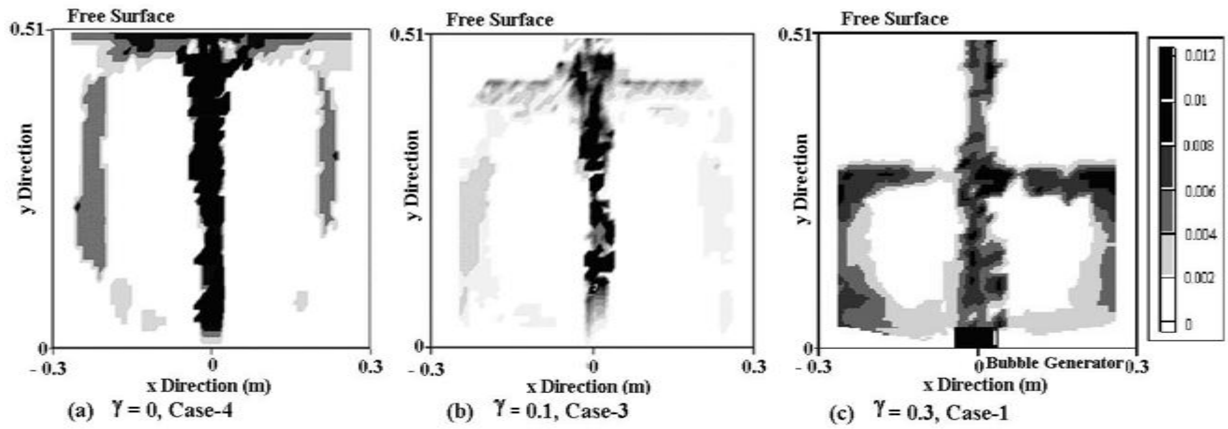

Figure 5. The kinetic energy distribution $(m/s)^2$

Figure 4 demonstrates the two-phase flow pattern of the time-averaged velocity vector maps of these cases which were obtained by using the BDCC (Brightness Distribution Cross-Correlation) method. Figure 5 clarifies the kinetic energy distribution $(m/s)^2$.

10- The detailed structure of the surface flow generation process induced by a bubble plume is investigated by numerical simulation depending on the Eulerian-Lagrangian model. The model and numerical method are formulated with an emphasis on the accuracy of computing the local two-way interaction between two phases. The time-averaged horizontal velocity profile at the surface induced by a bubble plume with different bubble generation conditions is predicted qualitatively and introduced in detail. The relative error against surface velocity is about 5 percent. The two-dimensional and three-dimensional behavior is measured. The flow structure is sensitively modulated by the bubble generation conditions (gas flow rate and bubble size). The results of the experiments that were obtained by using flow visualization and image processing including the PIV measurements of our earlier papers (Hassan 2013), (Hassan 2014), (Hassan 2015), and (Hassan 2017) and the numerical results show a good correlation, and the main results can be summarized as follows:

a- The surface flow velocity induced by the bubble plume in the vicinity of the free surface is larger and stronger than that in other regions. Moreover, the surface flow is rapidly generated in the vicinity of the free surface. The maximum surface velocity increases with the gas flow rate at a power index of around 0.25 to 0.50. The increase of the surface flow velocity responds to the increase of liquid volume flux pumped by the bubbles. Moreover, the power index of the bubble diameter for the maximum surface flow velocity ranges from -0.75 to -0.25. Hence, the surface flow velocity increases with the gas flow rate. Moreover, the magnitude of the horizontal velocity is larger for the larger void fraction supplied. The horizontal velocity is approximately proportional to the distance from the center of the bubble plume to the power of around -0.35. This means that the surface flow is maintained for a wide area compared to the two-dimensional equation of continuity in the horizontal plane.

b- Large bubbles generate several large vortices or large-scale circulations of the liquid phase. However, small bubbles result in small vortex-shedding near the free surface. Therefore, the speed of the surface flow is basically faster in the large bubble case because of the low energy dissipation. However, when the bubble injection point is shallow, the surface flow is reduced more than that for the small bubble case.

c- When a bubble plume reaches the free surface, a liquid flow rapidly changes its orientation from vertical to horizontal. Therefore, the rapid distortion of the liquid phase results in just under the free surface. This is qualitatively different from (not found so clearly in) the case of single-phase liquid jet flow whose speed is equivalent to the bubble plume. This is because, for the bubble plume, the liquid phase is continuously accelerated by bubbles in the vertical direction up to the free surface, while it is only dissipated in the case of a single-phase jet.

d- The flow properties of kinetic energy, vorticity distribution, shear strain rate, and high shear stress are explained, and it is confirmed that the highest kinetic energy is generated in the center of the bubble plume and in the area of the surface flow where the flow changes its orientation from the vertical to the horizontal. This implies that the surface flow induces the largest kinetic energy. This observation confirms the fact that the bubble plume can generate a strong and wide surface flow over the bubble generation system. Moreover, the high vorticity distribution, high shear strain rate, and high shear stress rate are generated by the surface flow, which is induced by the bubble plume, and these phenomena appear in a layer under the free surface. In this layer, the liquid flow rapidly changes its orientation from the vertical to the horizontal. Therefore, it can be said that the initial surface flow is rapidly generated in this layer. These results indicate that a surface flow is more effectively generated through bubbles than by a liquid jet flow because the distortion point appears in the vicinity of the surface.

e- The liquid phase occupies (with small fluctuations) the entire tank. This fluctuation is at first caused by the interaction between two phases inside the bubble plume. Then, as time passes, the fluctuation component is transported by the liquid convection to all the positions of the flow field.

f- There is a high enstrophy layer located under the surface. If the top interface (surface) is covered by a non-slip film, two high enstrophy layers appear in parallel due to vorticity generation on the non-slip film. Moreover, the thickness and the speed of the surface flow, as well as the position and the size of liquid circulations near the bubble plume are drastically altered with the interface conditions. Furthermore, the vortex motion just under the surface is drastically changed in the case of small bubbles. The center of the liquid phase circulation in the case of large bubbles also changes to a deeper position. This means that the effective area is kept wider, and the speed of the surface flow is faster in the case of the free surface compared to the case of the solid surface. Hence, in the case that the free surface is covered by solid or impurity film, the flow is not induced widely. Also, the three-dimensional simulation shows that there is a possibility that involves the periodical velocity fluctuation in the case of creating radial surface flow.

Where the Eulerian-Lagrangian model (Murai and Matsumoto 1998) is adopted in their study. They used the following equations:

a) Governing Equations:

● **Mass Conservation Equation for the Liquid Phase:**

$$\frac{\partial f_L\rho_L}{\partial t} + \nabla.(f_L\rho_L u_L) = 0 \quad (2)$$

where, f_L is the liquid volume fraction, ρ_L is the density of the liquid, t is the time, and u_L is the liquid velocity vector.

● **Restriction on the Two Volume Fractions:**

$$f_L + f_G = 1 \quad (3)$$

where, f_G and f_L are the gas and the liquid volume fractions, respectively. f_G is given by Eq. 4:

● **Gas volume fraction**

$$f_G = \frac{1}{V}\int f_{GLocal}\ dV \quad (4)$$

where, V is the averaging volume of a grid element, f_{Glocal} is the phase indicator, i.e., f=1 in the gas phase and f=0 in the liquid phase. f_{Glocal} is calculated by the TD method (Murai et. al. 1998).

● **Bubble Tracking Equation**

$$x_G = x_{G0} + \int_0^t u_G\ (t)\,dt \quad (5)$$

where $\boldsymbol{x_G}$ is the position vector of the bubble center of gravity, $\boldsymbol{x_{G0}}$ is its initial value, and u_G is the translational velocity vector of the bubbles.

● **Momentum Conservation Equation for all Phases**

$$\frac{\partial f_L\rho_L u_L}{\partial t} + \nabla.(f_L\rho_L u_L u_L) + \frac{\partial f_G\rho_G u_G}{\partial t} + \nabla.(f_G\rho_G u_G u_G) = -\nabla P - (f_L\rho_L + f_G\rho_G)g + (F_{LL} + F_{GG}) \quad (6)$$

where, p is the pressure in the liquid phase. g is the gravitational acceleration. F_{LL} and F_{GG} are the shear stress in each phase and given for continuous phase components as:

$$F_{LL} = \nabla.\mu\left[\nabla u_L + (\nabla u_L)^T - \frac{2}{3}(\nabla.u_L)I\right] \quad (7)$$

We set F_{GG} =0. The viscosity is given by the effective viscosity of bubbly flows (Batchelor 1967): $\mu=(1+f_G)\mu_L$. This equation is valid for small Reynolds numbers less than 1; however, there is no general equation for higher Reynolds numbers so that this description is adopted as a first order approximation.

● **Translational Motion Equation for a Bubble:**

$$\frac{d}{dt}(\rho_G V_G u_G) + \frac{d}{dt}(\beta\rho_L V_G u_G) - \frac{DL}{Dt}(\beta\rho_L V_G u_L) + \rho_G V_G\, g + V_G\nabla P - V_G\,\mu\left[\nabla^2 u_L + \frac{1}{3}\nabla(\nabla.u_L)\right] + \frac{1}{2}\rho_L\pi r_G^2 C_D|u_s|u_s + \frac{1}{2}\rho_L V_G u_s\,(\nabla.u_L) = 0 \quad (8)$$

Many forces act on a bubble in a liquid flow, which is non-uniform and unsteady. These forces are self-inertia force, added inertia force, pressure force, viscous force, drag force, lift force, force of gravity, and history force. Here, the pressure and the viscous forces are transmitted to a bubble via the liquid phase motion surrounding the bubble. History forces like the Basset forces are ignored because the shape of the bubble is almost spherical and the vorticity generation at the clean bubble surface is quite low (the history force has not been formulated in a general and reliable form). β is the added mass coefficient for a spherical bubble and given by ½ (Murai and Matsumoto 1998, Hassan 2002, 2013 and 2014, Murai et. al 1998 and 1999, Matsumoto and Murai 1995). D_L/Dt is the substantial acceleration defined by $D_L/Dt=\partial/\partial t + u_L.\ \nabla$. V_G is the volume of a bubble. Since the volumetric change of a bubble due to a pressure fluctuation or to a pressure gradient in the flow field does not affect the translational motion of the bubble, an invariance condition for the bubble volume: $V_G = V_{G0}$ is employed. Here, V_{G0} is the initial volume of the bubble. C_D is the drag coefficient of a bubble, and the constitution formula for wastewater (Tomiyama et. al 1995) is adopted: C_D =max{C_{D1}, C_{D2})}, C_{D1} =(24/Re) (1+0.15$Re^{0.687}$), and C_{D2} =(8/3) [E/(E+4)]. Here, Re is the bubble Reynolds number defined by: $Re=2\ r_G\rho_L|\ u_s|/\mu_L$, and E is the Eotvos number. r_G is the bubble radius, u_s is the velocity vector of bubble relative to the liquid. The reason of using the formula for wastewater is that contaminations and impurities will concentrate on the bubble interface. In Eq. (8), C_L is the lift force for bubbles and is given by the equation of Auton (Auton 1987 and Auton et. al. 1988).

11- The Flow visualization of the bubble plume in two immiscible stratified fluids is carried out to improve the applicability of the bubble plume as an oil fence after recording images of the flow field around a bubble plume and for a range (many cases) of gas flow rates. The path lines are calculated then the covering effect of the oil layer on the free surface and the influence of the convection due to the bubble plume is investigated by using image processing and PIV measurements. The PIV measurements and the pathline measurement results of the internal flow structure of immiscible two-phase stratified liquids show that the velocity of the surface flow induced by the bubble plume in the vicinity of the oil-water interface is larger and stronger than that inside the oil layer. Moreover, the surface flow is particularly rapidly generated in the vicinity of the oil-water interface. It is confirmed by their research that the flow structure is sensitively modulated by the gas flow rate. The main results explore the following points:

A- There are two circulating flows of liquid near the bubble plume for both the water and the oil layers. The flow circulations inside the water layer are larger than those inside the oil layer.

B- The velocity of the liquid is high inside the bubble plume, in the water layer, and near the oil-water interface, but low in other regions.

C- It is recognized that as the gas flow rate increases, the magnitude of the velocity increases and the effective area of the bubble plume (the width of the surface flow) expands in the horizontal direction. Two effective areas could be recognized: the first one is located at the oil-water interface and the second is located on the free surface. Hence, the surface flow of the oil-water interface, which is induced by the bubble plume, is stronger and larger than that induced in the free surface over the oil layer.

D- For large gas flow rate values, a strong vortex motion (turbulent motion) is induced inside the deformed area. This vortex motion has a role in generating strong shear stress near the oil-water interface.

E- The highest kinetic energy is generated at a long distance inside the bubble plume and in the vicinity of the oil-water interface. This observation confirms the fact that the bubble plume can indeed generate a strong and wide surface flow over the bubble generation system.

F- The oil layer is easily broken by bubbles. It is confirmed that the oil stratum can be separated by a bubble plume especially when the bubble plume has a high void fraction and high gas flow rates.

G- The altitude Δh of the upheaval bulge of the two-phase stratified liquid interface which is induced by the bubble plume (which plays an important role in breaking and destroying the oil layer) is measured experimentally and calculated theoretically. The experimental results agree up to a certain limit with the theoretical result.

12- Flow visualization and image analysis of the bubble plume and bubble motion are carried out to improve the applicability of the bubble plume. The parameters of bubbles (the mean bubble diameter, the bubble velocity, the gas flow rate, the void fraction, and the distance between the bubble generator and the free surface, which is equivalent to the water height in the tank) are found and their relation is demonstrated. It was confirmed that the flow structure is sensitively modulated by the gas flow rate and bubble size. The main results can be summarized as follows:

A. As the gas volume flow rate increases the mean (average) bubble diameter and bubble velocity increase. Moreover, the void friction increases with the gas flow rate at a power index of around 0.8–1.0.

B. The bubble size increases as the water height in the tank increases.

C. The bubble velocity increases as the water height in the tank increases, and the magnitude of bubble velocity increases along the bubble plume. Moreover, it is also recognized that the bubble velocity magnitude in the middle region is almost 1.5 times the bubble velocity magnitude over the bubble generator. Moreover, the bubble velocity magnitude under the free surface is almost twice that of the bubble velocity magnitude over the bubble generator.

D. The width area of the bubble plume on the surface (the area which contains bubbles on the free surface, "the width of the surface flow" in the horizontal direction) increases approximately proportional to the square root of the gas flow rate.

E. Inside the bubble plume and near the free surface, the bubble velocity and hence the velocity of the two-phase flow is higher while it is slower in other regions. Hence the generation of this high-speed flow is considered the main contribution to induce a strong surface flow.

F. Large bubbles can generate surface flow more quickly than small bubbles.

13- Bubble velocity and bubble volume are important for studying bubble motion because they are closely related to a void fraction. However, the volume of a bubble is difficult to calculate exactly, especially for distorted bubbles. The main reason surface flows induced by bubble plumes are used in so many fields, as mentioned above, is the simplicity of installation. The characteristics of bubble parameters that induce surface flow, namely the gas volume flow rate, bubble size or mean bubble diameter, bubble velocity, void fraction, and internal two-phase flow structure of the bubble plume were investigated by Hassan 2021 and Hassan 2022. The results of an experimental investigation of bubble columns were studied in which the variation in bubble diameter and velocity as a function of water depth or the distance between the bubble generator and the free surface, which is equivalent to the water height in the tank (i.e., the height of the bubble plume). In addition, the effects of temperature on the bubble parameters and bubble motion were evaluated. Moreover, the variation in the width of the bubble column was studied as a function of the gas flow rate. The results clearly showed that the bubble plume, “which is a typical bubble flow,” is a key phenomenon and is an effective tool for many applications. The study of bubble plumes is motivated by the possibility to improve its performance and thereby increase its range of applications in many engineering fields. The bubble plume was monitored by flow visualization, following which the images were analyzed, and the bubble motion was deduced and studied. The bubble parameters were then calculated. After visualizing the flow of different sections of bubble regions, the images were processed to clarify the relationship between the bubble parameters, the water height in the tank, and liquid temperature. The relationship between the bubble parameters was explained, enabling an improvement in the efficiency with which the surface flow is induced by the bubble plume (i.e., rapidly generating a strong, high, and wide surface flow over the bubble-generation system). Moreover, this approach allows us to control the parameters of the surface flow, such as thickness, length, and velocity, and thereby control the surface-flow performance. The maximum speed of the surface flow induced by a bubble plume is governed by the flow structure in the initial region, where the rising flow changes into a surface flow. The flow structure and bubble parameters are strongly affected by the gas flow rate, bubble size, and liquid temperature. The surface flow is thus expected to be an effective tool to support the function of an oil fence because it can generate a strong and wide surface flow over the bubble generation system, and it dampens wave motion. This will help for designing real systems that rely on surface flow generated by a bubble plume for controlling and collecting surface floating substances in marine systems, lakes, seas, rivers, and oceans (especially for the oil layer that forms after large oil spills). Surface flows generated by bubble plumes are thus crucial phenomena in various types of reactors, engineering processes, and industrial processes that involve a free surface. The control of the surface flow process and increase its efficiency by finding the effect of water temperature, gas flow rate, and bubble plume height or water height (i.e., the distance between the bubble generation system and free surface) on the bubble parameters (bubble size or mean bubble diameter, bubble velocity, Reynolds number, E*ö*tv*ö*s number, Drag coefficient, and Morton number) were evaluated by Hassan 2022. The efficiency of the surface flow can be evaluated by improving its characteristics such as (velocity, height, width, and length) hence, (rapidly generating a powerful, high and broad surface flow overhead the bubble generator arrangement). The relations connecting these various parameters of bubbles that control their motion are found. The outcomes of the experimental study of bubble columns in which the variation in bubble parameters (diameter, velocity) as a function of the height of bubble plume, temperature, and gas flow rate are studied. Besides, the variation in the width of the bubble column is found to be dependent on the gas flow rate. Our results clearly show that a bubble plume is essential and is a powerful tool for several utilizations. The bubble plume is monitored by flow visualization, following which the images are analyzed, and bubble motion is deduced and studied. The parameters of the bubble (velocity, mean diameter), water temperature, gas flow rate, and plume height are calculated, and their inter-relationship is demonstrated. The results confirm that the flow is greatly affected by the bubble size, gas flow rate, and water temperature. The most important conclusions are paraphrased as follows:

(a) Bubble size increases as water temperature increases. The bubble diameter increases by about one mm for every 10℃ increment in water temperature. Moreover, the bubble size increases with increasing water height in the tank.

(b) Bubble velocity increases as water temperature increases. The results confirm that the bubble velocity increases by a factor of about 1.5 to 2 for every 10℃ increment in water temperature. In addition, the bubble velocity increases along the bubble plume as the height of water in the tank increases. Moreover, the magnitude of the bubble velocity at medium height in the tank is almost 50% greater than the magnitude of the bubble velocity just above the bubble generator. Furthermore, the magnitude of the bubble velocity just under the free surface is almost twice that just above the bubble generator.

(c) The void fraction decreases as the water height increases and as the water temperature increases. The void fraction decreases up to twofold for every 10℃ increment in water temperature.

(d) The length of the bubble plume on the surface (i.e., the area that contains bubbles on the free surface, or “the length of the surface flow” in the horizontal direction) increases with increasing water temperature. Thus, a higher water temperature leads to stronger surface flow. Moreover, this area increases approximately in proportion to the gas flow rate.

(f) Inside the bubble plume near the free surface, the bubble velocity and thus the velocity of the two-phase flow is greater, whereas the opposite is true in other regions. Thus, the generation of this high-speed flow is a primary contributor to the inducement of a strong surface flow.

(g) The higher range of uncertainties occurs in the upper region, where the flow starts to change its orientation from a horizontal into a vertical direction, forming the surface flow, and especially with the higher gas volume flow rates Q3 = 50×10^{-5} (m^3/s), where the flow starts to be turbulent.

(h) The following properties are desired to efficiently generate surface flow: higher temperature, larger bubble size, deeper water, longer bubble plume, increased gas flow rate, and higher velocity. To sustain the surface flow process and increase its efficiency to generate surface flow, the parameters should achieve are greater bubble size, higher velocity, higher temperature, and greater gas flow rate.

(i) The surface flow width increases with increasing both water temperature and gas flow rate. The width of the surface flow increases by about 2 to 4 mm for each 10℃ enhancement of the water temperature, while the surface flow thickness increases about 0.2 to 1 mm for each 10℃ enhancement, and the surface flow velocity increases about 0.1 to 0.2 m/s for each 10℃ enhancement. Thus, a higher water temperature leads to stronger surface flow.

(j) The bubble Reynolds number increases when both the gas flow rate and the temperature increase.

(k) Drag coefficient decreases when both the gas flow rate and the temperature increase.

(l) The E*ö*tv*ö*s number increases when the temperature increases while the Morton number decreases.

(m) The velocity of the bubble and thus the two-phase flow velocity in the bubble plume and near the free surface is greater, whereas the opposite is true in other sectors. Thus, the production of this kind of flow with high speed is recognized as a primary contributor to the inducement of a powerful surface flow.

The detailed investigation of an unstable meandering bubble plume created in a 2 m diameter vessel with a water depth of 1.5 m is reported for void fractions up to 4% and bubble size of the order of 2.5 mm. Simultaneous particle image velocity (PIV) measurements of bubble and liquid velocities and video recordings of the projection of the plume on two vertical perpendicular planes were produced to characterize the state of the plume by the location of its centerline and its equivalent diameter. The data were conditionally ensemble-averaged using only PIV sets corresponding to plume states in a range as narrow as possible, separating the small-scale fluctuations of the flow from the large-scale motions, namely plume meandering and instantaneous cross-sectional area fluctuations. Meandering produces an apparent spreading of the average plume velocity and void fraction profiles that were shown to remain self-similar in the instantaneous plume cross-section. Differences between the true local time-averaged relative velocities and the difference of the averaged phase velocities were measured; the complex variation of the relative velocity was explained by the effects of passing vortices and by the fact that the bubbles do not reach an equilibrium velocity as they migrate radially, producing momentum exchanges between high- and low-velocity regions. Local entrainment effects decrease with larger plume diameters, contradicting the classical dependence of entrainment on the time-averaged plume diameter. Small plume diameters tend to trigger ‘entrainment eddies’ that promote the inward-flow motion. The global turbulent kinetic energy was found to be dominated by vertical stresses. Conditional averages according to the plume diameter showed that the large-scale motions did not affect the instantaneous turbulent kinetic energy distribution in the plume, suggesting that large scales and small scales are not correlated. With conditional averaging, meandering was a minor effect on the global kinetic energy and the Reynolds stresses. In contrast, plume diameter fluctuations produce a substantial effect on these quantities (Marco et. al. 2009).

Older studies of bubble plumes (e.g., by Kobus 1968 and Milgram 1983) produced a basic understanding of their global behavior. More recent detailed bubbly flow experiments (Hassan et al. 1992, Delnoj et al. 1999, Kubasch 2001, Rensen and Roig 2001, Hassan 2003, Marco et al. 2006) were conducted with confined flows or bubble columns. Various effects including recirculation in the vessel and the presence of walls can make the plume centerline and boundaries oscillate in three dimensions. These effects can also produce large structures driving the dispersed phase. The three-dimensionality of air-water bubbly flows was revealed in various experiments; (Milgram 1983, Castello-Branco and Schwerdtfeger 1994, Kuwagi and Ozoe 1999, Johansen and Boysan 1988 and Johansen et al. 1988) discuss plume precession and swirling. The radial distributions of the void fraction and the velocities were investigated by several authors, e.g. (Tacke et al. 1985, Johansen and Boysan 1988 and Johansen et al. 1988).

Gas-liquid bubble columns are used extensively in the process industries for applications that require a large liquid bulk, i.e., applications involving a chemical reaction that is slow concerning the gas-liquid mass transfer or a chemical reaction that produces excessive amounts of heat. The gas-liquid two-phase flow prevailing in a bubble column is extremely complex, is dominated by a rich variety of coherent structures, and exhibits inherent unsteadiness. In recent years, a considerable effort has been made by various researchers to develop computational fluid dynamics (CFD) models for these gas-liquid two-phase flows (Lapin and LuK bbert 1994, Devanathan et. al. 1995, Delnoij et. al. 1997 a, b, c, 1998 a, Jakobsen et. al. 1997, Van den Akker 1998) Experimental validation of these CFD models is a prerequisite for the widespread acceptance of CFD models as a reliable (design) tool in the engineering community and indeed for the development of more sophisticated models. Contemporary CFD models predict the spatial and temporal distribution of key hydrodynamic variables associated with the two-phase flow in a bubble column. Accurate assessment of the validity of CFD results, therefore, requires an experimental technique that provides time-dependent and two- or three-dimensional information regarding these key hydrodynamic variables (i.e., velocity of both phases and void fraction) (Delnoij et. al. 1999). An ensemble correlation, double-exposure single-frame, particle image velocimetry (PIV) technique that can be applied to study dispersed gas-liquid two-phase flows discussed by (Delnoij et. al. 1999). The essentials of this technique were reviewed and several important issues concerning the implementation of the PIV technique were discussed. The capabilities of the newly developed PIV technique were demonstrated by examining the gas and liquid flow fields induced by a bubble plume rising in a rectangular bubble column (Delnoij et. al. 1999).

Gas-liquid two-phase flow is observed frequently in diverse engineering systems covering chemical and petroleum processing, oil and gas extraction and transportation, thermal and nuclear power generation, etc. Despite its wide applications, two-phase flow is one of the least understood domains of fluid dynamics. The two phases can get distributed in many varieties (commonly termed as flow regimes or flow patterns) through any conduit during their motion. This renders the analysis and prediction of flow behavior extremely difficult. For decades scientists and engineers are making tireless efforts to understand two-phase flow through experimental investigations (Serizawa et al., 1975, 2002, 2003; Zun, 1990; Liu and Bankoff, 1993; Liu and Wang, 2001; Lucas et al., 2005 and 2006) and to model them by developing appropriate theory (Ishii, 1975; Ishii and Mishima 1984; Drahos et al., 1991; Yeoh and Tu, 2006; Lucas et al., 2007). Most of such endeavors consider two-phase flow through circular tubes. The motivation for such a choice emerges from the wide use of circular geometry in engineering applications. Nevertheless, flow through the annular passage of circular cross-section also occurs frequently. Well-bores for the exploration and extraction of oil and natural gas, double pipe heat exchangers, different cooling passages, various gas lift devices are examples where two-phase flow occurs through the concentric circular annulus. Accordingly, the flow of a two-phase mixture through annular passage has been investigated by several researchers (Sadatomi et al., 1982; Caetano, 1984; Kelessidis and Dukler, 1989; Hasan and Kabir, 1992; Caetano et al., 1992; Das et al., 1999; Sun et al., 2004).

Sadatomi et al. (1982) studied air-water two-phase flow through the vertical annulus of 15 mm inner diameter and 30 mm outer diameter and determined the average void fraction using a quick closing valve technique. They also proposed the transition boundary for bubbly to slug flow. Caetano (1984) investigated air water and air kerosene two-phase flow through annuli and observed the transition of bubbly flow to slug flow at a void fraction of 18% and 25% for these two cases respectively. Kelessidis and Dukler (1989) conducted experiments for air-water flow in vertical concentric and eccentric annuli of 50.8 mm inner diameter and 76.2 mm outer diameter. They have used probability density function analysis of their conductivity probe signals to identify various flow regimes. Based on this a map has also been introduced for transitions of different flow patterns. Mathematical models based on the physical understanding of different flow patterns have also been developed that match well with their experimental results.

Hasan and Kabir (1992) studied the effect of the annular gap on two-phase hydrodynamics using three different annuli. They have used the drift flux model to predict the average void fraction. Caetano et al. (1992) proposed a transition criterion for bubbly to slug flow using a hydrodynamic model based on eight empirical constants. Their flow pattern map matches well with the data of Hasan and Kabir (1992).

Das et al. (1999) made an experimental observation for air-water upflow through concentric annuli of three different annuli (A: 50.8 mm/25.4 mm, B: 38.1 mm/12.7 mm, C: 25.4 mm/12.7 mm). To identify the distribution of void fraction in different flow regimes parallel plate type conductivity probe was used. Flow regimes were identified using a PDF of the signals obtained. Further, they have developed a transition model and compared the model prediction for bubbly to slug flow with different experimental results.

Recently, Sun et al. (2004) observed bubble distribution patterns in their 4.1 m long borosilicate glass tubing of the annular cross-section. The outer diameter of the tube is 38.1 mm, and the inner diameter is 19.1 mm. Impedance void meter is used to measure the average void fraction of the test rig. Using the signals obtained from an impedance probe flow patterns have been recognized through a neural network. Their analytical model predicts the transition from bubbly to slug flow at a void fraction of 0.191. Some efforts have also been made for two-phase flow through annular conduit in horizontal and inclined orientations. The investigations made by Osamasali and Chang (1988), Ekberg et al. (1999), and Wongwises and Pipathattakul (2006) are worth mentioning.

The review of the literature reveals that most of the previous works on two-phase flow through annulus are experimental in nature. From time to time some efforts have been made to analyze the flow phenomena through theoretical models. These are primarily phenomenological models developed for specific control volumes based on simplified assumptions. Moreover, in most cases, these phenomenological models were derived as extensions of the transition criteria previously proposed for circular geometry. Though these models are reasonably successful in predicting the regime boundary they do not provide much insight into the flow behavior at any location or its development along the conduit axis. It is needless to say that a continuum-based model that takes care of the spatial and temporal variation of the phase velocities along with the mutual interactions of the phases will not only be able to give a clear picture of the hydrodynamics but will also provide a better prediction of transition.

The direct application of continuum-based models of fluid dynamics which are commonly used in the case of single-phase flow poses some difficulty in the case of two-phase flow. Further, the presence of different regimes in the case of two-phase flow increases the complexities. To tackle these situations, flow regime-based models are best suited as the underlying physics behind the regimes are different. Among different types of flow regimes, bubbly flow can be described as a homogeneous mixture of gaseous bubbles and a primary liquid phase. This leads various researchers to model bubbly flow using a homogeneous flow model or drifts flux model (Zuber and Findlay, 1969). Later, efforts have been made with the two-fluid model (Wu et al., 1998; Fu and Ishii, 2003) and the population balance model (Yeoh and Tu, 2004; Cheung et al., 2006) to investigate bubbly flow in the circular conduit. Though different numerical techniques (Bunner and Tryggvason, 2002) are employed to simulate bubble evolution in a circular tube, population balance technique coupled with two-fluid model emerges as an effective and robust technique (Cheung et al., 2006; Das et al., 2009 a, b; Yeoh and Tu, 2004) for predicting interfacial behavior in bubbly flow. Unfortunately, not much effort has been made to simulate bubbly flow and its transition in an annulus through the computational approach.

Knowledge of bubbly flows is significant to various engineering systems such as nuclear waste treatment, biochemical reactors, and steel-making plants. Especially in the chemical engineering and industrial field, the mixing problems such as powder dispersion, solid blending, and gas dispersion into liquid have been an important issue because the resulting product quality and productivity are highly dependent on the mixing process (Luewisutthichat et. al. 1997, P. Tirto et. al. 2001 and X. Tu and C. Trägårdh 2002). In turbulent bubbly flow studies, there are two main interests: turbulence modification by bubbles and turbulent mixing due to bubble-driven liquid flows.

Field surveys were carried out to investigate the surface jet flows and the resulting circulation patterns generated by diffused aeration in a shallow lake. The experimental conditions included point-source bubble plumes with very high air flow rates (100–400 L/min) relative to the shallow water depth (1.5 m). The results indicate that the surface jet velocity can be described by linear profiles. A simple returning flow model was proposed to describe the circulation flow patterns induced by the bubble plumes. The results were also applied to assess the impact of circulation on vertical algae migration, which is important for water quality management [Tone et.al. 2017].

The flow in and around air-bubble plumes was studied. Two main ways of modeling, using either the entrainment assumption or the energy balance principle, are presented and briefly compared. Focusing attention on the entrainment coefficient α(z) which is found to be useful information for a plane plume, from the characteristics of the external flow (the "return flow"). A theory is presented for the external flow far outside a plane plume, at horizontal distances $x \geq 3D$, D being the water depth. A similar theory is presented for the surface flow close to the plume (both axisymmetric and plane cases covered). The theory replaces the physically non-permissible assumption about conservation of momentum around the turning region, used in earlier approaches, with an energy condition in which turbulent dissipation is included. Comparisons of the theories with experiments reported in the literature show reasonable agreement. [I Brevik, Ø Kristiansen 2002].

To enhance mixing efficiency for a bubble-driven mixer such as a high-temperature mixing condition, air bubbling can be used. In such a system, gas is injected into a liquid bath from an orifice located at the bottom wall of a liquid container. (Durst et al. 1984) performed experimental studies on bubble-driven laminar flows by investigating liquid circulation and bubble streets with the Laser-Doppler system. It was reported that the liquid-phase circulation pattern is not sensitive to the actual shape of the void fraction profiles. (Johansen and Boysan 1988 and Johansen et al. 1988) studied fluid dynamics in bubble-stirred ladles by employing a Laser-Doppler system to measure the axial and radial mean and fluctuating velocities of the liquid phase. Air was supplied through a porous plug placed in the bottom wall of a cylindrical perspex-water model of a ladle.

The recirculation flow motion and turbulence characteristics of liquid flow driven by air bubble stream in a rectangular water tank are studied by (Hyun et. al. 2010). The time-resolved Particle Image Velocimetry (PIV) technique is adopted for quantitative visualization and analysis. 532nm Diode CW laser is used for illumination and orange fluorescent (λex = 540nm, λem = 584nm) particle images are acquired by a 1280×1024 high-speed camera. To obtain clean particle images, a 545 nm long-pass optical filter and an image intensifier are employed, and the flow rate of compressed air is 3ℓ/min at 0.5MPa. The recirculation and mixing flow field is further investigated by the time-resolved Proper Orthogonal Decomposition (POD) analysis technique. It is observed that the large-scale recirculation resulting from the interaction between the rising bubble stream and the sidewall is the most dominant flow structure and there are small-scale vortical structures moving along with the large-scale recirculation flow. It is also verified that the sum of 20 modes of velocity field has about 67.4% of total turbulent energy (Hyun et. al. 2010).

The flow structure surrounding bubbles is one of the interesting topics in the field of two-phase bubbly flow. A great number of experimental studies have been carried out to understand the fundamental mechanism of two-phase flows. The quick closing valve is one of the simplest and early developed methods to measure the average void fraction of steady and uniform two-phase flow (Liu 1993). To measure local void fraction, probe techniques and radiation techniques have been used for a long time (Serizawa et. al 1975, 1992 and Herringe and Davis 1976). In recent years, a laser Doppler anemometer has been applied to the bubbly flow measurement as a strong device to investigate the flow structure in detail, such as local void fraction profile, liquid velocity, and its fluctuation (Martin et. al. 1984 and Monji and Matsui 1995).

Flow visualization techniques have also been used commonly in order to understand bubble deformation and coalescence phenomena (Tokuhiro et. al. 1998 and Takeda 1990).

A measurement technique that can easily measure the velocity profile around a gas-liquid interface is required, even though it is necessary to clarify the flow structure around the bubble surface to understand the microscopic mechanism of bubbly flows. (Masanori et. al. 2000).

A measurement system incorporating a UVP monitor has been developed and proposed for use in measuring multi-dimensional bubbly flow characteristics. The system has been applied to bubbly counter-current and co-current flows with a void fraction of less than 7% in a vertical rectangular channel to assess its capability.

(1) The proposed system can measure instantaneous mixture velocity profiles in the channel.
(2) By treating statistically, the measured instantaneous mixture velocity profiles, the velocity profiles of both phases, the void fraction profile and turbulence intensity of the liquid phase in the channel can be obtained.
(3) The phase discrimination method of the measured instantaneous mixture velocity profile was proposed using the probability density function of the mixed velocities.
    The position of the bubble surface was decided, and the data were rearranged according to the distance from the bubble surface. From the results, it can be seen that the liquid velocity field surrounding bubbles can be classified into the following three regions: viscous sublayer, buffer region, and turbulence region.
(4) In the laminar sublayer, the liquid velocity profile has a large gradient, and is greatly affected by the bubble motion but hardly affected by the liquid main flow.
(5) The buffer region plays a role as a transition zone between the laminar sublayer and the main flow region. The motion of both phases influences the flow structure in this region.
(6) The main flow region is far away from bubbles, so that bubble motion does not affect the continuous liquid phase. (Masanori et. al. 2000).

The movement of bubbles is a basic subject in gas-liquid two-phase flow research because bubbles in water play an important role in solving problems in a wide range of experiments and projects [B. H. Davis, (2002) J. Magnaudet and I. Eames, (2000)]. The state and motion of bubbles are closed within the operating conditions, the nature of the liquid, and the form of ventilation. Implementing a bubble state by using visual methods has helped the development of the chemical industry and related fields [Y. Murai, et. al. (2000), H. Abdulmouti (2013), B. Jager and R. Espinoza, (1962)]. The motion of bubbles is very complex. The upward path and change in the direction of a bubble are known to be strongly related to bubble shape [E. T. White and R. H. Beardmore (1962)]. The motion of spherical bubbles is usually rectilinear. Once the bubble deforms into an oblate ellipsoid, instability sets in and results in a spiral or zigzag trajectory. Both bubble shape and bubble velocity of oblate ellipsoidal bubbles exhibit chaotic features [W. Luewisutthichat, et. al. (1997)]. In turn, the fluctuation of bubble shape is likely to cause oscillations in the drag force, leading to the chaotic fluctuation of bubble velocity in the streamwise direction. Therefore, despite periodic macroscopic motion, bubbles exhibit highly chaotic fluctuations in both the lateral and axial components along the zigzag path of a bubble ascent. At the same time, bubble orientation changes in such a way that the trajectory of the bubble plume tends to be perpendicular to the direction of instantaneous motion [W. L. Haberman and R. K. Morton, (1953)). From gas-disengagement experiments, it was inferred that both large and small bubbles exist in churn-turbulent flow [R. Krishna, et. al. (1991)]. Large bubbles rise fast through the column, whereas small bubbles display a longer resident-time distribution. Beyond a certain transition gas velocity, the small bubble holdup remains constant, whereas the large bubble holdup continues to increase with gas velocity [X. Junli, (2004)]. Bubbles in motion are generally classified as spherical, oblate ellipsoidal, or ellipsoidal cap, etc. In gas-liquid upward flow, bubbles move faster than the surrounding liquid (due to buoyancy), and large bubbles have greater upward acceleration than small bubbles. The actual bubble shape depends on the relative magnitudes of the forces acting on the bubble, such as surface tension and inertial forces [D. Bhaga and M. E. Weber, (1981)].

The axisymmetric numerical calculations were used to investigate single Taylor bubbles' distinctive features and liquid flow around the bubbles. The tracking of the interface between two phases is accomplished by the solution of a continuity equation of the volume fraction of the gas phase. Natalia and Alexander 2007 consider a single air Taylor bubble rising through quiescent water in a long vertical tube, which allows it to reach a constant drift velocity. This allows us, in particular, to compare the calculated drift velocities with the analytical predictions of Davies and Taylor (1949).

The authors study the flow in the whole pipe, thus including the upstream region, film flow, and the wake area in a single numerical model. The calculations are performed considering the axisymmetric Navier-Stokes equation assuming the whole flow laminar and then are repeated applying k-ε standard, k-ε RNG, k-ω standard, and the Reynolds stress turbulent models. The calculated results are compared with the experimental PIV measurements of van Hout et al. (2002), measurements of the wall stresses by (Mao and Duckler 1990 and 1991), and analytical results of Davies and Taylor (1949). The comparisons show that only using the Navier-Stokes equation the results agree quantitatively with the experimental measurements and with the analytical predictions (Natalia and Alexander 2007).

Slug (or Taylor) flow is a flow regime important for many applications, for example, air-lift reactors, the flow of immiscible fluids in porous media, and monolithic and microchemical multiphase reactors. Among other advantages, the flow pattern between the bubbles increases mixing promotes a more uniform residence-time than single-phase flow, and the thin liquid film between the bubbles and the tube wall leads to extremely high heat and mass transfer coefficients (Kreutzer et al. 2005). Knowledge about the precise shape of the bubbles and the resulting variation in the thickness of the liquid film that separates the bubbles from the channel wall is of crucial importance for the prediction of heat and mass transfer rates. This knowledge, however, is difficult to predict theoretically, especially for non-circular channels and high Reynolds numbers. Experimental research is also difficult, especially in the monolith and micro-chemical reactors, where the dimensions of the system are small, leading to extremely small film thicknesses. Therefore, Computational Fluid Dynamics is believed to be a powerful tool in studying the two-phase hydrodynamics of slug flow in such channels (F. S. Sousa et. al. 2007). A hybrid front-tracking / front-capturing (F. S. de Sousa et al. (2004) method was used to simulate the flow of liquid slugs inside square cross-section channels. Second-order finite-difference discretizations are employed over a threedimensional cartesian staggered grid. The interface representation employed by their method allows an accurate prediction of the position of the interface, and therefore, accurate computations of the surface tension, which usually dominates this type of flow, are then obtained (F. S. Sousa et. al. 2007). Results of a single bubble rising through a quiescent fluid in a vertical square channel were present, at moderate Reynolds numbers. A comparison between circular and square cross-section channels is made by reporting bubble velocities and shapes for these two geometries. The velocities in the cross-sections of the channels are also reported, showing the presence of a secondary flow for the square channel. Differently from the axisymmetric geometries, the flow of Taylor bubbles in square channels leads to an increased wall shear at the corners of the channel was also shows that what is important to take into account in the determination of heat and mass transfer coefficients (F. S. Sousa et. al. 2007).

Air-water bubbly jets are studied experimentally in a relatively large water tank with a gas volume fraction, Co, of up to 80% and nozzle Reynolds Number, Re, ranging from 3500 to 17,700. Measurements of bubble properties and mean axial water velocity are obtained and two groups of experiments are identified, one with relatively uniform bubble sizes and another with large and irregular bubbles. For the first group, dimensionless relationships are obtained to describe bubble properties and mean liquid flow structure as functions of Co and Re. Measurements of bubble slip velocity and estimates of the Drag Coefficient are also provided and compared to those for isolated bubbles from the literature. The study confirms the importance of bubble interactions to the dynamics of bubbly flows. Bubble breakup processes are also investigated for bubbly jets. It was found that a nozzle Reynolds Number larger than 8000 is needed to cause a breakup of larger bubbles into smaller bubbles and to produce a more uniform bubble size distribution. Moreover, the Weber Number based on the mean water velocity appears to be better criteria than the Weber Number based on the bubble slip velocity to describe the onset of bubble breakup away from the nozzle, which occurs at a Weber Number larger than 25 [Laime et. al. 2008].

Recently, the studies on two-phase flow in the capillary tubes have much attention because of its useful applications such as micro cooler, heat exchanger, and microreactor. Particularly, the slug bubble flow mode provides good performance for heat and mass transfer. For the design of those devices, the control of the two-phase flow pattern must be required. It is known that the coalescence and breakage of bubbles are often negligible in the capillary tube. Therefore, it is very important to predict the slug bubble size formed at the two-phase flow supply system. (Kreutzer, et. al. 2005, Takashi and Koichi 2007). A slug bubble formation model in a capillary tube is proposed. On the other hand, the effects of gas flow rate, nozzle diameter, liquid velocity, and capillary diameter on the shape and volume of bubbles formed in the capillary tube were experimentally investigated. To ensure the proposed model, the calculated results were compared with the experimental results. The bubble volume rapidly increased during the early period of bubble growth and then it increased proportionally to the time (Kreutzer, et. al. 2005, Takashi and Koichi 2007).

When gas and liquid flow simultaneously in a pipe, a variety of configurations (dispersed, annular, and transition flow) related to the spatial distribution of the two phases can be observed. These configurations termed flow patterns can be recognized by the flow maps Mandhane (1974). The one most configuration frequently occurs over certain ranges of flow rates is slug flow. This flow is encountered in large industrial processes as such oil and gas wells, gas-liquid pipeline reactors, and process vaporizers. It is a complicated flow pattern as reported by Fernandes et al., 1983, Orell, and Rembrand (1986). It is characterized by a quasi-periodic alteration of long bubbles and liquid slugs. In vertical flow and at low liquid viscosity, the Dumitrescu-Taylor bubble Clanet et al. (2004) has a generally spherical nose and a flat bottom. It fills most of the pipe cross-section and around it, the liquid moves in the form of a film. The Dumitrescu-Taylor bubble has been the subject of numerous studies Dumitrescu (1943), Davies and Taylor (1950), Collins (1978), Mao, and Dukler (1990), Polonsky et al. (1999), Nogueira et al. (2006), etc. Generally, most of these studies were done in stagnant and co-current vertical flows; few of them were conducted in counter current vertical flows in small tubes Griffith et al. (1961), Nicklin (1962), and Martin (1976). The comprehension of the behavior of the bubble inflow is important to understand the general phenomenon of gas-liquid flow. So, the flow around the individual bubble remains always a very attractive subject of research and any additional contribution of experimental data is useful for the progression of the physical model development (S. Benattalah et. al. 2011).

When a liquid flow through a tube, the motion of the long bubbles results from the complex influence of both buoyancy and the mean motion of the liquid. In upwards flow, the motion of the bubble has been studied by several authors Griffith et al. (1961), Nicklin et al. (1962), Collins (1978), Bendiksen (1985) while in downward flow few studies are carried out Martin et al. (1976), Griffith et al. (1961) and Nicklin et al. (1962). The study of the hydrodynamics of liquid film surrounding the Dumitrescu-Taylor bubble has required various works both experimental and numerical, Goldsmith et al. (1962), Brown (1965), Mao and Dukler (1990), Polonsky (1999), Van Hout (2002), Nogueira et al. (2006) and Bugg et al. (1998) and Bugg and Saad 2002. For the flow which occurs behind the bottom of the Dumitrescu-Taylor bubble, one can quote works of Campos and Guedes (1988) and those of Pinto and Campos (1996), and very few studies have been concerned with the field of flow inside the Taylor bubble. The first visualization of the flow velocity fields inside the gas Dumitrescu-Taylor bubble was carried out by Filla et. al. (1976), by forming a white smoke inside the Dumitrescu-Taylor bubble using a simple chemical reaction. The method consists to form an Ammonia NH3 bubble which will cross a column of liquid made up of two immiscible layers. The first layer is carbon tetrachloride enough deep to give the bubble the possibility to reach the limit velocity. The second is a chloride acid solution HCL. The emergence of the NH3 bubble into the acid leads to form an Ammonium Chloride fog near the interface which was swept down to the bottom of the bubble. Soon, after the chemical reaction, a downward motion near the interface was clearly shown, indicating a toroïdal vortex. When the diameter is small, this method allows only to see furtive vortex but cannot obtain quantitative velocity profiles as for the first measurements of gas velocities within a Dumitrescu- Taylor bubble which were realized by Eccles (1972), by using a miniature hot wire anemometer. The Dumitrescu-Taylor bubble is held stationary by a counter-current flow in a 27 mm diameter tube. The measurements were carried out in the upper hemispherical portion of the bubble (L/D<2.6) with a hot wire which doesn't enable the detection of the flow direction. It is seen that these results are in excellent agreement with the theoretical predictions. It is noted also that the theoretical predictions and experimental measurements have divergences at the level velocities in the center, and those inside the interface of gas/liquid (S. Benattalah et. al. 2011).

An experimental investigation on the Dumitrescu-Taylor bubble in counter-current laminar downward flow in the vertical pipe of a small internal diameter pipe is presented by (S. Benattalah et. al. 2011). The experimental design is realized to work for low and stable liquid flow rates. The Dumitrescu-Taylor bubble may be stationary or can be in motion with an ascending or descending velocity, and this displacement depends on the downward liquid flow rates. Consequently, the advantage of this device is to carry out the measurements of the velocities inside the gas Dumitrescu-Taylor bubble by Laser Doppler Velocimetry (LDV). Starting from the visual observations and image acquisitions with a fast camera, a qualitative description was brought on the hydrodynamic behavior of the liquid film and the ripples created at the bottom of the Dumitrescu-Taylor bubble. The experimental results show a presence of a long toroïdal vortex inside the gas bubble. It should be noted that before (S. Benattalah et. al. 2011)'s work using a hot wire does not show the existence of this vortex. Additionally, other hydrodynamic magnitudes were measured as the liquid film thickness, the Dumitrescu-Taylor bubble rising velocity as well as the erosion bubble. Detailed descriptions are brought concerned with this erosion. Strange phenomena have been observed primarily ahead of the nose of the bubble and on the side of its end (S. Benattalah et. al. 2011).

An upward air-water bubbly flow in a pipe was studied experimentally, with special attention being paid to the transition from bubbly flow to slug flow. The pipe diameter was 72 mm and the height 18 m. The Reynolds number based on liquid flow was low-to-moderate (Us_l < 0:2 ms-1), so that bubble break-up due to turbulence was nearly absent. Three different inlet devices were used, which had a significant influence on the initial bubble size and initial bubble concentration distribution. The transition from bubbly flow to slug flow was shown to be strongly dependent on the inlet configuration, particularly on the bubble size. Several theoretical models for the transition from bubbly flow to slug flow were reviewed. The (Y. Taitel et al. 1980) approach was combined with a bubble-size-dependent critical void-fraction expression of (C. H. Song et al. 1995). This new formulation for the transition from bubbly flow to slug flow was in good agreement with the measurements (S. Guet et. al. 2002).

It was shown experimentally that the efficiency of the gas-lift technique at low liquid flow conditions is very dependent on the inlet device used for injecting the gas. When small bubbles are generated during gas injection, the transition from bubbly flow to slug flow occurs at higher values of the void fraction than for large bubbles. Large values of the void fraction under bubbly flow conditions lead to large values of the liquid flow. This is not the case when large bubbles are generated during injection, as large bubbles would lead to slug-flow conditions already at low values of the void fraction. In addition, it is known that slug flow has a very detrimental effect on the efficiency of the gas-lift technique (S. Guet et. al. 2002).

It was also shown that the transition from bubbly flow to slug flow as a function of the injected bubble size can reliably be predicted by (Y. Taitel et al. 1980) criterion, combined with the critical void-fraction relation of (C. H. Song et al. 1995). When for a practical application the size of the injected bubbles is known, the critical void fraction (for the transition from bubbly flow to slug flow) can be calculated with the critical void-fraction relation of (C. H. Song et al. 1995). (Y. Taitel et al. 1980) criterion can then be used to calculate the optimal influence of the injected gas flow rate on the liquid flow rate (S. Guet et. al. 2002).

Gas-liquid flows are of great importance for many industrial processes. A well-known example is the gas lift technique that is for instance applied in the oil industry. In this technique, an increase, or a generation of an upward liquid flow in a vertical pipe is achieved by injecting gas at the bottom of the pipe. The range of conditions for the liquid flow rate (before gas injection) can be very wide, from conditions without a net liquid flow to conditions with a fully developed turbulent flow (S. Guet et. al. 2002).

Bubbly flow and its transitions in vertical annuli are studied using the population balance technique. Bubble breakup and coalescence are accounted separately to track the evolution of the bubble size during the simultaneous flow of gas and liquid. The conventional two-fluid model is used to simulate hydrodynamics. The model enables the prediction of a void age profile at any axial location. The presence of a peak in the void distribution at the walls of the annulus, center of the annulus, and both at walls and centers are observed depending on the phase superficial velocities. Further, the transition from bubbly to slug and bubbly to dispersed bubbly is predicted based on the evolved bubble size. The model prediction gives a good match with the experimental data and existing theory. A shift in the transition boundary is noted due to the variation in the inlet bubble size and the dimension of the annulus (A.K. Das and P.K. Das 2010).

The effect of bubble-bubble interaction in homogeneous bubbly flow is investigated by direct numerical simulation and a bubbly mixture model for bubbly shock flows at void fraction 0.4%– 13%. It is found that the bubble-bubble interaction effect is significant at a void fraction higher than O (1) % and decreases the amplitude and wavelength of the macroscale oscillations in the dispersive shock structure. For the modeling of the bubble-bubble interaction effect, the local volume averaged Rayleigh–Plesset (LVARP) equation, which is an extended version of the original Rayleigh–Plesset equation, is proposed. The results of the bubbly mixture model using LVARP agree well with the direct simulation results for bubbly shock flows at a void fraction up to 13%. The bubble-bubble interaction in nonuniform bubbly flows is also investigated in bubbly flows with randomized initial bubble positions. It is found that the LVARP model predicts the ensemble-averaged behavior with reasonable accuracy (Jung et. al. 2010).

The continuum bubbly mixture model (L. Van 1968, 1972, A. Biesheuvel and L. Van 1984, L. D'Agostino et. al. 1988 and C. E. Brennen,1995) in which macroscopic conservation equations are coupled with the microscopic bubble dynamics equation has been considered as a sound approach to the study of bubbly flows (liquid flow containing small gas bubbles). Several authors (D'Agostino et. al. 1988, L. D'Agostino and C. E. Brennen 1989, Y. C. Wang and C. E. Brennen 1999, T. Colonius et. al. 2000 and A. T. Preston et. al. 2002) used this model to study dilute bubbly cavitating flows and showed that the model is capable of resolving flow features which cannot be captured with barotropic two-phase models. The bubbly mixture model has also been applied to practical cavitating flows by several researchers (A. Kubota et.al. 1992 and Y. Chen and S. D. Heister 1996). In these studies, the Rayleigh–Plesset equation (or its simplification/ modification) and additional assumptions are used to describe the bubble dynamics. For practical cavitating flows, however, additional effects on bubble dynamics such as thermal diffusion, bubble-bubble interaction, and relative motion between bubbles and liquid should be carefully considered to obtain quantitative results. Many authors stressed the importance of the thermal diffusion effect on the bubble dynamics, and among the many mathematical analyses of the thermal diffusion effect, the model of Prosperetti (A. Prosperetti 1991) is notable. With the development of computational methods, the study of thermal diffusion has progressed rapidly. Kameda and Matsumoto (M. Kameda and Y. Matsumoto 1996) took into account the thermal diffusion effect in their bubbly shock flow simulation by solving the full set of partial differential equations (i.e., compressible Navier– Stokes equations) for spherical bubbles. This is computationally demanding but they obtained good agreement with experiments. Recently (A. T. Preston 2007) proposed a reduced-order model of diffusive effect on the bubble dynamics and showed its validity by comparing the results with computations of the full partial differential equations. Their model is applicable to practical, complex bubbly flow computations.

The bubble-bubble interaction is another important effect for nondilute bubbly flows. In practical cavitating flows, the local void fraction (gas volume fraction) often exceeds the dilute limit [O (1) % typically] and the bubble-bubble interaction effect is particularly significant in the high void fraction regions. The original Rayleigh–Plesset equation derived for single bubble dynamics is not valid in that regime.

There have been several studies, (R. E. Caflisch et.al. 1985, J. Rubinstein 1985, and A. S. Sangani 1991) in which bubbly flows at nondilute, finite void fraction was investigated in terms of "effective" equations intended to capture wave phenomena. (R. E. Caflisch et. al.1985) derived an effective wave equation for nondilute bubbly mixture applying the multiple-scale method in the linearized regime. (Rubinstein 1985) applied the approach of Caflisch et al. to the nonlinear analysis of a periodic lattice multi bubble system and derived an “improved” Rayleigh– Plesset equation, which includes the effects of interactions between the bubbles. (A. E. Beylich and A. Gülhan 1990) tried to find the correction factor for the bubble-bubble interaction effect by fitting the result of the model equation to their experimental data for a bubbly shock flow. (G. L. Chahine and R. Duraiswami 1992) studied the response of a few bubble clusters to a prescribed outer pressure (i.e., P_∞) with an asymptotic approach and a boundary element method. (A. (Kubota et.al. 1992) modeled the bubble bubble interaction in their hydrofoil computation by adding the velocity potential of other bubbles with the assumption of local homogeneity, which is the simplified approach of (G. L. Chahine and R. Duraiswami 1992 and G. L. Chahine 1983). Recently (C. F. Delale 2001) proposed a similar model and applied it to quasi-one-dimensional (quasi-1D), cavitating nozzle flow. (Y. Chen and S. D. Heister 1996) considered bubbly cavitating flow at high void fraction using a form of the Rayleigh–Plesset equation that was rewritten in terms of the density equation by volume averaging.

The diversity of applications of bubble plumes has triggered a host of experimental contributions, aimed at determining time-averaged velocities in tanks ranging from 1 m in diameter up to sinkholes of 50 m in depth (Milgram, 1983). Needless to say, the interpretation and comparison of results coming from such a variety of scales are complex. In fact, the shape of containers, different tank sizes and geometries, and the complex nature of the problem make the interpretation of results somewhat cumbersome. This is complex even in non-stratified conditions. Tools to extrapolate bubble-plume behavior in small tanks to big tanks are largely needed.

Experimental evidence regarding the behavior of bubble plumes in two tanks of different sizes, under non-stratified conditions, was presented by (L. E. Rincón et. al. 2004). The smaller vessel has been geometrically scaled down from the larger one with a relation 1:10. Velocity measurements were performed in both tanks with acoustic sensors (ADVs) and time-averaged velocity profiles obtained at both scales were compared. This comparison was used to support a methodology to scale vertical and horizontal (radial) distances in bubble plumes, while allowing for the simulation of portions of the reservoirs. The bubble-slip velocity and length scale D were determined as the relevant scales in the analysis. The previous scaling of bubble plumes, based on the preservation of the number MH (Asaeda and Imberger, 1993) and the use of the ratio diffuser depth/airflow rate, appear as a special case of this more general theory (L. E. Rincón et. al. 2004).

One of the reasons why bubbly flows are difficult to simulate correctly is that the forces exerted on the bubbles are mainly coming from the surrounding fluid and not from the inertia of the bubble itself. Therefore, a thorough understanding of the interaction between the bubbles and the fluid is needed. To this end, a 2D experimental technique is necessary, which can give accurate information concerning both the speed and diameter of the bubbles as well as the speed of the surrounding fluid (S. Dehaeck et. al. 2005).

The functional of bubble columns dependence on the velocity of an air bubble has been determined experimentally by numerous investigators. When rising through an infinite stagnant liquid, the single bubble’s terminal velocity is of fundamental importance in two-phase flow M. A. R. Talaia, (2004), as well as in other types of flow. The knowledge of bubble properties, including bubble velocity, bubble size, gas holdup, and specific interfacial area, is of prime importance for the proper design and operation of bubble columns A. Tomiyama, (2004) and A. Tomiyama, et. al. 2001.

There exist many techniques today, which give only a part of the required information. Backlighting is one of these. It is a well-known technique that simply records the shadow images of diffusively illuminated bubbles. Although this technique can give the size and velocity of the bubble, it cannot give its precise location along the optical axis of the camera since the position and dimension of the detection volume are uncertain. This makes accurate gas-water interface studies almost impossible, and measurements of the void fraction are crippled because of it. Another, more recent technique in droplet diagnostics is Interferometric Laser Imaging for Droplet Sizing (ILIDS) (Koenig et al. (1986); Glover et al. (1995)), which is also known under different names as IPI (Interferometric Particle Imaging) in Damaschke et al. (2002a) or PPIA (Planar Particle Image Analysis) in Hess (1998). It is based on the interference pattern observed when reflection and refraction spots on the droplet surface (glare points) are seen out-of-focus. The main advantage of this technique is its ability to measure microscopic particles while maintaining a relatively large field of view. However, observing an interference pattern that can be 10 to 100 times larger than the actual bubble, leads to a severe restriction on the allowable amount of bubbles per mm^3 since only a minimal overlap of the images is allowed. This concentration limit was investigated for different optical configurations in Damaschke et al. (2002b). The configurations examined by these authors also demonstrate a second drawback of the technique: its low dynamic range (dmax/dmin ≈10). The concentration limit can be improved if the glare points are observed out-of-focus in only one dimension through the use of a cylindrical lens, as proposed by Akasaka et al. (2002). Possibilities to increase the dynamic range were investigated by several authors. Damaschke et al. (2002a) suggested the use of a second laser sheet under a small inclination angle (15-40°) in their Global Phase Doppler technique (GPD). If the size ranges of the ILIDS- and the GPD-mode are made to overlap, an extension of the dynamic range can be accomplished (≈ 100). Another possibility to overcome both the concentration limit as the limited dynamic range is the use of holographic techniques as suggested by Burke et al. (2002). After identifying different particles in the reconstructed in-focus image, each particle is processed individually through the application of a mask. In this way, an isolated ILIDS pattern can be reconstructed for the smallest particles from the holographic recording, which is then processed to yield the droplet size. This masking procedure distinctly increases the allowable number density. Larger droplets are reconstructed in focus and their glare point pattern gives the diameter of the particle. The largest diameter that can be measured in this way is of the same order of magnitude as the field of view of the camera, leading to a considerable increase in dynamic range. Apart from size measurements, velocity measurements are probably equally important in investigating bubbly flows. Typically, such measurements with ILIDS would involve cross-correlating two pulsed out-of-focus images (Maeda et al. (2002). Another approach was presented by Dantec Dynamics (2003) and Damaschke et al. (2002a). They observed the glare points in-focus with a second camera to yield more accurate (PTV-like) velocity information, despite a more cumbersome set-up and associated calibration procedure. Although most of the development on ILIDS has been performed on droplets, Niwa et al. (2000) showed how it could be applied to bubbly flows if an observation angle of 45° is used (S. Dehaeck et. al. 2005).

A novel measuring technique for bubbly flows, named Glare Point Velocimetry and Sizing (GPVS), was developed to measure both bubble size and velocity with high accuracy in a 2D plane. This is accomplished by observing glare points in focus under an observation angle of 96°. When a second laser sheet is added, even higher accuracies are obtained, and the relative refractive index of the bubble can be measured. It also allows non-spherical bubbles to be rejected and arbitrary angles to be used (e.g., 90°). The accuracy of the size and refractive index measurements was found to be within 1,3% (S. Dehaeck et. al. 2005).

Computation of two-phase flows and, in particular, bubbly flows is a very active research topic in computational fluid dynamics (CFD), see, for instance (F.S. de Sousa et. al. 2004, Esmaeeli and Tryggvason 1998, M. Sussman and E. Puckett 2000, G. Tryggvason et. al. 2001 and 2006, S.P. van et. al. 2005 and 2008, J. Hua and J. Lou 2007, E. Marchandise et. al. 2007, R. Singh and W. Shyy 2007 and M. Sussman et. al. 2007). Understanding the dynamics and interaction of bubbles and droplets in a large variety of industrial processes is crucial for an economically and ecologically optimized design. Two-phase flows are complicated to simulate because the geometry of the problem typically varies with time and the fluids involved can have very different material properties. A simple example is that of air bubbles in water, where the densities vary by a factor of about 800. Mathematically, bubbly flows are modeled using the Navier–Stokes equations coupled with an interface advection equation, which can be approximated numerically using operator-splitting techniques. In these schemes, equations for the velocity and pressure are solved sequentially at each time step, and the fluid density is explicitly advected. In many popular operator-splitting methods, the pressure correction is formulated implicitly, requiring the solution of a linear system at each time step. This system takes the form of a Poisson equation with discontinuous coefficients. Solving these systems typically consumes the bulk of the computing time, even though the operator is elliptic.

The numerical simulation of two-phase fluid flow, where bubbles or droplets of one phase move against a background of the other phase was considered by (S.P. MacLachlan et. al. 2008). Such flows are governed by the Navier-Stokes equations, the solution of which may be approximated using a pressure-correction approach. Within such an approach, the computational cost is often dominated by the solution of a linear system corresponding to a discrete Poisson equation with discontinuous coefficients. The efficient solution of these linear systems using robust multilevel solvers was explored, such as deflated variants of the preconditioned conjugate gradient method, or robust multigrid techniques. These families of methods were considered in more detail and compared to their performance in the simulation of bubbly flows. Some of these methods turn out to be very effective and reduce the amount of work to solve the pressure-correction system substantially, resulting in efficient calculations for two-phase flows on highly resolved grids (S.P. MacLachlan et. al. 2008).

The mean gas fraction distribution in the two-phase flow of a gas-liquid bubble plume set to develop adjacent either to a wall or to another bubble plume was described. When this happens, the plume exhibits a type of Coanda effect, bending either towards the wall or the other plume. The local mean gas fraction measurements are carried out using the electro-resistivity probe technique in an air-water system. The deflection angle of the plumes is shown to present dependence on the modified Weber and Froude numbers of the bubbles. A Gaussian distribution for the mean gas fraction profile, observed to exist for axisymmetric single plumes, is shown not to occur in flow geometries where the Coanda effect is allowed to set in. The transition zone between the downstream flow where two Gaussian plumes are observed and the far upstream flow where the plumes are seen to merge onto a single plume is characterized. Photographs of the flow are shown to illustrate the phenomenon. Results are present for two- and three-dimensional mean gas fraction distributions. Furthermore, a simple theory based on integral methods is advanced for the prediction of the plume deflection angle; the theory considers a variable entrainment coefficient (Atila et. al. 2002). Buoyant plumes in multi-phase flows are a common occurrence in the chemical and metallurgical industries. Indeed, bubble plumes provide an effective and relatively simple way of achieving large degrees of agitation in the flow of fluids which are otherwise hostile to intrusive elements. For example, in the steelmaking industry, gas stirred melt ladles are commonplace. The upward movement of inert gas into a bath provokes a large agitation in the molten metal, resulting in the chemical and thermal homogenization of the mixture, as well as in an acceleration of the absorption of harmful non-metallic inclusions into an overlaying slag. The liquid metal homogenization can indistinctly be performed by a single gas plume, by a combination of geometrically arranged plumes, or by a curtain of bubbles. The degree of agitation – and consequently the flow properties provided by rising bubbles of inert gas in the liquid metal medium must hence be determined to achieve minimum mixing times and maximum recoveries of alloy additions at optimum flow rates. To measure the main characteristics of the plumes, an electro-resistivity probe system was used. This system was chosen for being simple while still being capable of conveying much useful information on the phenomenon. Here, it suffices to say that by an analysis of the experimental data through the mean gas fraction profiles, the deflection of the plume has been evaluated as a function of several parameters of interest including the gas flow rate and the distance between the point sources (Atila et. al. 2002).

The single bubble plume flow has been extensively studied both theoretically (Ditmars and Cederwall, 1974; Milgram, 1983; Brevik and Killie 1996) and experimentally (Milgram, 1983; Castillejos and Brimacombe, 1987; Barbosa and Bradbury, 1996) by many authors in the past three decades. For the integral approaches, the flow has been divided into three distinct regions where some dominant effects prevail (Milgram, 1983). The buoyancy-dominated region is normally referred to as the ‘‘zone of established flow’’. This was the region of main interest by (Atila et. al. 2002).

Bubble columns are intensively utilized as multiphase contactors and reactors in chemical, petrochemical, biochemical and metallurgical industrials. For the operation of two-phase flows in bubble columns, insight into primary parameters such as bubble size, shape, and velocity as well as a void fraction is essential. The measurements of bubble properties in heterogeneous bubbly flows in a square bubble column were performed. A four-point optical fiber probe was used for this purpose. The accuracy and intrusive effect of the optical probe were investigated first. The results show that the optical probe underestimates bubble properties, such as bubble velocity, local void fraction. The presence of the probe in the bubble column influences the local flow conditions. Particularly, when the probe is placed close to the liquid surface, this influence is more pronounced. Furthermore, two methods determining the interfacial area were compared. The results from both methods agree quite well at low superficial gas velocity, whereas large discrepancies are found when superficial gas velocity increases. Finally, the effect of column height on bubble properties was studied. No significant difference was found for the three investigated columns (W. Bai et. al. 2010). Optical fiber probes (Cartellier 1990, Mudde and Saito 2001) have the advantage of low cost, simplicity of setup, and easy interpretation of the results. With an optical fiber probe, the measurement of local void fraction becomes possible. Furthermore, using a four-point optical probe, properties of bubbles can also be studied, such as bubble velocity and bubble size. The effect of column height on the bubble properties, such as bubble velocity, local void fraction, interfacial area, and equivalent diameter, was discussed. (W. Bai et. al. 2010).

Bubble columns are widely used across a range of industries. The work described by (Bennett et. al. 1999), although applied to minerals separation flotation columns, is equally applicable in the wider context of bubble columns. In flotation columns, several flow regimes may be obtained and are difficult to visualize and detect. An Electrical Capacitance Tomography (ECT) sensor has been applied to investigate the potential of ECT for flotation column visualization and control. Different methods of flow regime analysis are reported including a repeatable and robust analytical procedure that has been designed to quantify heterogeneity. The use of ECT is examined for distinguishing homogeneous bubble flow and churn flow. Then a quantification of these flow regimes is compared to simple secondary parameters (derived from multiple frame measurements) obtained from images and capacitances. A wide variety of conditions were created to test the viability of the method using different spargers, frother concentrations, and height between sparger and sensor (Bennett et. al. 1999). ECT can be used to obtain information on flow regime, bubble size, gas concentration radial profile and flow heterogeneity in liquid/gas flows in bubble columns and flotation processes where conductivity is low (Bennett et. al. 1999). It was realized that aside from the actual flow regime many inter-related aspects of flow contributed to the sensor measurement including bubble size and size distribution, bubble swarming, and radial gas concentration (radial profile). Due to its high sensitivity and low noise, it was also believed that the sensor showed promise in highlighting furthermore detailed aspects of flow and these were investigated (Bennett et. al. 1999).

Water quality in reservoirs is affected by several factors, including thermally induced stratification coupled with eutrophication. Specifically, “a density and temperature structure with a well-mixed top surface layer which is separated from a deep bottom layer by an intermediate layer of strong temperature gradients” is created by Lemckert and Imberger 1993. This intermediate layer inhibits vertical heat and mass transport between the upper and bottom layers. As a result, water quality may deteriorate significantly due to algal blooms in the upper layer and anoxic conditions in the bottom layer when reservoirs are eutrophic (Schladow 1993). Since the early 1950s, bubble plumes produced by air diffuser systems have been widely used for destratification and/or to add oxygen to the bottom layer without causing destratification to improve water quality. The main advantages of this approach are economic efficiency and technical soundness (Sahoo and Luketina 2005; Yum et al. 2005). Air diffuser systems are employed in many source water reservoirs in Korea, but field engineers are demanding more detailed design and operational guidelines so that they can better address various field conditions for consistent performance (Sung et. al. 2010).

Bubble plumes in liquid media have been the subject of numerous studies, as they are widely used in industry for various purposes. Many studies have focused on the structure of bubble plumes and their interactions with the surrounding water environment (McDougall 1978; Baines and Leitch 1992; Leich and Baines 1989; Asaeda and Imberger 1989, 1993; Chen and Cardoso 2000; Sahoo and Luketina 2003; Socolofsky and Adams 2003, 2005; Bombardelli et al. 2007). Researchers have developed various plume models with different variables to address different questions and obtain related data (Sung et. al. 2010). Effects of bubble size, bubble diffusing area, and other parameters in air diffusers on destratification are studied using laboratory- and pilot-scale tanks with two layers. A dimensionless group involving such variables as bubble size, bubble diffusing area, and tank area are used to quantify these effects. Based on the results of experiments, a model is developed to predict destratification efficiency. Bubble diameter and overall tank area are found inversely related to destratification efficiency while bubble diffusing area is directly related to destratification efficiency (Sung et. al. 2010).

For studies on the characteristics of bubble flow in a rectangular channel (20×100mm), a new electrode-mesh tomograph has been applied. The measuring principle is based on local conductivity measurement. The applied sensor scans the local void fraction distribution in 2 parallel planes, separated 1.5 mm in the flow direction, with a resolution of 3.0×2.2 mm and an overall sampling rate of 1200 Hz (all 256 points). Algorithms for the calculation of the local instantaneous void fraction distribution and the true gas velocity are presented. Based on these values the approximate shape of bubbles was reconstructed and the gas volume flow through the sensor was evaluated. The superficial gas velocity, as well as the local distribution of the gas volume flux, was calculated. An extensive sensitivity study illustrating applicability and accuracy is presented, based on experimental observations as well as theoretical considerations. The evaluated results are compared with high-speed video observations of the flow field as well as data comparing the reconstructed volume flow with measurements by a laminar flow meter. Good agreement can be stated in general. (Steffen and Masanori 2002).

A limitation on the metal throughput of a gas fluxing unit is posed by splashing and spraying of metal droplets as the gas throughput is increased to keep pace. In an investigation at Berkeley funded by DOE (OIT DE-FC07-01ID14192) and Alcoa, droplets ejected because of bubble rupture at the free surface of molten metal are examined via high-speed digital photography and image tracking software. Experiments are carried out in a custom-built, glass-walled vessel designed for observation of splashing and spraying at the surface of a low melting temperature alloy. A controlled bubble release system permits variation in bubble size, the release of single or multiple bubbles, or a continuous stream of bubbles. The effects of melt depth in the vessel, oxide formation at the melt surface and the presence of a second liquid on droplet behavior are also examined. Droplet numbers, velocities, trajectories, and size distributions are determined for the aforementioned conditions with image analysis software (Autumn and James 2005).

Bubble plumes of various void fractions and sizes were produced by varying the flow velocity of a water jet impinging normally on a water surface. The bubbles entrained at the surface were carried downwards by the fluid flow to depths ranging from 33 to 65 cm and formed roughly cylindrical plumes with diameters ranging from 12 to 27 cm. The acoustic emissions from the plumes were recorded onto digital audio tape using a hydrophone placed outside the cloud at distances ranging from 50 cm to 16.0 m. Closeup video images of the individual bubbles within the plume were also taken to gain knowledge of the bubble size distributions. The experiments were performed in both fresh-water and salt-water environments. The fresh-water clouds emitted sounds with a modal structure that was significantly different from that produced by the salt-water clouds. Furthermore, the smaller bubbles present in the salt-water clouds have a fundamental effect on the amplification of turbulence noise, generating sound at significant levels for frequencies up to several hundred Hertz (Gregory and Michael 2000).

Detailed measurements of bubble composition, dissolved gas concentrations, and plume dynamics were conducted during a 9-month period at a very intense, shallow (22-m water depth) marine hydrocarbon seeps in the Santa Barbara Channel, California. Methane, carbon dioxide, and heavier hydrocarbons were lost from rising seep bubbles, while nitrogen and oxygen were gained. Within the rising seawater bubble plume, dissolved methane concentrations were more than 4 orders of magnitude greater than atmospheric equilibrium concentrations. Strong upwelling flows were observed, and bubble-rise times were ~40 s, demonstrating the rapid exchange of gases within the bubble plume (Jordan et. al. 2003).

A theoretical model for bubble formation and weeping has been developed. Potential flow theory is used to describe bubble formation at the orifice. The influence of detached, rising bubbles on liquid pressure at the orifice is predicted by Oseen's modification to potential flow. Model predictions of bubble volumes, weeping flow rates, and weep points agree well with experimental results (Wenxing and Tan 2000). Weeping may occur during the period between successive bubbles and is influenced by the liquid wake pressure due to the detached bubble and the gas chamber pressure. Oseen's modification to potential flow theory is used to provide a more realistic prediction of wake pressure behind a steadily rising bubble. Results for bubble volumes, weeping rates, and weep points are compared with experimental results both from published literature and from (Wenxing and Tan 2000). A new theoretical model to predict bubble frequencies and weeping rates at a submerged orifice with liquid crossflow has been developed. The model predicts a significant influence of liquid crossflow velocity on bubble formation frequency, and especially on liquid weeping. Simulated values of weeping rates for different orifice diameters, gas flow rates, and liquid crossflow velocities show good agreement with experimental data (Wenxing and Tan 2000).

Theoretical models for bubble formation with liquid crossflow have been also developed by Tsuge, Hibino, and Nojima (1981), Kawase and Ulbrecht (1981), Morgenstern and Mersmann (1982), Wace et. al. (1987), Marshall, Chudacek, and Bagster (1993) and Kim, Kamotani, and Ostrach (1994). They are generally based either upon a force balance on the bubble or a potential flow analysis of the surrounding liquid. All these models assume spherical bubble shapes and rely on arbitrary criteria for bubble detachment and several incorporate experimental correction factors or fitted parameters to improve the fit with their experimental data (R. B. H. Tan et. al. 2000). A non-spherical model for bubble formation at an orifice with liquid crossflow has been developed. The interface element approach is applied to describe the dynamics of bubble formation. The effect of liquid crossflow on the bubble formation process is modeled by a combination of tilting of the bubble axis and liquid pressure analysis of each element on the bubble interface. Model predictions compare well with the experimental results available in the literature for different conditions of gas flow rate, orifice diameter, and liquid crossflow velocity. Simulated bubble shapes are highly non-spherical, especially at high liquid velocities, and bear a striking resemblance with the experimental high-speed video sequences (R. B. H. Tan et. al. 2000).

Bubble formation at two, three, four, and six symmetrical orifices has been investigated by high-speed photography and analysis of chamber pressure fluctuations. Regimes of synchronous, alternative, and unsteady bubbling were identified, and the effects of orifice spacing and liquid depth on bubbling synchronicity and frequency were studied. Theoretical predictions of bubble frequency and average radius were found to be in good agreement with experimental data when the bubble regime was highly synchronous (Shuyi and Reginald 2003). The dispersion of gas bubbles in liquids plays an important role in bringing about efficient mass and heat transfer between the two phases. Important devices include bubble columns and sieve plate columns, in which bubbles are generated by introducing a stream of gas through orifices into the liquid phase. Investigations on bubble formation mainly concern bubble frequency, size, shape, the influence of wake pressure of preceding bubbles, and liquid weeping accompanying bubble formation and detachment (Shuyi and Reginald 2003). As a fundamental phenomenon, bubble formation at a single orifice has been widely studied, although it is not in wide use practically. Numerous theoretical models have been developed to predict bubble size, shape, frequency, and rising velocity in single orifice bubbling (Davidson and SchBuler, 1960; Tan and Harris, 1986; Terasaka and Tsuge, 1990; LoubiCere and HDebrard, 2002). On the other hand, some experimental studies of bubble formation from industrial perforated plates have been undertaken (Zuiderweg, 1982; Wijn, 1998). Few studies have addressed the case of multiple orifices as an extension of single orifice bubble formation (Titomanlio et. al. 1976) found that the bubble size generated at a single orifice approximates that of simultaneous bubbles at two orifices with double the gas chamber volume and double the gas 6ow rate (Miyahara et. al. 1983) investigated the size of bubbles generated from a perforated plate experimentally. For single orifice bubbling, gas chamber volume was observed to play a very important role in determining bubble volumes and frequencies. However, for the bubble formation at multiple orifices, they found that the effect of this parameter weakens as the number of orifices is increased and disappears when there were more than 15 orifices. Ruzicka et. al. 1999, 2000) investigated bubble formation at two orifices and identified two types of bubbling modes using analysis of pressure fluctuations in the gas chamber. They extended their work to more orifices (three to thirteen) and found more types of bubbling modes based on various plate configurations (McCann 1969) developed a bubble interaction model to predict bubble frequencies placed in a line of five orifices with 2:3 cm spacing. The results showed that bubble frequency depends on the total chamber volume, but the model did not appear to be applicable to other orifice configurations (Shuyi and Reginald 2003).

Two-phase bubbly flows are widely applied in engineering and environmental processes. The interaction of the dispersed phase with the continuous phase has a great effect on transfer processes between the phases. The interstitial relative velocities between the phases and the interfacial area and the shape of the dispersed phase are the key-dependent parameters in the drag, heat, and mass transfer between the phases. Although the physical understanding of bubbles rise in a liquid is of significant practical importance in many areas of engineering, neither the interactions between bubbles in clusters nor the bubble-induced pseudo-turbulence (i.e., the generation of velocity fluctuations by bubbles and their wakes in a laminar flow) are fully understood. The modeling of bubbly flows with the Computational Fluid Dynamics (CFD) codes requires detailed information about the full field velocity close to the bubble and its wake. Such information is not widely available. Experimental data exist mainly from point measurement techniques, which offer the advantage of having high time resolution, but their spatial resolution is poor, and information about the vorticity field is lacking. Many investigations have been carried out over the past three decades using hot-film and hot-wire anemometry. However, the use of hot-film anemometry in two-phase flows, raise many questions that remain unanswered. In particular, the interactions between the sensors as X-probe, liquid, and bubbles are not well known and can lead to errors in the determination of correct turbulence parameters. The deformation of the bubble surface is caused by sensor penetration through the bubble. Recently, an interesting number of direct numerical simulation studies of bubbly flows have cast considerable light on the evolution of bubbly flow (Esamaeeli andTryggvason, 1998, 1999; Burner and

Tryggvason, 2002, Yassin 2003). This communication is to present the results of an optical technique known as particle image velocimetry (PIV) utilized in multiphase flow investigations. PIV provides instantaneous velocity fields in a 2-D plane, and it can be extended to 3-D situations. Recently, increasing numbers of successful investigations are reported. In this brief, PIV is applied to study bubbly flows and the component phases are separated during analysis. With the improvement of digital imaging technology in recent years, PIV measurement techniques are now capable of capturing high-resolution digital images of gas/liquid two-phase flows, in which the continuous liquid phase and the dispersed gas phase are unsteady and multidimensional (Yassin 2003).

4. The Application of Bubble Plume

In recent years, multifluid systems including gas injection techniques (which is the most popular model in the field of bubble dynamics) have been widely used and play an important role in many natural and industrial processes and many engineering fields such as materials; combustion; petroleum refining; chemical, mechanical, environmental engineering; cleaning, promoting heat and mass transfer, and high-pressure evaporators. They also have been used to improve chemical reactions, waste treatment, gas mixing, resolution, and other engineering processes [A. Bankovic, et. al. (1984), S. Hara, et. al. (1984), and N. A. Hussain and B. S. Narang, (1984)). Furthermore, because of their simple construction and ease of operation, bubble columns are widely used in the petrochemical, pharmaceutical, and metallurgical industries as multiphase reactors and contactors. Moreover, the gas-liquid two-phase flow has seen wide use in many areas, such as biological fermentation, polymer polymerization, industrial wastewater treatment, and environmental protection [A. M. Leitch and W. D. Baines, (1989), and Y. Y. Sheng and G. A. Irons, (1992)]. Although the gas injection model has been used with varying degrees of success to describe bubble plumes, more information on this subject is needed because generating surface flow can still be made more efficient. The rising of a buoyancy-driven bubble in a liquid is a typical process in multifluid systems, so a sound understanding of the fundamentals of rising bubbles is crucial in a variety of practical applications, ranging from the rise of steam in boiler tubes to gas bubbles in oil wells. Because of the strong nonlinearity accompanied by large bubble deformations, it is difficult to study the mechanisms behind bubble behavior solely through theoretical methods [H. Wang, et. al. (2010), A. R. Talaia, (2007), G. P. Celata, et. al., (2001) and M. A. R. Talaia (2000)]. An understanding of bubble-fluid interactions is important in a broad range of natural, engineering, and medical settings. Air-sea gas transfer, bubble column reactors, oil and/or natural gas transport, boiling heat transfer, ship hydrodynamics, ink-jet printing, and medical ultrasound imaging are just a few examples where the dynamics of bubbles play a role [J. W. A. De Swart and R. Krishna, (1995), K. A. Shollenberger, et. el., (1997)., B. Eisenberg, et. el., (1994)].

Beyond that, air bubble systems have been used extensively and for a variety of purposes such as pneumatic breakwaters, prevention of ice formation, as barriers against saltwater intrusion in rivers and locks, for stopping the spreading of oil spills on the water surface, for the reduction of underwater explosion waves and agitation and mixing operations in process industries. However, the technique may also be used for destratification and water quality control Management of lakes and, reservoirs in which case the characteristics of the air-bubble plume are of more interest than the induced horizontal flow in the surface layer (Klas and John 1970).

Bubbly flows encompass a vast domain of natural and artificial flow conditions. They are encountered, for instance, in the surroundings of surface ships' hulls (Carrica et al., 1998) and nuclear-engineering devices, such as outputs from vessel cores and pipes passing through cooling systems. Bubble plumes constitute a special case of bubbly flows in which the flow is driven by buoyancy (strictly speaking). Bubble plumes have received considerable attention in the last four decades due to their large range of applications. For example, they have been proposed as a means of containing surface-floating substances, such as oil from large oil spills in rivers and estuaries; they have been employed to augment convective heat and mass transfer rates in various chemical applications; they have been used as pneumatic breakwaters; they have been employed for preventing icing in navigational waterways. One area of application that has received a great deal of recent attention is the use of bubble plumes as a destratification device, inducing mixing while introducing dissolved oxygen for improving water quality in lakes and reservoirs (Schladow, 1992).

The Mixing Processes induced by a Bubble Plume in Density Stratification and Destratification

Understanding the flow and mixing processes induced by a bubble plume in density stratification is of primary concern in the design of air bubble diffusers for lake/reservoir destratification and aeration (e.g., Asaeda and Imberger 1993; Lemckert and Imberger 1993; McGinnis et al. 2004; Schladow 1993), chemical reactors (e.g., Leitch and Baines 1983), and planning of deep-sea CO2 sequestration (e.g., Crounse et al. 2007; Socolofsky et al. 2008). Air bubble plumes in density-stratified environments have been the subject of numerous studies using laboratory-scale experiments (Asaeda and Imberger 1993; Baines and Leitch 1992; Leitch and Baines 1989; McDougall 1978; Socolofsky and Adams 2003, 2005), field-scale measurements (Lemckert and Imberger 1993; McGinnis et al. 2004), and integral numerical modeling (Asaeda and Imberger 1993; McDougall 1978; Schladow 1993; Socolofsky et al. 2008).

The study on the destratification of reservoirs with bubble columns attempts to specify the relevant parameters for models of the processes which contribute to both artificial and natural destratification. The long residence time of the water in such reservoirs permits algal bloom to occur, and this can be a major problem in maintaining the water quality. In practically all cases thermal stratification leads to an oxygen deficit near the bottom which can be prevented by extra mixing. Artificial mixing is usually achieved by air injection from the reservoir bottom and the resulting flows are presented. The upward flow of water induced by a bubble column and its coupling with the near field are discussed. A general model for such unconfined plumes is presented which predicts the vertical liquid volume flow (50 to 150 times the gas rate) and momentum flux. The isothermal near field determined by the radial outflow from a bubble column is discussed. The theory assuming constant eddy viscosity is shown to agree with experiments simulating an infinitely deep reservoir. A discussion is presented on the stratified near field. The original two-layered system is destratified by bubble columns in such a way that a third layer (the interlayer) is pumped in between the upper and lower layers at the level of the original thermocline. A model is presented in which a cold outflowing stream from the bubble column mixes with warm epilimnion water (upper layer) and splits into an interlayer and a return flow towards the column. The far-field with insolation is also discussed. A one-dimensional model is presented to calculate vertical temperature profiles in the far-field of a bubble column [Goossens, L. 1997].

Two-phase flows have received much attention in the past few decades due to their importance in the power and process industries, to name a few. Consequently, there is a continuous need to enhance knowledge of the parameters affecting two-phase flows in piping systems. Although a significant body of knowledge on two-phase flow was generated, available experimental data tend to be limited to two-phase flow in small diameter pipes. In the analysis of two-phase flow thermal-hydraulics, various formulations such as the homogeneous flow model drift flux model, and two-fluid model has been proposed. The two-fluid model considers each phase separately, in terms of two sets of conservation equations that govern the balance of mass, momentum, and energy of each phase, and accounts for interface exchange through additional interfacial terms in the governing equations. Because of its detailed treatment of phase interactions, the two-fluid model can be considered the most accurate. However, the accuracy of the two-fluid model, and thus its usefulness in applications, depends on accurate modeling of the interfacial transfer terms. The Interfacial Area Concentration (IAC) is the main parameter in the interface exchange formulation and its importance can explicitly be seen in the basic conservation equations of the two-fluid model. Many models and empirical relations have been proposed to formulate the IAC in terms of flow parameters such as gas and liquid superficial velocities, void fraction, and pressure drop. However, available models are based on limited data for flows in small diameter pipes. The validity of these models for use in large-diameter pipes have been determined by (Ihab 1999). Two-phase flow structure of an air-water, bubbly, upward, cocurrent flow in a large diameter pipe, 20 cm, were investigated experimentally by (Ihab 1999). Local flow parameters such as void fraction, bubble velocity, bubble diameter, and interfacial area concentration were measured using a dual fiber-optic probe. A well-calibrated air-water testing loop was used to conduct the experimental work. A computerized data acquisition system was used to analyze the probe output signals and so measuring the different flow parameters. The local time-averaged bubble diameter was measured using a direct averaging method and Uga's statistical method. The interfacial area concentration was measured using two methods; the bubble diameter-based method and the direct method proposed by (Kataoka et al. 1986).

Flow properties of a bubble plume in density-stratified conditions are studied using planar laser-induced fluorescence (PLIF) flow visualization. The entrained ambient fluid is identified by applying an image intensity threshold to the PLIF images of the passive dye tracer injected at the bubble diffuser. The density stratification gradually arrests the entrained ambient fluid, causing detrainment, or peeling, of the continuous phase fluid from the bubble plume core and intrusion of the detrained fluid at a level of neutral buoyancy; bubbles continue to rise above each detrainment zone. The peel and intrusion heights for the first detrainment event above the diffuser are measured from the thresholded PLIF images. The non-dimensional frequency of fluctuations in the detrainment and intrusion heights fz/u_s is measured as 0.35 (where f = frequency; z = height above the diffuser; and u_s = terminal rise velocity of the bubbles in a quiescent fluid), and this value compares well to the plume wandering frequency for similar experiments in unstratified reservoirs (Dong et. al. 2009).

An important aspect of stratified bubble plumes affecting mixing and warranting further study is the detrainment process, whereby entrained ambient fluid is arrested by the stratification and ejected from the bubble plume core, forming a downdraft outer plume and flowing into an intrusion layer at a level of neutral buoyancy. To observe the instantaneous spatial structure of the entrained ambient fluid in a bubble plume, including the peeling process and intrusion formation, (Dong et. al. 2009) applied the planar laser-induced fluorescence (PLIF) method for flow visualization in a laboratory-scale stratified bubble plume. While this data is largely qualitative due to complications for quantitative PLIF caused by the stratifying agents (salt and ethanol) and the presence of bubbles, these data are useful to highlight some of the peeling and intrusion dynamics important for the mixing processes induced by a bubble plume in ambient stratification and suggest a plume-induced mechanism for bubble column wandering in unstratified environments.

In stratified multiphase plumes, the entrained ambient fluid driven by the dispersed phase (here, bubbles) is detrained or peeled, from the bubble core when it decelerates due to its negative buoyancy exceeding the lifting capacity (drag force) of the dispersed phase. The detrained water creates an annular structure of a downdraft outer plume surrounding the bubble core and descends to a neutral buoyancy level, where the lateral intrusion of the fluid takes place (Asaeda and Imberger 1993; Socolofsky and Adams 2003, 2005). (Asaeda and Imberger 1993 and Socolofsky and Adams 2005) classified different types of bubble plume behavior based on the strength of the density stratification and the slip velocity (terminal rise velocity in a quiescent fluid) and the buoyancy flux of the dispersed phase. Each identified plume type demonstrates different forms of the entrainment/detrainment process, ranging from discrete, quasi-steady peeling to random unsteady peeling. (Dong et. al. 2009) focused on the first peeling event above the diffuser, which always exhibits a sudden detrainment and quasi-steady intrusion (Dong et. al. 2009).

Density stratification of lakes and water storage reservoirs is a common occurrence (Imberger and Patterson 1990). When its duration is sufficiently long, oxygen depletion resulting from biochemical and biological demand can occur in the hypolimnetic waters that have become isolated from the water surface. The immediate consequences of this are varied and can include the formation of iron and manganese compounds in solution and suspension, and widespread fish kills (Mortimer 1941, 1942).

Artificial destratification has been practiced countering these effects. Of the methods used, bubble-plume destratification is one of the more widespread. Here, compressed air is forced through a diffuser located near the bottom of the reservoir. The rising columns of bubbles are accompanied by the entrainment of ambient water to form a combined bubble and water plume. (In what follows this combined plume will simply be referred to as the bubble plume.) There is potentially a terminal height to which any buoyant plume will rise, before spreading out at some level of intermediate density below the plume's maximum height of rising (Morton et al. 1956). In the case of a bubble plume, the bubbles would continue to rise to the water surface and not be shed with the entrained water. The bubbles would cause the entrainment of a further plume above the level of the initial one. This process could be repeated several times before the bubbles reach the surface, as evidenced by the laboratory experiments of McDougall (1978), Asaeda and Imberger (1989), and Hassan 2003. The process is illustrated schematically in Fig. 6 (S. Geoffrey 1993).

Thermal stratification during summer may result in lowered dissolved oxygen levels below the thermocline of lakes and reservoirs. To avoid further deterioration of water quality, artificial destratification was practiced by (S. Geoffrey 1993). He presented a totally new design methodology for the design of bubble plume destratification systems. It is based on the interaction that occurs between a buoyant bubble plume and the density stratified water column through which it rises. Two dimensionless parameters, M and C, universally describe the behavior of such plumes. M represents the bubble source strength compared to the total pressure head, and C represents the effect of the stratification compared to the bubble source strength. By selecting appropriate values for these parameters, the individual bubble plumes can be designed to operate within high-efficiency bands. The number of such plumes that are required to destratify the lake can then be calculated by a simple energy balance. The method is validated using a combination of a dynamic reservoir simulation model (DYRESM) and a bubble-plume model. A comparison of the design recommendations with those produced from conventional practice suggests that large cost savings may be realized (S. Geoffrey 1993).

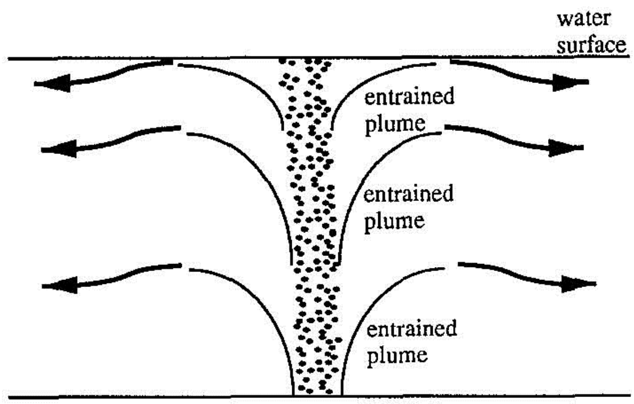

Figure 6. Schematic of Bubble-Plume Discharging into Density Gradient, with Two Internal Detrainment Levels and Surface Detrainment (S. Geoffrey 1993)

Simple plume models have been considered in various contexts. (Morton et al. 1956) used a simple plume model in their paper introducing the entrainment hypothesis. (Milgram 1983) compared his experimental results with the values predicted by a simple plume model, whereas (W¨uest et al. 1992) used both a simple plume model with the entrainment hypothesis to describe the effect of dissolving plumes. The work of (Brevik 1977) is also based on a simple plume formulation, though without making use of the entrainment hypothesis. (McDougall 1978) modeled the system as an inner circular plume containing the gas bubbles and some entrainment water, and an annular plume containing only water. The formalism of McDougall was generalized by (Asaeda and Imberger 1993, and Crounse et al. 2007), simplifying the implementation of density effects of dissolving bubbles. An extensive comparison between mixed and two-fluid models based on the entrainment hypothesis is given by (Bhaumik 2008). The advantages of the integral models are that the governing equations allow insight into the flow dynamics; they are computationally efficient and produce reasonable results in many cases. A drawback is that the integral models lose their validity, as the plume becomes less self-similar (Socolofsky et al, 2001 and 2003), the kinetic energy approach to buoyant plumes (Brevik 1977 and Brevik and Killie 1996) is generalized to allow for the dissolution of gas. The model is compared to experiments carried out by (Milgram 1983) and is found to reproduce experimental data with satisfactory accuracy. The results presented suggest that the model presented yields a good starting point for the description of the dynamics and dissolution of gas in the zone of established flow for an air-bubble plume, given that the turbulent correlation parameter is chosen correctly (Kristian and Iver 2008).

Liquid weeping remains a significant problem for the operation of distillation and absorption processes involving sieve trays. Hydraulically, weeping can affect the liquid hold-up on the tray deck and can influence the tray pressure drop and other wet-tray hydraulic characteristics. In terms of process performance, weeping results in a bypassing of gas-liquid contact, and thereby contributes to decreased tray efficiencies. A fundamental understanding of the parameters affecting weeping and the prediction of weeping rate is important for improving the design and operation of such processes (Wenxing and Tan 2000).

It is well-known that weeping occurs, most readily, at low-vapor flow rates, corresponding to the 'bubbling' regime (Sundar and Tan, 1999). An investigation of liquid weeping must therefore necessarily include a study of the complementary process of bubble formation at the submerged orifice. McCann and Prince (1969) presented a model for bubble formation and weeping at a single orifice, in which the weeping rate is determined principally by the transient pressure difference between the liquid at the orifice and the gas chamber. The authors applied potential flow theory to predict liquid pressure distribution in the wake of an upward accelerating bubble. The 'wake pressure' term played a significant role in the prediction of weeping rates. Subsequently, Kupferberg and Jameson (1970), following their earlier work (Jameson and Kupferberg, 1967), attempted to predict weeping based on a loss of hydraulic pressure at the orifice giving rise to a negative 'residual head'. Miyahara and Takahashi (1984) observed experimentally that bubble formation accompanied by weeping resulted in larger bubbles than in the case with no weeping. They proposed a complex theoretical model to predict bubble volumes for bubble formation accompanied by weeping. Antoniadis, Mantzavinos, and Stamatoudis (1992) studied the effect of chamber volume on bubble formation and weeping. Their measured values of weep points (i.e., the gas flowrate above which no discernible weeping occurs) were significantly lower than corresponding predictions by the model of Kupferberg and Jameson (1970).

The Mitsubishi Air Lubrication System (MALS) was the first air lubrication system in the world to be applied to a newly built ship and resulted in a substantial reduction in the ship's resistance. Therefore, a performance estimation method using computational fluid dynamics (CFD) needs to be established as soon as possible to apply the MALS to general commercial ships. The bubble distribution around ships with the MALS using CFD was predicted, and a method to determine the reduction in flow resistance based on the bubble coverage around the hull was developed. Furthermore, the intrusion of bubbles on the area of propeller disks was predicted, which could deteriorate the performance, and confirmed that the deterioration in propeller disk performance was negligible (Makoto et. al 2011). The development of energy-saving ships has been greatly anticipated by the shipping industry as a countermeasure against the surging prices of raw materials, including oil, arising from the economic growth of developing countries, and environmental issues such as CO2 emission regulations for international shipping operations. The air lubrication method, which reduces the resistance of the hull by using air bubbles, has been studied by many institutes because the method is expected to result in prominent energy-saving effects. (Kodama et al. 2000) performed tests using a flat-plate model ship with a total length of 50 m and confirmed that the total resistance working on the model ship and the local frictional force working on the ship bottom was reduced by bubbles. Verifications on actual ships have also been conducted; (Kodama et al. 2004, 2008) demonstrated an energy-saving effect of 5% in an actual ship test using a cement carrier (Makoto et. al 2011). Research on the use of computational fluid dynamics (CFD) to predict the effect of bubbly flow has also been promoted. (Murakami et al. 2008) simulated the flow around the cement carrier used by (Kodama et al. 2008) for experiments and evaluated the effects of changes in the ship posture and location of the bubble outlets on the resistance reduction ratio for the ship and the void fraction on the propeller disk area. The Nagasaki Shipyard and Machinery Works of Mitsubishi Heavy Industries, Ltd., (MHI) completed YAMATAI, a module carrier belonging to the NYK-Hinode. Line, Ltd., in April 2010. An air lubrication system was installed on a ship for the first time on this occasion. The ship achieved an energy-saving effect of more than 10% at sea trials prior to delivery (Makoto et. al 2011). While developing the Mitsubishi Air Lubrication System (MALS) installed on YAMATAI, air bubble predictions utilizing CFD technology were performed in addition to tests on the model and actual ship. The tests on a model ship confirmed the flow of bubbles along the bottom of the ship and were used to evaluate the effect of the void fraction on the propeller disk area on the propeller characteristics and fluctuating pressure (Takano et al. 2010). CFD with the same model-scale ship was used to predict the distribution of the air bubble void fraction on the hull surface, which is required to predict the reduction of the hull resistance, as well as the distribution of the void fraction on the propeller disk area, which affects the propeller performance (Makoto et. al 2011). The air bubble distribution around the hull surface is believed to be an important parameter for reducing the resistance working on the hull, and must, therefore, be predicted accurately. The predicted void fraction distribution due to air bubbles on the hull surface is reported. The void fraction is the ratio of the air volume to the air-fluid mixture (Makoto et. al 2011).

Natural convection heat transfer:

Natural convection heat transfer along a heated plate is widely seen in a variety of heat exchangers such as solar water heaters. The heat transfer enhancement for the natural convections provides high efficiency to the heat exchangers. So far there has been gas-bubble injection as one of the techniques of enhancing the heat transfer for the natural convection of liquid along with a heated vertical plate. In (Kenji et. al. 2007) study, the micro-bubble injection technique was used to enhance the heat transfer for the water natural convection along with a heated vertical plate. In most cases, the residential time of the micro-bubbles in a boundary layer is relatively long because the micro-bubble diameter is much smaller than the boundary layer thickness. Therefore, the micro-bubbles interact with liquid in the vicinity of a heated plate for a long time, and as a result, it is possible to enhance the heat and momentum transports of liquid remarkably at a relatively low bubble flow rate. However, flow and heat transfer characteristics for the natural convections of water with micro-bubbles have been fully explained by (Kenji et. al. 2007). (Kenji et. al. 2007) experimentally investigated the effects of the micro-bubble injection on the water natural convection along with a vertical plate with uniform heat flux. The thermocouples and the PTV (Particle Tracking Velocimetry) technique are, respectively, applied to temperature and velocity measurements (Note that the temperature measurement is performed for both laminar and turbulent regimes while the velocity measurement is performed for only the laminar regime). The relationship between the wall heat flux and the heat transfer coefficient ratio hx/hx_0 (at x=70 and 170 mm) in the laminar regime was shown. Where, hx_0 is the heat transfer coefficient without the micro-bubble injection, and the error bar is the standard deviation. The results are as follows:

(1) For all the cases, the heat transfer coefficient ratios are much higher than 1.0 because of the micro-bubble injection. This result enables us to expect that the micro-bubble injection is a promising technique for effectively enhancing the heat transfer.

(2) At both measurement positions, the heat transfer coefficient ratios increase with the bubble flow rate. Also, the differences in the heat transfer coefficient ratio for different bubble flow rates are roughly unchanged in most of the wall heat fluxes. In general, the number of bubbles attached to the wall increases with the bubble flow rate. These bubbles lead to a decrease in the mean thermal conductivity near the heated plate because the thermal conductivity of hydrogen bubbles is much lower than that of water. Therefore, it is possible that the increasing rate of the heat transfer coefficient ratio for the bubble flow rate decreases at high bubble flow rates.

(3) At both measurement positions, the heat transfer coefficient ratios decrease as the wall heat flux increases. This means that the micro-bubble injection technique is effective under a relatively low wall heat flux condition (Kenji et. al. 2007).

Nucleate boiling in a microchannel,

Nucleate boiling in a microchannel, being one of the most efficient modes of heat transfer, has recently received increasing attention as an effective cooling method for next-generation high-power-density microprocessors. Despite many experimental studies (Peng and Wang 1993, Balasubramanian and Kandlikar 2005), the bubble dynamics coupled with boiling heat transfer in a microchannel are still not well understood due to the technological difficulties in obtaining detailed measurements of microscale two-phase flows. Hence, a complete numerical simulation is performed by (Woorim and Gihun 2007) to further clarify the physics of nucleate boiling in a microchannel. The numerical formulation is based on the level set approach modified by (Son et al. 1999). In carrying out numerical simulations of nucleate boiling in a microchannel, the properties of saturated water at 1 atm are used (Woorim and Gihun 2007). The effect of channel height, H, on bubble growth was shown. For H = 3 *mm*, as the buoyancy force increased with bubble growth becomes dominant over the surface tension force, the bubble departs from the bottom wall and rises out of the thermal boundary layer. However, when the channel size is reduced to 0.4 *mm*, the bubble grows until it occupies the entire cross-section of the channel. Thereafter, the bubble expands along the channel and develops into a slug. The slug formation results in a significant increase in the bubble growth rate as well as the heat transfer rate (Woorim and Gihun 2007). The effect of contact angle φ on bubble growth was shown. When the contact angle is increased to 50°, a large increase in bubble growth rate is not observed, in contrast with the smaller contact angle cases. This behavior is explained by the fact that the bubble can more easily expand into the channel corner with a larger contact angle. The liquid layer between the bubble and the channel corner does not exist for $\varphi > 45°$ under (Woorim and Gihun 2007) computational conditions. The non-existence of the liquid layer results in a reduction of the wall heat flux. Also, the receding contact angle is found to have the dominant effect on the bubble growth over the advancing contact angle (Woorim and Gihun 2007).

Bubble column reactors

Two-phase flows appear in nature and everyday life. Yet, gas-liquid bubbly flows also play a tremendous role in many engineering applications for example, in chemical processing, oil and gas industry, biochemical operations, and loop reactors or metal foaming, etc. Especially for the prediction of gas-liquid systems with high gas hold-ups, accurate modeling of closure is important. The first results of the validation of a free surface lattice Boltzmann model and a volume of the fluid method were presented by (Vivek et.al. 2010). In the first stage, the rise velocity of single bubbles is examined. Validation occurs by comparing to data of experiments that were performed. While the overall agreement of the methods to the experimental data was reasonably well, the direct comparison of the methods show deviances (Vivek et.al. 2010). Some of the important gas-liquid reactors are bubble columns, stirred tanks, and loop reactors. The development of computational flow models, which can be used as a tool for the design and scale-up of these reactors is of great importance. Over the last decade, the hydrodynamics of gas-liquid flows has been investigated by many researchers using models from computational fluid dynamics (CFD) based on the continuum and the discrete particle approaches. Though, the above-mentioned models can predict the time-averaged and dynamic characteristics of gas-liquid quantitatively well for simple systems with low gas hold-ups (Vivek et.al. 2010).

Gas-liquid bubble columns are employed throughout the chemical, biochemical, and petrochemical industries. Typical applications usually involve gas-liquid mass transfer and (exothermal) chemical reactions. The gas-liquid two-phase flow prevailing in these bubble columns has a profound impact on the performance of the bubble column as a chemical reactor. Yet, many important fluid dynamical aspects of this two-phase flow are still poorly understood. This explains to some extent the considerable effort made by various researchers to develop sophisticated CFD models for gas-liquid bubble columns (Lapin and LuK bbert, 1994, Devanathan et. al. 1990 and 1995, Delnoij et. al. 1997a, b, c, Jakobsen et. al. 1997). From these numerical studies, mainly devoted to the behavior of a bubble column operated in the homogeneous regime, the gas-liquid flow is known to be highly time-dependent and dominated by a rich variety of coherent structures (Delnoij et. al. 2000).

Contrary to numerous studies reported on experimental analysis of a plunging jet system, there have been very few numerical studies. It is only recently that developments in Computational Multiphase Flow have started to achieve a level that such complex turbulent multiphase flow problems can be investigated. Readers are referred to studies investigating CFD simulation of air-water flow in bubble columns (Akhtar et al., 2006, Becker et al., 1994, Becker et al., 1999, Rampure et al., 2007, Ranade and Tayalia, 2001, Sokolichin and Eigenberger, 1994 and Ali et al., 2008). Sanyal et al. (1999) presented a comprehensive study on simulation of bubble column reactors using CFD software Fluent. Bravo et al. (2007) discussed the potential of commercially available CFD codes for the simulation of bubble plumes. Chen et al. 2003 and W. B. Chen and Reginald B. H. Tan 2003) discussed the application of population balance modeling in the three-dimensional simulation of a bubble column.

In chemical bubble-column reactors, bubbly flows are used to mix the flow and increase the efficiency of the reactions. Bubble column reactors are often used because of their simple construction, low operating cost, and excellent heat transfer characteristics at immersed surfaces (Shah et al., 1982). Gas injection into liquid reservoirs has been also widely used to promote mixing, for example, in the most current steelmaking and lake de-stratification processes (Castillejos and Brimacombe, 1987; Sheng and Irons, 1992.

Bubble column reactors are used in many technological applications where intense contact between gas and liquid phases is desired. The overall performance of these contacting and reacting vessels depends strongly on the hydrodynamics of the bubbly mixture. An important 'elementary process' in generating the bubbly mixture is bubble formation and detachment. Due to its complexity (nonlinear dynamics, strong coupling between gas and liquid phases), the flow field induced by bubble plumes in confined setups such as bubble column reactors has been investigated (Jaromír et. al. 2007). The experimental studies have shown that the number of vertical circulation cells generated in these setups is close to the ratio of column height to diameter or width (Mudde 2005). A general description of the effect of tank size and geometry, ranging from confined setups to larger-scale tanks, has been provided by (Iran et. al. 2008). The dynamics of the bubble generation process were studied by both direct numerical simulations and experiments. The formation of air bubbles was investigated by 2D axisymmetric CFD simulations. The volume-of-fluid (VOF) model was used, as it is implemented in the commercial flow solver Fluent 6.2. The interest of the study was in the detailed dynamics of bubble formation, namely in the investigation of the synchronous and asynchronous modes of bubbling from multiple orifices. The bubble formation was considered both form a needle and an orifice on a plate above a gas plenum. The problem was approached with both the CFD and experiment (Jaromír et. al. 2007).

Bubbly flows can be found in many industrial processes, nuclear power, and chemical plants, stirred reactors, and bioreactors. Concrete examples of bubbly flows in nuclear power plants can be found in the so-called pressure suppression pools of Boiling Water Reactors (BWR) (Arnold et al., 1997). In passive cooling systems of such reactors, decay heat removal may be achieved by venting steam mixed with non-condensable gases into the suppression pool to reduce the pressure in the reactor system. (Walsche and de Cachard 2000) and investigated these venting phenomena. In their particular example, they provided a better important understanding of the condensation and the mixing phenomena controlling the effectiveness of such suppression pools, to avoid incomplete steam condensation and stratified conditions in the pool which led to higher pressures and possibly to an over-design of the containment building.

Mory and Sano 1981, Iguchi et al., 1992, Goossens, 1979 reported that in all these applications, the main interest is to predict the currents induced by the dispersed phase evolving in the liquid and to determine the resulting mixing. Clearly, the performance of all these systems is considerably influenced by the motions of the bubbles and their interactions with the liquid flow; They, therefore, addressed the important understanding of these effects. In nature (lakes and oceans), and as well as in certain technical applications, bubbly flows are characterized by strong three-dimensional (3D) effects and are influenced by the superposition of different characteristic length scales. These effects are even stronger in non-confined bubble flows. As the effects of scale and instability on the 3D flow structure are complex, there is a need to conduct studies in large facilities closer in scale to real industrial applications. One of the most fundamental forms of a bubbly flow system is the bubble column reactor. The operation of this device is quite simple: a vertical column is filled with liquid, which can be either flowing or stationary, and gas is introduced to the system through a distributor at the base of the column. Several variants of the bubble column reactor have been produced, as described in detail by (Deckwer 1985).

Process intensification in the production of fine chemicals can be achieved using various types of microreactors. One of the suitable arrangements for electrochemical reactions is a thin gap microreactor (Rode et al. 2004). A thin-gap microreactor can be used as a single-pass flow-through reactor, with electrodes built in the front and rear walls. In the case of electro-organic oxidation, the desired reaction takes place on the anode, whereas on the cathode hydrogen is generated from the solvent as a counter-reaction. The evolution of gas leads to the formation of a two-phase system inside the microreactor (Jiˇrí et. al. 2007). (Jiˇrí et. al. 2007) experimentally investigate the two-phase gas-liquid flow in a thin-gap channel. The cross-section of the microchannel is 10 × 0.266 mm^2, orientation is vertical. Bubbles are generated on the electrode surface. The amount of generated gas is determined by controlling an electric current applied to the electrodes. Two-phase flow in the thin-gap channel is visualized with a digital camera, and images are processed in Matlab to obtain reported flow characteristics. Flow pattern and void fraction are evaluated for different operating conditions, e.g., liquid flow rates and applied electric current. For the entire range of investigated operating conditions, only bubbly flow was observed. However, with the increasing superficial gas velocity, a distinct difference in bubble size distribution appeared. Void fraction data were fitted with a modified empirical correlation of Chung and Kawaji (2004) and show a strongly nonlinear dependence on volumetric quality. Experimental results suggest that the bubble size distribution has a stronger effect on the microreactor performance than the overall void fraction (Jiˇrí et. al. 2007).

Bubble columns are two-phase gas-liquid systems in which a gas is dispersed through a sparger and bubbles through a liquid in vertical cylindrical columns (Figure 7), with or without internals such as heat exchangers. When fine solids are suspended in the liquid, a slurry phase is formed. Accordingly, it can be called a two-phase or three-phase (slurry) bubble column. With respect to the gas flow, the liquid/slurry phase flow can be co-current, counter-current, or in batch mode. The size of the solid particles typically ranges from 5 to 150 μm and solids loading ranges up to 50% volume (Krishna et al., 1998). The gas phase contains one or more reactants, while the liquid phase usually contains products and/or reactants (or sometimes is inert). The solid particles are typically catalysts. Generally, the operating liquid superficial velocity (in the range of 0 to 2 cm/s) is an order of magnitude smaller than the superficial gas velocity (1 to 50 cm/s).

Three-phase (gas, liquid, and solid) inverse fluidization was first recognized by (Page 1970). Its application, especially to wastewater treatment, resulted in a patent by (Shimodaira et al. 1981). During the past decades, three-phase inverse fluidization has gained attention, as this mode of operation is very promising for wastewater treatment, biochemical, and other industrial applications (Ibrahim et al. 1996 and Farag et al. 1997). In three-phase inverse fluidized bed bioreactors, the biofilm thickness can be controlled within a narrow range, and it has been experimentally shown that this kind of bioreactor is very efficient for biological aerobic wastewater treatment at both laboratory scales and pilot-plant scale (Nikolov and Karamanev 1987 and 1990).

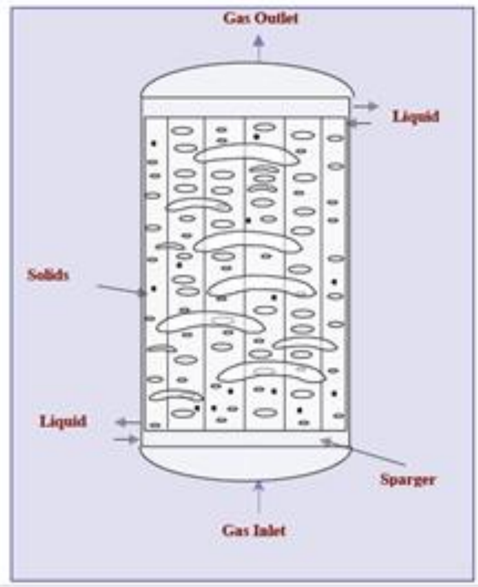

Figure 7. Schematic diagram of the bubble/slurry bubble column

For conventional three-phase inverse fluidization, the solid particles have a lower density than the liquid phase, and the gas phase flows upwards while the liquid phase flows downwards. Operating in this kind of counter-current flow mode, the gas bubbles must have a rising motion. If the liquid velocity becomes too large, the bubbles are not able to rise, and they become entrained by the liquid. This maximum liquid velocity corresponds to the limiting velocity of the rise of the bubbles (Legile et al. 1992). Experimental results (Fan et al. 1982, Chern et al. 1983) showed that three main flow regimes exist, namely, dispersed bubble regime, bubbling regime, and inverse slugging regime in three-phase inverse fluidization. At high gas velocities, bubbles tend to coalesce leading to increased agitation and shear, and less effective liquid-solid phase contact. In three-phase inverse fluidized bed bioreactors, the three phases (gas, liquid, and solid) make direct contact. It is now well established that gas sparging can damage microorganisms. Besides, the damage to cells was found to result from the appearance of bubbles in the bioreactor (Chalmers and Bavarian 1991, Cherry and Hulle 1992, Trinh et al. 1994, Michaels et al. 1995).

Airlift reactors have been known to be efficient contractors for processes involving gas, liquid, and solid phases. Their relatively simple mechanical design, low shear rate, high capacity, good mixing, absence of mechanical agitators, and low cost make them a versatile type of bioreactor (Douek et al. 1995, Snape et al. 1995, Dhaoudi et al. 1996, Gavrilescu and Tudose 1997). Currently, there are mainly two types of airlift reactors, i.e., internal, and external airlift reactors. Nikolov et al. 1982 proposed an inverse fluidization airlift bioreactor which was composed of two concentric tubes with air sparged in the inner tube. Garnier et al. 1990 experimentally investigated the effects of the operating parameters on the hydrodynamic characteristics within such a reactor. External-loop airlift reactors have been used as gas-liquid-solid contacting devices in biotechnology processes, preferentially at a large scale, due mainly to their high and readily controllable liquid circulation velocity (Akita et al. 1994). It has also been shown that external-loop airlift reactors have a high efficiency of homogenization and introduce intense mixing so that they can be applied to the industrial bioprocess which involves highly viscous fluid (Saunder et al. 1986, Siegel and Robinson 1992).

A gas-liquid-solid inverse fluidization airlift bioreactor was proposed by combining the advantages of external-loop airlift reactors and inverse fluidized beds (S. J. HAN et. al. 2000). This airlift bioreactor comprises a gas-liquid riser, a gas separator, a liquid-solid inverse fluidized downcomer, and a bottom connector. The effects of the gas velocity and the particle loading on the gas holdup in the riser and the liquid circulation velocity in the loop were investigated. Liquid-solid inverse fluidization in the downcomer was also studied. The gas holdup in the riser was experimentally found to increase with the increase in the particle loading and the gas velocity. The liquid circulation velocity decreased with the increase in the particle loading whereas it increased with the gas velocity. It was found that the Richardson and Zaki model fitted experimental data of bed expansion of liquid-solid inverse fluidization in the downcomer well. Based on an energy balance, two hydrodynamic models were proposed to predict the liquid circulation velocity in the present bioreactor. It was shown that the present models gave a good fit to experimental data in this bioreactor (S. J. HAN et. al. 2000).

The bubble columns offer numerous advantages: good heat and mass transfer characteristics, no moving parts, reduced wear and tear, higher catalyst durability, ease of operation, and low operating and maintenance costs. One of the main disadvantages of bubble column reactors is significant back-mixing, which can affect product conversion. Excessive back-mixing can be overcome by modifying the design of bubble column reactors. Such modifications include the addition of internals, baffles (Deckwer, 1991), or sieve plates (Maretto and Krishna, 2001). Bubble column reactors have been used in chemical, petrochemical, biochemical, and pharmaceutical industries for various processes (Carra and Morbidelli, 1987; Deckwer, 1991; Fan, 1989). Examples of such processes are the partial oxidation of ethylene to acetaldehyde, wet-air oxidation (Deckwer, 1991), liquid phase methanol synthesis (LPMeOH), Fischer-Tropsch (FT) synthesis (Wender, 1996), hydrogenation of maleic acid (MAC), hydroconversion of heavy oils and petroleum feedstocks, cultivation of bacteria, cultivation of mold fungi, production of single-cell protein, animal cell culture and treatment of sewage (Lehman et al., 1978).

Due to varied flow behavior, the demarcation of hydrodynamic flow regimes is an important task in the design and scale-up of bubble column reactors. (Ashfaq and Muthanna 2007) reviewed most hydrodynamic studies performed for flow regime identification in bubble columns. They began with a brief introduction to various flow regimes. Then they examined experimental methods for measurement of flow regime transition. A few experimental studies were presented in detail, followed by the effect of operating and design conditions on flow regime transition (Ashfaq and Muthanna 2007).

Plunging Liquid Jet System:

A liquid jet plunging in a pool of liquid entrains gas at the gas-liquid interface. Entrained gas is dispersed in a liquid pool in the form of bubbles. This simple phenomenon of gas entrainment is widely observed in nature and bears great industrial significance. For example, oceans absorb atmospheric gases including human-generated CO2 emissions by plunging breaking water waves (Chanson et al., 2006). The same mechanism of air entrainment is responsible for the formation of long bubbly wakes behind naval ships by breaking bow waves. This bubbly flow alters flow hydrodynamics around the ship and produces unintended acoustic and optical signatures (Moraga et al., 2008). Extensive research on plunging jets is also driven by an important application in the nuclear industry. During the loss of a coolant accident (LOCA) in a nuclear power plant, Emergency Core Cooling (ECC) is activated. In the process of ECC, a cold-water jet is injected into a cold leg partially filled with hot water and steam. Plunging cold water jet entrains steam which subsequently affects cold and hot water mixing. It is important to understand the cold and hot water mixing because this mixed water is used to cool the reactor pressure vessel. Undesirably cold water may result in high thermal loads at the reactor pressure vessel wall and affect its integrity (Schmidtke et al., 2009).

Plunging liquid jets have also been demonstrated as an efficient gas-liquid contacting device. Plunging jet-based systems are in use as chemical or biological reactors. Bin (1993), in his review article, demonstrated that plunging liquid jet-based downflow bubble columns have higher gas transfer efficiency than conventional bubble columns and stirred tanks. Due to this favorable property plunging jet-based downflow bubble columns have been used in the areas of mineral flotation, wastewater treatment, and other chemical industries. Jameson Cell is a widely used flotation unit based on this concept (Tasdemir et al., 2007).

In a CPLJ system, as shown in figure 8, the jet is allowed to fall in a narrow space of liquid. This leads to an increase in the penetration depth of bubbles over conventional plunging jet systems, figure 9. Before proceeding to further discussion, it is important to understand the process of lake destratification.

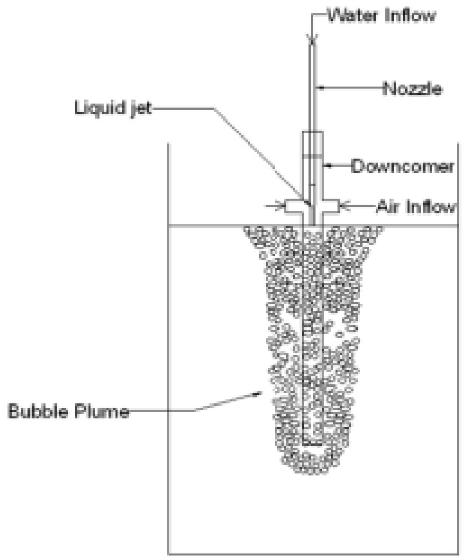

Figure 8. Confined Plunging Liquid Jet System

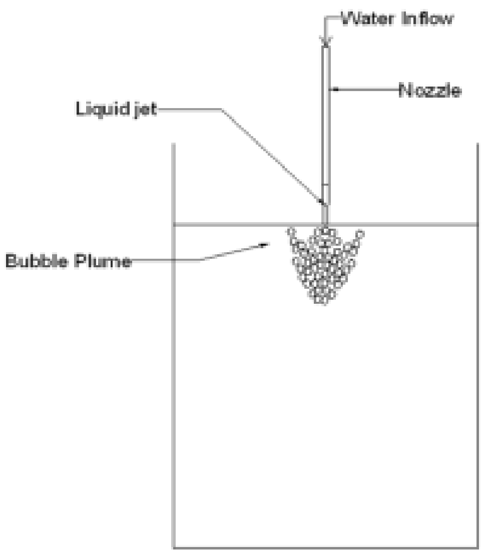

Figure 9. Plunging Liquid Jet System

Lake Destratification

During summers, lakes are often thermally stratified in three layers, warm upper layer (Epilimnion), thin middle layer (Metalimnion), and bottom cold layer (Hypolimnion), see figure 10. The warm upper Epilimnion layer is rich in nutrients and receives enough sunlight in summer to promote algal growth. Moreover, as the wind blows during summers water in the Epilimnion layer is mixed well, which ensures that oxygen-rich water from the surface is transported throughout the Epilimnion layer. However, the wind head is often not enough to move the cold water in Hypolimnion, which leads to a negligible supply of oxygen to this layer. Over summer, a limited amount of the oxygen contained in the Hypolimnion layer is gradually consumed by aerobic bacteria and other living animals.

Most of the nutrients are contained in the lake bottom (Hypolimnion), so lack of mixing in the whole lake also means that nutrients cannot be supplied to Epilimnion. Hence, Epilimnion has a limited amount of nutrients at the beginning of summer, which is consumed over summer to promote an algal boom. As the nutrients in Epilimnion dwindle, large destruction of algae may occur, which settles as organic matter at the bottom. Since most of the oxygen in Hypolimnion has already been consumed, this extra organic matter may lead the lake to an anoxic condition, where anaerobic bacteria may start to decompose the organic matter leading to the generation of harmful gases such as H2S (Hydrogen Sulfide) and NH3 (Ammonia). Lack of oxygen and the presence of harmful gases may lead to the destruction of aquatic life and the whole ecosystem in the lower part of the lake may be affected.

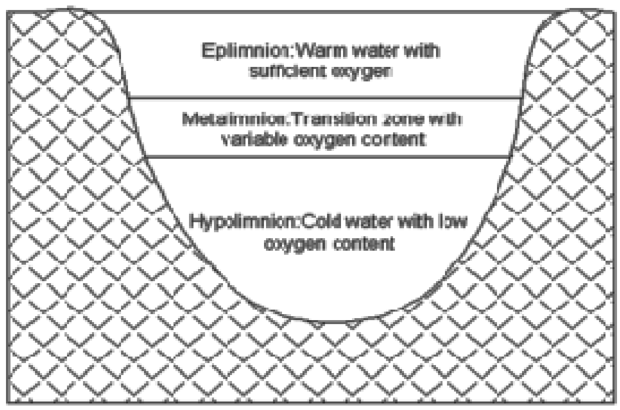

Figure 10. Stratification in a lake

In such cases, an artificial destratification of the lake is often recommended. Commonly, mechanical pumping techniques or bubble curtains are applied. Recently, bubble curtains have emerged as a favorable technology. In the bubble curtain technique, compressed air is injected into the lake bottom through an air diffuser. Rising air bubbles entrain the water and lift it to the lake surface, resulting in large-scale water circulation which not only breaks stratification but also performs aeration. However, this technology is cost-prohibitive due to high initial investments and operating costs. Michele and Michele (2002) proposed a free jet submerged in the lake for promoting artificial destratification. This liquid jet can transfer the oxygen-enriched water from the surface of the lake to the Hypolimnion. It is believed to be energetically more attractive than bubble curtains as it involves pumping of water which is mechanically more efficient than the air-compression process. However, using a free jet for destratification will require considerable operation time as aeration is dependent on the recirculation of natural oxygen-rich surface water, which is a slow process. A CPLJ system combines the strength of both these systems and offers a better prospect. It can not only provide aeration and destratification of the lake by dispersing the entrained air in the Hypolimnion Layer (same as bubble curtains) but also transfer the oxygen-enriched warm water from the surface of the lake to the cold Hypolimnion (same as free liquid jet), leading to considerably faster destratification than bubble curtains or the free liquid jet. Similar requirements also exist in wastewater treatment plants, where wastewater containing a large amount of organic matter is needed to be aerated for removal of the organic content by the oxidation process.

Apart from the above-mentioned advantages, CPLJ based systems offer other benefits too. It has already been demonstrated to be more efficient for wastewater aeration than conventional bubble columns and stirring devices (Bin, 1993). A CPLJ system does not require any compressor or stirring devices, which leads to a closed-loop hydraulic system, which is easier to operate and maintain. Since bubbles move against their buoyancy, in these systems gas residence time is considerably higher than conventional systems.

The mechanism of air entrainment by a liquid jet plunging in a liquid pool has been investigated by many authors. However, there is no conclusive information available about the mechanics of air entrainment at the impact point. Despite this, previous studies have successfully identified key parameters involved in the process of air entrainment. Early publications in this area showed that air entrainment occurs when liquid velocity exceeds a minimum critical velocity value (Ervine and Elsawy, 1975, Cummings and Chanson, 1999 and Danciu et al., 2009). For a given liquid-gas interface, apart from the physical properties of the gas and liquid, air entrainment rate is mainly controlled by jet surface turbulence, nozzle geometry, jet length, and liquid flow rate (Van de Sande and Smith, 1976, Lin and Donnelly, 1966). It was shown that the maximum bubble size is correlated to jet surface disturbance. Also, it was found that the maximum bubble size to be 1/4 of the jet surface disturbances. Bin (1993) published a comprehensive review on plunging jets detailing various mechanisms of air entrainment and empirical correlations of bubble size, plume penetration depth, and air entrainment rate. Ohkawa et al. (1986) proposed that if a liquid jet is allowed to plunge in a confined space, e.g., a tube of 4-6 times the diameter of the nozzle, then sufficient liquid flow velocity can be obtained in the downward direction in the tube to overcome buoyancy forces on the bubbles and bubble penetration depth can be increased. Subsequently, various studies probing the confined plunging liquid jet bubble columns have been published, where pressurized gas is externally supplied to the downcomer through an air inlet, and liquid to gas flow rate is independently controlled (Majumder et al., 2005). Contrary to the setup used in those studies, in the work of (Avanish 2011) and Ohkawa et al. (1986) gas is entrained naturally by a plunging jet and no external gas compressor is needed. Ohkawa et al. (1986) also demonstrated that for the same nozzle liquid velocity (VN), the diameter of the nozzle (DN) and free jet length (distance from the nozzle to free surface of the liquid, HN) gas entrainment rate is higher in a CPLJ system than in an ordinary plunging liquid jet system.

Deswal (2007) obtained a volumetric oxygen transfer coefficient by conducting aeration studies on a deoxygenated water pool. He showed plunging liquid jet system to have higher oxygen transfer efficiency (kg O2/kWh) than turbine agitators and small and large bubble size dispersers (bubble curtains). Recently, Botton and Cosserat et al. (2009) published oxygen mass transfer studies on a gas-liquid contacting system similar in spirit to that of Ohkawa et al. (1986). They found plunging jet aerators to provide a higher volumetric gas-liquid mass transfer coefficient for the same input power per unit volume of liquid than conventional gas-liquid stirred tanks and bubble columns.

Ma et al. (2010) developed a sub-grid air entrainment model for the prediction of the rate of air entrainment. They implemented this sub-grid air entrainment model as a source term in the bubble population balance equation in a RANS type two-fluid Euler-Euler CFD code. They obtained close agreements with corresponding experimental results of time and circumferentially averaged void fraction distributions reported by Chanson et al. (2004). Schmidtke et al. (2009) tested the impact of various drag models on air void fraction and discussed various approaches for modeling air entrainment by a plunging jet. Krepper et al. (2011) also performed a two-fluid Euler-Euler simulation of a liquid flow field generated by a plunging water jet and assessed its impact on fiber transport in a sump.

In a confined plunging liquid jet (CPLJ) system, a liquid jet is allowed to fall in a partially submerged narrow downcomer tube. Liquid jet impingement at the gas-liquid interface leads to entrainment of gas, which is dispersed down the downcomer tube into the outer pool in the form of bubbles. This simple phenomenon of gas entrainment bears great industrial significance. It facilitates an efficient gas-liquid contacting device, which can be used for wastewater aeration and lake destratification etc. A confined plunging liquid jet system was experimentally and numerically analyzed by (Avanish 2011). On the experimental front, a laboratory-scale CPLJ setup was developed. Impact of change in jet height, water flow rate and nozzle diameter on, bubble plume size, and surrounding flow field was investigated through high-speed camera photography and Particle Image Velocimetry. Image processing programs were developed in MATLAB for extracting plume boundaries in high-speed camera images. Experimental results showed that bubble plume width and the flow field are only weakly dependent on jet height. With an increase in water flow rate, bubble plume size, and airlifted water velocity increases. An increase in nozzle diameter, at a constant water flow rate and jet height, decreases both the plume size and upward water velocity.

On the numerical front, a 3D Euler-Euler two-fluid CFD simulation of bubble plume dispersion was performed for the test case of 7 mm nozzle diameter, 100 mm jet length, and 12.5 LPM water flow rate. Grid generation was done in GAMBIT while CFD software ANSYS CFX 12.1 was used for CFD simulations. The air phase was modeled as a polydispersed fluid with eight-size bins. In CFD modeling, interfacial drag, lift, wall lubrication, and turbulent dispersion forces were incorporated through appropriate correlations. Numerical and experimental results were found to agree with each other. CFD results showed that at least 85% of the inlet air breaks through the downcomer tube into the outer water tank (Avanish 2011).

Aeration

Aeration is a usual engineering measure, while bubble plume is a complex two-phase fluid generated in the aerating process (Murai, Y., Matsumoto, Y., Yamamoto, F 2000). Many scholars have got great achievements in the optimization of aerating types of equipment, however, such important factors as the flow pattern of gas-liquid two-phase flow, the mass transfer between the gas phase and liquid phase, and the mechanism of oxygen transfer are to be clarified and known little more nowadays. Studying the change of bubble plume structure is important to improve the aerating efficiency and widen the application range of bubble plume (L. Xu et. al. 2003). Based on this purpose, some experiments were done by (W.H. Liu et al. 2010), and particle image Velocimetry (PIV), which is a new measurement technique for the flow field, is employed in their study. Some bubble plume images in different conditions were obtained by CCD. Each digital image was divided into a white-back graph by binarization. The Recursive Cross-Correlation (Y. Murai, Y. Matsumoto 2000) (RCC) arithmetic was used to calculate the whole flow field by analyzing those images (W.H. Liu et al. 2010).

The flow pattern of gas-liquid two-phase flow in an aeration tank is of critical effect upon mass transfer by the convection. Bubble plume provides unsteadily fluctuating two-phase flow during the aeration. The study on the unsteady structure of bubble plume is dealt with from the experiment by (W.H. Liu et al. 2010). The time serial bubble plume images of different cases in the tank were analyzed. The RCC-PIV was employed to calculate the velocities in those cases, and then the time-serial vortex, the total turbulence intensity, the time-serial streamline was obtained. It was shown that the aspect ratio and void fraction are the dominant factors influencing the unsteady structure of the bubble plume. When the aspect ratio is unity and the void fraction gets higher, the bubble plume has a symmetrical vortex structure and the longest residence time, which is beneficial for optimizing the aeration system and enhancing the applied range of the bubble plume.

The gas transfer in aeration systems is broken into two processes: gas transfer at the bubble interface and gas transfer at the water surface. Experiments were conducted to separate these two sources of dissolved gas. The oxygen absorption was measured in a laboratory tank with air being diffused through a porous diffuser and then with nitrogen gas being diffused. The combination of these experiments along with the reformulation of the theoretical transfer equation permit separation of the gas transfer at the water surface and in the rising bubble plume. Estimates of the exchange coefficient for the plume and surface are given (Steven and Sandra 1992).

Diffused aeration systems for oxygen absorption are typically used in wastewater treatment. These systems usually use porous diffusers to generate a bubble plume that induces mixing and gas transfer. Design information for these diffuser systems is given as the product of the 1iquid film exchange coefficient, k_L, and the specific surface area, a. This product, k_La, is generally referred to as the overall mass-transfer coefficient or the exchange coefficient and has units of hr^{-1}. It represents the sum of the oxygen absorption that occurs in the rising bubble plume and at the water surface of the test tank (Metcalf and Eddy, Inc. 1979).

Diffused aeration systems have been considered and have been installed at a few locations for the improvement of dissolved oxygen (DO) in deep reservoirs and lakes. The level of confidence in applying manufacturer-supplied estimates of the exchange coefficient decreases with increasing reservoir depth since coefficients were derived from tank tests having water depths significantly less than those of deep reservoirs and lakes. While the relative contribution to the overall oxygen transfer by the water surface may be similar between laboratory flumes and shallow wastewater treatment facilities, the contribution to total gas transfer by absorption at the water surface would be significantly reduced for a very deep reservoir. For example, consider the oxygen transfer that occurs in a 5-m-deep test facility: part results from absorption from the bubbles and part from the transfer with the atmosphere at the water surface. If the depth of the facility is 50 m, the mass of oxygen transferred across the water surface remains nearly the same (assuming no change in the overall mixing characteristics at the water surface). However, the total gas transfer would increase dramatically with the diffusers located at a 50-m depth due to the hydrostatic pressure on the bubbles. According to Henry's law, hydrostatic pressure enhances oxygen transfer by increasing the saturation concentration in the bubbles (Hydraulics Research Station 1978, McDonald, and Gulliver 1990).

Bubble plume models are applied to study the de-stratification of lake water, aeration of reservoirs, wastewater treatment, and gas injection into liquid metals. Several existing models exemplify numerical modeling as problem-specific art, solve a mixture momentum equation, and have limitations in the availability of documentation, the definition of boundary conditions, and post- and pre-processing capabilities. The transfer of problem-specific models to a client or a multidisciplinary research and development team is a difficult process. The questions addressed in (Bravo et. al. 2007) study were as follows: (a) can one use a commercial code as a basis to develop a user-friendly, efficient model that simulates two-phase flow in bubble plumes? (b) what are the capabilities and limitations of such a model?

The two-fluid model developed has flexibility in the definition of the multiphase and viscous models, easily understood definition of boundary conditions, simple definition of spatial dimensionality and time dependency, efficient numerical solution, clear documentation, and user-friendly pre-and post-processing capabilities. Water and air phase velocities, water turbulent kinetic energy, and air volume fraction are predicted with accuracy like that of existing problem-specific models. A strategy to overcome some under-dispersion and include air-water mass transfer effects through user-defined functions is discussed (Bravo et. al. 2007).

The development of a bubble plume model for the aeration of deep reservoirs in a typical case can be studied. The designer of the aeration system wants to use the model to reproduce the geometry of bubble diffusers and test the effectiveness of different aeration devices. Interpretation of model results requires knowledge of the model hypotheses, limitations, and structure on part of the user. The specialist in air-water mass transfer may want a model that allows him/her to easily explore different formulations for gas transfer coefficients and the load imposed by oxygen demand, and their relationship with flow turbulence. The model buyer wants a user-friendly model that can efficiently model a whole deep reservoir. Every involved party wants a model that produces quantitative, reliable results on which decisions can be based (Bravo et. al. 2007).

Several existing models are developed specifically for a problem, are difficult to use by the designer or the specialist in air-water mass transfer and have limitations in the availability of documentation and post- and pre-processing capabilities. The definition of boundary conditions in problem-specific codes can lead to inconsistencies or difficulties in the exploration of air-water mass transfer. This typical disparity between expectations and existing software occurred in the research and development efforts aimed to design the aeration system for the McCook Reservoir. This scenario leads to the main questions addressed in (Bravo et. al. 2007) study as follows: (a) can one use a commercial code as a basis to develop an efficient user-friendly model that simulates two-phase flow in bubble plumes? (b) what are the capabilities and limitations of such a model?

Let us briefly discuss bubbly flow models in general, aeration of a deep reservoir, and a couple of models developed specifically for this application. Models for studying bubbly flows have been generally divided into EulereLagrange, or EeL (Sheng and Irons, 1995), and EulereEuler or EeE models (Bernard et al., 2000; Buscaglia et al., 2002; Mudde and Simonin, 1999; Sokolichin and Eigenberger, 1995; Smith, 1998). In the EeL formulation, the liquid phase is treated as a continuum, while the dispersed gas phase is solved by tracking bubbles. The liquid flow field is calculated with an initial estimate for the void fraction. Many bubble trajectories are then calculated so that a new void fraction can be calculated. This new void fraction is then used to recalculate the liquid flow field, and iteration continues until the void fraction and liquid flow field converge (Sheng and Irons, 1995). In the EeE representation, the two phases are treated as interpenetrating fluids. The concept of phasic volume fraction is introduced since the volume of a phase cannot be occupied by another phase. The EeE model family includes the mixture model (Wuest et al., 1992; Manninen et al., 1996) and the two-fluid model. The mixture model solves the mixture momentum equation and prescribes relative velocities to describe the dispersed phase. In the two-fluid model, the two phases are represented by two sets of mass and momentum balances, which have similar structures for all phases (Mudde and Simonin, 1999). These equations are solved by providing certain constitutive relations that are obtained from empirical information.

The design of deep reservoirs for combined (stormwater and wastewater) flows leads to various water quality challenges, and aeration is one possible solution. In most cases, the depth of the reservoirs is beyond the proven range of validity of existing design methods for aeration systems. One notable case is the almost 80-m deep McCook Reservoir being planned by the US Army Corps of Engineers (USACE) for Chicago, Illinois. The design of aeration systems for deep reservoirs requires a practical capability for numerically simulating the effect of submerged diffusers on reservoir flow and aeration (Bernard, 1998). The design of the McCook Reservoir is supported by a combination of experiments and computational modeling.

Large-scale experiments on aeration-induced flows (Soga and Rehmann, 2004), water quality, and air-water mass transfer are underway. Computational efforts include those by Bernard (1995, 1997, 1998, 2002), Bernard et al. (2000), and Buscaglia et al. (2002). The PAR3D mixture model developed by Bernard (1995, 1998) and Bernard et al. (2000) is capable of reproducing observed velocities within a factor of two. The current version of the PAR3D code includes the simulation of air-water mass transfer (Bernard, 2002). The authors' review of the PAR3D model (Bernard, 2002) revealed the limitations in terms of documentation availability, the definition of boundary conditions, post- and pre-processing capabilities, and model efficiency. Buscaglia et al. (2002) developed a mixture model coupled to a mass transfer model and applied it to typical conditions of isolated aeration plumes in deep wastewater reservoirs. Buscaglia et al.'s (2002) model predictions compared well with those of the 1D model proposed by Wuest et al. (1992) but combine a mixture model with boundary conditions defined for the individual phases (Bravo et. al. 2007).

To treat organic wastewater, the biological method is usually used in many industries and water purification plants. The aerobic microorganism's inactive sludge decompose organic compounds to low molecular ones with oxygen consumption in the aeration tank. On many **aeration systems**, the oxygen supply into water limits the rate of wastewater treatment. To improve the oxygen dissolution into water, it is available that the size of air bubbles is reduced. If bubbles are crushed by some additional power devices such as pump, stirrer, and so on, however, the cost must increase. In (Yoshihito and Koichi 2007) study, a novel aerator that consumes almost no additional power was developed to generate bubbles that diameter is smaller than 1 mm (Yoshihito and Koichi 2007).

Slit orifice aerator

When gas is inputted from a round orifice to water, bubbles grow so stably that their size is to be large. On the other hand, when the shape of the orifice is slit-like, the instability is caused by bubble expansion. The developed aerator consists of multiple layered slit plates. Every plate has a slit orifice so that the number of orifices can be changed by laminating (Yoshihito and Koichi 2007). The mean size *d* of N2 bubbles dispersed in tap water was measured using a high-speed video camera. The effects of the width *W* and the length *L* of the slit orifice on the bubble size were investigated. The suitable pitch of the orifices was also investigated. As a result, the slit orifice aerator with no additional power device was developed. When the width was less than 30 μm, the submilli-sized bubbles were distributed (Yoshihito and Koichi 2007).

Hypolimnetic Aeration and Oxygenation Systems

When properly designed, hypolimnetic aeration and oxygenation systems can replenish dissolved oxygen in water bodies while preserving stratification. A comprehensive literature review of design methods for the three primary devices was completed. Using fundamental principles, a discrete-bubble model was first developed to predict plume dynamics and gas transfer for a circular bubble-plume diffuser. This approach has subsequently been validated in a large vertical tank and applied successfully at full-scale to an airlift aerator as well as to both circular and linear bubble-plume diffusers. The unified suite of models, all based on simple discrete-bubble dynamics, represents the current state-of-the-art for designing systems to add oxygen to stratified lakes and reservoirs (Vickie 2008).

An existing linear bubble plume model was improved, and data collected from a full-scale diffuser installed in Spring Hollow Reservoir, Virginia (U.S.A.) were used to validate the model. The depth of maximum plume rise was simulated well for two of the three diffuser tests. Temperature predictions deviated from measured profiles near the maximum plume rise height but predicted dissolved oxygen profiles compared very well to observations. Oxygen transfer within the hypolimnion was independent of all parameters except the initial bubble radius. The results of (Vickie 2008) work suggest that plume dynamics and oxygen transfer can successfully be predicted for linear bubble plumes using the discrete-bubble approach (Vickie 2008).

To model the complex interaction between a bubble plume used for hypolimnetic oxygenation and the ambient water body, a model for a linear bubble plume was coupled to two reservoir models, CE-QUAL-W2 (W2) and Si3D. In simulations with a rectangular basin, the predicted oxygen addition was directly proportional to the update frequency of the plume model. W2 calculated less oxygen input to the basin than Si3D and significantly less mixing within the hypolimnion. The coupled models were then applied to a simplified test of a full-scale linear diffuser. Both the W2 and Si3D coupled models predicted bulk hypolimnetic DO concentrations well. Warming within the hypolimnion was overestimated by both models, but more so by W2. The lower vertical resolution of the reservoir grid in W2 caused the plume to rise height to be overpredicted, enhancing erosion of the thermocline (Vickie 2008).

Hypolimnetic Aeration and Oxygenation Devices

Mercier and Perret [1949] developed one of the earliest aeration systems, which utilized mechanical agitation of water pumped from the hypolimnion into a splash basin on the surface of a lake. Another type of aeration method is layer aeration, which redistributes available dissolved oxygen obtained from algal photosynthesis and contact with the atmosphere [Kortmann, 1994; Kortmann et al., 1994]. Airlift devices have also been used for hypolimnetic aeration. Partiallift systems operate by injecting compressed air near the bottom of the hypolimnion. The air-water mixture travels up a vertical tube to a given depth in the lake from which the remaining gas bubbles are vented to the atmosphere through a pipe to the surface. The oxygenated water is returned to the hypolimnion. Full-lift systems are similar except the air-water mixture rises to the surface before residual gas bubbles are released. Regarding hypolimnetic oxygenation, one technique involves withdrawing water to the shore, injecting it with pure oxygen gas under high pressure, and then returning it to the hypolimnion. This is known as side-stream pumping and is one of the earliest reported oxygenation systems [Beutel and Horne, 1999; Fast, A. W., and M. W. Lorenzen (1976]. Another side-stream method entails mixing air or pure oxygen into withdrawn water, pumping, or passing the bubble-water mixture down a deep U-tube to enhance gas transfer, and returning oxygenated water that is discharged at the top of the tube [Bruijn and Tuinzaad, 1958; Speece and Adams, 1968]. In submerged contact systems, oxygen is injected into an enclosed chamber usually located in the hypolimnion, and water is either pumped or entrained into the device [Beutel and Horne, 1999]. Oxygen transfer occurs within the chamber, and oxygenated water is discharged to the hypolimnion. A Speece Cone employs this principle [Speece et al., 1973]. Finally, either compressed air or pure oxygen gas can be introduced into the hypolimnion through diffusers to form a rising, unconfined bubble plume.

The primary types of hypolimnetic aeration and oxygenation systems currently in use include airlift aerators, Speece Cones, and bubble plume diffusers [McGinnis and Little, 2002].

Bubble-Plume Diffuser

Bubble-plume diffusers generally have a linear or circular geometry and inject either air or oxygen at a relatively low gas flow rate [McGinnis and Little, 2002]. These systems are most suitable for deep lakes where the bulk of the bubbles dissolves in the hypolimnion and the momentum generated by the plume is low enough to prevent significant erosion of the thermocline [Wuest et al., 1992]. Gas bubbles are injected into the water column through a porous diffuser creating a gas/water mixture that rises and gains momentum due to a positive buoyancy flux. The buoyant mixture entrains water at the boundaries, which increases the water flow rate and cross-sectional area, but decreases the momentum. The plume rises against the vertical density gradient until the depth of maximum plume rise (DMPR) is reached, which is where the plume momentum is zero. The plume water at this depth is negatively buoyant and is expected to fall back to an equilibrium depth (ED) where the plume density equals the ambient density [McGinnis et al., 2004]. Upon reaching the ED, the plume water disperses horizontally into the far-field [McGinnis et al., 2004].

Numerous studies have been conducted documenting the physical, chemical, and biological effects of hypolimnetic aeration and oxygenation on lakes and reservoirs. These studies have been reviewed by Fast and Lorenzen [1976], Taggart and McQueen [1981], Pastorok et al. [1981; 1982], McQueen, and Lean [1986], and, more recently, Beutel and Horne [1999]. In their extensive review of literature on the effects of hypolimnetic aeration on water quality, lake biota, and stratification, McQueen and Lean [1986] summarized the results of the studies:

(1) well designed aeration systems have maintained stratification and have not increased hypolimnetic water temperature significantly.
(2) hypolimnetic oxygen levels increased,
(3) iron, manganese, hydrogen sulfide, and methane levels decreased.
(4) zooplankton populations were generally unaffected.
(5) chlorophyll levels were usually not altered.
and (6) depth distributions of cold-water fish populations increased. The effects of hypolimnetic aeration on phosphorus levels have been more variable. McQueen et al. [1986] attribute this to pH levels and iron availability for phosphorus sedimentation. The published effects of aeration on nitrogen levels have not been consistent either; ammonium and total nitrogen decreased in some studies but increased in others. McQueen and Lean [1986] concluded that this is also related to pH levels. It has been reported that gaseous nitrogen concentrations were elevated to supersaturation levels during hypolimnetic oxygenation with compressed air, and there has been some concern expressed over this causing gas bubble disease in fish [Fast et al., 1975b]. However, there have been no reported adverse effects of hypolimnetic aeration on fish populations [McQueen and Lean, 1986].

Beutel and Horne [1999] conducted a comprehensive literature review on the effects of hypolimnetic oxygenation and reported the following after evaluation of several detailed case studies:

(1) unlike some hypolimnetic aeration systems, oxygenation projects-maintained stratification and only caused minor increases in hypolimnetic temperature,
(2) average hypolimnetic dissolved oxygen concentrations were maintained at greater than 4 mg L-1,
(3) induced oxygen demand reported for oxygenated lakes and reservoirs was lower than values reported for aerated waterbodies,
and (4) oxygenation decreased hypolimnetic concentrations of dissolved phosphorus, ammonia, manganese, and hydrogen sulfide by 50-100%.

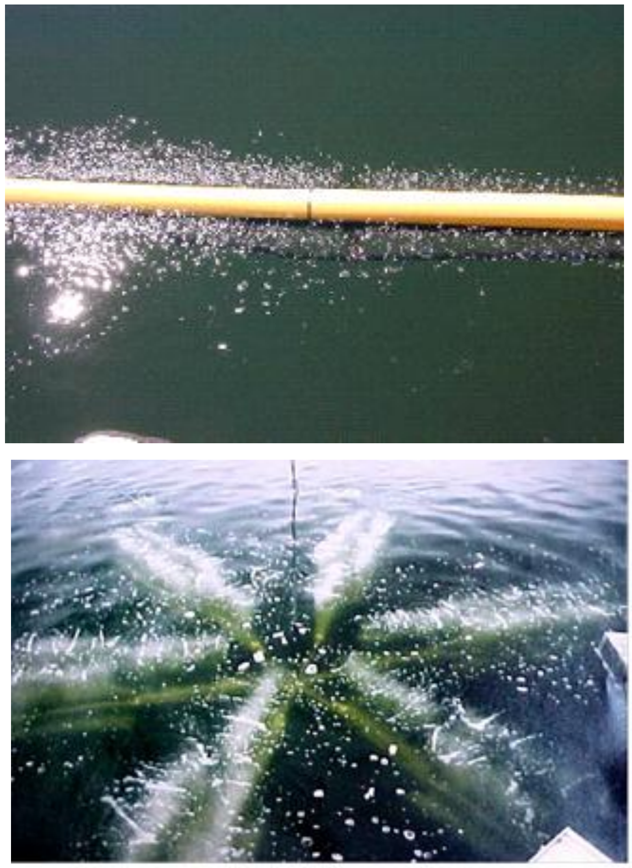

Figure 11. Photographs of linear (top) and circular (bottom) bubble-plume diffusers. (Photo of the linear diffuser from Mark Mobley of Mobley Engineering, Inc. Photo of the circular diffuser from Swiss Federal Institute for Aquatic Science and Technology (Vickie 2008)

A survey of the literature on hypolimnetic aeration effects published since the review of McQueen and Lean [1986] generally supports the findings of that paper [Ashley, 1988; Gachter and Wehrli, 1998; Gemza, 1995; Gibbons et al., 1994; Jaeger, 1990; Nordin et al., 1995; Soltero et al., 1994]. Similarly, a survey of the effects of hypolimnetic oxygenation reported since the review of Beutel and Horne [1999] confirms the conclusions of that work (Sondergaard et al., 2000).

While the vast majority of studies regarding hypolimnetic aerators and oxygenators have focused on their effects, relatively little work has been undertaken to examine the parameters that impact system performance. A review of these early design studies of full-lift aerators and bubble plume diffusers was presented. Because the Speece Cone has not been as widely used as other oxygenation devices, no earlier design literature was available. Figure 11. illustrates photographs of linear (top) and circular (bottom) bubble-plume diffusers. (Photo of the linear diffuser from Mark Mobley of Mobley Engineering, Inc. Photo of the circular diffuser from Swiss Federal Institute for Aquatic Science and Technology (Vickie 2008).

Discrete Bubble Model

A significant unifying advance in hypolimnetic aeration and oxygenation system design is the use of the discrete-bubble model for predicting oxygen transfer. In each of the three primary devices, the interfacial gas transfer is accomplished through individual bubbles in contact with water. Bubble size is an important parameter because it is directly related to the interfacial surface area, bubble-rise velocity [Clift et al., 1978; Haberman and Morton, 1954], and the mass-transfer coefficient [Clift et al., 1978; Motarjemi and Jameson, 1978]. Besides, bubble size may vary significantly as the bubbles pass through the system or ascend the water column. For these reasons, Wuest et al. [1992] developed a discrete-bubble model for a circular bubble plume that accounts for volumetric changes due to gas transfer as well as changing hydrostatic pressure and water temperature. The method has subsequently been applied to diffused-bubble aeration in a large vertical tank [McGinnis and Little, 2002], an airlift aerator [Burris and Little, 1998; Burris et al., 2002], a Speece Cone [McGinnis and Little, 1998], and a linear bubble-plume diffuser [Little and McGinnis, 2001; Singleton et al., 2005].

Because bubble plumes are encountered in a variety of natural and man-made systems, numerous studies have been conducted on plume dynamics. Less work has been performed on bubble plumes in stratified environments [Asaeda and Imberger, 1993; Lemckert and Imberger, 1993; McDougall, 1978; Schladow, 1993], and even fewer investigations on bubble plumes incorporating gas transfer [Sahoo and Luketina, 2003; Speece and Murfee, 1973; Speece and Rayyan, 1973; Tsang, 1990]. Bubble plumes intended for hypolimnetic oxygenation must be capable of increasing dissolved oxygen concentrations, and most lakes and reservoirs have vertical density and concentration gradients. Therefore, only design methods that account for gas transfer and stratification were reviewed. Also, because (Vickie 2008) work focuses on oxygenation methods that preserve stratification, destratification models [Asaeda and Imberger, 1993; Davis, 1980; Sahoo and Luketina, 2003; Schladow, 1993] were not reviewed.

A model was developed by Rayyan and Speece [1977] to describe the hydrodynamics of circular bubble plumes in stratified environments. The model accounts for non-linear stratification and oxygen transfer. The model predicts maximum plume rise height, centerline velocity and nominal half-width, and density and temperature differences between the plume and the ambient water column. Conservation principles were applied to a circular plume to derive equations for water mass flux, oxygen flow, momentum flux, buoyancy flux, and heat flux. These equations are functions of characteristic plume width, entrainment coefficient, water and bubble rise velocities, gas concentration, bubble and water spreading coefficients, and local plume and ambient water densities and temperatures. The entrainment coefficient was set equal to 0.04 for low flow rates in the laboratory and 0.055 for higher flow rates in the field. The water and bubble spreading coefficients were 1.25 and 0.2, respectively. Bubble size varies along with the height of the circular plume and is a function of oxygen transfer and the local hydrostatic pressure. It was assumed that the velocity and density profiles are similar at all heights above the diffuser, and normally distributed. The Boussinesq assumption was invoked (Vickie 2008).

Hypolimnetic oxygenation using bubble plumes released from areal sources was modeled by Tsang [1990]. The author described bubble plume dynamics as consisting of two primary mechanisms: hydrodynamics (macroscopic) and gas/bubble dynamics (microscopic). Tsang applied fundamental principles to relate the various parameters that govern bubble plume dynamics and gas transfer, which resulted in three equations. The conservation of mass and energy were used to obtain equations for average water velocity across the plume W(z) and volumetric gas flux. The gas flux equation accounts for bubble radius variations with depth due to changing hydrostatic pressure and gas transfer. For the third equation, formulas describing the absorption of gas across bubble walls and isothermal expansion of gas bubbles were combined. The three equations can be solved simultaneously to determine the three unknowns: the entrainment coefficient α, average water velocity W(z), and bubble radius Rb(z). The following assumptions were made by Tsang [1990] during his theoretical analysis of bubble plumes. The areal diffuser source is considered to be circular, and a top-hat distribution for vertical velocity is assumed. The plume expansion angle, number flux of bubbles, and bubble rise velocity are assumed to be constant. The potential and kinetic energy fluxes of the gas phase are negligible compared to those for the liquid phase. It is also assumed that the ambient dissolved gas concentration is constant during the bubble ascent. Lastly, it is unclear whether the model accounts for stratified ambient conditions.

Early literature on the design of airlift aerators and bubble plumes for hypolimnetic oxygenation provides useful insight and field observations of factors affecting device performance. However, each of the models has deficiencies that can result in incorrect sizing of oxygenation devices and/or gas supply facilities. Lorenzen and Fast [1977] provided practical guidance and information about the major variables that affect the performance of airlift aerators. However, their aerator sizing method makes several critical assumptions that are unverified. Taggart and McQueen’s [1982] model presents a simple, straightforward approach for the hydrodynamic design of airlift aerators. However, the model lacks key elements, namely the prediction of oxygen transfer. Also, the effect of gas flux on induced water velocity was not considered. The authors did account for gas flow when developing a correlation to estimate induced water flow rate as a function of volumetric airflow and riser depth. Ashley [1985] presented a detailed, stepwise method to size airlift aerators and provided helpful information on engineering aspects such as compressors, power supply, oxygen transfer, and oxygenation capacity. The model was field-tested by Ashley et al. [1987], but the aeration system was unable to satisfy hypolimnetic oxygen demand because the induced water velocity and oxygen input were overestimated during design. The model proposed by Little [1995] was the first attempt at using a fundamental approach to predict oxygen transfer in airlift aerators, but the model relies on empirical equations to determine critical variables. Also, nitrogen transfer can be significant for deep installations and will affect bubble volume and bubble-size dependent properties like the rise velocity and mass transfer coefficient. The bubble-plume model of Rayyan and Speece [1977] is based on fundamental principles and captures many of the key hydrodynamic features of plumes. However, the model does not account for nitrogen transfer, ambient salinity gradients, or the effect of changing bubble size on rising velocity and the mass transfer coefficient. While hydrodynamic predictions from the model have been verified with laboratory and field testing, oxygen transfer estimates have not been validated. Similarly, the bubble-plume model of Tsang [1990] has not been validated with data. Also, the effect of changing bubble size on rising velocity is not considered. Lastly, it is unclear whether Tsang's model accounts for ambient concentration gradients (Vickie 2008).

In each oxygenation device, gas bubbles in contact with water facilitate the interfacial transfer of oxygen, nitrogen, and other soluble gases. Using fundamental principles, a discrete bubble model was first developed to predict plume dynamics and gas transfer for a circular bubble plume diffuser. The discrete-bubble approach has subsequently been validated using oxygen transfer tests in a large tank and applied successfully at full-scale to an airlift aerator as well as to both circular and linear bubble plume diffusers. The discrete-bubble approach has also been extended to the Speece Cone, but the model has not yet been validated due to a lack of suitable data (Vickie 2008).

Bubble Plumes in Stratified Waterbodies

During hypolimnetic oxygenation with bubble plumes, compressed gas is continually supplied to diffusers, usually located immediately above the sediments, and is allowed to bubble freely. A gas-water plume mixture that is less dense than the ambient water is created, which causes the mixture to ascend through the hypolimnion. As the mixture rises, ambient water is entrained into the plume, and the plume width increases. The entrained fluid produces a double plume structure, consisting of an inner core that contains the bubble-water mixture surrounded by an outer annulus that contains plume water relatively free of bubbles [McDougall, 1978]. As the outer annulus entrains stratified hypolimnetic water, the plume width increases, and the density decreases. When the negative buoyancy of the entrained fluid exceeds the positive buoyancy imparted by the bubbles, the plume detrains water at a rate nearly equal to that previously entrained [Lemckert and Imberger, 1993]. At this depth, the velocity of the relatively dense water within the plume decreases to zero and the plume stops rising. The detraining plume water then forms an annular downward flow immediately outside the outer annulus of the upward flowing plume water. The detraining plume water entrains ambient water until a depth of neutral buoyancy is reached, where a horizontal intrusion is created into the hypolimnion [Asaeda and Imberger, 1993]. The undissolved bubbles remaining in the bubble-water mixture separate from the inner core flow and continue to rise to the surface, repeating the entire process (Vickie 2008).

Two-phase plumes have historically been studied in a variety of situations, including bubble breakwaters, bubble curtains for contaminant containment, bubble jets for destratification in lakes and prevention of ice formation in harbors, reaeration in lakes and reservoirs, bubble barriers for shockwave protection from underwater explosions, and oil well blow-outs (Asaeda and Imberger 1993, Jones 1972, McDougall 1978). Recently, two-phase plumes have played a role in the proposed deep ocean sequestration of carbon dioxide to help mitigate potential global climate change (Liro et al. 1991, and Caulfield 1996). Figure 12 shows a schematic of a deep-ocean CO2 release and identifies key nomenclature. Contrary to deep-ocean plume behavior, most of the existing studies of two-phase plumes focus on highly energetic plumes in weakly stratified and step-stratified shallow waters, which form a single intrusion layer near the peak density gradient of the stratification (Lemckert and Imberger 1993, Baines and Leitch 1992, and Patterson and Imberger 1989). Deep-ocean plumes of CO2 in either a bubble or droplet form would experience a linear ambient stratification and would be designed so that all of the injected CO2 and entrained seawater would trap below the thermocline, having several detrainment events from the injection point to the crest of the plume (Caulfield 1996, Liro et al. 1991). The environmental impacts of such a CO2 plume depend on the detrainment and secondary plume start-up processes that are not fully understood.

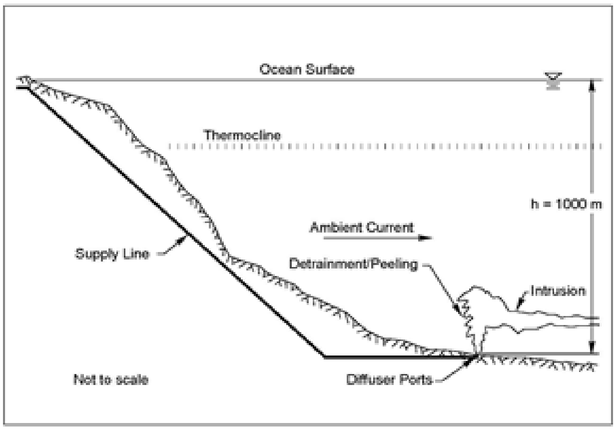

Figure 12. Schematic of a deep-ocean CO2 plume with related nomenclature

In a review of CO2 injection methods, Adams and Herzog (1996) found that bubble and droplet plumes were the most promising disposal methods because they are the simplest and the least costly both in terms of energy and maintenance. Several modeling investigations of CO2 plumes have approached plume design by predicting the distribution of

CO_2 in the water column and the resulting environmental impacts. An integral model of a CO_2 plume for a 500 MW power plant was developed by Liro et al. (1991 and 1992); the model accounted for the dissolution of CO_2 from the plume into the water column and the possibility of several peeling events. Caulfield et al. (1997) extended the Liro et al. (1991) model to include the density change of the entrained seawater due to the dissolution of CO_2 and predicted the resultant pH change in the far-field water column. Caufield et al. (1997) also developed a stochastic random-walk model to quantify the time-history pH experience of a passive organism swept through the plume. Based on dose-response data compiled by Auerbach et al. (1997), the model was then used to estimate the organism mortality for various plume designs. Among the important parameters determining the organism mortality flux were the intrusion layer thickness, the number of intrusions, and the intrusion layer flux (Caulfield 1996, Adams et al. 1997). The droplet size and the possible formation of clathrate hydrate scales were also important factors and are under investigation at several research institutes. Although these models and a similar model by Thorkildsen et al. (1995) predict many peeling events, the models must arbitrarily set parameters controlling the peeling process because of a lack of experimental observations; thus, organism mortality remains uncertain.

Other researchers have used more physically based models of the peeling process (e.g. Alendal et al. 1998, Asaeda and Imberger 1993, and McDougall 1978); however, the amount of peeled water at each detrainment and the location of detrainment events remains largely arbitrary. The Alendal et al. (1998) model has the highest level of complexity, solving a three-dimensional, eddy-diffusivity model on a fine mesh in the near-field of the plume. However, detrainment is too fine scale of an event to be modeled explicitly, even in such a complete model. The sensitivity analysis by Caulfield (1996) and Adams et al. (1997) shows that potential organism impacts for CO_2 plume injections for a 500 MW power plant could be avoided by a variety of designs if the peeling parameters could be quantified. The efficiency and performance of each design would also depend in large part on a detailed understanding of the plume peeling and intrusion dynamics. Therefore, experimental studies of the peeling process for two-phase plumes in stratified environments have been initiated.

Asaeda and Imberger (1993) assume that all of the plume fluid peels at each peeling event and that peels occur when the net plume momentum reaches zero. Similarly, McDougall (1978) assumes that all the fluid outside the narrow bubble core (approximately 70% of the plume fluid) peels at the same height as Asaeda and Imberger (1993). By contrast, Liro (1991) and Caulfield (1996) assumed that half of the fluid peels and that peels occur when the net buoyancy flux is zero.

Numerical plume models began out of an interest in forced, convective, single-phase plumes in the atmosphere, first summarized in the classic paper by Morton, Taylor, and Turner (1956). Morton et al. (1956) demonstrated the flexibility of the entrainment assumption, first identified by Taylor in the 1940s and later popularized in a review lecture by Batchelor (1954), which forms the essential part of the analysis of buoyant, turbulent plumes in stratified environments (Turner 1986). Stated simply, the entrainment assumption predicts that the mean inflow velocity across the edge of a turbulent flow is proportional to a characteristic velocity in the flow at the level of inflow (Turner 1986). The ordinary similarity solutions for a plume in a uniform environment do not apply when there is stratification because, as the plume entrains ambient fluid and changes density, it passes through a level of neutral buoyancy, where the downstream velocity vanishes and the plume is said to trap (Morton et al. 1956, Turner 1986). The entrainment assumption, however, is still assumed to be valid for the stratified case, implying the same kind of turbulence structure and balance of forces, but without relying on similarity solutions of the usual kind (Morton et al. 1956). This approach is robust in stratified environments because the entrainment coefficient enters the governing equations with weak sensitivity (Turner 1986). Morton (1956) also showed that continuous, distributed sources could be approximated by virtual point sources and treated by the analysis of Morton et al. (1956). Using a single entrainment coefficient for pure plumes, these models have successfully been applied to a range of problems, from laboratory scales of fractions of a meter, up to the scales of forest fires and volcanic eruptions, where plumes have reached heights of 40,000 m (Turner 1986).

The first successful analysis of the flow induced by two-phase (air-bubbles) plumes was by Kobus (1968) for a uniform ambient environment. In laboratory experiments in a 4.7 m deep basin, Gaussian profiles were fit to the velocity measurements and were postulated for the density defect in the plume. An integral plume model was proposed based on an entrainment assumption, the Gaussian profiles, and considering the changing air volume with depth and an experimental effective transport rate of buoyancy due to the velocity difference between the bubbles and the plume fluid (Kobus 1968). Ditmars and Cederwall (1974) extended Kobus' model to include the bubble slip velocity directly. Ditmars and Cederwall (1974) also estimated the entrainment rate as a function of gas flow rate and found it to lie between values for pure jets (0.057) and pure plumes (0.082). Other researchers have found a wider range of values for the entrainment coefficient (Milgram 1983, Kobus 1968, Hugi 1993). Milgram (1983) found a dependence of the entrainment coefficient on the plume center-line gas fraction, the bubble flow rate, and the bubble size. Milgram (1983) reports measured entrainment coefficients between 0.035 and 0.16. Researchers at the Eidgenossiche Technische Hochschule (ETH) Z¨urich also report a range of entrainment coefficients from 0.01 to 0.10 (Hugi 1993). The lowest values of entrainment were for a straight-tube diffuser (large, fastmoving bubbles) and a large (15 cm diameter) porous plate (small, diffuse bubbles), but for airflow rates much lower than for Milgram (1983), Kobus (1968), or

Cederwall and Ditmars (1974). Together, the data follow a general trend from low values at low flow rates towards the pure plume value of 0.082 with increasing flow rate; however, other factors were also important (Hugi 1993). In further modeling studies, estimates of the spreading ratio between the density defect and velocity profiles indicated an exact correlation with the turbulent Schmidt number (Ditmars and Cederwall 1974). The Schmidt number, therefore, enters the equations but is not an independent parameter. Finally, based on experiments in a deep well and a review of the literature, Milgram (1983) added a momentum amplification factor to the integral model developed by Kobus (1968) and Ditmars and Cederwall (1974) to account for the momentum carried in the plume turbulence. Although this coefficient can be as high as 2.8, Liro et al. (1991) showed that there is little sensitivity in the results in constant values of the momentum amplification factor and stated that it is approximately unity for a prototype CO2 plume.

Additional experimental studies of bubble plumes have quantified many characteristics of the two-phase flow using a wide range of techniques (Tacke et al. 1985, Sun and Faeth 1986, Cheung and Epstein 1987, and Castello-Branco and Schwerdtfeger 1996, Hugi 1993). Tacke et al. (1985) developed an electro-resistivity probe to measure gas concentration, bubble frequency, and bubble velocity. Their measurements confirmed the use of Gaussian profiles for the density defect in the plume. Sun and Faeth (1986) measured the turbulent properties of bubble plumes. Bubble size distributions were measured using photographic techniques. Bubble and plume fluid velocities were measured using a modified laser-Doppler anemometer (LDA) technique. The measurements by Sun and Faeth (1986) showed that bubble slip is important throughout the established plume, and that turbulent dispersion is important everywhere in the plume. Both Milgram (1983) and Kobus (1968) used propeller anemometers to measure plume liquid velocities. Marco et. al. (1996) used particle image velocimetry (PIV) in a scaled-down vessel to investigate recirculation currents for an eccentric plume. Hugi (1993) used PIV techniques with a moving bubble source to measure the trailing vortices of a bubble plume in a uniform crossflow.

These experimental studies have been limited by the inability to control bubble size and by the physical size of experimental basins. Kobus (1968) was the first to report that bubble size was purely dependent on gas flow rate, independent of the orifice diameter for a straight-tube diffuser. Matsunashi and Miyanaga (1990) confirmed this finding for the field-scale plume. McDougall (1978) created smaller bubbles by adding octanoic acid (30 ppm) to his laboratory tank. Reingold (1994) proposed a solution for bubble size control whereby sediment was used as the buoyancy source, and the plume was inverted. In trials comparing sediment to bubbles having similar slip velocities and carrying equal buoyancy, sediment was shown to be an acceptable model for air bubbles for predicting plume peeling heights in stratified environments (Reingold 1994). Reingold's (1994) tank (1.0 × 3.0 × 0.8 m deep) was not deep enough, however, to investigate several peels. Experimental basins in the literature vary widely in the lateral dimension, but most are about 1±0:3 m deep. Exceptions include Kobus (1968): 4.7 m deep, Marco et al. (1996): 2.25 m deep, and Hugi (1993): 3.0 m deep, none of whom investigated stratification.

Models of bubble plumes in stratified environments began with the integral and double-plume models of McDougall (1978), designed to predict the distribution of oil in the water column after an oil-well blow-out. The effects of gas expansion and bubble slip velocity for the stratified case were incorporated with the model of Cederwall and Ditmars (1974) as a first attempt to model the problem (McDougall 1978). Bubble plumes differ from single-phase plumes by the bubbles, which rise through the point where the simple plume traps and then are assumed to create an iterated structure of similar plumes above the periodic intrusions. McDougall (1978) does not apply his simple integral model beyond the first peel. Liro et al. (1991), however, did include the peeling process and resulting secondary plume start-up in a simple integral model. Peeling occurs in the Liro et al. (1991) model whenever the negative buoyancy of the water has a greater magnitude than the positive buoyancy of the bubbles. At that point, one-half of the volume flux, one-half of the momentum flux, and three-quarters of the buoyancy flux are arbitrarily ejected from the plume (Liro et al. 1992). The secondary plume resumes after similar adjustments to the plume width and velocity to maintain continuity.

McDougall (1978) modeled peeling in a more complicated model, called a double plume model, where the inner plume contained the bubble core and an outer, ring-shaped plume contained water only. This model was developed out of experiments he performed in a 0.6 × 0.6 × 1.3 m deep tank. The double-plume model was integrated simultaneously up to a point where the outer plume radius increased rapidly, and the velocity became negligible. At that point, the plume was beginning to peel. Several attempts were made to restart the model at a point just above the peeling zone, where the upward and downward fluxes of water in the inner and outer plumes, respectively, were balanced. The only stable solution, however, was to restart the plume just above the point where the downdraught of the peel began. At that level, the inner plume quantities remain unchanged from the previously calculated level, and the outer plume is re-started with zero volume and momentum flux. Experiments did not show quite such a dramatic necking-down of the outer plume as assumed in the model (McDougall 1978). The double-plume model was able to simulate several peeling events but underestimated the level of the first peel in the experiments by up to 40%. Baines and Leitch (1992) also reported that McDougall's (1978) double-plume analysis underpredicted the height of the first peel for their linearly stratified case.

Baines and Leitch (1983) and Lemckert and Imberger (1993) performed additional experiments in linear and step-stratified environments, confirming the qualitative findings of McDougall (1978). Asaeda and Imberger (1993) used a 1.0 × 1.0 × 0.75 m deep tank with linear stratification and variable bubble source strengths, and their observations led them to develop a hybrid double-plume model. They identified three distinct flow regimes (labeled Types 1, 2, and 3, shown qualitatively in Figure 13) and classified each flow using two non-dimensional numbers: MH and PN. MH represents the bubble source strength compared to the total pressure head, and PN represents the effect of the stratification compared to the bubble source strength. Type 1 plumes are vigorous enough that they carry all their entrained water to the surface, forming one intrusion layer. At a critical value of PN, Type 2 and 3 plumes appear. For low MH (Type 3), the plume appears to continuously peel, forming dozens of randomly spaced, finger-like peels throughout the length of the plume. Type 2 plumes occur for higher values of MH, forming several distinct peels, each remaining independent from the rest. Shadowgraph visualization of the Type 2 plumes showed that an outer plume forms a downward flowing ring from the flow separation down to the level where the intrusion layer forms. In the model proposed by Asaeda and Imberger (1993) a simple integral plume model is integrated from the source to the point where the upward momentum is zero. At that level, a second, outer plume model, is started, such that the upward flux of the inner plume is balanced by the downward flux of the outer plume (i.e 100% of the plume fluid peels). McDougall (1978) showed that the two plume fluxes should balance below this point. The outer plume entrains fluid from the inner plume and the ambient water as it descends until it reaches a level of neutral buoyancy where it is allowed to intrude. The secondary plume starts up again with zero volume flux, the buoyancy of the bubbles, and the width of the inner plume at the level where the outer plume began. This method predicted multiple peeling events better than McDougall's (1978) model but remains arbitrary in setting the initial flux in the downdraught plume and the start-up conditions of subsequent plumes.

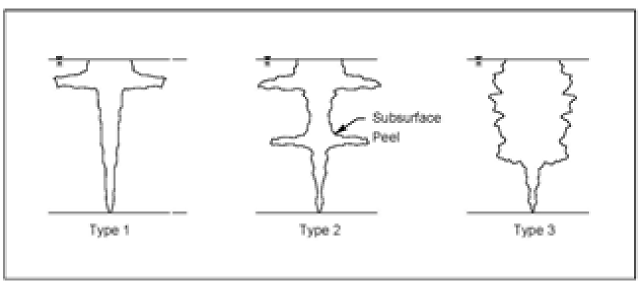

Figure 13. Schematic of plume classification as given in Asaeda and Imberger (1993)

While models are still developing, applications of bubble plumes in stratified environments have been made extensively for lake and reservoir management, both to enhance vertical mixing and to provide reaeration to the hypolimnion (Goossens 1979, Patterson and Imberger 1989, W¨uest et al. 1992, and Schladow 1993). Measurements of the surface intrusion, including the radial extent to the plunge line, the volume flow rate, and the level of the intrusion in the far-field, have been reported by several researchers for field and laboratory experiments and scale with the stratification and bubble source characteristics (Lemckert and Imberger 1993, Goossens 1979, Schladow 1993, Baines and Leitch 1992, Leitch and Baines 1989).

To assess the far-field effects of bubble plumes for reservoir management, models have been developed coupling simple integral models to various dynamic reservoir models (Goossens 1979, Patterson and Imberger 1989, and W¨uest et al. 1992). Patterson and Imberger (1989) developed a coupled model, using the simple integral model of McDougall (1978) and the one-dimensional dynamic reservoir model dyresm. They discretized the plume at the same levels as the layers in dyresm and simulated the entrainment and transport of water between layers. When the vertical velocity becomes zero, the plume is ejected horizontally (mixing across the layer instantaneously) and is restarted at the next layer. They were able to predict the new turn-over time for a reservoir that was mixed by a bubble plume and used the model to enhance the plume system design. W¨uest et al. (1992) developed a simple integral plume model, similar to Patterson and Imberger (1989), to study both reaeration and reservoir mixing. The model included gas transfer between the bubbles, calculated the concentrations of gases in the air and water, and tracked the water quality changes in the reservoir due to the presence of the plume. As the basis for a design methodology for reservoir mixing bubble plumes, Schladow (1993a, 1993b, and 1991) proposed using two important non-dimensional parameters: M and C (Modified versions of MH and PN). His design methodology was validated in a coupled plume-reservoir model like Patterson and Imberger (1989). Although simple integral models involving gas transfer, buoyancy transfer between layers, and intermediate plume peeling have been developed in these reservoir studies, detailed analysis of the peeling and intermediate intrusion dynamics have not been necessary because most of the plumes are of Type 1, having no intermediate peels. In the case of step stratification, peeling can occur at the thermocline and the surface (a form of a Type 2 plume), but the steep density gradient reduces uncertainty in the location of the peel and the level at which the intrusion layer will form (Lemckert and Imberger 1993).

Two-phase plumes play an important role in the more practical scenarios for ocean sequestration of CO2 - i.e., dispersing CO2 as a buoyant liquid from either a bottom-mounted or ship-towed pipeline. Despite much research on related applications, such as reservoir destratification using bubble plumes, our understanding of these flows is incomplete, especially concerning the phenomenon of plume peeling in a stratified ambient. To address this deficiency, a laboratory facility was built by (Scott et. al. 1999) in which fundamental measurements of plume behavior could be made. Although they used air, oil, and sediments as sources of buoyancy (rather than CO_2), by using models, the results can be directly applied to field-scale CO_2 releases to help to design better CO_2 injection systems, as well as plan and interpret the results of their up-coming international field experiment (Scott et. al. 1999).

(Tomomi and Shoji 2010) propose a three-dimensional vortex method for bubbly flow. The method is extended from the authors' two-dimensional vortex method (Uchiyama and Degawa 2006). It can consider the change of vorticity owing to the stretch, contraction, and rotation of the vortex, which are ignored in the two-dimensional method. (Tomomi and Shoji 2010) the study also applies the proposed vortex method to simulate a bubble plume, which was experimentally investigated by (Alam and Arakeri 1993), to validate the method. In a tank containing water, small hydrogen bubbles are released from the bottom of the tank. The bubbles rise due to the buoyant force and induce the water flow around them. The simulation for the plume at the starting period highlights that the rising bubbles induce large-scale eddies at their top and that a bubble cluster of a mushroom shape appears owing to the entrainment of the bubbles into the eddies. This indicates that the threedimensional transient bubbly flow, which is known to occur in a plume at the starting period, is successfully simulated by the vortex method. For the developed plume, large-scale complicated vortical flows are analyzed around the rising bubbles, and the meandering motion of the plume is also simulated. These numerical results are confirmed to agree well with the corresponding experiments, demonstrating the validity of the proposed vortex method (Tomomi and Shoji 2010).

Airlift Aerator

Full-lift hypolimnetic aerators typically consist of 1) a vertical riser tube, 2) a diffuser inside the bottom of the riser tube, 3) an air-water separation chamber at the top of the riser, and 4) one or two return pipes, called downcomers [McQueen and Lean, 1986]. Compressed air is delivered to the aerator and bubbles freely from the diffuser. This creates a positively buoyant gas-water mixture that ascends the riser. At the top of the riser, some of the bubbles are released to the atmosphere, although some may be entrained in the water that enters the downcomers. The oxygenated water flows through the downcomers and is returned to the hypolimnion [Burris et al., 2002]. One of the earliest attempts to design airlift aerators, developed by Lorenzen and Fast [1977], consists of determining approximate specifications for the compressor. The design airflow rate is based on the hypolimnetic oxygen depletion rate and the induced water flow rate through the aeration device. The authors assumed that water reaching the top of the aerator is saturated with oxygen. The water flow rate needed is found using the hypolimnetic depletion rate and volume and the change in the DO concentration. The airflow rate required to induce this water flow rate is a function of the aerator dimensions. The authors assumed that the theoretical head available in the full-lift aerator results from the difference in density between the air-water mixture in the riser and the ambient lake water. It was also assumed that half of the theoretical head is used to convey water to the surface and that the remainder is dissipated as water exits the aerator through the downcomer (Vickie 2008). The method of Taggart and McQueen [1982] involves determining the dimensions of the riser and downcomer when compressor capacity is known. The authors presented a detailed, empirically based approach for establishing full-lift aerator specifications including diffuser depth, air flow rate, water flow rate, and riser and downcomer cross-sectional areas. The water flow rate is calculated with an empirical equation that was developed using a proportionality relationship from the literature and regression of data collected from 20 published experiments. To determine the riser cross-sectional area, the authors assumed that the maximum induced water velocity is a function of the median estimated bubble rise velocity (Vickie 2008). Another empirical full-lift aerator design model was proposed by Ashley [1985]. In addition to aerator sizing, Ashley also discussed other practical design aspects including air supply, rated and actual airflow, and performance specifications. The model was derived from the work of Lorenzen and Fast [1977] and Taggart and McQueen [1982] as well as experience with a full-scale system. Ashley developed a stepwise procedure for sizing compressors and full-lift aerators. The model assumes that the induced water flow rate will completely satisfy the oxygen consumption in the hypolimnion measured during spring stratification. The model also requires an estimate of the increase in the DO concentration produced by the aerator. Determination of the DO increase is an important variable, and Ashley [1985] suggested that this parameter may be difficult to predict. Little [1995] developed a model to predict oxygen transfer in a full lift hypolimnetic aerator. Cocurrent flow of water and gas, the variation of the saturated DO concentration as a function of depth, and depletion of gaseous oxygen are accounted for in the model. Input parameters include aerator dimensions, volumetric airflow rate, diffuser depth, and ambient water conditions. To calculate the water flow rate, an empirical correlation that is a function of superficial gas velocity and riser length was developed. The correlation was derived from the same data set used by Taggart and McQueen [1982], except dependence on riser diameter was eliminated. Mass balance equations were used to determine the amount of oxygen transferred from the bubbles to the water. Literature correlations, originally developed for bubble columns and airlift reactors, were used to estimate the mass transfer coefficient and gas holdup in the riser. The model assumes that gas-phase holdup is small, that water is in plug flow, and that nitrogen transfer may be neglected. Figure 14. Shows a photograph of a full-lift aerator prior to installation. (Photo from Bob Kortmann of Ecosystem Consulting Service, Inc., used with permission. (Vickie 2008).

Figure 14. Photograph of full-lift aerator before installation. (Photo from Bob Kortmann of Ecosystem Consulting Service, Inc., (Vickie 2008)

Speece Cone

Figure 15. Photographs of Speece Cone and diffuser before installation at Camanche Reservoir, California. (Photos from Rod Jung of East Bay Municipal Utility District (Vickie 2008)

The Speece Cone, developed by Dr. Richard Speece, was originally known as a downflow bubble contact system [Speece et al., 1973; Thomas et al., 1994]. The system consists of a source of oxygen gas, a conical bubble contact chamber, a submersible pump, and a diffuser that disperses highly oxygenated water into the hypolimnion. Ambient water and oxygen gas bubbles are introduced at the top of the cone. As water flows down the cone, the velocity decreases because of the cross-sectional area of the cone increases. The system is designed so that the downward velocity of the water is sufficient to overcome the rise velocity of the bubbles at all levels. The applied water flow rate and slope of the cone walls control the water velocity and, therefore, the time available for gas transfer. Figure 15. Shows photographs of Speece Cone and diffuser prior to installation at Camanche Reservoir, California. (Photos from Rod Jung of East Bay Municipal Utility District., used with permission. (Vickie 2008) [McGinnis and Little, 1998].

Linear Bubble Plume Model for Hypolimnetic Oxygenation

As stated previously, bubble plume diffusers are one of the primary types of hypolimnetic oxygenation devices. Two areal diffuser geometries are typically installed, circular and linear. A bubble plume model to predict oxygen transfer from linear diffusers was presented by McGinnis et al. [2001], based on the model for a circular diffuser developed earlier by Wuest et al. [1992]. While several models for point-source or circular bubble plumes have been proposed [Asaeda and Imberger, 1993; Brevik and Killie, 1996; Brevik and Kluge, 1999; Cederwall and Ditmars, 1970; Ditmars and Cederwall, 1974; Fannelop and Sjoen, 1980; Johansen, 2000; Kobus, 1968; McDougall, 1978; Milgram, 1983; Rayyan and Speece, 1977; Sahoo and Luketina, 2003; Schladow, 1992; Speece and Rayyan, 1973; Tsang, 1990; Wuest et al., 1992; Zheng et al., 2002] less work has been conducted on linear (also referred to as twodimensional or planar) bubble plumes. Kobus [1968] developed one of the first detailed analytical models for linear bubble plumes, but the model calculates the transport rate of buoyancy empirically using experimental data as a function of air discharge rate and bubble size [Ditmars and Cederwall, 1974]. Cederwall and Ditmars [1970] and Ditmars and Cederwall [1974] presented a model similar to that of Kobus [1968] but included bubble slip velocity. Brevik [1977] proposed a phenomenological theory for two-dimensional bubble plumes comparable to that of Cederwall and Ditmars [1970], except that a kinetic energy equation was used to predict entrainment as opposed to assuming that entrainment is proportional to the vertical plume velocity. Wilkinson [1979] proposed that full-scale linear plumes could be characterized by a Weber number. Laureshen and Rowe [1987] presented a model for two-dimensional bubble plumes that assumed constant bubble slip velocity. Plume spreading, entrainment, and momentum amplification were assumed to be functions of the plume Weber number and empirical constants. Fannelop et al. [1991] developed a model for linear plumes in shallow water and studied the resulting surface currents and recirculation cells. Other researchers that have studied linear bubble plumes include Brevik and Kluge [1999], who expanded a previous phenomenological theory to account for the influence of vertical turbulence.

Although much insight into plume dynamics was gained, the previous models before (Vickie 2008) for linear or two-dimensional bubble plumes did not account for ambient stratification or gas transfer. The first linear bubble plume model to include gas transfer was presented by McGinnis et al. [2001], who converted the circular bubble plume model of Wuest et al. [1992] to linear geometry. The incorporation of gas transfer is critical because the rapid dissolution rate of oxygen, and nitrogen when compressed air is used, strongly influence the buoyancy of the plume [Wuest et al., 1992]. The gas transfer is especially important in deep water bodies and for weak plumes because the increased contact time allows greater gas exchange. Lastly, the prediction of oxygen addition from hypolimnetic oxygenation systems is facilitated. Despite the usefulness of the linear bubble plume model, it has not yet been validated at full scale and over a range of operating conditions. Figure 16. Shows photograph and schematic of linear bubble plume diffuser in Spring Hollow Reservoir, VA, U.S.A. (Courtesy of Mark Mobley, Mobley Engineering, Inc.) (Vickie 2008).

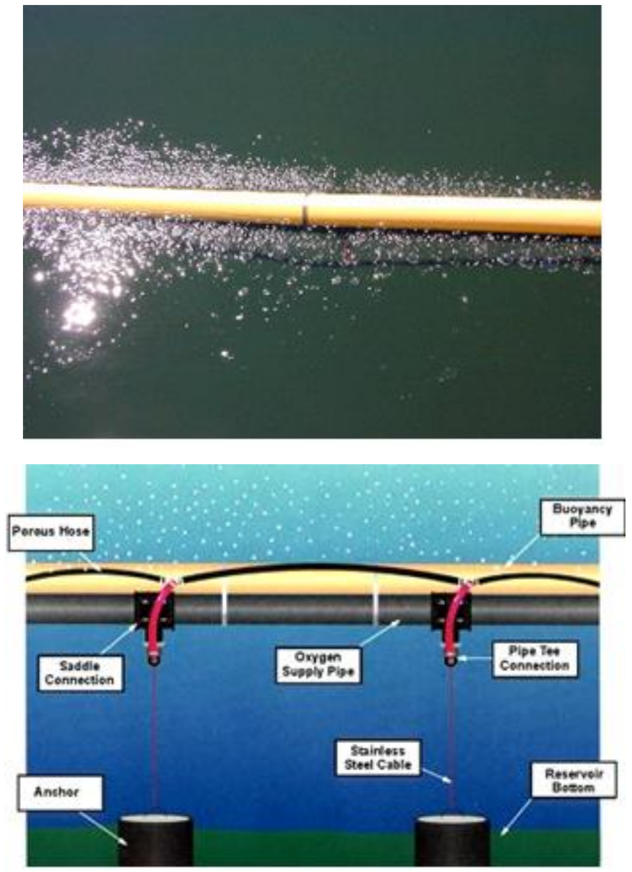

Figure 16. Photograph and schematic of linear bubble plume diffuser in Spring Hollow Reservoir, VA, U.S.A. (Courtesy of Mark Mobley, Mobley Engineering, Inc.) (Vickie 2008)

Coupled Bubble-Plume/Reservoir Models for Hypolimnetic Oxygenation

While bubble plumes are successful at adding oxygen, the added energy may induce large-scale hypolimnetic mixing. An unconfined bubble plume is in intimate contact with the ambient water column and is strongly influenced by the local density profile. Plume-induced mixing changes the thermal structure of the reservoir, and plume performance depends strongly on the vertical density gradient, establishing a feedback loop that continually changes plume behavior [McGinnis et al., 2004]. Mixing may partially erode the thermocline and subsequently lead to warming of the hypolimnion and even premature destratification of the reservoir. Higher hypolimnetic temperatures and plume-induced mixing may also be responsible for increased sediment oxygen uptake (SOU). Many studies have reported that small increases in water velocity above lake sediments can significantly increase SOU [Arega and Lee, 2005; Beutel, 2003; Hondzo, 1998; Josiam and Stefan, 1999; Lorke et al., 2003; Mackenthun and Stefan, 1998]. Because the sediment is the largest sink of oxygen in most lakes and reservoirs, the effect of plume-induced mixing must be included to avoid serious under-sizing of oxygenation systems. The specific plume-induced mixing mechanisms should be identified and incorporated in a coupled bubble-plume/reservoir model for successful design and operation (Vickie 2008).

Several models for predicting plume dynamics and/or oxygen transfer from bubble plumes have been developed [Singleton and Little, 2006], but less research has focused on modeling the interaction between bubble plumes and ambient water bodies. Most of the coupled bubble-plume/reservoir models proposed in the literature involve whole-lake artificial circulation or destratification systems and, consequently, do not account for oxygen transfer from the bubbles [Johnson et al., 2000; Schladow, 1993]. Similar to Schladow [1993], Lindenschmidt and Hamblin [1997] coupled the one-dimensional hydrodynamic model DYRESM with stirrer and bubbler modules to simulate mixing induced by Limnox hypolimnetic aerators, an enclosed type of aeration device. To analyze the effectiveness of bubble plume destratification on reducing algal blooms, Imteaz and Asaeda [2000] coupled DYRESM with a bubble plume model and an ecological model that tracks factors related to phytoplankton growth. Bravo et al. [2007] used a comprehensive and commercially available hydrodynamic model, FLUENT, and constructed a two-fluid, dispersed turbulence model to simulate bubble plume dynamics. Despite their performance and applicability, none of these coupled models included mass transfer between the bubbles and water, which is critical to predicting the performance and evaluating the effectiveness of hypolimnetic oxygenation systems (Vickie 2008).

A destratification system:

Water bodies, such as lakes and reservoirs, experience seasonal temperature stratification with warmer water at the surface and colder water at the bottom. Temperature stratification is strongest during the late summer months because of the high incidence of solar radiation. This energy input warms the surface of the reservoir, causing large thermal gradients in the water body. The thermal gradients impede circulation and internal mixing and restrict the transport of oxygen from the surface layers to the bottom. As a consequence, the cold water (hypolimnion) deep in the reservoir becomes isolated from the warmer surface water (epilimnion). Biochemical processes in the reservoir water and at the reservoir bottom use oxygen. Because oxygen is not transported to the hypolimnion from the epilimnion, low oxygen concentrations, or even anaerobic conditions are created at these lower depths. Under anaerobic conditions, water quality suffers because of trace metal dissolution, nutrient release that stimulates eutrophication, production of hydrogen sulfide gas, and a lowering of the pH (Kreshimir and Hienz 1994).

Destratification, as its name implies, has the objective of disrupting thermal stratification to allow natural processes to improve the quality of the lake. The induced mixing and circulation acts to cool the epilimnion and warm the hypolimnion, resulting in a more uniform temperature profile throughout the water column. Destratification of a lake or reservoir eliminates or minimizes the undesirable anaerobic conditions of the lower layers by mixing the hypolimnion and epilimnion and exposing the water to the surface where oxygen absorption occurs. A destratification system operates by adding energy to the water body through an artificial means to destratify the lake or reservoir. Depending upon its specific character, usually, a destratification system results in the cyclical mixing of the water column (Figure 17). The induced circulation brings the cooler, oxygen-deficient bottom water to the surface where reaeration occurs. The warmer, oxygen-rich surface waters are entrained and displaced to the lower depths causing an increase in the temperature and dissolved oxygen content of the bottom water (Kreshimir and Hienz 1994).

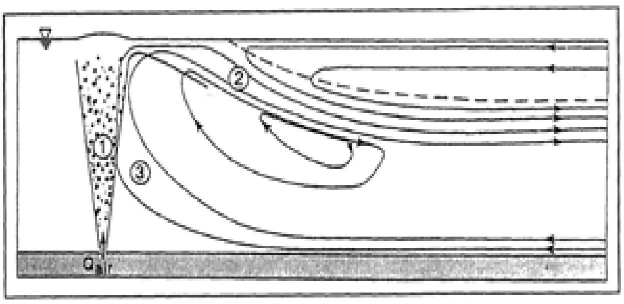

Figure 17. Destratification systems

The two types of destratification systems used are classified as hydraulic or pneumatic devices. The hydraulic systems pump water as the mechanism for imparting energy to the reservoir for destratification. Axial flow pumps or direct drive mixers are examples of hydraulic destratification systems (Price 1988; Punnet 1991). These axial flow pumps generate a low-velocity jet by rotating a large-diameter propeller (6- to 15-ft) at a slow speed. On the other hand, the direct-drive mixers generate a high-velocity jet by rotating a small-diameter propeller (1- to 2-ft) at high speed. The axial flow pumps generate a high discharge because of the large diameter propeller; however, the flow is at low velocity. The direct drive mixers produce a high-velocity jet; therefore, they add more momentum to the jet but must rely on entrainment to increase the pumped volume of water (Kreshimir and Hienz 1994).

Pneumatic systems operate by introducing a continuous stream of air bubbles to the water column. As the air is released, a bubble plume is formed consisting of air bubbles and entrained water. The bubble plume creates a flow of water from the hypolimnion to the surface. When the bubble plume reaches the surface, the entrained hypolimnetic water spreads horizontally until density causes it to plunge to a region of neutral density. This cycle continues until the density difference of the water column above the diffuser is essentially zero. Occasional operation of the pneumatic diffuser after uniform density is reached maintains a destratified condition by continually disrupting newly established stratification in the reservoir. Pneumatic systems are usually composed of three parts: an onshore air compressor, a supply line, and a diffuser system. Diffuser systems may be a point source or line source. A line source diffuser is often fabricated by drilling holes in a pipe that permits air to escape. This type of diffuser allows the bubble plume to form vertical recirculation cells on either side of the line diffuser. A point source diffuser releases air at essentially a single point along the supply line and forms a radial circulation pattern (Kreshimir and Hienz 1994).

The airflow discharged into water rapidly expands, due to the pressure drop across the nozzle, and breaks up into bubbles of discrete size. This initial formation of the gas bubbles has been studied both theoretically and experimentally, see for instance, (Davidson and SchUler 1960). Several studies on the motion of gas bubbles in liquid are reported in the literature. (Haberman and Morton 1954) carried out a comprehensive investigation on the rise velocity of single air bubbles in still water (Klas and John 1970).

The similarity between the air-bubble plume and a simple buoyant plume was first pointed out by (Taylor 1955) in a discussion on the use of pneumatic breakwaters. (Bulson 1962) derived semiempirical relations for maximum velocity and thickness of the layer of horizontal surface flow. (Sjoberg 1967 and Kobus 1968) have studied the flow induced by air-bubble systems both experimentally and theoretically using the similarity to jet and plume mixing.

Bubble Pump:

Contrary to conventional dual and triple pressure absorption refrigeration cycles, a single pressure absorption cycle does not require mechanical work to pump fluid from the absorber to the higher-pressure generator. However, the single pressure cycle does require a mechanism to lift the fluid from the generator to the absorber against gravity and friction. A bubble pump, or vapor-lift pump, is used for this task because it requires only thermal energy input as the driving force, which is the same as that required to drive the absorption cycle. In a bubble pump, heat addition creates vapor, thereby increasing the buoyancy of the fluid causing it to rise through a vertical tube under two-phase flow conditions. Airlift pumps have been used for decades in the oil industry that run on the same principles, however, instead of bubbles forming from the phase change involved with boiling the liquid, the air is injected into the flow, creating the same buoyancy effect (Susan 2001). While two-phase vertical flow and air-lift pumps have been studied since the early part of the last century, experimental studies are performed by (Susan 2001) while different existing two-phase flow models' results are compared to the experimental data. The best-suited model is used to carry out parametric studies and to optimize for maximum efficiency under various operating conditions. Optimum efficiency is defined as the liquid pumped per unit of bubble pump heat input. The results show there is an optimum bubble pump tube diameter for a given set of operating conditions. The results are discussed, and conclusions are drawn regarding designing a bubble pump for a single pressure absorption cycle that will lift the required liquid fluid flow rate with the minimum bubble pump thermal input (Susan 2001).

Conventional vapor compression and absorption refrigeration systems are dual pressure cycles where the saturation temperature difference between the condenser and evaporator is produced by a system pressure difference. This requires a mechanical input to drive the compressor or pump needed to generate this change in pressure, which adds significantly to the noise level and cost of the system while reducing the reliability and portability. On the other hand, single pressure absorption refrigeration systems, such as the Platen and Munters (1928) diffusion-absorption cycle and the Einstein cycle (1928), use at least three working fluids to create temperature changes by imposing partial pressures on the refrigerant. While termed "single pressure" there are still slight overall pressure variations within these cycles due to low friction and gravity. So, despite there being no need to pump the fluid to a much higher pressure to create a change in saturation temperature, a mechanism is needed to move the fluid through the cycle against flow friction and gravity. To eliminate the need for a mechanical input, a heat-driven bubble pump is used for this purpose. The bubble pump component is analyzed so that design for optimum performance can be achieved (Susan 2001).

Dual Pressure Absorption Cycles

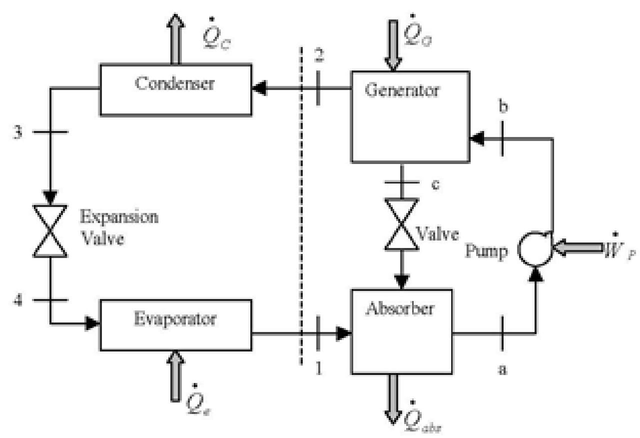

Figure 18. Dual Pressure Absorption System (Moran and Shapiro 1996)

In a dual pressure absorption system, the refrigerant circulates through the condenser, the expansion valve, and the evaporator in much the same way as in a vapor compression system (Figure 18). However, an absorption-generation process replaces the compressor. Now, instead of compressing a vapor between the evaporator and the condenser as in a vapor compression refrigeration cycle, the refrigerant is absorbed by a secondary substance, called an absorbent, to form a liquid solution. The liquid solution is then pumped to a higher pressure (Susan 2001).

Because the average specific volume of the liquid solution is much less than that of the refrigerant vapor, significantly less work is required than in a vapor compression cycle. Accordingly, absorption refrigeration systems have the advantage of relatively small work input compared to vapor-compression systems (Moran and Shapiro, 1996). A generator is needed in the absorption cycle to separate the refrigerant vapor from the liquid solution before the refrigerant enters the condenser. This involves heat transfer from a relatively high-temperature source. The refrigerant then flows to the condenser, while the absorbent is throttled back to the lower pressure as it falls to the absorber (Susan 2001).

Single Pressure Absorption Refrigeration

Two single pressure absorption refrigeration cycles are the Einstein Cycle (Einstein and Szilard 1928) and Platen and Munters' diffusion absorption cycle (von Platen and Munters 1928). Because of their single pressure operation, they can completely avoid the need for electric power, along with its associated central power plant and electric distribution infrastructure, and instead, rely on a direct thermal energy source. This helps avert the need to wastefully convert heat to work and then back to heat. They also use environmentally benign fluids, an increasingly important issue as several manmade refrigerants are phased out over the next few years. Additionally, they are portable, reliable, operates silently, and are inexpensive to build. However, with relatively low refrigeration COP's, they have limited applications. When used for heating, both cycles can achieve efficiencies over 100% (Schaefer, 2000). In this situation, when competing against direct-fired heating devices, the low COP is less of an issue (Susan 2001).

The Platen-Munters Cycle

The Platen-Munters (1928) cycle is similar to a dual-pressure ammonia-water absorption cycle with an inert gas, usually, hydrogen, diffused through the system to maintain a uniform system pressure throughout the cycle. As shown in Figure 19, the diffusion-absorption cycle consists of a generator, bubble pump, absorber, and condenser with ammonia, water, and hydrogen as the working fluids. When heat is supplied to the generator (5), bubbles of ammonia gas are produced from the ammonia-water mixture. The ammonia bubbles rise and lift with them the weak ammonia-water solution, (weak in ammonia), through the bubble pump lift tube. The weak solution is sent to the absorber (6), while the ammonia vapor rises to the condenser (1). In the condenser, heat is removed from the ammonia vapor causing it to condense to a liquid at the system's total pressure. The condensed ammonia flows down into the evaporator (2). The hydrogen supplied to the evaporator passes across the surface of the ammonia, lowering the partial pressure on the liquid ammonia. This reduction in the partial pressure allows the liquid ammonia to evaporate at a lower temperature. The evaporation of the ammonia extracts heat from the evaporator, providing refrigeration to the desired space. The mixture of ammonia and hydrogen vapor falls from the evaporator to the absorber (3). A continuous trickle of weak ammonia-water solution enters the upper portion of the absorber (6). It is fed by gravity from the bubble pump. This weak ammonia-water solution absorbs the vapor ammonia leaving the light hydrogen to rise back to the evaporator (4). Finally, the strong ammonia-water solution flows back into the generator/bubble pump system (5), thus completing the cycle (Susan 2001).

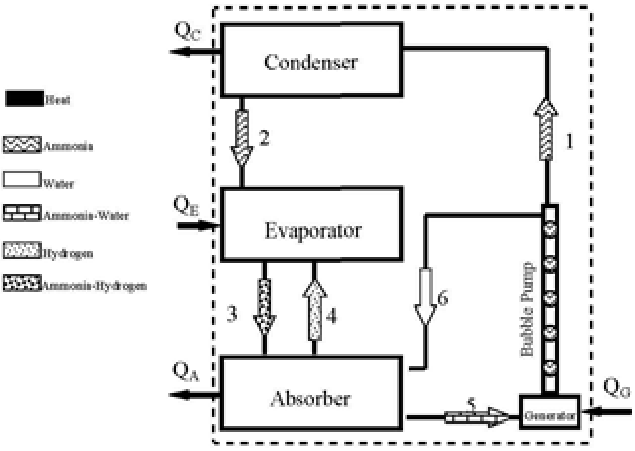

Figure 19. Diffusion-Absorption Cycle

The diffusion-absorption cycle has a niche market in the recreational vehicle and hotel room refrigerator markets (Herold et. al. 1996). It is manufactured in many parts of the world today. These units have a COP of approximately 0.15 to 0.2. Since its invention, several attempts have been made to make it more competitive with dual pressure cycles by improving its efficiency, but at refrigeration temperatures, a COP of approximately 0.3 is the best-published efficiency (Chen et. al. 1996).

The Einstein Cycle

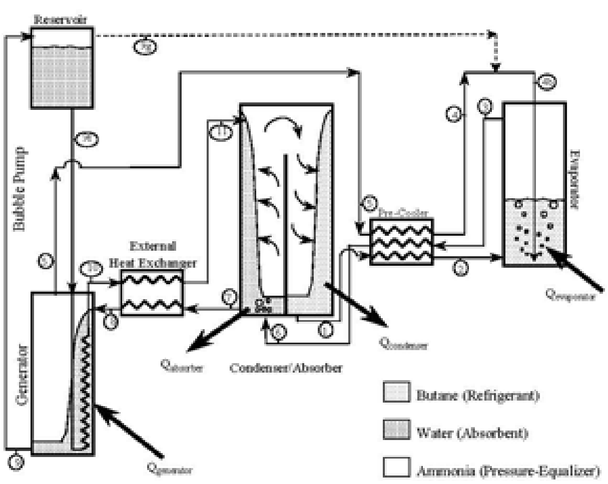

Figure 20. The Einstein Refrigeration Cycle

In 1928 Einstein and Szilard also patented a single pressure absorption cycle. Delano (1998) performed a design analysis of the cycle and added two regenerative heat exchangers to improve efficiency. These include an internal regenerative heat exchanger in the generator and an evaporator pre-cooler. His cycle schematic can be seen in Figure 20. Unlike the Platen-Munters cycle, the Einstein cycle uses a pressure-equalizing absorbate fluid rather than an inert gas. In the Einstein cycle, butane is the refrigerant, water remains the absorbent, and ammonia becomes the pressure-equalizing fluid. The generator, bubble pump, and evaporator are the same as the Platen-Munters cycle, but the condenser and absorber are combined into a single unit. It also operates as a single pressure system. In the evaporator, the partial pressure on the entering liquid butane is reduced by ammonia vapor, allowing it to evaporate at a lower temperature. In the condenser/absorber, the partial pressure of the butane vapor coming from the evaporator is increased when the ammonia vapor is absorbed by liquid water, thus allowing the butane to condense at a higher temperature. The liquid butane and liquid ammonia-water naturally separate due to their respective density differences and the fact that ammonia water is immiscible with butane at the condenser/absorber's temperature and pressure. The ammonia is then separated from the water in a generator by the application of heat (Susan 2001).

While early models predicted the cycle's cooling COP to be about 0.4, more recent studies have shown it to be about 0.2 (Shelton, et. al. 1999), which is relatively low compared to the thermal efficiency of dual pressure refrigeration cycles, but competitive with the diffusion-absorption cycle. One advantage of the Einstein cycle is its use of a different generator absorbate, ammonia, than that used in the evaporator, butane. This decouples the temperature difference between the generator/condenser and the condenser/evaporator allowing more flexibility in cycle design (Susan 2001).

Information on bubble pumps, also known as vapor-lift pumps, is sparse in the open literature. Percolating coffee makers are a well-known application of bubble pumps. Heat addition to the fluid at the base of a vertical tube creates vapor, thereby increasing the buoyancy of the fluid causing it to rise through the vertical tube under two-phase flow conditions, as seen in figure 21. The work of (Delano 1998) has addressed the design of a bubble pump for use in a single pressure absorption refrigeration cycle, with others (Schaefer 2000, Sathe 2001) referencing this model.

Air-lift pumps are very similar to vapor-lift pumps, with a different mechanism to increase the buoyancy of the fluid. There is much more information available in the open literature on air-lift pumps. Most are based on the assumption of two-phase slug flow. Additionally, few have the same range of lift (~0.5 to 1 m) and diameters (~6 to 10 mm) that are applicable to the current study. Both air and vapor-lift pumps, however, are simply two-phase flow in a vertical tube; therefore, two-phase flow models can be used to analyze the system (Susan 2001).

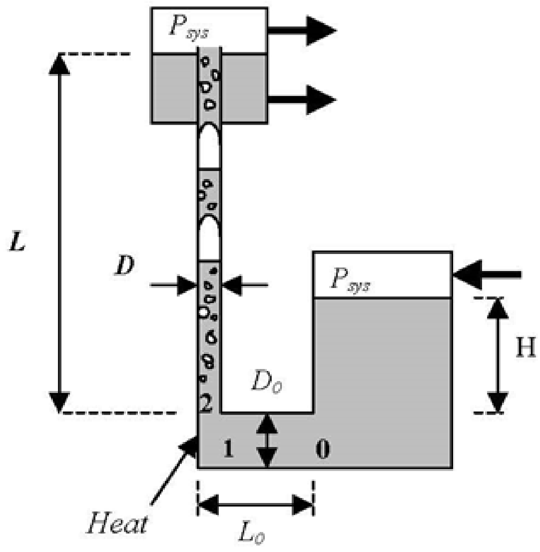

Figure 21. Bubble Pump Configuration

Einstein Cycle Bubble Pump

Delano (1998) designed a model, based on the air-lift pump analysis of Stenning and Martin (1968), and analyzed the performance of the bubble pump of the Einstein cycle. It uses momentum balances and assigns a value recommended by Stenning and Martin (1968) for the slip ($S=V_G/V_L$) between phase velocities to model the two phases involved. Schaefer (2000) used Delano's (1998) model with a turbulent single-phase friction factor instead of an experimentally determined one. In addition, Schaefer analyzed the relationship of diameter, submergence ratio, mass flow rate, and heat input to maximize performance.

Platen-Munters Cycle Bubble Pump

Recently there has been a lot of interest in the Platen and Munters cycle. Herold et. al (1996) give a review of the details of its operation and performance. Chen et. al (1996) investigated the diffusion-absorption cycle for enhancing its performance. The result was a new design for the bubble pump/generator configuration. The original design combines the generator and the bubble pump into one component, with only one heat addition. The modified version heats the strong ammonia solution first, extracting most of the ammonia from the water so that a weak ammonia solution is sent to the bubble pump where another heater causes the solution to boil and rise, due to increased buoyancy, through the lift tube. This design is virtually identical to the bubble pump/generator configuration in the Einstein cycle; therefore, the same bubble pump model can be used for both cycles (Susan 2001). Chen et al (1996) experimentally found that this new configuration increased the cycle COP by about 50%, however, a detailed theoretical model was not developed in this publication. Earlier, Hassoon (1989) provided a theoretical model and experimental results for a bubble pump that used injected steam for lift instead of vaporizing the liquid in the tube. However, it modeled a lift tube that was cooled along its length. Its application was for an ammonia-water absorption heat pump. More recently, Sathe (2001) used Delano's (1998) methodology applied to the Platen-Munters' bubble pump.

Air-Lift Pumps

Air-Lift pumps run on the same principles as vapor-lift pumps except that air is injected to increase the buoyancy of the fluid instead of bubbles forming from liquid vaporization. Although air-lift pumps have a wide variety of possible applications, most studies have been concerned with dewatering mines or raising oil from dead wells. More recently, the importance of airlifts in moving liquids at nuclear fuel reprocessing plants has been realized, requiring more accurate design equations (Clark and Dabolt 1986). There is a large amount of literature on air-lift pumps, and since their operation is similar to that of bubble pumps, their analyses can be readily applied to bubble pumps. Stepanoff (1929) used a thermodynamic approach to investigate air-lift pumps and was able to physically describe their performance but offered no empirical data to back up the analysis. Pickert (1932) analyzed the performance of air-lift pumps, but as with many other studies, this was prior to the development of the two-phase flow theory. It must also be mentioned that most of these publications refer to generally large lift tubes, diameters 25-300 mm and lengths 10-200 m, well out of the range of the current study. However, Nicklin (1963) speculated that increased efficiency might be obtained by using small-diameter tubes at low flow rates, realizing along with White and Beardmore (1962) and Zukoski (1966) that as the tube diameter is decreased below 20 mm, the effects of surface tension on the dynamics of vertical slug flow become increasingly important.

With recent progress during the second half of the last century in understanding two-phase flows, Stenning and Martin (1968) introduced the basic principles of two-phase flow and momentum for investigating relatively small diameter and low lift air-lift pumps. Stenning and Martin's (1968) model is the starting point for Delano's (1998) analysis of the bubble pump. A study of the performance of the air-lift pump is carried out in the Stenning and Martin study. Liquid water volume flow rate (Q_L) is plotted versus air volume flow rate (Q_G) for various submergence ratios (H/L). It was determined that there is an airflow rate that produces a maximum water flow rate for a given tube diameter. Delano (1998) produces the same plots in his study and defines his bubble pump to operate at this maximum water flow rate. Lately, Kouremenos and Staicos (1985) carried out their investigations on small diameter air-lift pumps down to 12 mm diameters and low lift in the range of 1 to 3 m, with submergence ratios between 0.55 and 0.7. In the current study, the lift tube diameters considered are slightly smaller than this, with a larger range of submergence ratios. Also, Kouremenos and Staicos devised their experiments to obtain "perfect" slug flow. For the current study, the flow regime was originally not constrained, however after performing experiments it was found that the most efficient flow regime was slug flow. Clark and Dabolt

(1986) published a model to predict the height to which an airlift pump operating in the slug flow regime can lift a given volumetric flow rate of liquid, given the airflow rate and the pressure at the point of gas introduction. The focus of their study was on accurately designing very tall airlifts for nuclear fuel reprocessing, but it did not attempt an accurate description of the frictional pressure losses in the lift tube and used an approximation of the general Lockhart-Martinelli (1949) correlation (de Cachard and Delhaye 1996). More recent studies investigating the application of air-lift pumps in nuclear fuel reprocessing, such as de Cachard and Delhaye (1996), have been most interested in the accuracy of the air-lift pump model rather than with the efficiency. The extent to which they explore the two-phase fluid flow details around Taylor bubbles in the lift tube to obtain the frictional pressure drop is beyond the scope of this study. Certain assumptions have been made to simplify the model considerably, without risking much degradation inaccuracy due to the small scale of the bubble pump to be used (Susan 2001).

Theory of Small Diameter Airlift Pumps

A typical airlift pump configuration is illustrated in figure 22. A gas, usually air, is injected at the base of a submerged riser tube. As a result of the gas bubbles suspended in the fluid, the average density of the two-phase mixture in the tube is less than that of the surrounding fluid. The resulting buoyant force causes a pumping action. The slug flow regime is most widely encountered in airlift pump operation and is characterized by bubbles large enough to nearly span the riser tube. The length of the bubble's ranges from roughly the diameter of the tube to several times this value. The space botWG8n the bubbles is mostly liquid-filled and is referred to as a liquid slug (Govier and Aziz, 1972). The large gas bubble is also referred to as a gas slug or Taylor bubble (Douglas 1987). Extensive experimental and theoretical work has been done on airlift pumps in the slug flow regime (Apazidis, 1985; Clark and Dabolt, 1986; Hjalmars, 1973; Higson, 1960; Husain and Spedding, 1976; Jeelani et al., 1979; Nicklin, 1963; Richardson and Higson, 1962; Sekoguchi et al., 1981; Slotboom, 1957; Stenning and Martin, 1968). These studies have been confined to air/water systems in tubes with a diameter greater than 20 mm in which the effects of surface tension are small and have therefore been neglected (Douglas 1987). As tube diameter is decreased below 20 mm, the effects of surface tension on the dynamics of vertical slug flow become increasingly important (Bendiksen, 1985, Nickens, and Yannitell, 1987; Tung and Parlange, 1976; White and Beardmore, 1962; Zukoski, 1966). It has been speculated that increased efficiency might be obtained by using small diameter tubes at low flow rates (Nicklin, 1963).

The results and discussion of a study of the effects of tube diameter on vertical slug flow, specifically as it relates to 3 -25 mm airlift pump performance are presented by (Douglas 1987). The theory previously presented by Nicklin (1963), is extended into this range of tube diameters by considering the effects of surface tension on bubble rise velocity. Differences are noted between the rise velocity of a single gas slug and a train of gas slugs in small vertical tubes. Comparisons are made between experimental observations and theoretical predictions (Douglas 1987). A difference has been observed between a single bubble and bubble train slug flow in air-water systems at low Reynolds numbers. When a single gas slug rises in a moving liquid stream the velocity profile coefficient approaches a value of 2.0 for low Reynolds number flow in air/water systems. This indicates a laminar velocity profile in the liquid ahead of the gas slug. When a series of gas slugs rise concurrently with a series of liquid slugs, the velocity profile coefficient remains at a value of 1.2 for Reynolds numbers as low as 500. This indicates turbulent flow in the liquid slugs. It is believed that this difference is the result of vorticity generated in the liquid film surrounding the gas slugs and, in their wake, (Douglas 1987). It has been shown that including this effect and the effects of surface tension on bubble rise velocity allows the airlift pump theory previously described by Nicklin (1963) to be extended to lower tube diameters of from 3 mm to 20 mm. It has also been shown that airlift efficiency and optimal submergence ratio increase in this range of tube diameters. The theory described by (Douglas 1987) can be used with confidence to design small diameter airlift pumps.

Hydrodynamics of the Airlift Pump in Bubble and Bubbly-Slug Flow

A typical airlift pump configuration is illustrated in figure 22. A gas, usually air, is injected at the base of a submerged riser tube. As a result of the gas bubbles suspended in the fluid, the average density of the two-phase mixture in the tube is less than that of the surrounding fluid. The resulting buoyant force causes a pumping action. Extensive experimental and theoretical work has been done on the airlift pump (Castro et al., 1975; Clark and Dabolt, 1986; Kouremenos and Staicos, 1985; Murray, 1980; Nicklin, 1963; Reinemann et al., 1987; Richardson and Higson, 1962; Slotboom, 1957; Stenning, and Martin, 1968; Todoroki et al., 1973). These studies have been confined, however, to the slug flow regime (Douglas 1987). In slug flow, the gas phase is contained in large bubbles that nearly span the tube and range in length from the tube diameter to several times this value. These are referred to as gas slugs or Taylor bubbles. The liquid filling the space between the Taylor bubbles is referred to as the liquid slug. The liquid between the Taylor bubbles and the tube wall is referred to as the liquid film (see figure 22) (Douglas 1987).

Other flow patterns are possible in vertical gas/liquid flow. In bubble flow, the bubble diameter is much smaller than the tube diameter and the bubbles are distributed over the pipe cross-section. Bubbles remain close to their initial size, and there is little interaction between bubbles (see figure 23). The bubble flow pattern has been largely neglected in the studies of the airlift pump because it has been assumed to be absent in the useful operating regime. Clark et al (1985) presented a theoretical treatment of the airlift in the bubble flow regime but offers no experimental verification and does not clearly define the bubble flow operating regime (Douglas 1987). An intermediate regime referred to as bubbly-slug flow has been observed in several studies (Akagawa and Sakaguchi, 1966; Fernandes et al., 1983; Mao and Duckler, 1985; Nakoryakov and Kashinsky, 1982; Nakoryakov et a1., 1986, Serizawa et a1., 1975 and 1992; Shipley, 1984). In bubbly-slug flow, small bubbles are found in the liquid slug (see figure 22). The presence of these bubbles is due to the region of extreme turbulence encountered at the tail of the Taylor bubble. Small bubbles are broken off the Taylor bubble and dispersed in the liquid slug (Douglas 1987).

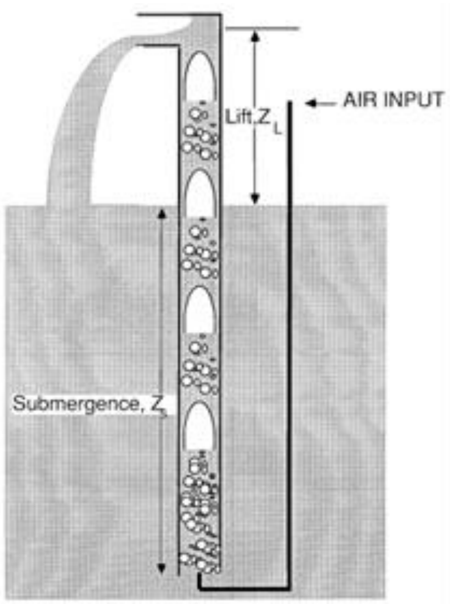

Figure 22. Typical Airlift Pump

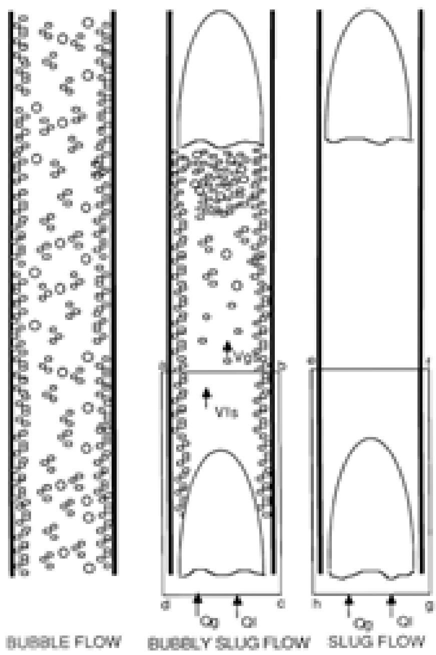

Figure 23. Flow Patterns in Airlift Pump Operation

In previous studies of bubble and bubbly-slug flow dynamics, the liquid motion has been pump-driven (Akagawa and Sakaguchi, 1966; Clark and Flemmer, 1985; Fernandes et al., 1983). In airlift operation, the sole driving force is that developed by buoyancy. As a result of this difference, many of the previous two-phase flow studies have been conducted at flow velocities much higher than those encountered in airlift operation. The objective of the (Douglas 1987) study is to determine the hydrodynamics of bubble and bubbly slug flow in the range of gas concentrations and liquid velocities generally encountered in airlift pump operation. The results and discussion of a study of the flow dynamics of a 38 mm diameter airlift pump are presented by (Douglas 1987). Flow patterns ranged from dispersed bubble flow to bubbly-slug flow. The effects of initial bubble size and water quality on flow dynamics and flow pattern transition are examined. Experimental data are compared with previous two-phase flow models and a new prediction equation is presented for the bubbly-slug flow regime. Equations have been presented to describe the operation of the airlift pump in the bubble and bubbly-slug flow. The effect of small bubbles dispersed in the liquid slug on the average gas velocity in bubbly-slug flow has been accurately predicted. The stable operating regimes for bubble and bubbly-slug flow have been identified. The transition from bubble flow to bubbly-slug flow was found to be sensitive to gas/liquid surface contamination. Surface contamination did not however significantly influence flow dynamics. Due to bubble breakup and dispersal in the liquid slug, it is doubtful that true slug flow will ever exist in the normal operating regime of airlifts except for narrow diameter tubes (D < 20 mm, for air/water systems (Douglas 1987).

Oxygen Transfer in Airlift Pumping

The airlift pump has been of practical use as a pumping device for many decades (see figure 22). It has been reported that the famous Roman water distribution system used airlifts 2000 years ago. Airlifts also found application in removing water from mines in the late 1800s. The first recorded pumping studies were performed at that time and have continued to the present. Airlifts have become popular in the aquaculture industry and in wastewater treatment plants where large volumes of water must be both circulated and aerated. Several studies have been done on the aeration properties of the airlift (Nagy, 1979; Zielinski et al., 1978) but no theory or predictive equation for oxygen transfer rates was given before (Douglas 1987). The flow dynamics of the airlift pump have been described previously (Reinemann et al., 1987). Complicating the prediction of the hydrodynamics of the airlift is the fact that there are two flow patterns possible in airlifts when tube diameters are greater than about 20 mm. When the initial bubble size is much smaller than the tube diameter and the gas void ratio is low, the bubble flow pattern results. Small bubbles are distributed over the pipe cross-section. Bubbles remain close to their initial size, and there is little interaction between bubbles (see figure 23). If the gas void fraction is above some critical value, coalescence occurs, and bubble size increases (Douglas 1987).

Bubbles with an average diameter greater than about 0.7 times the riser tube diameter are referred to as gas slugs or Taylor bubbles. The presence of Taylor bubbles only is referred to as the slug flow regime. The slug flow regime has been found to occur only when the riser tube diameter is below 20 mm (Reinemann et al., 1987).

In the bubbly-slug flow regime, small bubbles are found suspended in the liquid slug between the Taylor bubbles. The presence of these bubbles is due to the region of extreme turbulence encountered at the tail of the Taylor bubble. Small bubbles are broken off of the tail of the Taylor bubble and dispersed in the liquid slug. Experiments were performed in both the bubble flow and bubbly slug flow regimes to determine if any significant difference existed between the gas transfer properties in these two regimes (Douglas 1987). The results of an experimental study of the oxygen transfer properties of a 38 mm diameter airlift pump are presented. The effects of varying initial bubble size, flow rate, flow pattern, and water quality on oxygen transfer are examined. A model to predict oxygen transfer in airlift pumping is presented by (Douglas 1987). Oxygen transfer was not significantly affected by flow pattern, initial bubble size, or the wastes present in the water studied. Wastes in the water did however influence the transition from bubble to slug flow. An empirical correlation is presented relating the oxygen transfer coefficient (Kla (20)), to the two-phase pipe Reynolds number. It is not advantageous to use a small pore gas diffuser to increase gas transfer in airlift pumps. Reducing the orifice size increases the pressure drop across the diffuser and the gas transfer rate will not increase (Douglas 1987).

As a summary (Douglas 1987) conducted a theoretical and experimental study pertaining to the pumping and aeration properties of the airlift pump and its application in intensive aquaculture facilities. The results and discussion of a study of the effects of tube diameter on vertical slug flow, specifically as it relates to 3 -25 mm airlift pump performance, are presented: Theory of Small Diameter Airlift Pumps. The theory previously presented by Nicklin (1963) is extended into this range of tube diameters by taking into account the effects of surface tension on bubble rise velocity. Differences are noted between the rise velocity of a single gas slug and a train of gas slugs in small vertical tubes. Comparisons are made between experimental results and theoretical predictions. The results and discussion of a study of the flow dynamics of a 38 mm diameter airlift pump were presented as experimental flow patterns ranging from dispersed bubble flow to bubbly-slug flow to study the Hydrodynamics of the Airlift Pump in Bubble and Bubbly-Slug Flow. The effects of initial bubble size and water quality on flow dynamics and flow pattern transition are examined. Experimental data are compared with previous two-phase flow models and a new prediction equation is developed for the bubbly-slug flow regime. The results of an experimental study of the oxygen transfer properties of a 38 mm diameter airlift pump are presented: Oxygen Transfer in Airlift Pumping. The effects of varying initial bubble size, flow rate, flow pattern, and water quality on oxygen transfer are examined. A model to predict oxygen transfer in airlift pumping is presented (Douglas 1987).

The propagation of pressure waves and breaking waves

Gas bubbles may be released at high points in liquid lines after rapid pressure reduction. This may happen in a force main when the sudden stoppage of a pump occurs either during normal operation or because of an emergency condition such as power failure. This may also happen in a long gravity main owing to the closure of a valve located near the upstream end of the main. The presence of gas bubbles in liquids, even in minute quantities, has important effects on the propagation of pressure waves in closed conduit flow. The combination of high compressibility of the gas phase and large inertia of the liquid phase yields a very low acoustic velocity for the two-phase mixture, which may be much lower than the acoustic velocity of the gas phase alone (Phu D. Tran 2011).

Campbell and Pitcher (1958) studied the propagation of finite-amplitude pressure waves in a shock tube containing a stationary mixture of liquid and gas bubbles. By neglecting the compressibility of the liquid phase and pipe wall elasticity and applying conservation equations across the shock wave, an expression for the shock velocity was derived that assumed a particularly simple form when the temperature rise across the wave was also neglected. Mori et al. (1975) extended the work of Campbell and Pitcher to include the effect of pipe wall elasticity on the velocity of pressure waves and found that this effect should not be neglected for mixtures at atmospheric pressure with void fraction below 0.01. Enever (1967, 1972) was the first to apply Campbell and Pitcher's method to the analysis of pressure waves attributable to sudden valve closure in a pipe containing an initially flowing bubbly mixture. The pressure wave was rendered stationary by a velocity transformation; conservation equations were then written across the wave, considering the compressibility of the liquid phase while ignoring pipe wall elasticity and temperature change across the wave. Bryant (1975) extended Enever's work to include the effects of pipe wall elasticity and temperature change across the wave. Both Enever's and Bryant's models result in polynomial equations in two unknown variables, which require a complex iterative procedure to yield numerical solutions for wave velocity and pressure ratio. Moreover, Bryant ignored the effects of pipe anchoring and wall force in the momentum equation and only included the effect of temperature change on internal energy in the energy equation while ignoring the effect of pressure change. Martin and Padmanabhan (1975), Martin et al. (1976), Padmanabhan et al. (1978a), and Chaudhry et al. (1990) applied a numerical method to the analysis of pressure wave attributable to sudden valve closure in two-component bubbly flow. They considered the case of isothermal homogeneous flow whereby liquid compressibility and pipe wall elasticity were included, but relative velocity between the two phases and temperature change across the wave was neglected. The emphasis of their work was on how the pressure wave attenuated as it propagated against the incident flow and how it reflected at the system boundary. This approach was adopted by Akagawa et al. (1983), who also investigated the reflection of the pressure wave at the interface between a flowing single-phase liquid column and a two-phase bubbly column. Considerable research efforts have been made in the past decade, notably by Guinot (2001), to improve the numerical methods for the simulation of transient two-phase flows. By using the experimental data by Chaudhry et al. (1990), Leon et al. (2008) found that the Godunov method can be used to simulate pressure wave propagation in bubbly flows as accurately as the method of characteristics but more efficiently in terms of computing time. The studies of Martin, Akagawa, Guinot, Leon, and their coworkers did not elaborate on how wave velocity and pressure rise would change with initial pressure, fluid velocity, and void fraction; these are aspects of interest in engineering.

Martin and Padmanabhan (1975), Martin et al. (1976), and Padmanabhan and Martin (1978b) carried out the earliest experimental investigations on pressure surges generated by rapid closure of a valve in two-component, horizontal, and vertical bubbly flows with a pressurized reservoir as the upstream system boundary, with initial void fraction at the valve in the range of 0.015–0.047 and superficial liquid velocity in the range of 1.4–3.2 m/s. Akagawa and coworkers (1979, 1980, 1983) conducted experimental investigations of pressure surges generated by rapid closure of a valve at the end of a horizontal pipe with a pressurized reservoir as the upstream system boundary in two-component bubbly flow and in flow including an interface between a liquid column and a bubbly column, with initial void fraction at the valve in the range of 0.025– 0.24 and superficial liquid velocity in the range of 1.4–3.2 m/s. Huang et al. (2005) measured the velocity of pressure waves generated by the oscillation of a membrane located near the upstream end of a flowing bubbly mixture, with a void fraction in the range of 0.05–0.30 and superficial liquid velocity in the range of 0.5–1.5 m/s.

The propagation of pressure waves in two-component bubbly flow was analytically and experimentally investigated. An analysis is presented that accounts for the effects attributable to liquid compressibility, pipe elasticity, and temperature rise across pressure waves. Analytical results indicate that the effects of liquid compressibility and pipe wall elasticity are important at low gas content, although the effect of temperature change is generally negligible. Pressure waves were generated in the laboratory by a rapid closure of a valve at the downstream end of a horizontal pipe. The experimental results indicate that there were two major pressure surges generated by valve closure; the first was attributable to the stoppage of the two-phase mixture at the valve, and the second was attributable to the arrest of the liquid column at the upstream end of the mixing device. The transient flow model provides a satisfactory prediction of the initial pressure rise at the valve and the average velocity of the initial pressure waves (Phu D. Tran 2011).

A pressure transient analysis for two-component bubbly flow in a horizontal pipe was presented by (Phu D. Tran 2011). The purpose of this analysis is to provide a general relationship between wave velocity and pressure rise concerning the initial pressure, velocity, and void fraction, considering the effects of temperature change across the pressure wave, pipe wall elasticity, and liquid compressibility. This general relationship is expressed in the form of a polynomial equation that can be reduced to simple cases such as isothermal flow, with allowance for liquid compressibility, pipe wall elasticity, and isothermal flow with incompressible liquid and rigid pipe (Phu D. Tran 2011).

Wave propagation in bubbly fluids has attracted investigators for many decades because of its special properties. Bubbly fluids have the unique feature that even a minute bubble concentration (volume fraction less than one percent) significantly increases the compressibility of the system. The system transports energy at a speed considerably lower than the sound speeds in both phases because of the energy exchange between the liquid and the bubbles. When additional effects such as vaporization and condensation play a role, e.g., in cavitating flows, further phenomena, still little understood, are superimposed upon the basic behavior of bubbly flows. The rich internal structure of bubbly flows endows the medium strikingly complex behavior (Tianshi et. al. 2007).

The wave propagation in bubbly fluids has been studied using a variety of mathematical models. Significant progress has been achieved in the study of systems consisting of noncondensable gas bubbles (Beylich and Gülhan 1990, Caflisch and Miksis 1985, Watanabe and Prosperetti 1994, van 1972) and vapor bubbles (Finch and Neppiras 1973 and Hao and Prosperetti 1999). The treatment of the kinetic and thermal properties of the medium, e.g., the compressibility of the liquid and the thermal conduction, by different authors, varies. But they shared a common feature that the two phases were not separated explicitly, i.e., the bubble radius and concentration were considered as functions of time and space. The Rayleigh-Plesset equation or the Keller equation governing the evolution of spherical bubbles has been used as the kinetic connection between the bubbles and fluid. These models include many important physical effects in bubbly systems such as viscosity, surface tension, and thermal conduction. Numerical simulations of such systems require relatively simple algorithms and are computationally inexpensive. Nevertheless, homogenized models treat the system as a pseudofluid and cannot capture all features of the rich internal structure of the bubbles. They exhibit sometimes large discrepancies with experiments (Watanabe and Prosperetti 1994) even for systems of noncondensable gas bubbles. Their range of validity is limited to small void fractions and small amplitude waves. These models are also not suitable if the bubbles are distorted severely by the flow or even fission into smaller bubbles, as it may happen in cavitating and boiling flows (Ceccio and Brennen 1991 and

Kuhn et. al. 1995).

The direct numerical simulation (DNS) method, which solves the full nonlinear system of compressible fluid dynamics equations in every component of the multiphase domain, is potentially free of these deficiencies. DNS is based on techniques developed for free surface flows. (Welch 1995) numerically investigated the evolution of a single vapor bubble using the interface tracking method. (Juric and Tryggvason 1998) simulated the boiling flows using the incompressible flow approximation for both liquid and vapor and a simplified version of interface tracking. 3D simulations of very large volume fraction fluids using a method of front tracking with incompressible liquid approximation were also reported (Delale et. al. 2005). DNS simulations of small void fraction bubbly fluids using front tracking for compressible fluid equations were performed (Tianshi et. al. 2007).

(Taylor 1955) explained how bubble-breakwaters were operated employing a surface jet produced by a bubble plume. He also demonstrated theoretically that the surface flow in the direction against the waves can break them.

Taylor has proposed the use of such plumes as wave breakers. To be effective the surface current generated should be stable for a distance of the order of the wavelength, which in turn could be several times the depth. It appears that the formation of recirculating cells can affect the wave-breaking potential of line bubble plumes. The flow structure in the far-field of line-source bubble plumes in shallow water is investigated. The influence of the cross-sectional geometry of the channel on the cell structure is investigated experimentally. Observations and measurements of the cell structure associated with line bubble plumes as obtained in a model towing basin of dimensions 1 × 1 × 40 m. Different criteria for the definition of the cell length have been examined, such as the surface flow rate, the surface velocity, and surface flow patterns. Flow velocities in the plane of symmetry have been measured using a propeller anemometer. These results have been supplemented by measurements with an acoustic Doppler velocimeter. The velocity distributions show a strong influence on the cross-sectional geometry. For an analysis of the flow in the far-field, a model based on an analogy of the surface flow with a free (half) jet with counterflow is proposed. The study contains a complete theory for line bubble plumes, including the effects of compressibility, bubble slip, and finite release volume, as well as a simplified similarity analysis useful in estimating plume properties and horizontal-current depth and velocity [I. R. Riess and T. K. Fanneløp 1998 and Fannelop, T., Hirschberg, S., & Küffer, J. (1991)].

Recent progress is reviewed in the understanding of the relationship between the dynamics of breaking and the sound generated by breaking waves. Gently Breaking waves entrain a small number of bubbles that may break up, resonate and relax toward their equilibrium shape. Measurements of the sound spectrum under gently spilling waves are shown to be consistent with a simple model of the acoustics based on the resonant relaxation of individual bubbles. More energetic breaking may lead to significant entrainment with recent laboratory and field measurements showing void fractions of O (10^{-1}) or more. At these large void fractions, the entrained air becomes dynamically significant and up to 50% of the energy lost from the surface wave field by breaking may be expected by entraining air against buoyancy forces. Bubble clouds of the large void fraction may oscillate collectively and radiate sound at frequencies such as lower than the resonant frequencies of the individual bubble (W. K. Melville et. al. 1992).

Bubbles are ubiquitous in the near-surface ocean and are important in the climate system. They are known to elevate the net air-sea gas transfer rate, enhance the equilibrium gas saturation level [e.g., Woolf, 1997; Hare et al., 2004; D'Asaro and McNeil, 2007; Wanninkhof et al., 2009], and modify the optical and acoustical properties of the near-surface ocean at moderate to high ocean surface wind speeds [e.g., Lamarre and Melville, 1991; Zhang et al., 1998; Terrill et al., 2001; Anguelova and Webster, 2006]. They are also used as passive tracers to study upper ocean dynamics, such as the distribution of breaking waves at the ocean surface [Melville and Matusov, 2002], and the evolution of Langmuir circulations (LCs) [Zedel and Farmer, 1991; Farmer and Li, 1995] as well as tidal fronts [Baschek and Farmer, 2010].

Bubbles near the ocean surface are generated during the breaking of surface gravity waves. A few laboratory studies [e.g., Lamarre and Melville, 1991; Asher and Farley, 1995; Deane and Stokes, 2002] have been carried out to investigate the bubble field during and immediately after the breaking of surface gravity waves. Lamarre and Melville [1991] found that up to 50% of the wave energy lost during wave breaking is used to entrain bubbles. Deane and Stokes [2002] showed that bubbles formed under breaking waves have a well-defined size spectrum. The spectrum implies that bubbles with a radius smaller than the Hinze scale (~1 mm) are generated due to entrainment while larger bubbles are fragmented by the turbulent flows. The evolution of bubbles in a laboratory channel has also been investigated numerically [Shi et al., 2010; Liang et al., 2011; Ma et al., 2011]. Wave breaking generates a vortex in the cross-wave direction [Melville et al., 2002; Sullivan et al., 2004]. This vortex, propagating in the wave direction, advects both the bubbles and the dissolved gases from bubbles.

(Shoichi et. al. 1984, Shoichi et. al. 1985, and Hassan et. al 1998) have examined the air- bubble curtains (bubble plumes) i.e., two-dimensional water flows induced by rising air bubbles as a new type of oil control barrier. They obtained velocity distribution, momentum, and width of the tidal current. They also examined the hydrodynamical performance of the plume. Observing the oil leakage through the plume fundamentally by using both grains polyethylene and actual oil films. They examined the profile of the horizontal water velocity behind the plume in the current and the performance of the surface flow breaking waves. Furthermore, they investigated the critical velocity of the current under which the air-bubble curtain can prevent spilled oil from spreading with waves. They also found that the efficiency of breaking waves is 27% against waves of 3 m height without current and decreases as both wavelength and the current velocity increase. The upper limit of the current velocity against the surface flow, which can prevent spilled oil from spreading, is found to be 0.3 m/sec for the co-existence of waves of 10 m wavelength and 0.5 m wave height. Furthermore, they examined the vertical distribution of the water velocity behind the plume in the current and in the waves, and the performance of the plume for breaking waves.

The evolution of bubbles in a turbulent oceanic boundary layer is different from in a laboratory flume due to the presence of boundary layer turbulence. After injection by breaking surface gravity waves, bubbles move with oceanic boundary layer turbulence, exchange gases with ambient water, and change size. Large bubbles will burst at the ocean surface, and small bubbles will fully dissolve into the ocean (Figure 24). Some early in situ observations show that the mean bubble number density decreases exponentially with depth [e.g., Johnson and Cooke, 1979; Thorpe, 1982; Crawford and Farmer, 1987]. Bubbles of radius between 50 µm and 150 µm are more abundant than smaller and larger bubbles [e.g., Farmer et al., 1998; Garrett et al., 2000]. Recent observations focus on the detailed structure of bubble plumes and the correlation of bubble penetration and surface wind speed [e.g., Trevorrow, 2003; Vagle et al., 2010]. There are very few numerical modeling studies of bubble distribution in the ocean. Thorpe et al. [2003] model bubbles of 70 µm under the influence of idealized Langmuir cells. They conclude that Langmuir cells are effective in subducting bubbles of that size and note that sophisticated models including the information of boundary layer turbulence are needed for a better understanding of subsurface bubble distributions. Because of the incomplete knowledge of subsurface bubble evolution, the role of bubbles in upper-ocean dynamics and climate is not well understood. The abundance of near-surface bubbles suggests that their buoyancy may weaken the downward branch of Langmuir circulations [Smith, 1998]. By examining the in-situ measurements of subsurface bubble distributions, Thorpe et al. [2003] conclude that the buoyancy effect of bubbles is not important at a wind speed of 11 m/s. Gases pass in and out of the ocean through both the atmosphere-ocean interface as well as bubbles [e.g., Woolf, 1997]. Due to hydrostatic pressure and surface tension exerted on bubbles, the air-sea gas transfer rate is larger, and the equilibrium saturation level is higher in the presence than in the absence of bubbles. Although the conceptual idea of how bubbles contribute to air-sea gas exchange is widely accepted, there has not been a consensus on the functional form of bubble-mediated air-sea gas transfer parameterization [e.g., Woolf and Thorpe, 1991; Asher et al., 1996; Woolf, 2005; McNeil and D'Asaro, 2007; Wanninkhof et al., 2009]. Liang et al. [2011] recently reported on a bubble model that calculates the concentrations of bubbles of multiple sizes with multiple gas components. The model successfully simulates essential bubble processes including gas dissolution, size change, buoyant rising, and advection by turbulent flows. The bubble model is coupled with a Large Eddy Simulation (LES) model capable of simulating boundary layer turbulence [Sullivan and McWilliams, 2010].

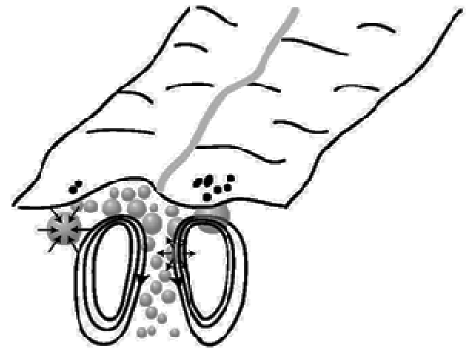

Figure 24. The evolution of subsurface bubbles after injection by breaking waves

The evolution of bubbles in a turbulent oceanic boundary layer is simulated using a multi-size multi-gas bubble model coupled with a Large Eddy Simulation model. Bubbles injected by breaking waves are brought into the boundary layer by episodic bubble plumes, and they form near-surface streaks in the convergence zone of Langmuir circulations. The equilibrium bubble distribution decays exponentially with depth and is a manifestation of intermittent bubble plumes whose bubble number density is at least one order of magnitude higher than the mean bubble number density. Bubble distribution in the injection zone is influenced by injection, turbulent transport, and dissolution. Bubble distribution below the injection zone is determined by the strength of turbulence and dissolution. For a given sea state, bubble e-folding depth increases linearly with friction velocity. Wave age is an additional governing parameter for bubble e-folding depth. The buoyancy of bubbles weakens both Langmuir circulations and near-surface turbulent kinetic energy dissipation. The buoyancy effect increases with wind speed. Gas flux through bubbles depends on both wind speed and wave age. For a given sea state, the bubble flux increases with wind speed to the fifth power (Jun-Hong et. al. 2012).

Bubble plumes are used in a variety of industrial and environmental applications including mixing in chemical reactors, stripping of dissolved gases, containment of spills, prevention of ice formation, protection of harbors from damaging waves [Fannelop et al., 1991], and destratification of lakes and reservoirs [Schladow, 1992]. In addition to airlift aerators [Burris et al., 2002] and Speece Cones [McGinnis and Little, 1998], bubble plumes are commonly used for hypolimnetic aeration and oxygenation, which preserves stratification of water bodies while adding oxygen to the deepest layer. Hypolimnetic anoxia negatively affects the drinking-water treatment process, cold-water fisheries, and water quality downstream of hydropower reservoirs. In the U.S., releases from hydropower reservoirs typically must comply with state water quality criteria for minimum dissolved oxygen (DO) concentrations [Peterson et al., 2003]. Oxygen depletion may lead to increases in hydrogen sulfide, ammonia, and phosphorus, and the release of reduced iron and manganese from the sediments. Hydrogen sulfide, iron, and manganese in drinking water usually require additional treatment [Cooke and Carlson, 1989]. Finally, hypoxia can affect sex differentiation and development, resulting in male-dominated populations with reduced reproductive success [Shang et al., 2006].

A bubble plume model to predict oxygen transfer from linear diffuser systems was presented by McGinnis et al. [2001], based on the model for a circular diffuser developed earlier by Wuest et al. [1992]. While several models for point-source or circular bubble plumes have been proposed [Asaeda and Imberger, 1993; Brevik and Kluge, 1999; Ditmars and Cederwall, 1974; Fannelop and Sjoen, 1980; Johansen, 2000; Kobus, 1968; McDougall, 1978; Milgram, 1983; Rayyan and Speece, 1977; Sahoo and Luketina, 2003; Schladow, 1992; Wuest et al., 1992; Zheng et al., 2002] less work has been conducted on linear (also referred to as a line, twodimensional, or planar) bubble plumes. Kobus [1968] developed one of the first analytical models for linear bubble plumes, which uses an empirical correlation to calculate buoyancy flux. Ditmars and Cederwall [1974] presented a model similar to that of Kobus [1968] but included bubble slip velocity. Brevik [1977] proposed a phenomenological theory for two-dimensional bubble plumes comparable to that of Ditmars and Cederwall [1974], except that kinetic energy was used to predict entrainment. Wilkinson [1979] proposed that full-scale linear plumes could be characterized by a Weber number. Laureshen and Rowe [1987] presented a model for two-dimensional bubble plumes in which plume spreading, entrainment, and momentum amplification were assumed to be functions of the plume Weber number and empirical constants. Fannelop et al. [1991] developed a model for linear plumes in shallow water and studied the resulting surface currents and recirculation cells. Lastly, Brevik and Kluge [1999] expanded an existing model for linear bubble plumes to account for vertical turbulence. Although much insight into plume dynamics was gained, none of these models for linear or two-dimensional bubble plumes accounted for ambient stratification or gas transfer. The first linear bubble plume model to include gas transfer was presented by McGinnis et al. [2001], who converted the circular bubble plume model of Wuest et al. [1992] to linear geometry. The incorporation of gas transfer is critical because the rapid dissolution rate of oxygen, and nitrogen when compressed air is used, strongly influence the buoyancy of the plume [Wuest et al., 1992]. A gas transfer is especially important in deep water bodies and for weak plumes because the increased contact time allows greater gas exchange. Lastly, the prediction of oxygen addition from hypolimnetic oxygenation systems is facilitated. Despite the usefulness of the linear bubble plume model, it has not yet been validated at full scale and over a range of operating conditions (Vickie 2008).

Using extensive, high spatial-resolution CTD (conductivity and temperature as a function of depth) transect data collected in Spring Hollow Reservoir (SHR), VA, the U.S.A. during diffuser operation in 2003 and 2004, the performance of the linear bubble plume model is evaluated. The motivation for (Vickie 2008) work includes verification of model performance before use for design and investigation of critical model parameters through sensitivity analysis. Also, the accuracy of model predictions for the depth of maximum plume rise (DMPR) and induced water flow rate should be assessed prior to coupling with lake/reservoir hydrodynamic and water quality models, such as CE-QUAL-W2 [McGinnis et al., 2001]. An improved linear bubble plume model is presented by (Vickie 2008), observations and model predictions are compared, and results of sensitivity analysis are discussed (Vickie 2008).

Gas-liquid mixing in stirred vessels is ubiquitous within the industry. For bioreactors, gas dispersions are traditionally carried out using radial disc turbines such as the Rushton turbine. However, improved performance has been observed with axial flow impellers. Additionally, the use of an up-pumping mode has been demonstrated as a more efficient means of dispersing the gas phase than a down-pumping mode for some types of hydrofoil impellers (Nienow *et al*., 2004).

Cell damage is also an issue in the operation of bioreactors, particularly for animal cells where the cells are of delicate construction due to the lack of a cell wall. Despite substantial evidence that cells are not damaged by fluid shear, but by the action of bursting bubbles at the liquid free surface which can be mitigated by the addition of anti-foam agents (e.g. Pluronic^{TM}), this myth still persists within the industry. Some newly designed ‘Elephant Ear Impellers’ (EE), with large solidity ratio and deep blades, have been marketed as low shear impellers due to their large swept volume and good gas dispersion characteristics (Hui et. al. 2007). Particle Image Velocimetry (PIV) is a ‘whole field’ imaging technique that obtains a near-instantaneous velocity field within a plane in a flow illuminated usually by a laser sheet. Average flow field behavior and turbulent flow parameters can be extracted from multiple image pairs. This technique has been applied to gas-liquid flows by Aubin *et al*. (2004), who compared mixing performance in an aerated tank using both up-and down-pumping pitched blade turbines (PBT) (Hui et. al. 2007). To perform PIV in a two-phase system, it is necessary to separate the movement of the seeding particles, which are assumed to follow the liquid, from the motion of the gas bubbles. This was accomplished by using red fluorescent seeding particles that emit light at 575 nm. A 545 nm bandpass filter is fitted to the camera, which only allows light with a wavelength greater than 545 nm to pass through and this blocks out incident laser light (532 nm) which is scattered by gas bubbles or the liquid free surface. Hence this allows the velocity field of the liquid phase only to be obtained (Hui et. al. 2007). In (Hui et. al. 2007) paper, the hydrodynamics of the liquid phase in a model aerated bioreactor of diameter, *T*=0.15 m, stirred by up-and down-pumping ‘Elephant Ear’ (EE) impellers (D/T=0.45) have been studied using Particle Image Velocimetry (PIV). Airflow rates, of 0.01 to 0.05 vvm (typical for animal cell culture) and 0.5 vvm were used. PIV was used to obtain the average velocity field from 500 image pairs in a vertical plane in the tank. The Power number, global flow field, and turbulent quantities have been studied. Measured turbulent power numbers *Po* were not affected upon gassing, i.e., Pog/Po ≈ 1 for the up-pumping mode. For the down-pumping EE impeller, *Po* decreased by up to 30% at the highest gas flow rate. The presence of gas does not have a significant effect on the global flow field and mean liquid velocities at lower gas flow rates, but for a higher flow rate of 0.5 vvm, aeration slightly alters the liquid flow pattern and liquid velocities were decreased by aeration for both up-and down-pumping EE impellers. Maximum values of turbulent kinetic energy (TKE) are also relatively unaltered, but the distribution of TKE in the bulk of the liquid phase changes significantly and the mean values are decreased. Flow numbers decrease by 20-30% from the single-phase values at the highest gas flow rate studied. The results show that the up-pumping mode provides a more stable flow configuration with higher gas-hold-up than the down-pumping mode for these classes of agitators (Hui et. al. 2007).

Enhanced mass transfer and water purification:

Enhanced mass transfer associated with bubble plumes is widely observed and exploited in engineering applications, with water purification using ozone bubble plumes being one of them. The plume mass transfer efficiency is one of the key parameters in practice as it is desirable to achieve high mass transfer efficiency when an expensive gas such as ozone is used (Xiaobo et.al. 2006). A simple analysis of the mass transfer inside a bubble plume reveals that the mass transfer process is affected by several factors. They are the gross area of the contact surfaces between the gas and liquid phases, the contact time of bubbles with the liquid, and the mass transfer rate of individual bubbles. The gross contact area depends on the bubble diameter. At the same void fraction, the contact area increases as the size of the bubble decreases. The contact time depends mainly on the bubble diameter that which increases when the bubble size reduces as smaller bubbles rise slower than big ones. However, simply reducing the bubble size may not be the most cost-effective solution for achieving high mass transfer efficiency, when we consider the difficulty of generating small bubbles in practices. In addition, the contact time is also affected by the detailed plume structure such as flow circulation since it affects the rising speed of bubbles in the plume as well. Furthermore, the mass transfer rate of individual bubbles cannot be determined easily as it depends on the interaction between the mass transfer process and the detailed plume structure. Therefore, to find the optimal operation conditions, a realistic model must be used that considers the complex and transient nature of the flow structures inside the plume (Xiaobo et.al. 2006).

In contrast to the ensemble-average analysis that averages the variables both in time and space, modeling the mass transfer process in bubble plumes from the viewpoint of fluid mechanics will help us to understand the mechanisms of the phenomena more fundamentally. Fleischer et al. (1996) were the first to set up a one-dimensional model for studying the dissolution of carbon dioxide in an aqueous solution of sodium hydroxide. Bauer and Eigenberger (1999) proposed a multi-scale approach in which a simplified reactor model interacts with detailed models for hydrodynamics, mass transfer, and bubble interactions. Based on a two-fluid approach, they analyzed the influence of hydrodynamics on local and global mass transfer processes. The multi-scale modeling concept was further applied in their successive study (Bauer and Eigenberger, 2001) in which a bubble column reactor with a non-isothermal reaction was modeled and simulated. In contrast to Bauer and Eigenberger’s works which employed a bubble density function to determine the mean local bubble size, models based on the Euler-Lagrange representation, which tracks individual bubble size, have been reported by Machane et al. (1999), Darmana et al. (2004, 2005) and Gong et al. (2004). Under this Euler-Lagrange framework, the motion and diameter change of individual bubbles are tracked explicitly, and previous work on plume structure and mass transfer properties of single bubbles could be readily incorporated into the study of the mass transfer process in bubble plumes.

The mass transfer process inside a bubble plume is closely related to the local plume structure inside a confined container, which depends on the location and motion of individual bubbles. The presence of bubbles in an initially quiescent liquid inside a confined container leads to buoyancy-driven circulations. Continuously injected bubbles induce a mean upward flow of the liquid-bubble mixture (the plume region), and the unsteady vortices generated at the boundary of the main plume region and the surrounding liquid cause transient and spatial variations of the plume. The plume structure of bubble columns has been numerically and experimentally studied extensively in recent years for various engineering applications, as reviewed by Joshi et al. (2002). Sokolichin et al. (2004) reviewed and assessed the modeling and simulation of buoyancy-driven bubble flows. Starting from the two-fluid approaches, the two-way coupling method using a gas-liquid mixture equation, which was referred to as a weaker two-way coupling compared with the two-way coupling proposed by Drew (1983), was introduced, and discussed in detail. Among the four most extensively discussed problems as analyzed in Joshi et al. (2002), the numerical comparison between the Euler-Euler and the Euler-Lagrange approaches is the first on the list. As reported by Sokolichin and Eigenberger (1997), both approaches may agree with each other quantitatively if a proper discretization method is used for the Euler-Euler method. Generally, it is believed that to capture the essential features in a bubble column, a 3D dynamic model might be necessary (Delnoij et al. 1997; Pfleger et al. 1999; Sokolichin and Eigenberger 1999; Pfleger and Becker 2001).

Many of the numerical studies conducted in recent years use the standard k-ε turbulent model (Sokolichin and Eigenberger 1999; Pfleger et al. 1999; Borchers et al. 1999; Pfleger and Becker 2001) or large-eddy simulations based on the Smagorinsky model (Deen et al. 2001; Darmana et al. 2004, 2005). These computations are applicable to engineering applications with a large gas flow rate and the liquid flow is usually in the turbulent regime. Detailed studies of the transient properties of the plume at small gas flow rates, which are important for validating numerical models, are not as common. Valuable work on the instability of plane bubble plumes can be found in Alam and Arakeri (1993) in which experiments with fine hydrogen bubbles (diameter around 130μm) at a low void fraction (from 0.03% to 0.08% at the bubble generating zone) were performed to study the transition height, wavelength, and wave velocity of an unstable plane plume. Murai and Matsumoto (1998) investigated the effect of the bubble diameter and void fraction on the plume structure. More recently Caballina et al. (2003) studied the effect of the Grashof number on the height of transition in a plane plume using 2D numerical simulations.

(Xiaobo et.al. 2006) study the mass transfer process of ozone dissolution in a bubble plume inside a rectangular water tank, as a model problem for a water purification system. The effect of bubble diameter and plume structure on the mass transfer efficiency of ozone in bubble plumes is investigated numerically. To capture the detailed plume structure, interaction between liquid and bubbles is treated by a two-way coupling Euler-Lagrange method. The motion of the continuous phase (a mixture of liquid and gas bubbles) is solved using a finite difference method in an Eulerian framework. The motion of the dispersed phase (bubbles) is tracked individually in a Lagrangian fashion. The ozone transfer process from bubbles to liquid is computed by modeling the mass transfer rate of individual bubbles. Their numerical results show a nonlinear dependence of the ozone dissolution efficiency on the initial bubble size. The dissolution efficiency varies rapidly when the initial bubble size reaches a certain value while the change of efficiency is much slower at other bubble sizes. Therefore, for a given tank size it is not necessary to generate bubbles much smaller than the optimal size. This result is of importance for engineering since it is difficult to generate small bubbles in practice. Their results also show that the instantaneous dissolution rate of ozone could be increased by increasing the initial volumetric fraction of ozone inside bubbles even up to 20% while maintaining the dissolution efficiency (Xiaobo et al. 2006).

Environmental application (drinking water treatment, lakes, reservoirs, …)

Excess phosphorous loading in lakes and reservoirs increases the content of organic matter, which, through decomposition, increases oxygen demand. Many eutrophic lakes do not contain sufficient hypolimnetic dissolved oxygen (DO) to meet this demand during the stratified season and become anoxic before the advent of deepwater convection in winter [Beutel and Horne, 1999]. As a result, anoxic products such as methane, hydrogen sulfide, ammonia, iron, manganese, and phosphorus are formed [Ga¨chter and Mu¨ller, 2003]. These conditions cause environmental and drinking water treatment problems, which vary depending on the water use. For drinking water sources, water depletion of DO may lead to taste and odor problems, increased treatment costs, and increased formation of disinfection by-products [Cooke et al., 1993]. For cold-water fisheries, low hypolimnetic DO stresses or eradicates fish populations, and eggs deposited in anoxic sediments may not develop. Hypoxia itself has been shown to be an endocrine disruptor and negatively impacts fish reproduction [Wu et al., 2003]. Anoxic reservoir releases also negatively impact downstream water quality [Beutel and Horne, 1999]. Preventing the occurrence of anoxia in the hypolimnion may be achieved with oxygenating bubble plumes [Wuest et al., 1992] or other oxygenation systems such as the Speece Cone [McGinnis and Little, 1998] or airlift aerator [Burris et al., 2002]. The advantage of hypolimnetic oxygenation is the ability to replenish DO while preserving thermal stratification [Nakamura and Inoue, 1996; Beutel and Horne, 1999]. Bubble-plume diffusers inject air or oxygen with a relatively weak gas flow rate using small (<2 mm diameter) bubbles [Wuest et al., 1992; McGinnis and Little, 2002]. This application lends itself to deeper lakes where the bulk of the bubbles dissolve in the hypolimnion, and the plume momentum is small enough to prevent intrusion into the thermocline, which would otherwise lead to warming of the hypolimnion [Wuest et al., 1992]. Penetration of phosphorus-laden plume water into the photic zone can also fuel further algal growth. Minimizing these potential problems requires a better understanding of the performance of bubble plumes. Besides, the plume-lake interaction, particularly in the near field, may play a significant role in determining plume behavior. Many bubble plume models have been developed, most were tested in laboratory settings (McDougall, 1978; Asaeda and Imberger, 1993; Borchers et al., 1999; Brevik and Kristiansen, 2002] or in limited in situ studies [Wuest et al., 1992; Lemckert and Imberger, 1993; Mobley, 1997; Johnson et al., 2000).

Previous models before (D. F. McGinnis et. al. 2004) typically assume steady-state conditions and do not account for short- and long-term temporal and spatial alteration of the density structure or water quality with the associated change in plume dynamics. Such changes may result from seasonal (climatic) warming and cooling, reservoir operation (withdrawal), inflow, seiching, and the plume-lake interaction itself. A steady-state bubble-plume model is evaluated using full-scale temperature, salinity, and dissolved oxygen data collected in a Swiss lake by (D. F. McGinnis et. al. 2004). The data revealed a plume-generated near-field environment that differed significantly from the ambient far-field water column properties. A near-field torus of reduced stratification developed around the plume, the extent of which is on the same lateral scale as the horizontal dislocations generated by persistent first mode seiching. The plume fallback water was found to penetrate much deeper than expected, thereby maintaining reduced vertical gradients in the near-field torus. The plume entrains a portion of the fallback water leading to short-circuiting, which generates a complex plume-lake interaction and reduces far-field downwelling relative to the upward plume flow. As the integral plume model incorporates the entrainment hypothesis, it is highly sensitive to near-field environmental conditions. After identifying appropriate near-field boundary conditions the plume model predictions agree well with the field observations (D. F. McGinnis et. al. 2004).

Oil Fence:

The above shows that bubbly flow has very wide applications in many aspects of life. One important application is using it as a new type of oil fence that can generate a strong and wide surface flow over the bubble generation system.

In case of accidents of tankers and seaside oil refineries, oil barriers (oil fences) are usually set on the water surface to prevent spilled oil from spreading. Many types of barriers were developed so far. However, the existing oil control devices are not always effective for containing oil slicks on actual sea surfaces. Hence, improvements in the performance of barriers are required especially for high values of current velocity, wave height, and wind velocity (Hassan 2002, 2003, 2006, 2011, 2012, 2013, Hassan and Tamer 2006, Abdulmouti, et. al. 2000, Hassan et. al. 1997, 1998, 1999-No. 1, 1999- No. 2 and 2001, Hassan and Esam, 2013).

Figure 25. The Japan Sea in Fukui disastrously polluted by heavy oil leakage from a Russian oil tanker in early 1997

Figure 26. Oil pollution in the Japan Sea

Figure 27. Oil fence on a polluted sea area

Figure 28. People cleaning the Japan Sea from oil (1997)

It is well known that seas and oceans are exposed to pollution by oil leakages. The Japan Sea including Echizen-Kaigan in Fukui was disastrously polluted by heavy oil leakage from a Russian oil tanker in early 1997 as shown in Figs. 25- 29. Another accident in Boston in June 2000 happened due to a tanker collision with a small ship as shown in Fig. 30 and Fig. 31. Many other accidents have happened in many areas of the world. These incidents are the motivation for the development of a new bubbling jet flow type employing the bubble plume to support the function of an oil fence, as one of the most important applications of a bubble plume. The most important functions of the oil fence (as shown in Fig. 32) are as follows: a) to encircle an area of water surface over which oil has leaked and then to limit the polluted area. b) to encircle a special area like a power plant, factory, or station in the sea and protect them by keeping oil far away from these areas. A conventional oil fence is sufficient when sea waves are weak but fails when wave amplitude becomes large. In this case, the oil will concentrate near the inside border of the oil fence and then will leak beyond it, either by passing over or under the oil fence. Hence it is very important to find an effective way to support the function of the oil fence and to restrain the expansion of the oil spot. If the spot of oil can be kept inside the oil fence and far from its boundary, the oil will not leak even when waves become higher. Thus, it is considered possible to use the bubble plume as an effective way to control the density and transportation of surface-floating substances since the plume can generate a strong and wide surface flow over the bubble generation system. Moreover, it is expected to be an effective tool to support the function of an oil fence, and able to damp the wave motion especially for high values of current velocity, wave height, and wind velocity. The bubble plume decreases the intensity of the wave motion and restrains the waves passing over an oil fence body (i.e. decrease the intensity of the wave motion) (Hassan 2002, 2003, 2006, 2011, 2012, 2013, Hassan and Tamer 2006, Abdulmouti, et. al. 2000, Hassan et. al. 1997, 1998, 1999- No. 1, 1999- No. 2 and 2001, Hassan and Esam, 2013, Murai et. al. 2000, Fire Department of Fukui Prefecture 1998).

Figure 29. Oil pollution in the Japan Sea

Figure 30. Ship accident in Boston (June 2000)

Figure 31. Oil tanker accident in Boston on June 2000

The annual average of oil accidents in the sea around Japan for the last 30 years is about 500 accidents. Beyond that, one big oil leakage accident happens every two years in the world. Table 4 shows the distribution of the percentage of oil accidents. Most accidents occur on the seas and oceans.

Table 4. Distribution of accidents

Accidents	Percentages of accidents %
Seas, Oceans, Ships, Tankers…etc	77.9 %
On the ground or land	2.4 %
Others	0.2 %
Unknown	19.7 %

Figure 32. Oil fence (photos taken from the Japan Sea 1997)

Fig. 33 shows the bad effects of the oil on marine life. Oil has bad effects not only on fish but also on sea birds, other sea animals, naval plants, nature, and so on. Bad effects of the oil can occur in various ways:

(a) Oil can evaporate from the oil spots floating on the sea.
(b) Oil can diffuse and expand either inside the sea water or by floating on the sea surface.
(c) Oil can sink or fall to the bottom of the sea. Drops or balls of oil can be formed.
(d) Oil can be absorbed by the sea, by animals, naval plants, etc.

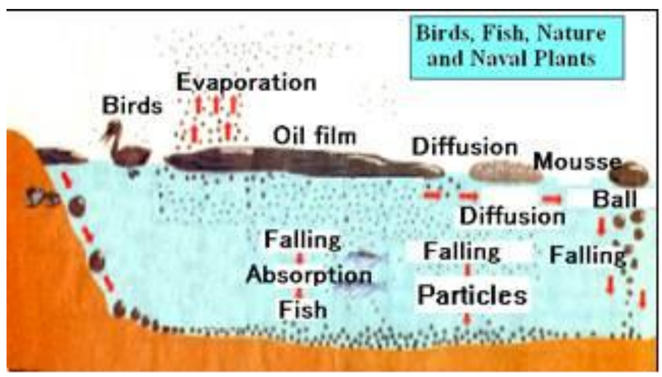

Figure 33. The effects of oil on marine life

Fig. 34 shows ways used to extract oil from the sea:
(a) Suction devices.
(b) Human power.
(c) Absorption sheets.
(d) Processing materials.

Figure 34. Ways used to clean seas and oceans from oil

(Shoichi et. al. 1982) also have made an analytical treatment of the two-dimensional flow of a vertically rising plume under restricted conditions using the data by (Kobus 1968). They measured the velocity profile of the plume and performed numerical analysis on the velocity and width of the plume. Moreover, experimental constants were taken for a numerical calculation with the presence of a tidal current.

The precise theoretical prediction (and explanation) of water wave damping has been a long-standing open problem (Henderson and Miles 1994). Its solution is essential for various purposes, including the appropriate modeling of weakly nonlinear water dynamics. Three sources of damping are readily identified:

(a) Viscous dissipation in both the oscillatory boundary layers and the bulk. The latter is second order as viscosity goes to zero and was systematically omitted in the literature. But for the usual small-but-fixed values of viscosity, this effect must not be ignored if the contact line is pinned, as shown by (Martel, Nicolas, and Vega 1998), who obtained results in good agreement with experiments in (Howell et. al. 2000).

(b) Contact line dynamics, which is not well-understood, is modeled by phenomenological formulas but can be avoided by pinning the contact line.

(c) Surface contamination, again a not-well-understood effect that is most likely to be present in water unless much care is taken in the experimental setup. It is modeled by phenomenological formulas (Dorrestein 1951, Levich 1962, Miles 1967) that also apply to thin films of highly viscous Newtonian fluids on surfaces (Jenkins and Dysthe 1997, Jose a. Nicolas and Jose m. Vega 2000).

(Hassan 2002, 2003, 2006, 2011, 2012, 2013, Hassan and Tamer 2006, Abdulmouti, et. al. 2000, Hassan et. al. 1997, 1998, 1999- No. 1, 1999- No. 2 and 2001, Hassan and Esam, 2013) investigated the following research:

1- The detailed of the liquid flow pattern (flow structure) of a bubble induced convection in both cases of one layer (water) and stratified liquid (two layers), which governs the efficiency of the surface flow generation, in order to improve the applications of the bubble plume and to collect surface-floating substances especially an oil layer during large oil-leakage accidents to protect naval systems, rivers, and lakes.

2- The multi-dimensional transportation of oil due to bubbles. And the interaction mechanism between the surface flow generated by the bubbles and the oil layer for applications to actual oil fences. And the mixing effects of the oil layer to improve the system performance. In other words, the interaction pattern between a bubble plume and the oil layer.

3- The separation mechanism of oil due to bubbling by focusing on the actual oil transportation phenomenon due to the bubble plume and its effects considering the stratified layer of oil on a free surface. Their results showed that the oil layer is easily broken by bubbles. It was confirmed that the oil stratum can be separated by a bubble plume especially when the bubble plume has a high void fraction and high gas flow rates.

4- The experimental measurement of the oil-water interface motion. And the altitude of the upheaval bulge of the interface of the two-phase stratified liquids induced by the bubble plume, which is a very important factor in breaking the oil layer and depends on the bubbling conditions (such as gas flow rate, bubble radius, and void fraction).

5- An additional function of the surface flow, the wave-damping effects. The efficiency and applicability of the bubble plume as an actual oil fence application by the measurement of fundamental factors such as wavelength, wave height, frequency, bubble size, the relationship between waves and bubbles, and the applicability of the bubble plume as a new type of oil fence. Their results indicated that the bubble plume reveals a remarkable and efficient effect on wave damping due to the surface flow. It is a very effective tool to decrease the wave parameters and extinct the wave motion on the free surface. Furthermore, the wave damping effect is much greater for the bubbling case than for the non-bubbling case. The effect of the wave damping with bubbles is 3.3 to 8.8 times greater than without bubbles.

Other applications:

Marine sediments contain some of the largest reservoirs of methane in the world. These reservoirs include shallow gas hydrates that have both biogenic and thermogenic sources (Kvenvolden 1993, 1995; Sassen et al. 1999), and deeper hydrocarbon accumulations. Leakage from these reservoirs is potentially a significant source of atmospheric methane, one of the most important greenhouse gases. Additionally, marine seeps are significant sources of dissolved hydrocarbons and oil in coastal waters (Clark et al. 2000; MacDonald et al. 2000; NRC 2002).

Estimates of the magnitude of the global methane flux from marine sediments to the atmosphere are based upon statistical analysis of very limited field measurements of seepage rates (Hovland et al. 1993; Judd et al. 1997; Kvenvolden et al. 2001; Judd et al. 2002). Because most measurements of seepage rates have been made near the seafloor, these estimates are primarily for leakage from sediments into the ocean (Judd et al. 2002). Methane released at the seafloor forms bubble plumes that travel through the water column before entering the atmosphere. Hence, before the atmospheric flux can be estimated, oceanic processes governing methane bubble dissolution must be considered (Jordan et. al. 2003).

The extent to which methane and other gases exchange between bubbles and seawater depends upon the immediate seep and bubble plume environment (Leifer et al. 2000; Leifer and Clark 2002; Leifer and Patro 2002). Models that consider only gas transfer out of single rising bubbles within a stagnant fluid (Cline and Holmes 1977) are simplifications that overestimate the amount of methane that dissolves because bubble plume processes and ambient conditions are not considered. While some of these processes have been examined in the laboratory, some studies of marine bubble plumes have been conducted (McDougal 1978; Leifer and Patro 2002).

The dispersion of gases through submerged orifices, slots, or holes is an efficient and commonly used method of creating large interfacial area per unit volume in process equipment such as distillation columns, absorption towers, flotation cells, aerated stirred tanks, biological wastewater treatment systems, and metallurgical smelters. In many industrial gas-liquid operations, the continuous phase is caused to flow normally across the emerging gas at the orifices either by bulk liquid motion tangential to the orifice or by the motion of the orifices as in gas-sparged impellers or rotary spargers. Bubble formation under such conditions of liquid crossflow is known to produce smaller bubbles when compared with formation under stagnant or quiescent liquid conditions. Another advantage of cross-flowing liquids is that the detached bubbles tend to be swept away from the region of the orifice, thereby reducing the likelihood of coalescence (R. B. H. Tan et. al. 2000).

A model for bubble formation from a single submerged orifice is developed using the boundary-integral method. Since the flow field is assumed to be irrotational, the potential-flow theory is used to predict the growth of the bubble. The effects of the surface tension and the liquid circulation around the bubble are included in the calculation. Predictions of bubble shape, chamber pressure, and the effect of surface tension are presented to compare with reported experimental data (Zongyuan Xiao and Reginald 2004).

Two-phase flow is found in many systems used in nuclear and chemical engineering. Mixtures of liquid and gas may be steam and water, such as in the heat-transfer apparatus. However, it is still difficult to describe quantitatively boiling two-phase flow due to the extreme complexity of flow behavior. Recently, the nonlinear points were introduced to the boiling two-phase flow. But many nonlinear studies reported in open literature focused on pool nucleate boiling system due to the simple configuration from which it was easy to address fundamental issues. Investigation on the flow boiling system is more urgent because the accuracy design, optimum operation and effective control of flow boiling heat exchangers such as the evaporator and nuclear reactor are still quite difficult due to the complexity of the flow boiling phenomena. Ming-yan Liu et al, (2005) have procured some achievement in flow boiling system. Although these analyses are valuable for enhancing the physical understanding of such a system, most of the experimental work is performed for adiabatic (no heat addition) two-phase flow or at different exchanger devices. However, in industrial processes, in many cases, two-phase flow develops under nonadiabatic. So, in (Yan et. al. 2007) paper, the effect of heat flux on pressure fluctuation was stressed studied.

Because pressure fluctuation measurements reflect many hydrodynamic phenomena, like bubble passage, bubble coalescence, and bubble eruption, experiments are carried out to study the feature of pressure fluctuating in a vertical tube for boiling two-phase flow. There are many ways to characterize the pressure fluctuations in order to quantify a change in the two-phase flow behavior. In (Yan et. al. 2007) paper, time-series analysis for this purpose operated in the time domain, frequency domain, and state-space, the latter being used in non-linear time-series analysis. Also, analyses of pressure fluctuation time series were carried out by using the standard deviation, the power spectrum density function, the Hurst exponents, Kolmogorov entropy, and correlation dimension (Yan et. al. 2007). Experimental results show that heat flux has a great influence on the fluctuation feature. In different velocities of flow, the standard deviation (SD) of the pressure fluctuation time-series decreased firstly and increased lately with the increase of heat flux. And as the velocity of flow is bigger than 0.6 m/s, an increase of SD is obvious. The power spectrum density function of the pressure fluctuation time series shows an exponential decrease at a semi-logarithmic coordinate. At lower heat flux, the PSD is characterized by the lower major frequency with a larger fluctuation scale. At higher heat flux, the PSD is featured by a higher major frequency with a smaller fluctuation scale. For the heat flux, the values of H were found to be between 0.5 and 1, indicating that the time series displays persistent behaviors under the conditions examined. The Kolmogorov entropy and correlation dimension have changed with a difference of heat flux and A positive, nonfinite estimate of the Kolmogorov entropy provides further evidence that pressure fluctuation signals behave chaotically. It can be concluded that the flow pattern map and transition theories based on adiabatic flow cannot be extrapolated directly to the boiling two-phase system (Yan et. al. 2007). Further work is required to determine the effect that local heat-transfer coefficients and system pressure of boiling two-phase flow have on the pressure fluctuation feature. Further information would be desirable to investigate the transition mechanisms of flow patterns for the boiling two-phase flow system (Yan et. al. 2007).

It is widely accepted that two complementary mechanisms exist in the influence area of the nucleation site which contributes to efficient cooling of heating surface in partial nucleate boiling regime. The first one is adhesive microlayer evaporation beneath the base of the growing bubble which takes place during the contact time (Judd and Hwang, 1976). Transient heat conduction is the second mechanism, and it governs thermal boundary layer reformation during the waiting time. Periodical stripping of thermal energy accumulated in the superheated liquid layer caused by cyclic bubble activity in the influence area is often referred to as enhanced convection. In this approach, convective contribution to overall heat flux is included merely indirectly through the frequency of the ebullition cycle (Benjamin and Balakrishnan, 1996).

Most mechanistic models dedicated to this regime treat bubbles as passive agents whose hydrodynamics features after departure does not affect heat transfer to a great extent. It is known that a solid body that moves through initially quiescent fluid induces flow in its vicinity. This induced fluid movement, named drift flow, distorts initially fixed material surface situated perpendicular to the body path, displacing fluid forward in regions close to where the body passes, and displacing fluid far from the body backward. Benefits from drift flow analysis developed in the past for the translational movement of a rigid body through the inviscid fluid is considerably restricted when more complex flow conditions exist. Viscosity effects, boundary constraints due to the boiling surface, and zero-shear-stress interface of the moving bubble have all to be considered in the assessment of drift flow contribution in the wake of rising bubbles over the nucleation site. In contrast to enhanced convection mentioned before, a drift flow mechanism can be recognized as the direct contribution of convection caused by bubble activity (Beer and Durst, 1968).

To quantify this contribution, a partial nucleate boiling regime has been investigated experimentally using the PIV measurement technique. A single nucleation site has been artificially produced on a highly smoothed Si wafer. Upward facing boiling surface of this wafer has been immersed in deionized water at atmospheric pressure and uniformly heated maintaining constant wall superheat by circulating fluid on its lower side. A pulsed laser sheet has been directed to pass through the bubble chain originating from the nucleation site and illuminate seeding particles entrained in the flow. Time-delayed particle displacements within interrogation areas of the CCD chip have been captured by synchronically triggered PIV cameras.

Velocity distribution over the influence area of the nucleation site is evaluated through the different stages of the ebullition cycle. It has been recognized that after inception the bubble interface passes through five different stages. Successively, these stages are hemispherical expansion, vertical elongation, base shrinking, bubble departure, and rising. For each of these stages, and instantaneous velocity distribution is presented qualitatively by PIV plots and quantitatively by the velocity component distribution diagrams. Statistically evaluated morph-cinematic matrices have been introduced to describe characteristic vapor bubble formations of non-interacting and interacting bubbles. By virtue of the findings presented, it might be possible to estimate a convective contribution in the overall heat flux removed from the boiling surface in a partial nucleate boiling regime (Sani and Leopold 2007).

Many manufacturing processes include bubble columns for mass transfer promotion, high-pressure evaporators, and so on. The functional dependence of the velocity of an air bubble has been determined experimentally by numerous investigators. When rising through an infinite stagnant liquid, the single bubble's terminal velocity is of fundamental importance in the two-phase flow [M. A. R. Talaia, (2007)] as well as in other types of flow. The knowledge of bubble properties, including bubble velocity, bubble size, gas holdup, and specific interfacial area, is of prime importance for the right design and operation of bubble columns. [G. B. Wallis, (1969), and J. W. A. De Swart and R. Krishna, (1995)]. An understanding of bubble-fluid interactions is vital in a broad range of natural, engineering, and medical settings. Bubble column reactors, air-sea gas transfer, boiling heat transfer, gas and/or oil transport, ship hydrodynamics, medical ultrasound imaging, and ink-jet printing are just a couple of examples where the dynamics of bubbles play a task [B. H. Davis, (2002)]. The movement of bubbles may be a basic subject in gas-liquid two-phase flow research. The motion of bubbles is extremely complex. The upward path and alter within the direction of a bubble are known to be strongly associated with bubble shape [E. T. White and R. H. Beardmore, (1962)]. The motion of spherical bubbles is typically rectilinear. Once the bubble deforms into an oblate ellipsoid, instability sets in and leads to a spiral or zigzag trajectory. [W. Luewisutthichat, et. al. (1997)] found that both bubble shape and bubble velocity of oblate ellipsoidal bubbles exhibit chaotic features. In turn, the fluctuation of bubble shape is probably going to cause oscillations within the drag force, resulting in the chaotic fluctuation of bubble velocity within the streamwise direction. Therefore, despite periodic macroscopic motion, bubbles exhibit highly chaotic fluctuations in both the lateral and axial components along the zigzag path of a bubble ascent. At an equivalent time, bubble orientation changes in such how that the trajectory of the bubble plume tends to be perpendicular to the direction of instantaneous motion [W. L. Haberman and R. K. Morton, (1953)]. [Krishna et. al. (1991)] inferred from gas-disengagement experiments that both large and little bubbles exist in churn-turbulent flow. Large bubbles rise fast through the column, whereas small bubbles display an extended resident-time distribution. Beyond a particular transition gas velocity, the tiny bubble holdup remains constant, whereas the massive bubble holdup continues to extend with gas velocity [X. Junli, (2004)]. Bubbles in motion are generally classified as spherical, oblate ellipsoidal, or ellipsoidal cap, etc. In gas-liquid upward flow, bubbles move faster than the encompassing liquid (due to buoyancy), and enormous bubbles have greater upward acceleration than small bubbles. The particular bubble shape depends on the relative magnitudes of the forces working on the bubble, like physical phenomenon and inertial forces [D. Bhaga and M. E. Weber, (1981)].

Summary of Applications:

Bubbly flows are a very common subset of gas-liquid flows; a list of industrial processes that employ bubbly flow is given in Table 1, and Table 2 lists the environmental and naval engineering applications of bubbly flow, while Table 3 illustrates the applications: aerospace, biomedical, electrical, and mechanical.

5. Conclusions

As a result, it is clear that the bubble plume "which is a typical bubble flow" is a key phenomenon to be studied and investigated, and it is an effective tool for many applications and can indeed contribute to various improvements. The motivation to study the bubble plume is the demand to improve its performance and its applications. Especially in many engineering fields as materials, chemicals, mechanical, modern industrial technologies, and in the environment in order to protect the natural environment, the naval planets, navel systems, rivers, lakes, etc from pollution. Hence these engineering fields are expected to benefit from the improvement and development of the bubble plume. Surface flows are more effectively generated by bubble plumes compared to liquid jet flows because the distortion point appears in the vicinity of the surface.

The present work demonstrates, reviews, and summarizes the major finding of previous research of the following points:

1) The differences of surface flow generation mechanisms among single-phase liquid jet, single-phase buoyant plume, and bubble plume.
2) The study of bubble plumes, their properties, characteristics, features, and their effects on the applications.
3) The important applications of bubbly flow and gas-liquid two-phase flow especially on bubble plumes and their associated surface flow since they can contribute to improvements in various directions including the conventional oil fence (function, problems, oil accidents on seas and oceans). The techniques of gas injection have been widely utilized in many engineering fields. The surface flows generated by bubble plumes are considered key phenomena in many kinds of processes in modern industries. It is utilized as an effective way to control surface floating substances on lakes, oceans, as well as in various kinds of reactors and industrial processes handling a free surface.
4) Summary of the above applications as a table of industrial processes that employ bubbly flow, a table of the environmental and naval engineering applications of bubbly flow, and a table of the applications: aerospace, biomedical, electrical, and mechanical.

REFERENCES

[1] A. Castillejos and J. Brimacombe. Measurement of physical characteristics of bubbles in gas-liquid plumes: Part II. Local properties of turbulent air-water plumes in vertically injected jets. Metall. Trans. B, 18B, 659–671 (1987).

[2] A. Fujiwara, D. Minato, and K. Hishida, Effect of Bubble Diameter on Modification of Turbulence in an Upward Pipe Flow, International Journal of Heat and Fluid Flow, 25 (2004) 481-488.

[3] Abdel-Aal H. K., Stiles G. B. and Holland C. D. 1966. Formation of Interfacial Area at High Rates Gas Flow Through Submerged Orifices. ALCHE J. 12, pp. 174-180.

[4] Abdulmouti H., Murai Y., Ohno Y., Yamamoto F. 2000. Measurement of Bubble Plume Generated Surface Flow Using PIV, Journal of the Visualization Society of Japan. Vol. 21. No. 2. Pp. 31-37.

[5] Abramovich, G. N. (1963). The theory of turbulent jets, MIT, Cambridge, Mass.

[6] Akagawa, K., and T. Sakaguchi, 1966, "Fluctuation of Void Ratio in Two-Phase Flow (2nd Report, Analysis of Flow Configuration Considering the Existence of Small Bubbles in Liquid Slugs) and (3rd Report, Absolute Velocities of Slugs and Small Bubbles, and Distribution of Small Bubbles in Liquid Slugs)," Bulletin of JSME, Vol. 9, No. 33, pp. 104-120.

[7] Akagawa, K., Sakaguchi, T., Fujii, T., Sugiyama, M., Yamaguchi, T., and Ito, Y. (1979). "Shock phenomena in bubble and slug flow regimes." Two-Phase Flow Dynamics, Japan–U.S. Seminar, A. B. Bergles and S. Ishigai, eds., Hemisphere Publishing, Washington, DC, 217–238.

[8] Akagawa, K., Sakaguchi, T., Fujii, T., Fujioka, S., and Sugiyama, M. (1980). "Shock phenomena in air-water two-phase flow." Proc., Multiphase Flow and Heat Transfer Symposium Workshop, Vol. 3, Hemisphere Publishing, Washington, DC, 1673–1694.

[9] Akagawa, K., Fujii, T., and Ito, Y. (1983). "Analyses of shock phenomena in a bubbly flow by two-velocity model and homogeneous model." Advances in two-phase flow and heat transfer, fundamentals and applications,

[10] Akasaka, Y., Kawaguchi, T., and Maeda, M. (2002). Application of interferometric laser imaging technique to a transient spray flow. In 11th International Symposium on Applications of Laser to Fluid Mechanics, Lisbon.

[11] A.K. Das and P.K. Das. Modelling bubbly flow and its transitions in vertical annuli using population balance technique. International Journal of Heat and Fluid Flow 31 (2010) 101–114.

[12] Akita, K., Nakanishi, O. and Tsuchiya, K., 1994, Turn-around energy losses in an external-loop airlift reactor, Chem Eng Sci, 49: 2521.

[13] Akhtar, M. A., Tadé, M. O. and Pareek, V. K. (2006), "Two-fluid Eulerian simulation of bubble column reactors

with distributors", Journal of Chemical Engineering of Japan, vol. 39, no. 8, pp. 831-841.

[14] A. Kubota, H. Kato, and H. Yamaguchi, “A new modeling of cavitating flows: A numerical study of unsteady cavitation on a hydrofoil section,” J. Fluid Mech. 240, 59 (1992).

[15] Alam M. and Arakeri V. H., Observations on Transition in Plane Bubble Plumes. J. Fluid Mech., 254, 1993, 363-380.

[16] Al Tawell A. M. and Landau J. 1977. Turbulence Modulation in Two-Phase Jets. Int. J. Multiphase Flow 3, pp. 341-353.

[17] Alexander B. Tayler. Experimental Characterisation of Bubbly Flow using MRI. Trinity College. Ph. d. Thesis. May 2011. The University of Cambridge.

[18] American, S., 2021. Scientific American. Available at: https://www.scientificamerican.com/article/the-bubbles-produced-by-u/.

[19] Antoniadis, D., Mantzavinos, D., and Stamatoudis, M. (1992). Effect of chamber volume and diameter on bubble formation at plated orifices. Transactions of the Institution of Chemical Engineers, Part A, 70, 161-165.

[20] Apazidis, N., 1985, "Influence of Bubble Expansion and Relative Velocity on the Performance and Stability of an AirLift Pump," International Journal of Multiphase Flow, Vol. 11, No.4, pp. 459-475.

[21] A. Prosperetti, “The thermal behavior of oscillating gas bubbles,” J. Fluid Mech. 222, 587 (1991).

[22] Arega, F., and J. H. W. Lee (2005), Diffusional mass transfer at sediment-water interface of cylindrical sediment oxygen demand chamber, J. Environ. Engineer., 131(5), 755-766.

[23] Arnold, H., Yadigaroglu, G., Gonzales, A., Rao, A. S., 1997. An economic passive plant design. Jahrestagung Kerntechnik 97. Aachen, Germany.

[24] Asaeda, T., and Imberger, J. (1989). “Behaviors of bubble plumes in a linear stratification.” J. Jpn. Soc. Civ. Eng., 411, 55–62 (in Japanese).

[25] Asaeda, T., and Imberger, J. (1993). “Structure of bubble plumes in linearly stratified environments.”. J. of Fluid Mechanics, Vol. 249, pp. 35-57.

[26] Ashfaq Shaikh and Muthanna H. Al-Dahhan. A Review on Flow Regime Transition in Bubble Columns. International Journal of Chemical Reactor Engineering. Volume 5. 2007 Review R1.

[27] Asher, W. E., and P. J. Farley (1995), Phase-Doppler anemometer measurement of bubble concentrations in laboratory-simulated breaking waves, J. Geophys. Res., 100, 7045–7056.

[28] Asher, W. E., L. M. Karle, B. J. Higgins, P. J. Farley, E. C. Monahan, and I. S. Leifer (1996), The influence of bubble plumes on air-seawater gas transfer velocities, J. Geophys. Res., 101(C5), 12,027–12,041, doi:10.1029/96JC00121.

[29] Ashley, K. I. (1985), Hypolimnetic aeration: Practical design and application, Water Res., 19(6), 735-740.

[30] Ashley, K. Hay, S., Scholten, GH., (1987), Hypolimnetic aeration: Field test of the empirical sizing method, Water Res., 21(2), 223-227.

[31] Ashley, K. I. (1988), Hypolimnetic aeration research in British Columbia, Verh. Internat. Verein. Limnol., 23(1), 215-219.

[32] Asiagbe, K. S., Fairweather, M., Njobuenwu, D. O., & Colombo, M. (2017). Large eddy simulation of microbubble transport in vertical channel flows. In Computer Aided Chemical Engineering (Vol. 40, pp. 73-78). Elsevier.

[33] Atila P. Silva Freire, Davi D’E. Miranda, Leonardo M.S. Luz, Guilherme F.M. Franc_a. Bubble plumes and the Coanda effect. International Journal of Multiphase Flow 28 (2002) 1293–1310.

[34] A. Tomiyama, Drag, lift and virtual mass forces acting on a single bubble, in Proc. of the 3rd International Symposium on Two-Phase Flow Modelling and Experimentation, Edizioni ETS, Pisa, Italy (2004).

[35] A. T. Preston, T. Colonius, and C. E. Brennen, “A numerical investigation of unsteady bubbly cavitating nozzle flows,” Phys. Fluids 14, 300 (2002).

[36] A. T. Preston, T. Colonius, and C. E. Brennen, “A reduced-order model of diffusive effects on the dynamics of bubbles,” Phys. Fluids 19, 123302 (2007).

[37] Avanish Mishra. Numerical And Experimental Investigation Of A Confined Plunging Liquid Jet System. MSc (Research). Cranfield University. 2011.

[38] Autumn Fjeld and James W. Evan. Characterization of Droplets Produced by Bubbles Bursting: San Francisco, CA. TMS 2005 (134th) Annual Meeting: Technical Program.

[39] A.W.G. de Vries. Path and Wake of a Rising Bubble. ISBN 90 365 15262. 2001. Enschede, The Netherlands.

[40] Aubin, J., Sauze, L.N., Bertrand, J., Fletcher, D., Xuereb, C., PIV measurements of flow in an aerated tank stirred by a down- and an up-pumping axial flow impeller. Experimental Thermal and Fluid Science, Vol. 28, 447-456 (2004).

[41] Baines W. D. and Hamilton G. F. 1959. On the Flow of Water Induced by a Rising Column of Air Bubbles. Intl Assoc. For Hydraulic Research, Proceedings of 8th Congress., Monteral, 24-29 August, pp. 7D1-7D17.

[42] Baines W. D. 1961. The Principles of operation of Bubbling Systems. Proc. Symp. Air Bubbling, Ottawa.

[43] Baines W. D. 1983. A Technique for the Direction Measurement of Volume Flux of a Plume. J. Fluid Mech. 132, 247-256.

[44] Baines W. D. and Leitch A. M. 1992. Destruction of Stratification by Bubble Plume. Journal of Hydraulic Engineering. Vol. 188, No. 4, April, 1992. No. 26602. Pp. 559-577.

[45] Balasubramanian, P. and Kandlikar, S.G. Experimental study of flow patterns, pressure drop, and flow instabilities in parallel rectangular minichannels. Heat Transfer Engineering, Volume 23, 20-27 (2005).

[46] Baltimore, Maryland, August 2–6, 1992. Published by American Society of Civil Engineers. Hydraulics Research Station. 1978. "Air Bubbles for Water Quality Improvement," Report No. 00/12, April, Hydraulics Research Station, Wallingford, England.

[47] Bankovic A., Currie, I. G. and Martin W. W. 1984. Laser-Doppler Measurements of Bubble Plumes. Phys. Fluids 27, pp. 348-355.

[48] Barbosa, J.R.J., Bradbury, L.J.S., 1996. Experimental investigations in round bubble plumes. In: Proc. 6th Brazilian National Meeting on Thermal Sciences (ENCIT), Florianopolis, pp. 1073–1078.

[49] Bauer, M., Eigenberger, G., 1999. A concept for multi-scale modelling of bubble columns and loop reactors, Chemical Engineering Science, 54, 5109-5117

[50] Bauer, M., Eigenberger, G., 2001. Multiscale modeling of hydrodynamics, mass transfer and reaction in bubble column reactors, Chemical Engineering Science, 56, 1067-1074

[51] Bardina, J., Ferziger, J. H. and Reynolds, W. C. (1980) Improved Subgrid Models for Large Eddy Simulation. AIAA paper, 1980.

[52] Baschek, B., and D. M. Farmer (2010), Gas bubbles as oceanographic tracers, J. Atmos. Oceanic Technol., 27, 241–245.

[53] Becker, S., Sokolichin, A. and Eigenberger, G. (1994), "Gas-liquid flow in bubble columns and loop reactors: Part II. Comparison of detailed experiments and flow simulations", Chemical Engineering Science, vol. 49, No. 24, pp. 5747-5762.

[54] Becker, S., De Bie, H. and Sweeney, J. (1999), "Dynamic flow behaviour in bubble columns", Chemical Engineering Science, vol. 54, no. 21, pp. 4929-4935.

[55] Beer, H.; Durst, F.: Mechanismen der Wärmeübertragung beim Blasensieden und ihre Simulation. *Chemie Ingenieur Technik*, 40/13, 632-638, (1968).

[56] B. Eisenberg, L. L. Ansel, R. A. Fiato, and R. F. Bauman, Advanced gas conversion technology for remote natural gas utilization, GPA Convention, New Orleans, Louisiana (1994).

[57] Bel Fdhila, R., Simonin, O., 1992. Eulerian prediction of a turbulent bubbly flow downstream of a sudden pipe expansion. Workshop on Two-phase flow predictions, 30 March–2 April, Erlangen.

[58] Benjamin, R.J.; Balakrishnan, A.R.: Nucleate pool boiling heat transfer of pure liquids at low to moderate heat fluxes. International Journal of Heat and Mass Transfer, 39,2495-2504, (1996).

[59] Bendiksen, K. (1985). On the motion of long bubbles in vertical tubes. Int. J. Multiphase Flow, Vol. 11(6), 797- 812.

[60] Bernard, R.S., 1995. Preliminary Development of a Three-dimensional Numerical Model for Reservoir Hydrodynamics. Technical Report HL-95-9, Waterways Experiment Station. US Army Corps of Engineers, Vicksburg, MS.

[61] Bernard, R. S. 1997. ‘‘Extension and validation of the MAC3D numerical model for applications involving bubble diffusers.’’ Proc., Int. Association of Hydraulic Research Congress on Environmental and Coastal Hydraulics, ASCE, New York, 833–838.

[62] Bernard, R.S., 1998. MAC3D: Numerical Model for Reservoir Hydrodynamics with Application to Bubble Diffusers. Technical Report CHL-98-23, Waterways Experiment Station. US Army Corps of Engineers, Vicksburg, MS.

[63] Bernard, R.S., Maier, R.S., Falvey, H.T., 2000. A simple computational model for bubble plumes. Applied Mathematical Modelling 24, 215e233.

[64] Bernard, R.S., 2002. User’s Manual for the PAR3D Numerical Flow Model, Version 2.0. ERDC Waterways Experiment Station. US Army Corps of Engineers, Vicksburg, MS.

[65] Beutel, M. W., and A. J. Horne (1999), A review of the effects of hypolimnetic oxygenation on lake and reservoir water quality, Lake Reservoir Manage., 15(4), 285-297.

[66] Beutel, M. W. (2003), Hypolimnetic anoxia and sediment oxygen demand in California drinking water reservoirs, Lake Reservoir Manage., 19(3), 208-221.

[67] Beylich, A. E., and Gülhan, A., 1990, “On the Structure of Nonlinear Waves in Liquids With Gas Bubbles,” Phys. Fluids A, 2-8, pp. 1412–1428.

[68] B. H. Davis, Overview of reactors for liquid phase Fischer-Tropsch synthesis, Catal. Today 71, 249 (2002).

[69] Bin, A. K. (1993), "Gas entrainment by plunging liquid jets", Chemical Engineering Science, vol. 48, no. 21, pp. 3585-3630.

[70] B. Jager and R. Espinoza, Advances in low temperature Fisher-Tropsch synthesis, Catal. Today 23, 17 (1995).

[71] B.J. Azzopardi. Multiphase Flow. Chemical Engineering and Chemical Process Technology - Vol. I – Encyclopaedia of Life Support Systems. ISBN: 978-1-84826-396-3 (eBook). ISBN: 978-1-84826-846-3 (Print Volume) 2012.

[72] Boufadel, M. and Socolofsky, S., 2021. *The Underwater Behavior of Oil and Gas Jets and Plumes*. [online] Eos. Available at: <https://eos.org/editors-vox/the-underwater-behavior-of-oil-and-gas-jets-and-plumes>.

[73] Bombardelli, F. A., Buscaglia, G. C., Rehmann, C. R., Rincón, L. E., and García, M. H. (2007). “Modeling and scaling of aeration bubble plumes: A two-phase flow analysis.” J. Hydraul. Res., 45_5_, 617– 630.

[74] Borchers, O., Busch, C., Sokolichin A., Eigenberger, G., 1999, Applicability of the standard k−ε turbulence model to the dynamic simulation of bubble columns. Part II: Comparison of detailed experiments and flow simulations, Chemical Engineering Science, 54, 5927-5935.

[75] Botton, R., Cosserat, D., Poncin, S. and Wild, G. (2009), "A simple gas-liquid mass transfer jet system", 8th World Congress of Chemical Engineering, Montréal, Canada.

[76] Boulton-Stone J. M. and Blake J. R. 1993. Gas Bubbles Bursting at a Free Surface. J. Fluid Mech. 1993, Vol. 254, pp.437-466.

[77] Boudreau, A., 2016. Bubble migration in a compacting crystal-liquid mush. Contrib Mineral Petrol (2016) 171:32. DOI 10.1007/s00410-016-1237-9. *Petrology*, 171(4).

[78] Bravo R. Hector, John S. Gulliver, Miki Hondzo. Development of A Commercial Code-Based Two-Fluid

Model For Bubble Plumes. Environmental Modelling and Software 22 (2007) 536-547.

[79] Brevik, I. (1977), Two-dimensional air-bubble plume, J. Waterway, Port, Coastal, and Ocean

[80] Div., Proc. American Soc. of Civil Engineers, 103(WW1), 101-115.

[81] Brevik, I., and R. Killie (1996), Phenomenological description of the axisymmetric air-bubble plume, Internat. J. Multiphase Flow, 22(3), 535-549.

[82] Brevik, I., and R. Kluge (1999), On the role of turbulence in the phenomenological theory of plane and axisymmetric air-bubble plumes Internat. J. Multiphase Flow, 25, 87-108.

[83] Brevik, I., and Ø. Kristiansen (2002), The flow in and around air-bubble plumes, Int. J. Multiphase Flow, 28(4), 617– 634. ISSN 0301-9322, https://doi.org/10.1016/S0301-9322(01)00077-5. (https://www.sciencedirect.com/science/article/pii/S0301932201000775).

[84] Brown, R. A. S., (1965). The mechanics of large gas bubbles in tubes I. Bubble velocities in stagnant liquids. Can. J. Chem. Eng., Vol. 43, pp. 217-223.

[85] Brankovic A; Currie IG; Martin WW (1984) Laser-Doppler measurements of bubble dynamics. Phys Fluid 27: 348-355

[86] Brennen, C.E., Cavitation and Bubble Dynamics, Oxford Engineering Sciences Series 44, Oxford University Press, New York, (1995).

[87] Bruijn, J., and H. Tuinzaad (1958), The relationships between depth of U-tubes and the aeration process, Journal of the American Water Works Association, 7, 879.

[88] Bryant, R.A.A. (1975). “Water hammer incompressible fluids.” Rep.FM/18/ 75, University of Salford, Dept. of Mechanical Engineering, Salford, UK.

[89] Bugg, J.D., K. Mack and K.S. Rezkallah (1998). Anumerical model of Taylor bubbles rising through stagnant liquids in vertical tubes. Int. J. Multiphase Flow 25(2), 271-281.

[90] Bugg JD, Saad GA (2002). The velocity field around a Taylor bubble rising in a stagnant viscous fluid: numerical and experimental results. Int J Multiphase Flow 28:791–803.

[91] Bulson, P. S., "Bubble Breakwater with Intermittent Air Supply," Res. Rept. 9-2, Military Eng. Exper. Estab., Christchurch, Hampshire, England, 1962.

[92] Bulson, P. S., "Large Scale Bubble Breakwater Experiments," Res. Rept. 9-3, Military Eng. Exper. Estab., Christchurch, Hampshire, England, 1962.

[93] Bulson P.S. 1968. The Theory and Design of Bubble Breakwaters. Proc. 11th Conf. Coastal Engng, London. 995.

[94] Bunner, B. and G. Tryggvason, “Dynamics of homogeneous bubbly flows. Part 1: Rise velocity and microstructure of the bubbles,” J. Fluid Mech. 466, 17-52 (2002).

[95] Bunner, B. and G. Tryggvason, “Dynamics of homogeneous bubbly flows. Part 2: Velocity fluctuations,” J. Fluid Mech. 466, 53 (2002).

[96] Burke, J., Hess, C., and Kebbel, V. (2002). Digital holography for whole field spray diagnostics. In 11th international symposium on application of laser techniques to fluid mechanics, Lisbon.

[97] Burris, V. L., and J. C. Little (1998), Bubble dynamics and oxygen transfer in a hypolimnetic aerator, Water Sci. Technol., 37(2), 293-300.

[98] Burris, V. L., McGinnis, DF., Little, JC., (2002), Predicting oxygen transfer and water flow rate in airlift aerators, Water Res., 36(18), 4605-4615.

[99] Buscaglia, G.C., Bombardelli, F.A., rouse, M.H., 2002. Numerical modeling of large-scale bubble plumes accounting for mass transfer effects. International Journal of Multiphase Flow 28 (11), 1763e1785.

[100] Caballina, O., Climent, E., Dusek, J., 2003. Two-way coupling simulations of instabilities in a plane bubble plume, Physics of Fluids, 15(6), 1535-1544

[101] de Cachard, F. and Delhaye, J.M. 1996. A slug-churn model for small-diameter airlift pumps. Int. J. Multiphase Flow, Vol. 22, No. 4, pp. 627-649.

[102] Caetano, E.F., 1984. Two-phase flow in a vertical annulus. TUFFP Report, University of Tulsa, OK.

[103] Caetano, E.F., Shoham, O., Brill, J.P., 1992. Upward vertical two-phase flow through an annulus, Part I: single-phase friction factor, Taylor bubble rise velocity and flow pattern prediction. In: Proceedings of 4th International Conference on Multiphase Flow, Nice, France.

[104] Caflisch, R. E., Miksis, M. J., Papanicolaou, G. C., and Ting, L., 1985, “Effective Equations for Wave Propagation in Bubbly Liquids,” J. Fluid Mech., 153, pp. 259–273.

[105] Caflisch, R. E. M. J. Miksis, G. C. Papanicolaou, and L. Ting, “Wave propagation in bubbly liquids at finite volume fraction,” J. Fluid Mech. 160, 1 (1985).

[106] Campbell, I. J., and Pitcher, A. S. (1958). “Shock waves in a liquid containing gas bubbles.” Proc. Royal Soc., Lon., Series A, 243, 534–545.

[107] Campos JBLM, Guedes de Carvalho JRF (1988). An experimental study of the wake of gas slugs rising in liquids. J Fluid Mech 196: 27–37.

[108] Cartellier, A. 1990 Optical probes for local void fraction measurements: characterization of performance. Rev. Sci. Instrum. 61 (2), 874- 886.

[109] Carra, Sergio; Morbidelli, Massimo, (1987). Gas-liquid reactors. Chemical Industries (Dekker), 26(Chem. React. React. Eng.), 545-666.

[110] Carrica, P., Bonetto, F., Drew, D., and Lahey, R. “The interaction of background ocean air bubbles with a surface ship.” Int. J. Numerical Methods in Fluids, 28:571-600, 1998.

[111] Castello-Branco, M. A. S. C. and Schwerdtfeger, K. (1994) Large-Scale Measurements of the Physical Characteristics of Round Vertical Bubble Plumes in Liquids. Metallurgical and Materials Transactions B, 25B, 359-371, 1994.

[112] Castro, W.E., P.B. Zielinski, and P.A. Sandifer, 1975, "Performance Characteristics of Airlift Pumps of Short Length and Small Diameter," Proceedings of the 6th annual meeting World Mariculture Society,

[113] Chaudhry, M. H., Bhallamudi, S. M., Martin, C. S., and Naghash, M. (1990). “Analysis of transient pressures in bubbly, homogeneous, gas-liquid mixtures.” J. Fluids Eng., 112(2), 225–231.

[114] Ceccio, S. L., and Brennen, C. E., 1991, “Observations of the Dynamics and Acoustics of Traveling Bubble Cavitation,” J. Fluid Mech., 233, pp. 633–660.

[115] Cederwall, K., and J. D. Ditmars (1970), Analysis of Air-Bubble Plumes, W. M. Keck Laboratory of Hydraulics and Water Resources, Division of Engineering and Applied Science, California Institute of Technology, Pasadena, CA.

[116] C. F. Delale, G. H. Schnerr, and J. Sauer, “Quasi-one-dimensional steadystate cavitating nozzle flows,” J. Fluid Mech. 427, 167 9(2001).

[117] Chalmers, J. J. and Bavarian, F., 1991, Microscopic visualization of insect-bubble interactions. II: the bubble . lm and bubble rupture, Biotechnol Prog, 7: 151.

[118] Chanson, H., Aoki, S. and Hoque, A. (2006), "Bubble entrainment and dispersion in plunging jet flows: Freshwater vs. seawater", Journal of Coastal Research, vol. 22, no. 3, pp. 664-677.

[119] Chanson, H., Aoki, S. and Hoque, A. (2004), "Physical modelling and similitude of air bubble entrainment at vertical circular plunging jets", Chemical Engineering Science, vol. 59, no. 4, pp. 747-758.

[120] Chen, J.; Kim, K.J.; Herold, K.E. 1996. Performance enhancement of a diffusion absorption refrigerator. Int. J. Refrig. Vol. 19, No. 3, pp. 208-218.

[121] Cheng wen, Wan tian, Liu wen-hong, Hu bao-wei. Research on unsteady structure of bubble plume in an aeration tank [C], 2008, Conference on Multi-phase of Engineering thermo-physics in China, Qingdao

[122] Cheng Wen, Liu Wen-Hong, Hu Bao-Wei, Wan Tian. Experimental Study on Gasliquid Two-Phase Flows in An Areation Tank by Using Image Treantment Method [J]. Journal of Hydrodynamics. 2008, 20(5): 650-655.

[123] Chern, S. H., Muroyama, K. and Fan, L. S., 1983, Hydrodynamics of constrained inverse fluidization and semi fluidization in a gas-liquidsolid system, Chem Eng Sci, 38: 1167.

[124] Cherry, R. S. and Hulle, C. T., 1992, Cell death in the . lm of bursting bubbles, Biotechnol Prog, 8: 11.

[125] Chesters A. K., Van Doorn M. and Goossens L. H. J. 1980. A General Model of Unconfined Bubble Plumes from an Extended Source. Int. J. Multiphase Flow 6, pp. 499-521.

[126] Cheung, S.C.P., Yeoh, G.H., Tu, J.Y., 2006. On the modelling of population balance in isothermal vertical bubbly flows—average bubble number density approach. Chemical Engineering Processing 46, 742–756.

[127] Christopher E. Brennen. Fundamentals of Multiphase Flows. California Institute of Technolog. Cambridge University Press 2005. ISBN 0521 848040.

[128] Christop Hugi. Modelluntersuchungen von Blasenstrahlen f¨ur die Seebel¨uftung. Ph.D. Thesis, Inst. f. Hydromechanik u. Wasserwirtschaft, ETH, Z¨urich, 1993.

[129] C. H. Song, H.C. No, M.K. Chung, Investigation of bubble flow developments and its transition based on the instability of void fraction waves, Int. J. Multiphase Flow 21 (1995) 381–404.

[130] Chung, P. M. Y. and Kawaji, M. The effect of channel diameter on adiabatic two-phase flow characteristics in microchannels. International Journal of Multiphase Flow, Volume 30, 735 – 761(2004).

[131] Clanet, C., P. Héraud and G. Searby (2004). On the motion of bubbles in vertical tubes of arbitrary cross-sections: some complements to the Dumitrescu-Taylor problem. J. Fluid Mech. 519, 359-376.

[132] Clark, N.N., T.P. Meloy, and R.L.C. Flemmer, 1985, "Predicting the Lift of Air-Lift Pumps in the Bubble Flow Regime," Chemsa Vol. 11, No.1, PP 14-17, January 1985.

[133] Clark, N.N., and R.L.C. Flemmer, 1985, "Predicting the Holdup in Two-Phase Bubble Upflow and Downflow using the Zuber and Findlay Drift-Flux Model," AIChE Journal, Vol. 31, No.3, PP 500-503, March, 1985.

[134] Clark, N.N., 1985, "Gas-Liquid Contacting in vertical Two-phase Flow," Industrial Engineering Chemistry Process Design and Development, Vol. 24, No.2, pp. 231-236.

[135] Clark, N.N., and R.J. Dabolt, 1986, "A General Design Equation for Airlift Pumps Operating in Slug Flow," AIChE Journal, Vol. 32, No.1, pp. 56-64.

[136] N. N. Clark and R. L. Flemmer, “Predicting the holdup in two-phase bubble upflow and downflow using the Zuber and Findlay drift-flux model,” AIChE J. 31, 500 (1985).

[137] Clark JF, Washburn L, Hornafius JS, Luyendyk BP (2000) Dissolved hydrocarbon flux from natural marine seeps to the southern California Bight. J Geophys Res 105: 11, 509–11, 522.

[138] Clift, R., Grace, J. R. and Weber, M. E., “Bubbles, Drops, and Particles”, Academic Press (1978). 380 pp., New York, NY.

[139] Cline JD, Holmes ML (1977) Submarine seepage of natural gas in Norton Sound, Alaska. Science 198:1149–1153

[140] Collins, R. (1978). The motion of a large gas bubble rising through liquid flowing in a tube. J. Fluid Mech. 89, 497-514.

[141] Cooke, G. D., and R. E. Carlson (1989), Reservoir Management for Water Quality and THM Precursor Control, 387 pp., American Water Works Association Research Foundation, Denver, CO.

[142] Cooke, G. D., E. B. Welch, S. A. Peterson, and P. R. Newroth (1993), Restoration and Management of Lakes and Reservoirs, 2nd ed., Lewis, Boca Raton, Fla.

[143] Crawford, G. B., and D. M. Farmer (1987), On the spatial distribution of ocean bubbles, J. Geophys. Res., 92(C8), 8231–8243, doi:10.1029/ JC092iC08p08231.

[144] C. R. Liro, E. E. Adams, and H. J. Herzog. Modeling the release of CO2 in the deep ocean. Technical Report MIT-EL 91-002, Energy Laboratory, Massachusetts Institute of Technology, June 1991.

[145] C. R. Liro, E. E. Adams, and H. J. Herzog. Modeling the release of CO2 in the deep ocean. Energy Conservation Management, 33(5-8):667-674, 1992.

[146] Crounse, B. C., Wannamaker, E. J., and Adams, E. E. (2007). “Integral model of a multiphase plume in quiescent stratification.” J. Hydraul. Eng., 133(1), 70–76.

[147] Cummings, P. D. and Chanson, H. (1999), "An experimental study of individual air bubble entrainment at a planar plunging jet", Chemical Engineering Research and Design, vol. 77, no. 2, pp. 159-164.

[148] Damaschke, N., Nobach, H., Nonn, T., Semidetnov, N., and Tropea, C. (2002a). Size and Velocity Measurements with the Global Phase Doppler Technique. In 11th international symposium on application of laser techniques to fluid mechanics, Lisbon.

[149] Damaschke, N., Nobach, H., and Tropea, C. (2002b). Optical limits of particle concentration for multi-dimensional particle sizing techniques in fluid mechanics. Experiments in Fluids, 32:143–152.

[150] Danciu, D. V., Da Silva, M. J., Schmidtke, M., Lucas, D. and Hampel, U. (2009), "Experimental investigation on air entrainment below impinging jets by means of video observations and image processing", WIT Transactions on Engineering Sciences, Vol. 63, pp. 481.

[151] Dantec Dynamics (2003). Flowmap Particle Sizer. Dantec Dynamics Newsletter, 10(7).

[152] Darmana, D., Deen, N.G., Kuipers, J.A.M., 2004. Modelling of Mass Transfer and Chemical Reactions in a Bubble Column Reactor using a Discrete Bubble Model, Proceedings of the 5th International Conference on Multiphase Flow, May30-June 4, Yokohama, Japan

[153] Darmana, D., Deen, N.G., Kuipers, J.A.M., 2005, Detailed modelling of hydrodynamics, mass transfer and chemical reactions in a bubble column using a discrete bubble model, Chemical Engineering Science, 60(12), 3383-3404.

[154] Das, G., Das, P.K., Purohit, N.K., Mitra, A.K., 1999. Flow pattern transition during gas liquid upflow through vertical concentric annuli—part I: experimental investigations. ASME Journal of Fluids Engineering 121, 895–901.

[155] Das, A.K., Das, P.K., Thome, J.R., 2009a. Transition of bubbly flow in vertical tubes: new criteria through CFD simulation. ASME Journal of Fluids Engineering 131 (9), 091303.1–091303.12.

[156] Das, A.K., Das, P.K., Thome, J.R., 2009b. Transition of bubbly flow in vertical tubes: effect of bubble size and tube diameter. ASME Journal of Fluids Engineering 131 (9), 091304.1–091304.6.

[157] D’Asaro, E., and C. McNeil (2007), Air-sea gas exchange at extreme wind speeds measured by autonomous oceanographic floats, J. Mar. Res., 66, 92–109.

[158] David I. Auerbach, Jennifer A. Caulfield, E. Eric Adams, and Howard J. Herzog. Impacts of ocean CO2 disposal on marine life: I. A toxicological assessment integrating constant concentration laboratory assay data with variable concentration field exposure. Environmental Modeling and Assessment 2, pages 333-343, 1997.

[159] Davidson, J. F. and Schuler, B.O.G., "Bubble Formation at an Orifice in a Viscous Liquid," Trans, of the Inst. of Chem. Eng., Vol. 38, p. 335–342, 1960.

[160] Davies R.M., Taylor G., 1949. The mechanics of large bubbles rising through extended liquids and through liquids in tubes. Proc. of Royal Soc. Of London, 200, 375-390.

[161] Davies, R. M. And G.I. Taylor (1950). The mechanics of large bubbles rising through extended liquids and through liquids in tubes. Proc. R. Soc., London Ser. A 200, 375-390.

[162] Davis, J. M. (1980), Destratification of reservoirs - A design approach for perforated-pipe compressed-air systems, Water Services, 84, 497-505.

[163] Davis, R. H. and Acrivos, A. 1985 Sedimentation of noncolloidal particles at low Reynolds numbers. Ann. Rev. Fluid Mech. 17, 91-118.

[164] D. Bhaga and M. E. Weber, Bubbles in viscous liquids: shape, wakes and velocities, J. Fluid Mech. 105, 61 (1981).

[165] Deane, G. B., and M. D. Stokes (2002), Scale dependence of bubble creation mechanisms in breaking waves, Nature, 418, 839–844.

[166] Deckwer, W., Bubble Column Reactors, John Wiley and Sons, 1991.

[167] Deckwer, W.D.,. Bubble column reactors. Wiley, Chichester. 1985.

[168] Deen, N. G., Solberg, T., Hjertager, B. H., 2001, Large eddy simulation of gas-liquid flow in a square cross-sectioned bubble column, Chemical Engineering Science, 56, 6341-6349

[169] Deen, N.G.. An Experimental and Computational Study of Fluid Dynamics in Gas-Liquid Chemical Reactors. Ph.D. thesis, Aalborg University Esbjerg, Denmark (2001).

[170] Delale, C. F., Nas, S., and Tryggvason, G., 2005, “Direct Numerical Simulation of Shock Propagation in Bubbly Liquids,” Phys. Fluids, 17, pp. 121705– 121708.

[171] Delano, A.D. 1998. Design Analysis of the Einstein Refrigeration Cycle, PhD Dissertation, Georgia Institute of Technology.

[172] Delnoij, E., Lammers, F. A., Kuipers, J. A. M., and van Swaaij, W. P. M. (1997a). Dynamic simulation of dispersed gas-liquid two-phase flow using a discrete bubble model. Chemical Engineering Science, 52(9), 1429-1458.

[173] Delnoij, E., Kuipers, J. A. M., and van Swaaij, W. P. M. (1997b). Computational fluid dynamics applied to gas-liquid contactors. Chemical Engineering Science, 52(21/22), 3623.

[174] Delnoij, E., Kuipers, J. A. M., and van Swaaij, W. P. M. (1997c). Dynamic simulation of gas-liquid two-phase flow: Effect of column aspect ratio on the flow structure. Chemical Engineering Science, 52(21/22), 3759.

[175] Delnoij, E., Kuipers, J. A. M., and van Swaaij, W. P. M. (1998). A threedimensional dimensional CFD model for gas-liquid bubble columns. Chemical Engineering Science, 54, 2217-2226.

[176] Delnoj, E., Westerweel, J., Deen, N. G., Kuipers, J. A. M. and van Swaaij, W. P. M. 1999. Ensemble correlation PIV applied to bubble plumes rising in a bubble column. Chemical Engineering Science 54 (1999) 5159-5171.

[177] Delnoij, E., Kuipers, J.A.M. and van Swaaij, W. and Westerweel, J., 2000. Measurement of gas-liquid two-phase flow in bubble columns using ensemble correction PIV. Chemical Engineering Science 55 (2000). Pp 3385-3395. PII: S 0 0 0 9 - 2 5 0 9 (9 9) 0 0 5 9 5 – 3.

[178] Deswal, S. and Verma, D. V. S. (2007), "Air-water oxygen transfer with multiple plunging jets", Water Quality Research Journal of Canada, vol. 42, no. 4, pp. 295-302.

[179] Devanathan, N., Moslemian, D. and Dudukovic, M.P., 1990. Flow mapping in bubble columns using CARPT. Chem. Eng. Sci., 45, pp. 2285-2291.

[180] Devanathan, N., Dudukovic, M. P., Lapin, A., and LuK bbert, A. (1995). Chaotic flow in bubble column reactors. Chemical Engineering Science, 50 (16), 2661.

[181] Dhaoudi, H., Poncin, S., Hornut, J. M. and Wild, G., 1996, Hydrodynamics of airlift reactor: experiments and modelling, Chem Eng Sci, 51: 2625.

[182] Ditmars, J. D., and K. Cederwall (1974), Analysis of air-bubble plumes, 14th Coastal Engineering Conference, Am. Soc. Civ. Engineers, Copenhagen, Denmark, 24-28 June. pp. 2209–2226 (Chapter 128).

[183] Juric, D., and Tryggvason, G., 1998, “Computation of Boiling Flows,” Int. J. Multiphase Flow, 24, pp. 387–410.

[184] Dissanayake, A., Gros, J. and Socolofsky, S., 2018. Integral models for bubble, droplet, and multiphase plume dynamics in stratification and crossflow. *Environmental Fluid Mechanics*, 18(5), pp.1167-1202.

[185] Dissanayake, A., Rezvani, M., Socolofsky, S., Bierlein, K. and Little, J., 2021. Bubble Plume Integral Model for Line-Source Diffusers in Ambient Stratification. *Journal of Hydraulic Engineering*, 147(5), p.04021015.

[186] Dong, F., Z.X. Jiang, X.T. Qiao and L.A. Xu, 2003. Application of Electrical Resistance Tomography to Two-Phase Pipe Flow Parameters Measurement. Flow Measurement and Instrumentation, 14: 183-192.

[187] Dong-Guan Seol; Duncan B. Bryant; and Scott A. Socolofsky, M.ASCE. Measurement of Behavioral Properties of Entrained Ambient Water in a Stratified Bubble Plume. Journal Of Hydraulic Engineering. Asce / November 2009 / 983-988. DOI: 10.1061/(ASCE)HY.1943 -7900.0000109.

[188] Donnelly, B., Murray, D. B., & O'Donovan, T. S. (2008). Bubble enhanced heat transfer from a vertical heated surface. Journal of Enhanced Heat Transfer, 15(2).

[189] Dougherty, E., 1991. Morphological granulometric analysis of electrophotographic images--size distribution statistics for process control. *Optical Engineering*, 30(4), p.438.

[190] Dorrestein R. 1951. General Linearized Theory of the effect of Surface Films on Water Ripples. Proc. K. Ned. Akad. Wet. B 54-260.

[191] Douek, R. S., Hewitt, G. F. and Livingston, A. G., 1995, A hydrodynamic study of the riser zone in a three phase airlift (TPAL) reactor, Trans IChemE, Part A, Chem Eng Res Des, 73 (A3): 336.

[192] Drahos, J., Zahradnik, J., Puncochar, M., Fialova, M., Bradka, F., 1991. Effect on operating conditions on the characteristics of the pressure fluctuations in a bubble column. Chemical Engineering Processing 29, 107–115.

[193] Drew, D.A., Lahey, R.T., 1982. Phase distribution mechanisms in turbulent low-quality two-phase flow in circular pipe. J. Fluid Mech. 117, 91–106.

[194] Drew, D. A. 1983 Mathematical modeling of two-phase flow. Ann. Rev. Fluid Mech. 15, 261-291.

[195] Dumitrescu, D. T., (1943). Strömung an einer Luftblase in senkrechten Rohr. Z. Angew. Math. Mech., Vol. 23, pp.139-149.

[196] Eccles, M.A. (1972). Research Project Report. Chem. Eng. Department, University of Cambridge, England.

[197] E. E. Adams and H. J. Herzog. Environmental impacts of ocean disposal of CO2. Technical Report MIT-EL 96-003, Energy Laboratory, Massachusetts Institute of Technology, 1996.

[198] E. Eric Adams, Jennifer A. Caulfield, Howard J. Herzog, and David I. Auerbach. Impacts of reduced pH from ocean CO2 disposal: Sensitivity of zooplankton mortality to model parameters. Waste Management, pages 375-380, 1997.

[199] Einstein, A. and Szilard, L. 1930. Refrigeration. (Appl. U.S. Patent: 16 Dec. 1927; Priority: Germany, 16 Dec. 1926).

[200] Einstein, A. and Szilard, L. 1928. Improvements Relating to Refrigerating Apparatus. (Appl. U.K. Patent: 16 Dec. 1927; Priority: Germany, 16 Dec. 1926)

[201] Ekberg, N.P., Ghiaasiaan, S.M., Abdel-Khalik, S.I., Yoda, M., Jeter, S.M., 1999. Gas– liquid two-phase flow in narrow horizontal annuli. Nuclear Engineering and Design 192, 59–80.

[202] E. Marchandise, P. Geuzaine, N. Chevaugeon, J. Remacle, A stabilized finite element method using a discontinuous level set approach for the computation of bubble dynamics, J. Comput. Phys. 225 (1) (2007) 949–974.

[203] Enes, K., 2010. Survey of gas-liquid mass transfer in biorectors. Ph.D. thesis, Iowa State University.

[204] Enever, K. J. (1967). “An introduction to pressure surges in gas-liquid mixtures.” 9th Members Conf., BHRA, Cranfield, UK.

[205] Enever, K. J. (1972). “Surge pressures in a gas-liquid mixture with a low gas content.” 1st Int. Conf. on Pressure Surges, BHRA, Cranfield, UK.

[206] Ervine, D. A. and Elsawy, E. M. (1975), "Effect silt a falling nappe on river aeration", Int Assoc for Hydraul Res, 16th Congr, Proc, Prepr, Fundam Tools To Be Used in Environ Prob, vol. 3 -Subj, pp. 390-397.

[207] E. Shams, J. Finn and S. V. Apte. A Numerical Scheme for Euler-Lagrange Simulation of Bubbly Flows in Complex Systems. International Journal For Numerical Methods In Fluids. 2010; 00:1-0

[208] Esmaeeli Asghar and Tryggvason, G Retar. (1998). Direct numerical simulation of bubbly flows. Part I- low Reynolds number arrays, J. Fluid Mech., vol. 377, pp. 313-345. Printed in the United Kingdom.

[209] Fabregat Tomàs, A., Poje, A., Ö zgökmen, T. and Dewar, W., 2016. Dynamics of multiphase turbulent plumes with hybrid

buoyancy sources in stratified environments. Physics of Fluids, 28(9), p.095109.

[210] Fabian A. Bombardelli. Characterization of Coherent Structures from Parallel, L.E.S. Computations of Wandering Effects in Bubble Plumes. World Water Congress 2003. ASCE 2004.

[211] Fabian A. Bombardelli, Gustavo C. Buscaglia, Marcelo H. Garc´ıa, and Enzo A. Dari. Simulation of Wandering Phenomena in Bubble Plumes Via A K-E Model and A Large-Eddy-Simulation (Les) Approach. Mec´anica Computacional Vol. XXIII G.Buscaglia, E.Dari, O.Zamonsky (Eds.) Bariloche, Argentina, November 2004

[212] Fannelop, T. K., and K. Sjoen (1980), Hydrodynamics of underwater blowouts, Norweg. Maritime Res., 4, 17-33.

[213] Fannelop, T. K., S. Hirschberg, and J. Kueffer (1991), Surface current and recirculating cells generated by bubble curtains and jets, J. Fluid Mech., 229, 629-657. DOI:10.1017/S0022112091003208.

[214] Fan, L. S., Muroyama, K. and Chen, S. H., 1982, Hydrodynamic characteristics of inverse fluidization in liquid-solid and gas-liquidsolid systems, Chem Eng J, 24: 143.

[215] Fan, L. S., Muroyama, K. and Chen, S. H., 1982, Some remarks on hydrodynamics of inverse gas-liquid-solid fluidization, Chem Eng Sci, 37: 1570.

[216] Fan, L.-S. (1989). Gas-Liquid-Solid Fluidization Engineering. Butterworth Series in Chemical Engineering, Boston, MA.

[217] Farag, I. H., Nikolov, V. R. and Nikov, I., 1997, Gas-liquid mass transfer in three-phase inverse fluidized bed, Advances in fluidization and fluid particle systems, AIChE Symposium Series, 93: 51.

[218] Farmer, D., and M. Li (1995), Patterns of bubble clouds organized by Langmuir circulation, J. Phys. Oceanogr., 25, 1426–1440.

[219] Farmer, D. M., S. Vagle, and A. D. Booth (1998), A free-flooding acoustical resonator for measurement of bubble size distributions, J. Atmos. Oceanic Technol., 15, 1132–1146.

[220] Fast, A. W., and M. W. Lorenzen (1976), Synoptic survey of hypolimnetic aeration, Journal of the Environmental Engineering Division, American Society of Civil Engineers, 102(EE6), 1161-1173.

[221] Fast, A. W., Overholtz, WJ., Tubb, RA., (1975b), Hypolimnetic oxygenation using liquid oxygen, Water Resour. Res., 11(2), 294-299.

[222] F. B. Cheung and M. Epstein. Two-phase gas bubble-liquid boundary layer flow along vertical and inclined surfaces. Nuclear Engineering and Design, 99(1):93-100, 1987.

[223] F. Durst, A. M. K. P. Taylor and J. H. Whitelaw, Experimental 3and Numerical Investigation of Bubble-driven Laminar Flow in an Axisymmetric Vessel, International Journal of Multiphase Flow, 10 (1984) 557-569.

[224] Fernandes, R.C., R. Semiat, and A.E. DuckIer, 1983, "Hydrodynamic Model for Gas-Liquid Slug Flow in Vertical Tubes," AIChE Journal, Vol. 29, No.6, pp. 981-989.

[225] Filla, M.J., J.F. Davidson, J.F. Bates and M.A. Eccles (1976). Gas phase controlled mass transfer from a bubble. Chem. Sc. 31, 359-367.

[226] Finch, R. D., and Neppiras, E. A., 1973, "Vapor Bubble Dynamics," J. Acoust. Soc. Am., 53, pp. 1402–1410.

[227] Finch, J.A. and Dobby, G.S., 1991. Column rotation: A selected review. Part I. Int. J. Min. Proc., 33, pp. 343 - 354.

[228] Finn Thorkildsen, Guttorm Alendal, and Peter M. Haugan. Modeling of CO2 droplet plumes. Technical report, Nansen Environmental, and Remote Sensing Center, Adv. Griegsvei 3A, N - 5037 Solheimsviken, Norway, 1995.

[229] Fire Department of Fukui Prefecture. (1998). Memories and Teaching on Oil-leakage Disaster of Russian Tanker. Committee of Disaster Record in Russian Tanker Oil-leakage Accidents.

[230] Fleischer, C., Becker S., Eigenberger, G., 1996. Detailed modeling of the chemisorption of CO2 into NaOH in a bubble column, Chemical Engineering Science, 51, 1715-1724.

[231] Fluent, Inc., 2001. Fluent 6.0 User's Guide. Fluent, Inc., Lebanon, NH. Goring, D.G., Nikora, V.I., 2002. Despiking acoustic Doppler velocimeter data. Journal of Hydraulic Engineering 128 (1), 117-126.

[232] F.S. de Sousa, N. Mangiavacchi, L.G. Nonato, A. Castelo, M.F. Tomé;, V.G. Ferreira, J.A. Cuminato, S. McKee, A front-tracking/front-capturing method for the simulation of 3d multi-fluid flows with free surfaces, J. Comput. Phys. 198 (2) (2004) 469–499.

[233] F. S. Sousa, L. M. Portela, M. T. Kreutzer, C. R. Kleijn. Numerical simulation of slug flows in square hannels using a front-tracking/front-capturing method International Conference on Multiphase Flow, ICMF 2007, Leipzig, Germany. July 9 – 13, 2007.

[234] Fu, X.Y., Ishii, M., 2003. Two-group interfacial area transport in vertical air–water flow I. Mechanistic model. Nuclear Engineering Design 219, 143–168.

[235] Gachter, R., and B. Wehrli (1998), Ten years of artificial mixing and oxygenation: No effect on the internal phosphorus loading of two eutrophic lakes, Environ. Sci. Technol., 32(23), 3659-3665.

[236] Ga¨chter, R., and B. Mu¨ ller (2003), Why the phosphorus retention of lakes does not necessarily depend on the oxygen supply to their sediment surface, Limnol. Oceanogr., 48(2), 929– 933.

[237] G. Alendal, H. Drange, and F. Thorkildsen. Two-phase modeling of CO2 droplet plumes. Technical Report 153, Nansen Environmental and Remote Sensing Center, 1998.

[238] García, C. M., and García, M. H. (2006). "Characterization of flow turbulence in large-scale bubble–plume experiments." Exp. Fluids, 41(1), 91–101.

[239] Garnier, A., Chavarie, C., Andre, G. and Klvana, D., 1990, The inverse fluidization airlift bioreactor, Chem Eng Comm, 98: 31.

[240] Garrett, C., M. Li, and D. M. Farmer (2000), The connection

between bubble size spectra and energy dissipation rates in the upper ocean, J. Phys. Oceanogr., 30, 2163–2171.

[241] Gavrilescu,M. and Tudose, R. Z., 1997, Mixing studies in external-loop airlift reactors, Chem Eng J, 66: 97.

[242] Gemza, A. (1995), Some practical aspects of whole lake mixing and hypolimnetic oxygenation: Ecological impacts of aeration on lakes and reservoirs in southern Ontario, Lake Reservoir Manage., 11(2), 141-142.

[243] Georges L. Chahine. Strong interactions bubble/bubble and bubble/flow. 1994 Kluwer Academic Publishers. Printed in the Netherlnnds. Pp. 195-206.

[244] G. K. Batchelor. Heat convection and buoyancy efiects in fluids. Quarterly Journal of The Royal Meteorological Society, 80:339-358, 1954.

[245] Gibbons, H. L., (1994), Worlds largest attempt at hypolimnetic aeration, Lake Reservoir Manage., 9(2), 76.

[246] G. L. Chahine, “Cloud cavitation: Theory,” Proceedings of the 14th Symposium on Naval Hydrodynamics, Ann Arbor, Michigan (National Academy Press, Washington D.C., 1983), pp. 161–195.

[247] G. L. Chahine and R. Duraiswami, “Dynamical interactions in a multibubble cloud,” ASME J. Fluids Eng. 114, 680 (1992).

[248] Glover, A., Skippon, S., and Boyle, R. (1995). Interferometric laser imaging for droplet sizing: a method for dropletsize measurement in sparse spray systems. Applied Optics, 34:8409–8421.

[249] Goossens, L., 1979. Reservoir destratification with bubble plumes. Delft University Press. Delft, The Netherlands, 1979. EDB-80-118650

[250] Govier, G.w., and K. Aziz, 1972, The Flow of Complex Mixtures in Pipes. Van Nostrand Reinold Co. New York, 792 pp.

[251] Goldsmith, H.L. and S.G. Mason (1962). The movement of single large bubbles in closed vertical tubes. J. Fluid. Mech. 14, 42-58.

[252] Gong, X., Takagi, S., Matsumoto, Y., 2004. A Numerical Study on the Detailed Structure and Mass Transfer of Ozone Plumes for Water Purification System, Proceedings of the 5th International Conference on Multiphase Flow, May 30-June 4, Yokohama, Japan

[253] Goosens L. H. J. and Smith J. M. 1975. The Hydrodynamics of Unconfined Bubble Columns for Mixing Lakes and Reservoirs. Chem. Eng. Tech. 47, 951. PP. 249-261.

[254] G. P. Celata, M. Cumo, F. D’Annibale, and A. Tomiyama, Terminal bubble rising velocity in one-component systems, in Proc. of 39th European Two-Phase Flow Group Meeting, paper F-3 (Aveiro, 2001).

[255] Gregory J. Orris and Michael Nicholas. Collective oscillations of fresh and salt water bubble plumes. 2000 Acoustical Society of America. [S0001-4966(99)03012-X] PACS numbers: 43.30.Nb, 43.30.Es {SAC-B}. J. Acoust. Soc. Am. 107 (2), February 2000. 771-787.

[256] Grevet J.H., J. Szekely, N. El-Kaddah, An experimental and theoretical study of gas bubble driven circulation systems, Int. J. Heat Mass Transfer 25 (4) (1982) 487-497.

[257] Griffith, P. And G.B. Wallis (1961). Two-phase slug flow. J. of Heat Transfer, Trans. ASME, Serie C 83, 307-320.

[258] Gross R. W. and kuhlman J. M. 1992. Three-Component Velocity Measurements in a Turbulent Recarculating Bubble-Driven Liquid Flow. Int. J. Multiphase Flow 18(3), 413-421.

[259] G. Tryggvason, B. Bunner, A. Esmaeeli, D. Juric, N. Al-Rawahi, W. Tauber, J. Han, S. Nas, and Y.-J. Jan. A Front-Tracking Method for the Computations of Multiphase Flow. Journal of Computational Physics 169, 708–759 (2001).

[260] Guinot, V. (2001). “Numerical simulation of two-phase flow in pipes using Godunov method.” Int. J. Numer. Methods Eng., 50(5), 1169–1189.

[261] Haberman, W. L. and Morton, R. K., "An Experimental Study of Bubbles Moving in Liquids," Trans ASCE Proc, Vol. 80, No. 387, Eng. Mech. Div., 1954. Soc. Civ. Eng., 80, 379-427. 2799, 227–252.

[262] Hao, Y., and Prosperetti, A., 1999, “The Dynamics of Vapor Bubbles in Acoustic Pressure Fields,” Phys. Fluids, 11(8), pp. 2008–2019.

[263] Hare, J. E., C. W. Fairall, W. R. McGillis, J. B. Edson, B. Ward, and R. Wanninkhof (2004), Evaluation of the National Oceanic and Atmospheric Administration / Coupled-Ocean Atmospheric Response Experiment (NOAA/COARE) air-sea gas transfer parameterization using GasEx data, J. Geophys. Res., 109, C08S11, doi:10.1029/2003JC001831.

[264] Hasan, A.R., Kabir, C.S., 1992. Two-phase flow in vertical and inclined annuli. International Journal of Multiphase Flow 18 (2), 279–293.

[265] Hassan Abdulmouti 2002. The Flow Patterns in Two Immiscible Stratified Liquids Induced by Bubble Plume. The International Journal of Fluid Dynamic. Vol. 6. Article 1.

[266] Hassan Abdulmouti 2002. Visualization of The Flow Patterns in Two Immiscible Stratified Liquids Due to Bubble Plume. The 10th International Symposium on Flow Visualization. Kyoto Japan. August 26-29.

[267] Hassan Abdulmouti 2003. Visualization and Image Measurement of Flow Structures Induced by a Bubbly Plume. Ph. D. thesis. Fukui University.

[268] Hassan Abdulmouti 2006. Bubbling Convection Patterns in Immiscible Two-phase Stratified Liquids. International Journal of Heat Exchangers (IJHEX). Vol. VII. No. 1. Pp. 123-143. ISSN 1524-5608. June 2006.

[269] Hassan Abdulmouti. Surface Flow Generation Mechanism Induced by Bubble Plume. Yanbu Journal of Engineering and Science (YJES). Second issue. PS-M02-28 (50-67). 2011.

[270] Hassan Abdulmouti. The Principle of Bubbly Flow and Its Application Especially to Oil Fence. Alzahrawi Encyclopedia for Arab Engineer. 1, 11, 2012.

[271] Hassan Abdulmouti. The Principle and Classification of PIV. Alzahrawi Encyclopedia for Arab Engineer. 19, 9, 2012.

[272] Hassan Abdulmouti. Particle Imaging Velocimetry (PIV) Technique: Principles and Application. Yanbu Journal of Engineering and Science (YJES). ISSN: 1658-5321. Vol. 6, April 2013.

[273] Hassan Abdulmouti. Particle Imaging Velocimetry (PIV) Technique: Principles, the typically used methods, classification and applications. Scholar's Press. ISBN-13: 978-3-639-51249-6. 6 March, 2013.

[274] Hassan Abdulmouti. Measurement of Flow Structures Induced by a Bubbly Plume Using Visualization, PIV and Image Measurement. Scholar's Press. ISBN-13: 978-3-639-51490-2. 7, June, 2013.

[275] Hassan Abdulmouti. Bubbly Two-Phase Flow: Part I- Characteristics, Structures, Behaviors and Flow Patterns. DOI: 10.5923/j.ajfd.20140404.03. American Journal of Fluid Dynamics. Scientific and Academic Publishing. Volume 4, Number 4, 4(4): 194-240. December 2014.

[276] Hassan Abdulmouti. Bubbly Two-Phase Flow: Part II- Characteristics and Parameters. DOI: 10.5923/j.ajfd.20140404.01 American Journal of Fluid Dynamics. Scientific and Academic Publishing. Volume 4, Number 4, 4(4): 115-180. December 2014.

[277] Hassan Abdulmouti. Parameter Measurements of Bubble Plume Structure. 19th Australasian Fluid Mechanics Conference. Melbourne, Australia. 8-11 December 2014.

[278] Hassan Abdulmouti. The Role of Kaizen (Continuous Improvement) in improving Companies' Performance: A Case Study. ISBN: 978-1-4799-6064-4. INSPEC Accession Number: 15091284. DOI: 10.1109/IEOM.2015.7093768. May 2015. IEEE Xplore Digital Library.

[279] Hassan Abdulmouti. Experimental Measurement for Surface Flow Characteristics Generated by a Bubble Plume. The Journal of Flow Visualization and Image Processing. 22 (1–3), 39–58. 2015. Begell House "USA". The Home for Science and Engineering.

[280] Hassan Abdulmouti. Experimental Measurements of Bubble Convection Models in Two-phase Stratified Liquids. Experimental Thermal and Fluid Science (2016). Volume 83C, May 2017. Pages 69-77. (ELSEVIER). https://doi.org/10.1016/j.expthermflusci.2016.12.010.

[281] Hassan Abdulmouti. 2D- numerical simulation of surface flow velocity and internal flow structure generated by bubbles. Multiphase Science and Technology 28 (2): 153–171 (2016). 0276–1459/16/$35.00 © 2016 by Begell House, Inc "USA". The Home for Science and Engineering. DOI: 10.1615/MultScienTechn.2017018926.

[282] Hassan Abdulmouti. The Measurements of Bubble Plume Structure Parameter. International Journal of Fluid Mechanics Research. Volume 44. Issue 4. pages 277-295. (2017). Begell House "USA". The Home for Science and Engineering. DOI: 10.1615/InterJFluidMechRes.2017014476.

[283] Hassan Abdulmouti. Numerical Simulation and Fundamental Characteristics of Surface Flow Generated by Bubbly Flows. International Journal of Fluid Mechanics Research. Volume 45, Issue 3, Pp. 263-282. (2018). ISSN Print: 1064-2277. ISSN Online: 2152-5102. DOI: 10.1615/InterJFluidMechRes.2018021875. Begell House "USA". The Home for Science and Engineering.

[284] Hassan Abdulmouti. Measurements of Thermal Effect on Bubble Parameter. The 3rd Thermal and Fluids Engineering Conference (TFEC). March 4-7, 2018. Fort Lauderdale, FL, USA.

[285] Hassan Abdulmouti. Numerical Simulation of Bubble Convection in Two-phase Stratified Liquids" Multiphase Science and Technology by Begell House, Inc "USA". Volume 31, Issue 2, pp. 133–149 (2019). The Home for Science and Engineering. DOI: 10.1615/MultScienTechn.2019029995. (Impact factor: 0.82, SJR:0.153- Q3= 0.184, H Index: 16, SINP 0.222, Cite Score 0.26).

[286] Hassan Abdulmouti. Measurement of Bubbles Properties to Generated Efficient Surface Flow. The 4th International Conference on Multiphase Flow and Heat Transfer (ICMFHT'19). April 10-12, 2019. Rome, Italy.

[287] Hassan Abdulmouti. Effect of Temperature on Surface Flow Generated by Bubble Plumes. The Journal of Flow Visualization and Image Processing. Vol. 29, Issue 1, Pp. 1-28. 2022. Begell House "USA". The Home for Science and Engineering. (Impact factor: 0.321, SJR: Q3= 0.214, H Index: 12). ISSN Print: 1065-3090, ISSN Online: 1940-4336; SNIP: 0.312. DOI: 10.1615/JFlowVisImageProc.2021038705.

[288] Abdulmouti, Hassan. 2021. "Improving the Performance of Surface Flow Generated by Bubble Plumes" MDPI. Fluids. Vol: 6, No. 8: 262. https://doi.org/10.3390/fluids6080262. Special Issue "Dynamics of Droplets and Bubbles". Multidisciplinary Digital Publishing Institute. (Impact factor: 1.81, SJR: Q2= 0.399, H Index: 14).

[289] Abdulmouti, Hassan. "SURFACE FLOW GENERATION MECHANISM INDUCED BY A BUBBLE PLUME." *Yanbu Journal of Engineering and Science* 2.1 (2021): 50-67.

[290] Hassan Abdulmouti, Esam Jassim. Visualization and Measurements of Bubbly Two-Phase Flow Structure Using Particle Imaging Velocimetry (PIV). Annual International Interdisciplinary Conference, IIC. Azores, Portugal. 24 -26 April 2013.

[291] Hassan Abdulmouti and Tamer Mohamed Mansour. The Technique of PIV and Its Applications. 10th International Congress on Liquid Atomization and Spray Systems (ICLASS-2006). Aug. 27-Sept. 1. Kyoto, Japan. 2006.

[292] Hassan Abdulmouti and Tamer Mohamed Mansour. Bubbly Two-Phase Flow and Its Application. 10th International Congress on Liquid Atomization and Spray Systems (ICLASS-2006). Aug. 27-Sept. 1. Kyoto, Japan. 2006.

[293] Hassan Abdulmouti, Fujio Yamamoto, Yuichi Murai, Yasuhiro Kobayashi, 1997. Research and Development for a New Bubble Curtain Type of Oil Fence. Journal of the Visualization Society of Japan. vol. 17 suppl. No. 1. Pp. 239~242.

[294] Hassan Abdulmouti, Yuichi Murai, junichi Ohat, Fujio Yamamoto 1998. PIV Measurement and Numerical Analysis of Flow around Bubble Curtain published in preprint of (J.S.M.E.) Japanese Society of Mechanical Engineer. No. 987-1. pp. 83~84.

[295] Hassan Abdulmouti, Yuichi Murai, junichi Ohat, Fujio Yamamoto 1999. PIV Measurement of Surface Flow Induced by Bubble Curtain. Journal of the Visualization

Society of Japan. Vol. 19 Suppl. No. 1. Pp.239~242.

[296] Hassan Abdulmouti, Yuichi Murai, junichi Ohat, Fujio Yamamoto 1999. PIV Measurement of Bubbly Flow Interaction with Water Surface. Journal of the Visualization Society of Japan. Vol. 19. Suppl. No. 2. Pp.209-210.

[297] Hassan Abdulmouti Yuichi Murai, Ohno Yasushi, Fujio Yamamoto 2001. Measurement of Bubble Plume Generated Surface Flow Using PIV, Journal of the Visualization Society of Japan. Vol. 21. No. 2. Pp. 31-37.

[298] Hassan Abdulmouti and Monsif Shinneeb. Investigation of Free-Surface Flow Induced by a Bubbly Plume Using PIV. 2020 (ASET). Electronic ISBN: 978-1-7281-4640-9. ISBN: 978-1-7281-4641-6. Print on Demand (PoD). Pp. 1-5. DOI: 10.1109/ASET48392.2020.9118203. Publisher: IEEE. Added to IEEE *Xplore*: 16 June 2020.

[299] Hassan Abdulmouti and Monsif Shinneeb. Investigation of Free-Surface Flow Induced by a Bubbly Plume Using PIV. The International Conference on Sustainable Environment and Urban Infrastructure (SEUI-2020 ASET). Advances in Science and Engineering Technology International Conferences. February 04-06, 2020.

[300] Hassan, Y. A., Blanchat, T. K., Seeley, Jr., C. H. and Canaan, R. E. 1992 Simultaneous velocity measurements of both components of a two-phase flow using particle image velocimetry. Intl J. Multiph. Flow 18 (3), 371–395.

[301] Hassoon, H. 1989. A two-phase investigation relating to circulating bubble absorbers. PhD thesis, Mechanical Engineering Department, University of Bristol, U.K.

[302] Herold, K.E.; Radermacher, R. and Klein, S.A. 1996. Absorption Chillers and Heat Pumps. CRC Press, Boca Raton, FL.

[303] Henderson D. M. and Miles J. W. 1994. Surface-Wave Damping in Circular Cylinder with a Fixed Contact Line. J. Fluid Mech. 275, 285-299 (hereinafter reefed to as HM94).

[304] Herringe, R.A., and Davis, M.R., Journal of Fluid Mechanics, 73 (1976), 97.

[305] Hess, C. F. (1998). Planar particle image analyzer. In 9th International Symposium on Applications of Laser Techniques to Fluid Mechanics, Lisbon.

[306] Hibiki, T., and Ishii, M., 1999, "Experimental Study on Interfacial Area Transport in Bubbly Two-Phase Flows," Int. J. Heat Mass Transfer, 42, pp. 3019– 3035.

[307] Hideki Murakawa, Hiroshige Kikura, Masanori Aritomi. Application of Multi-Wave Tdx For Multi-Phase Flow Measurement. 4th International Symposium on Ultrasonic Doppler Method for Fluid Mechanics and Fluid Engineering Sapporo, 6.-8. September, 2004.

[308] Higson, D.J., 1960, The Flow of Gas-Liquid Mixtures in vertical Pipes. Thesis, Imperial College of Science and Technology, England.

[309] Hjalmars, S., 1973, "The origin of Instability in Airlift Pumps," Journal of Applied Mechanics, June 1973, pp. 399-404.

[310] H. Karimi, M. R. Rahimi, "A Robust Classification method for the Prediction of Two-phase Flow Pattern, using Ensemble Classifiers Technique," in proc. 11th Int. Conf. on Multiphase Flow in Industrial Plants, Palermo, 2008, pp. 443-451.

[311] Hondzo, M. (1998), Dissolved oxygen transfer at the sediment-water interface in a turbulent flow, Water Resour. Res., 34(12), 3525-3533.

[312] Hoult D. P. Oil on the Sea. Plenum, 1969.

[313] Hovland M, Judd AG, Burke RA Jr (1993.) The global flux of methane from shallow submarine sediments. Chemosphere 26:559–578.

[314] Howell D., Heath T., Mckenna C., Hwang W. and Schatz M. F. 2000. Measurements of Surface-Wave Damping in a Container. Phys. Fluids 12, 322-326.

[315] Huang, F., Takahashi, M., and Guo, L. (2005). "Pressurewave propagation in air-water bubbly and slug flow." Prog. Nucl. Energy, 47(1-4), 648–655.

[316] Hubert Chanson. Air-Water Bubbly Flows: Theory and Applications. Ph. d. thesis. School of Engineering. The University of Queensland. January 1999.

[317] Hu, H. H. 1996 Direct simulation of flows of liquid-solid mixtures. Intl J. Multiphase Flow 22, 335-352.

[318] Hui Zhu, Mark Simmons, Waldek Bujalski and Alvin Nienow. Mixing of the Liquid Phase in a Model Aerated Bioreactor Equipped with 'Elephant Ear' Agitators using Particle Image Velocimetry. International Conference on Multiphase Flow, ICMF 2007, Leipzig, Germany, July 9–13, 2007.

[319] Husain, L.A., and P.L. Spedding, 1976, "The Theory of the Gas-Lift Pump," International Journal of Multiphase Flow, Vol. 3, pp. 83-87.

[320] Hussain N. A. and Siegel R. 1976. Liquid Jet Pumped by Rising Gas Bubbles, J. Fluids Eng., March 8. Pp. 49-62.

[321] Hussain N. A. and Narang B. S. 1984. Simplified Analysis of Air-Bubble Plumes in Moderately Stratified Environments. ASME. Journal of Heat Transfer. Vol. 106, pp. 543-551.

[322] H. Wang, Z.-Y. Zhang, Y.-M. Yang, and H. S. Zhang, Surface tension effects on the behavior of a rising bubble driven by buoyancy force. Chin. Phys. B 19, 026801 (2010).

[323] Hyun Dong Kim, Seung Jae Yi, Jong Wook Kim and Kyung Chun Kim. Structure analysis of bubble driven flow by time-resolved PIV and POD techniques. Journal of Mechanical Science and Technology 24 (4) (2010) 977~982. DOI 10.1007/s12206-010-0210-1.

[324] Iamandi, C., and Rouse, H. (1969) "Jet-induced circulation and diffusion." J. Hydr. Div., 95(2), 589–601.

[325] Ibrahim, Y. A. A., Briens, C. L., Margaritis, A. and Bergongnou,M. A., 1996, Hydrodynamic characteristics of a three-phase inverse fluidizedbed column, AIChE J, 42: 1889.

[326] Iguchi, M., Takeuchi, H. and Morita, Z. (1991) The Flow Field in Air-Water Vertical Bubbling Jets in a Cylindrical Vessel. ISIJ International, 31 (3), 246-253, 1991.

[327] Iguchi, M., Uemura, T., Yamamoto, F., Morita, Z., 1992. Multiphase flows in ironmaking and steel-making processes. Jpn J. Multiphase Flow 6, 54–64.

[328] Iguchi, M., Kondoh, T., Morita, Z., Nakajima, K., Hanazaki, K., Uemura, T. and Yamamoto, F. (1995) Velocity and Turbulence Measurements in a Cylindrical Bath Subject to Central Bottom Gas Injection. Metallurgical and Material Transactions B, 26B, 241-247, 1995.

[329] Iguchi, M., Shinkawa, M., Nakamura, H. and Morita, Z. (1995) Mean Velocity and Turbulence of Water Flow in a Cylindrical Vessel Agitated by Bottom Air Injection. ISIJ International, 35 (12), 1431-1437, 1995.

[330] Iguchi M., Okita K., Nakatani T., Kasai N. 1997. Structure of Turbulent Round Bubbling Jet Generated by Premixed Gas and Liquid Injection, Int. J. Multiphase Flow, Vol. 23, 2, pp.249-262.

[331] Ihab Edward Gerges. Two-Phase Bubbly Flow Structure In Large Diameter Pipes. Master of Engineering Thesis. Cairo University). March, 1999. ISBN. 3 9005 0219 9807 9.

[332] Imberger, J., and Patterson, J. C. (1990). "Physical limnology." Advances in applied mechanics, 27, 305-475.

[333] Imteaz, M. A., and T. Asaeda (2000), Artificial mixing of lake water by bubble plume and effects of bubbling operations on algal bloom, Water Res., 34(6), 1919-1929.

[334] Ishii, M., 1975. Thermo-Fluid Dynamic Theory of Two-Phase Flow. Eyrolles, Paris.

[335] Ishii, M., Mishima, K., 1984. Two-fluid model and hydrodynamic constitutive relations. Nuclear Engineering and Design 82, 107–126.

[336] Ishii, M. and Sun, X. Interfacial Characteristics of Two-phase Flow. Multiphase Science and Technology, Vol. 18, 1-29 (2006).

[337] Jakobsen, H. A., Sannaes, B. H., Grevskott, S., and Svendsen, H. F. (1997). Modeling of vertical bubble-driven flows. Industrial and Engineering Chemistry Research, 36, 4052.

[338] Jacobsen, H.A., 2008. Chemical reactor modeling. Springer-Verlag, Berlin.

[339] Jaeger, D. (1990), TIBEAN: A new hypolimnetic water aeration plant, Internat. Vereinigung fuer Theoret. und Angewandte Limnol., 24(1), 184-187.

[340] Jameson, G. J., and Kupferberg, A. (1967). Pressure behind a bubble accelerating from rest: Single theory and applications. Chemical Engineering Science, 22, 1053-1055.

[341] Jaromír Havlica, Miroslav Šimčík, Radovan Bunganič, Marek Večeř, Marek Ruzicka, Kamil Wichterle, Jiří Drahoš. A case study on bubble formation: numerics vs. measurements. International Conference on Multiphase Flow, ICMF 2007, Leipzig, Germany, July 9 – 13, 2007.

[342] J. Chahed, V. Roig, L. Masbernat. Eulerian–Eulerian two-fluid model for turbulent gas–liquid bubbly flows. International Journal of Multiphase Flow 29 (2003) 23–49.

[343] Jeelani, S.A.K., K.V. KasipatiRao, and G.R. Balasubramanian, 1979, "The Theory of the Gas-Lift Pump: A Rejoinder," International Journal of MuItiphase Flow, Vol. 5, pp. 225-228.

[344] Jeff Tyson. howstuffworks.com. Facweb.cs.depaul.edu. 2021. *How Inkjet Printers Work*. [online] Available at: http://facweb.cs.depaul.edu/sgrais/how_inkjet_printers_work.htm.

[345] Jenkins A. D. and Dysthe K. B. 1997. The Effective Film Viscosity Coefficients of a Thin Floating Fluid Layer. J. Fluid Mech. 344, 335-337.

[346] Jennifer Ann Caulfield. Environmental impacts of carbon dioxide ocean disposal: Plume predictions and time dependent organism experience. Master's thesis, Massachusetts Institute of Technology, Department of Civil and Environmental Engineering, 1996.

[347] Jennifer A. Caulfield, E. Eric Adams, David I. Auerbach, and Howard J. Herzog. Impacts of ocean CO2 disposal on marine life: II. Probabilistic plume exposure model used with a time varying dose-response analysis. Environmental Modeling and Assessment 2, pages 345-353, 1997.

[348] J. Hua and J. Lou. Numerical simulation of bubble rising in viscous liquid. J. Comput. Phys., 222(2): 769–795, 2007.

[349] Jiacai Lu and Gretar Tryggvason. Numerical study of turbulent bubbly downflows in a vertical channel. PHYSICS OF FLUIDS 18, 103302 (2006). American Institute of Physics. (DOI: 10.1063/1.2353399).

[350] Jiˇrí Kˇrišt'ál, Jaromír Havlica and Vladimír Jiˇriˇcný. Flow Patterns and Void Fraction in Thin-Gap Channel. International Conference on Multiphase Flow, ICMF 2007, Leipzig, Germany, July 9–13, 2007.

[351] Jirka, G., and Harleman, D. R. F. (1979). "Stability and mixing of a vertical plane buoyant jet in confined depth." J. Fluid Mech., 94, 275–304.

[352] Johansen, S. T., Robertson, D. G. C., Woje, K. and Engh, T. A. (1988) Fluid-Dynamics in Bubble Stirred Ladles: Part I. Experiments. Metallurgical Transactions B, 19B, 745-754, 1988.

[353] Johansen, S. T. and Boysan, F. (1988) Fluid-Dynamics in Bubble-Stirred Ladles: Part II. Mathematical Modelling. Metallurgical Transactions B, 19B, 755-764, 1988.

[354] Johansen, O. (2000), DeepBlow - a Lagrangian plume model for deep water blowouts, Spill Sci. and Tech. Bull., 6(2), 103-111.

[355] Johnson, B. D., and R. C. Cooke (1979), Bubble populations and spectra in coastal waters: A photographic approach, J. Geophys. Res., 84(C7), 3761–3766, doi: 10.1029/JC084iC07p03761.

[356] Johnson G, Hornewer N, Robertson D, Olson D, Gioja J (2000) Methodology, Data Collection, and Data Analysis For Determination of Water-Mixing Patterns Induced by Aerators And Mixers. Water Resources Investigation Report 00-4101. 48 pp, U.S. Geological Survey.

[357] J. Magnaudet and I. Eames, The motion of high-Reynolds-number bubbles in inhomogeneous flows, Ann. Rev. Fluid Mech. 32, 659 (2000).

[358] John C. Patterson and J¨org Imberger. Simulation of bubble plume destratification systems in reservoirs. Aquatic Sciences, 51(1):1 - 18, 1989.

[359] Jones W. T. 1972. Air Barriers as Oil-Spill Containment Devices. Society of Petroleum Engineers Journal, pages 126-142, April 1972.

[360] Jordan F. Clark, Ira Leifer, Libe Washburn, Bruce P. Luyendyk Compositional changes in natural gas bubble plumes: observations from the Coal Oil Point marine hydrocarbon seep field. Geo-Mar Lett (2003) 23: 187–193 DOI 10.1007/s00367-003-0137-y.

[361] Jose A. Nicolas and Jose M. Vega. 2000. A Note on the Effect of Surface Contamination in Water Wave Damping. J. Fluid Mech. 2000. Vol. 410. Pp. 367-373. Cambridge University Press. United Kingdom.

[362] Joshi J, Vitankar V, Kulkarni A, Dhotre M, Ekambara K (2002) Coherent flow structures in bubble column reactors. Chem Eng Sci 57:3157–3183.

[363] Josiam, R. M., and H. G. Stefan (1999), Effect of flow velocity on sediment oxygen demand: comparison of theory and experiments, J. Am. Water Resour. Assoc., 35, 433-439.

[364] Kouremenos, D.A., and J. Staicos, 1985, "Performance of a Small Air-lift Pump," International Journal of Heat Fluid Flow. Vol. 6, No.3, pp. 217-222

[365] J. Rubinstein, "Bubble interaction effects on waves in bubbly liquids," J. Acoust. Soc. Am. 77, 2061 (1985).

[366] J. S. Turner. Turbulent entrainment: the development of the entrainment assumption, and its application to geophysical flows. Journal of Fluid Mechanics, 173:431-471, 1986.

[367] Judd AG, Davies G, Wilson J, Holmes R, Baron G, Bryden I (1997) Contributions to atmospheric methane by natural seepages on the U.K. continental shelf. Mar Geol 140:427–455.

[368] Judd AG, Hovland M, Dimitrov LI, Garcia-Gil S, Jukes V (2002). The geological methane budget at continental margins and its influence on climate change. Geofluids 2: 109–126.

[369] Judd, R.L.; Hwang, K.S.: A Comprehensive Model for Nucleate Boiling Heat Transfer Including Microlayer

[370] Evaporation. *Journal of Heat Transfer*, 98, 623-629 (1976).

[371] Jung Hee Seo, Sanjiva K. Lele, and Gretar Tryggvason. Investigation and modeling of bubble-bubble interaction effect in homogeneous bubbly flows. PHYSICS OF FLUIDS 22, 063302 (2010).

[372] Jun-Hong Liang, James C. McWilliams, Peter P. Sullivan, and Burkard Baschek. Large eddy simulation of the bubbly ocean: New insights on subsurface bubble distribution and bubble-mediated gas transfer. Journal of Geophysical Research, Vol. 117, C04002, doi:10.1029/2011JC007766, 2012

[373] J. W. A. De Swart and R. Krishna, Effect of particles concentration on the hydrodynamics of bubble column slurry reactors, Chem. Eng. Res. Design, Trans. Ind. Chem. Eng. 73, 308 (1995).

[374] K. A. Shollenberger, J. R. Torczynski, D. R. Adkins, T. J. O'Hem, and N. B. Jackson, Gamma-densitometry tomography of gas holdup spatial distribution in industrial scale bubble columns, Chem. Eng. Sci. 52, 2037 (1997).

[375] Kawase, Y., and Ulbrecht, J. J. (1981). Formation of drops and bubbles in flowing liquids. Industrial and Engineering Chemistry, Process Design and Development, 20(4), 636-640.

[376] Kelessidis, V.C., Dukler, A.E., 1989. Modeling flow pattern transitions for upward gas–liquid flow in vertical concentric and eccentric annuli. International Journal of Multiphase Flow 15 (2), 173–191.

[377] Kenji Uchida, Keita Kosuge, Atsuhide Kitagawa and Yoshimichi Hagiwara. Heat transfer enhancement for water natural convection along a vertical plate by micro-bubbles. International Conference on Multiphase Flow, ICMF 2007, Leipzig, Germany, July 9–13, 2007.

[378] Kim, I., Kamotani, Y., and Ostrach, S. (1994). Modeling bubble and drop formation in flowing liquids in microgravity. AIChE Journal, 40(1), 19-28.

[379] Lim, Kang Yuan; Quinto-Su, Pedro A.; Klaseboer, Evert; Khoo, Boo Cheong; Venugopalan, Vasan; Ohl, Claus-Dieter. Nonspherical laser-induced cavitation bubbles. Physical Review E, vol. 81, Issue 1, id. 016308. Pub Date: January 2010. DOI: 10.1103/PhysRevE.81.016308 https://www.science.gov/topicpages/l/laser-induced+cavitation+bubble.

[380] Klas Cederwall and John D. Ditmars. Analysis of Air-Bubble Plumes. Report No. KH-R-24. September 1970. California Institute of Technology, Pasadena, CA, 1970.

[381] Kodama, Y. Kakugawa, A., Takahashi, T., Kawashima; H., Experimental Study on Microbubbles and their Applicability to Ships for Skin Friction Reduction, International Journal of Heat and Fluid Flow, Vol.21, Issue 5 (2000) p.582.

[382] Kodama, Takahashi, Hori, Makino, and Ueda, 3rd Int. Symp. on Two-Phase Flow Modelling and Experimentation, Pisa (2004).

[383] Kodama, Y. Kakugawa, A., Takahashi, T., Kawashima; H.A Full-Scale Air Lubrication Experiment Using a Large Cement Carrier for Energy Saving (Result and Analysis), Conference Proceedings, the Japan Society of Naval Architects and Ocean Engineers, Vol.6 (2008) p.163.

[384] Koenig, G., Anders, K., and Frohn, A. (1986). A new light scattering technique to measure the diameter of periodically generated moving droplets. Journal of Aerosol Sciences, 17:157–167.

[385] Kortmann, R. W., Knoecklein G. W., Bonnell., H. C., (1994), Aeration of stratified lakes: Theory and practice, Lake Reservoir Manage., 8(2), 99-120.

[386] Kortmann, R. W. (1994), Oligotrophication of Lake Shenipsit by layer aeration, Lake Reservoir Manage., 9(1), 94-97.

[387] Kreshimir Zic, Hienz G. Stefan. Destratification Induced by Bubble Plumes. Water Quality Research Program. Technical Report W-94-3. June 1994.

[388] Krepper, E., Weiss, F. -., Alt, S., Kratzsch, A., Renger, S. and Kästner, W. (2011), "Influence of air entrainment on the liquid flow field caused by a plunging jet and consequences for fibre deposition", Nuclear Engineering and Design, vol. 241, no. 4, pp. 1047-1054.

[389] Kreutzer, M., T., Heiszwolf, J., J. and Moulijn, J., A., AIChE Journal, 51, 9, 2428-2440 (2005).

[390] Kreutzer, M. T. Kapteijn, F. Moulijn J. A. and Heiszwolf J. J.. Chem. Eng. Science, Vol. 60, 5895–5916, 2005.

[391] Krishna, R. and van Baten, J.M., 1998. Simulating the motion of gas bubbles in a liquid. Nature, 398, p. 208.

[392] Krishna, R. and Sie, S.T., 2000. Design and scale-up of the Fischer-Tropsch bubble column slurry reactor. Fuel Proc. Tech., 64, pp. 73-105.

[393] Kristian Etienne Einarsrud and Iver Brevik. KINETIC Energy Approach To Dissolving Axisymmetric Multiphase Plumes. arXiv.org. physics. arXiv: 0804.2789v1. April 17, 2008.

[394] Kvenvolden KA (1993) Gas hydrates—geological perspective and global change. Rev Geophys 31:173–187.

[395] Kvenvolden KA (1995) A review of the geochemistry of methane in natural gas hydrate. Org Geochem 23:997–1008.

[396] Kvenvolden KA, Lorenson TD, Reeburgh WS (2001) Attention turns to naturally occurring methane seeps. EOS 82: 457.

[397] Kubasch, J. H. 2001 Bubble hydrodynamics in large pools. Doctoral dissertation, ETH No. 14398, Zurich, Switzerland.

[398] Kuhn de Chizelle, Y., Ceccio, S. L., and Brennen, C. E., 1995, "Observations and Scaling of Traveling Bubble Cavitation," J. Fluid Mech., 293, pp. 99–126.

[399] Kupferberg, A., and Jameson, G. J. (1970). Pressure fluctuations in a bubbling system with special reference to sieve plates. Transactions of the Institution of Chemical Engineers, 48, T140-T150.

[400] Kuwagi, K. and Ozoe, H. (1999) Three-Dimensional Oscillation of Bubbly Flow in a Vertical Cylinder. International Journal of Multiphase Flow, 25, 175-182, 1999.

[401] Lamarre, E., and W. K. Melville (1991), Air entrainment and dissipation in breaking waves, Nature, 351, 469–472.

[402] Lance, M. and Bataille J., 1991, Turbulence in the Liquid-phase of a uniform bubbly air water-flow. Journal of Fluid Mechanics, 222, Pp.95-118.

[403] Lance, M., Marrie, J.L., Bataille, J., 1991. Homogeneous turbulence in bubbly flows. J. Fluids Eng. 113, 295–300.

[404] Lapin, A., and LuK bbert, A. (1994). Numerical simulation of the dynamics of two-phase gas-liquid flows in bubble columns. Chemical Engineering Science, 49(21), 3661.

[405] Laureshen, C. J., and R. D. Rowe (1987), Modeling of plane bubble plumes, paper presented at 24th National Heat Transfer Conference and Exhibition, Am. Soc. Mech. Engineers, Pittsburgh, PA, 9-12 Aug.

[406] Leah Sarah Reingold. An experimental comparison of bubble and sediment plumes in stratified environments. Master's thesis, Massachusetts Institute of Technology, Department of Civil and Environmental Engineering, 1994.

[407] L. D'Agostino, C. E. Brennen, and A. Acosta, "Linearized dynamics of two dimensional bubbly and cavitating flows over slender surfaces," J. Fluid Mech. 192, 485 (1988).

[408] L. D'Agostino and C. E. Brennen, "Linearized dynamics of spherical bubble clouds," J. Fluid Mech. 199, 155 (1989).

[409] Lehman, J. and Hammer, J., (1978), Continuous fermentation in tower fermentor, I European congress on biotechnology, Interlaken, Part 1, 1.

[410] Leitch, A.M., and Baines, W. D. 1989. Liquid Volume Flux in a Weak Bubble Plume, J. Fluid Mech., Vol. 205. Pp. 77-90.

[411] Leitch, A. M., and Baines, W. D. (1989). "Measurement of liquid volume flux in a bubble plume." J. Fluid Mech., 205, 77–98.

[412] Leifer I, Clark JF (2002) Modeling trace gases in hydrocarbon seep bubbles: application to marine hydrocarbon seeps in the Santa Barbara Channel. Russian Geol Geophys 47:572–579.

[413] Leifer I, Patro RK (2002) The bubble mechanism for methane transport from the shallow sea bed to the surface: a review and sensitivity study. Cont Shelf Res 22: 2409–2428.

[414] Leifer I, Clark JF, Chen RF (2000) Modifications of the local environment by natural marine hydrocarbon seeps. Geophys Res Lett 27:3711–3714. 192

[415] Legile, P., Menard, G., Laurent, C., Thomas, D. and Bernis, A., 1992, Contribution to the study of an inverse three-phase fluidized bed operating countercurrently, Int Chem Eng, 32: 41.

[416] Lemckert, C. J., and Imberger, J. (1993). "Energetic bubble plumes in arbitrary stratification." J. Hydraul. Eng., 119(6), 680–703.

[417] Leon, Arturo S., Ghidaoui, M. S., Schmidt, A. R., and Garcia, M. H. (2008). "Efficient second-order accurate shock-capturing scheme for modeling one-and two-phase water hammer flows." J. Hydraul. Eng., 134(7), 970–983.

[418] L. E. Rincón, F. A. Bombardelli and M. H. García. Experimental Evidence for Scaling Laws in Bubble Plumes.World Water Congress 2004.

[419] Levich V. G. (1962). Physicochemical Hydrodynamics, Section 87, Prentice Hall, Engelwood Cliffs, N.J.

[420] Liang, J.-H., J. C. McWilliams, P. P. Sullivan, and B. Baschek (2011), Modeling bubbles and dissolved gases in the ocean, J. Geophys. Res., 116, C03015, doi:10.1029/2010JC006579.

[421] Lima Neto, Iran & David, Zhu & Rajaratnam, N. (2008). Bubbly jets in stagnant water. International Journal of Multiphase Flow. 34. 1130-1141. 10.1016/j.ijmultiphaseflow.2008.06.005.

[422] Lindenschmidt, K. E., and P. F. Hamblin (1997), Hypolimnetic aeration in Lake Tegel, Berlin, Water Res., 31(7), 1619-1628.

[423] Lin, T. J. and Donnelly, H. G. (1966), "Gas bubble entrainment by plunging laminar liquid jets", AICHE Journal, vol. 12, no. 3, pp. 563-571.

[424] Liu, T.J., Bankoff, S.G., 1990. Structure of air-water bubbly flow in a vertical pipe: I-Liquid mean velocity and turbulence measurements. Int. J. Heat Mass Transfer 36 (4), 1049–1060.

[425] Little, J. C. (1995), Hypolimnetic aerators: Predicting oxygen transfer and hydrodynamics, Water Res., 29(11), 2475-2482.

[426] Little, J. C., and D. F. McGinnis (2001), Hypolimnetic

oxygenation: Predicting performance using a discrete-bubble model, Water Science and Technology: Water Supply, 1(4), 185- 191.

[427] Liu, T.J., and S. G. Bankoff, "Structure of air-water bubbly flow in a vertical pipe. Part 2: Void fraction, bubble velocity and bubble size distribution," Int. J. Heat Mass Transfer 36, 1061 (1993).

[428] Liu, T.J., and S. G. Bankoff, "Structure of air water bubbly flow in a vertical pipe. Part I: Liquid mean velocity and turbulence measurements," Int. J. Heat Mass Transfer 36, 1049 (1993).

[429] Liu, T. J., and Bankoff, S. G., 1993, "Structure of Air-Water Bubbly Flow in a Vertical Pipe- I," Int. J. Heat Mass Transfer, 36, pp. 1049–1060.

[430] Liu, T. J., and Bankoff, S. G., 1993, "Structure of Air-Water Bubbly Flow in a Vertical Pipe- II," Int. J. Heat Mass Transfer, 36, pp. 1061–1072.

[431] Liu, T.J., Wang, S.J., 2001. Optimization of local and area-averaged interfacial area concentration correlations in two-phase bubbly flow. In: Proceedings of Fourth International Conference on Multiphase Flow, New Orleans, USA.

[432] Lockhart, R.W. and Martinelli, R.C. 1949. Proposed correlation of data for isothermal two-phase, two-component flow in pipes. Chem. Eng. Prog., Vol. 45, pp 39-48.

[433] Lopez de Bertodano, M., Lee, S.J., Lahey, R.T., Jones, O.C., 1994. Development of a k-ε model for bubbly two-phase flow. J. Fluids Eng. 116, 128–134.

[434] Lorke, A., Beat Müller, Martin Maerki, Alfred Wüest (2003), Breathing sediments: The control of diffusive transport across the sediment-water interface by periodic boundary-layer turbulence, Limnol. Oceanogr., 48(6), 2077-2085.

[435] Lorenzen, M. W., and A. W. Fast (1977), A Guide to Aeration/Circulation Techniques for Lake Management, 125 pp, U.S. Environmental Protection Agency Ecol. Res. Serv.

[436] LoubiCere, K., and HDebrard, G. (2002). Bubble formation from a 6exible hole submerged in an inviscid liquid. Chemical Engineering Science, 58, 135–148.

[437] L. Xu, G. Chen, J. Li, J. Shao, Study on development of Particle Image Velocimetry[J]. The Advance of Dynamic 2003, 04: 533-540.

[438] L. Van Wijngaarden, "On the equations of motion for mixtures of liquid and gas bubbles," J. Fluid Mech. 33, 465 (1968).

[439] L. Van Wijngaarden, "One-dimensional flow of liquids containing small gas bubbles," Annu. Rev. Fluid Mech. 4, 369 (1972).

[440] Lucas, D., Krepper, E., Prasser, H.M., 2005. Development of co-current air–water flow in a vertical pipe. International Journal of Multiphase Flow 31, 1304–1328.

[441] Lucas, D., Krepper, E., Prasser, H.M., 2007. Use of models for lift, wall and turbulent dispersion forces acting on bubbles for poly-disperse flows. Chemical Engineering Science 62 (15), 4146–4157.

[442] Lucas, D., Krepper, E., Prasser, H.-M., and Manera, A. Investigations on the stability of the flow characteristics in a bubble column. Chem. Engng. Tech. 29, 1066 (2006).

[443] M.A. Bennett, S. P. Luke, X. Jia, R.M. West and R.A. Williams. Analysis and Flow Regime Identification of Bubble Column Dynamics. 1st World Congress on Industrial Process Tomography, Buxton, Greater Manchester, April 14-17, 1999.

[444] MacDonald IR, Buthman DB, Sager WW, Peccini MB, Guinasso NL (2000) Pulsed oil discharge from a mud volcano. Geology 28: 907–910.

[445] Machane, R., Takemura, F., Takagi, S., and Matsumoto, Y., 1999. A first attempt at modelling mass transfer and gas dissolution dynamics in bubbly flows, Proceedings of the 3rd ASME/JSME joint fluid engineering conference, July 18-23, 1-7 San Francisco, California

[446] Mackenthun, A. A., and H. G. Stefan (1998), Effect of flow velocity on sediment oxygen demand: Experiments, J. Environ. Engineer., 124(3), 222-230.

[447] Maeda, M., Akasaka, Y., and Kawaguchi, T. (2002). Improvements of the interferometric technique for simultaneous measurement of droplet size and velocity vector field and its application to a transient spray. Experiments in Fluids, 33:125–134.

[448] Ma, G., F. Shi, and J. T. Kirby (2011), A polydisperse two-fluid model for surf zone bubble simulation, J. Geophys. Res., 116, C05010, doi:10.1029/ 2010JC006667.

[449] Mahmood Reza Rahimi and Hajir Karimi. Computational Fluid Dynamics Modeling of Downward Bubbly Flows. World Academy of Science, Engineering and Technology 73 (2011).

[450] Ma, J., Oberai, A. A., Drew, D. A., Lahey Jr., R. T. and Moraga, F. J. (2010), "A quantitative sub-grid air entrainment model for bubbly flows - plunging jets", Computers and Fluids, vol. 39, no. 1, pp. 77-86.

[451] Majumder, S. K., Kundu, G. and Mukherjee, D. (2005), "Mixing mechanism in a modified co-current downflow bubble column", Chemical Engineering Journal, vol. 112, no. 1-3, pp. 45-55.

[452] Makoto Kawabuchi, Chiharu Kawakita, Shuji Mizokami, Seijiro Higasa, Yoichiro Kodan, Shinichi Takano. CFD Predictions of Bubbly Flow around an Energy-saving Ship with Mitsubishi Air Lubrication System. Mitsubishi Heavy Industries Technical Review Vol. 48 No. 1 (March 2011).

[453] Mandhane, J.M, G.A. Gregory and K. Aziz (1974). A flow pattern map for gas-liquid flow in Horizontal pipe. Int. J. Multiphase Flow 1, 537-553.

[454] Manga, M. and Stone, H. A. 1993 Buoyancy-driven interactions between deformable drops at low Reynolds numbers. J. Fluid Mech. 256, 647-683.

[455] Manninen, M., Taivassalo, V., Kallio, S., 1996. On the Mixture Model for Multiphase Flow. VTT Publications 288. Technical Research Centre of Finland.

[456] Mao Z.S. and A.E. Duckler, 1985, "Rise Velocity of a Taylor Bubble in a Train of such Bubbles in a Flowing Liquid," Chemical Engineering science, Vol. 40, No. 11, pp. 2158-2160.

[457] Mao, Z. S., and Duckler, A.E., 1985. Brief communication: Rise velocity of a Taylor bubble in a train of such bubbles in a flowing liquid. Chemical Engineering Science, 40, 2158 - 2160

[458] Mao, Z. S. And A. Duckler (1990). The motion of Taylor bubbles in vertical tubes: I. A numerical simulation for the shape and rise velocity of Taylor bubbles in stagnant and flowing liquid. J. Comp. Phys. 91, 132-160.

[459] Mao Z.S., Dukler A.E., 1991.The motion of Taylor bubbles in vertical tubes-II. Experimental data and simulations for laminar and turbulent flow. Chemical engineering science, 46, No 8, 2055-2064.

[460] Marco A. S. C. Castello-Branco and Klaus Schwerdtfeger. Characteristics of eccentric bubble plumes in liquids. Metallurgical and Materials Transactions B, 27B:231-239, 1996.

[461] Marco Simiano. Experimental Investigation of Large-Scale Three Dimensional Bubble Plume Dynamics. Doctoral dissertation, Swiss Federal Institute of Technology Zurich. Ph.d. thesis. Diss. ETH No 16220. 2005.

[462] Marco Simiano, D. Lakehal, M. Lance and G. Yadigaroglu. Turbulent transport mechanisms in oscillating bubble plumes. J. Fluid Mech. (2009), vol. 633, pp. 191–231.

[463] Marco Simiano, Zboray, R., de Cachard, F., Lakehal, D. and Yadigaroglu, G. 2006 Comprehensive experimental investigation of the hydrodynamics of large-scale, three-dimensional bubble plumes. Intl J. Multiph. Flow 18 (32), 1160–1181.

[464] Maretto C. and Krishna R. Design and optimisation of a multi-stage bubble column slurry reactor for Fischer–Tropsch synthesis. Author links open overlay panel. 2001. Elsevier Science Direct.Volume 66, Issues 2-4, 30 March 2001, Pp. 241-248.

[465] Marks, C. H., and Cargo, D.G. 1974. Field Tests of Bubble Screen Sea Nettle Barrier, J. Mar. Tech.. Pp. 33-39.

[466] M. A. R. Talaia, Terminal Velocity of a Bubble Rise in a Liquid Column, World Academy of Science, Engineering and Technology 28, (2007)

[467] M. A. R. Talaia, Uma análise dimensional: Ascensão de uma bolha num líquido parado, Gazeta de Física, 23, 9 (2000).

[468] M. A. R. Talaia, Predicting the rise velocity of single gas slugs in stagnant liquid: Influence of liquid viscosity and tube diameter, in Proc. of the 3rd International Symposium on Two-Phase Flow Modelling and Experimentation, Edizioni ETS, Pisa, Italy (2004).

[469] Marshall, S. H., Chudacek, M. W., and Bagster, D. F. (1993). A model for bubble formation from an ori"ce with liquid cross-flow. Chemical Engineering Science, 48, 2049-2059.

[470] Martel C. Nicolas J. A. and Vega J. M. 1998. Surface wave Damping in a Brimful Circular Cylinder. J. Fluid Mech. 360, 213-228. See also Corrigendum, J. Fluid Mech. 373, 379 (referred to herein as MNV).

[471] Martin, C. S., and Padmanabhan, M. (1975). “Effects of free gases on pressure transients.” Energia Elettrica, 52(5), 262–267.

[472] Martin, C. S., Padmanabhan, M., and Wiggert, D. C. (1976). “Pressure wave propagation in two-phase bubbly air-water mixtures.” 2nd Int. Conf. on Pressure Surges, BHRA, Cranfield, UK.

[473] Martin, C. S. (1976). Vertically downward two-phase slug flow. J. of Fluids Eng. 98, 715-722.

[474] Masanori Aritomi, Hiroshige Kikura and Yumiko Suzuki. Ultrasonic Doppler Method For Bubbly Flow Measurement. 4th Workshop on Measurement Technique for Stationary and Transient Two-Phase Flows Rossendorf, Germany, November 16-17, 2000.

[475] Massimo Milelli, A Numerical Analysis Of Confined Turbulent Bubble Plumes. 2002. A dissertation submitted to the Swiss Federal Institute Of Technology Zurich. DISS. ETH No. 14799.

[476] McCann, D. J. (1969). Bubble formation and weeping at a submerged ori5ce. Ph.D thesis, The University of Queensland, Queensland, Australia.

[477] McCann, D. J., and Prince, R. G. H. (1969). Bubble formation and weeping at a submerged orifice. Chemical Engineering Science, 24, 801-814.

[478] McDonald, J. P., and Gulliver, J. S. 1990. "Methane Trace Technique for Gas Transfer at Hydraul ic Structures," Air-Water Mass Transfer, Selected Papers from the Second International Symposium on Gas Transfer at Water Surfaces, ASCE, pp 267-277.

[479] McDougall T. J. 1978. Bubble Plumes in Stratified Environments. Journal of Fluid Mechanics, Vol. 85 (4), 1978, pp. 655-672.

[480] McGinnis, D. F., and J. C. Little (1998), Bubble dynamics and oxygen transfer in a Speece Cone, Water Sci. Technol., 37(2), 285– 292.

[481] McGinnis, D. F., et al. (2001), Hypolimnetic oxygenation: Coupling bubble-plume and reservoir models, paper presented at Asian Waterqual 2001: First IWA Asia-Pacific Regional Conference, Intl. Wat. Assoc., Fukuoka, Japan, 12-15 Sept.

[482] McGinnis, D. F., and J. C. Little (2002), Predicting diffused-bubble oxygen transfer rate using the discrete-bubble model, Water Res., 36(18), 4627– 4635.

[483] McGinnis, D. F., Lorke, A., Wuest, A., Stockli, A., and Little, J. C. (2004). “Interaction between a bubble plume and the near field in a stratified lake.” Water Resour. Res., 40(10), W10206.

[484] McNeil, C., and E. D’Asaro (2007), Parameterization of air-sea gas fluxes at extreme wind speeds, J. Mar. Syst., 66, 110–121.

[485] McQueen, D. J., and D. R. S. Lean (1986), Hypolimnetic aeration: An overview, Water Pollution

[486] Research Journal of Canada, 21(2), 205-217.

[487] McQueen, D. J., Lean, DRS., Charlton, MN., (1986), Effects of hypolimnetic aeration on iron-phosphorus interactions, Water Res., 20(9), 1129-1135.

[488] Melville, W. K., and P. Matusov (2002), Distribution of breaking waves at the ocean surface, Nature, 417, 58–63.

[489] Melville, W. K., F. Veron, and C. J. White (2002), The

velocity field under breaking waves: Coherent structures and turbulence, J. Fluid Mech., 454203–233.

[490] Mercier, P., and J. Perret (1949), Aeration of Lake Bret, Monastbull, Schwiez, Ver. Gas. Wasser- Fachm, 29, 25.

[491] Metcalf and Eddy, Inc. 1979. Wastewater Engineering: Treatment/Oi sposa 7IReuse, 2d ed., revised by George Tchobanogl ous, McGraw-Hill, new York.

[492] Michaels, J. D., Nowak, J. E., Mallik, A. K., Koczo, K.,Wasan, D. T. and Papoutsakis, E. T., 1995, Analysis of cell to bubble attachment in sparged bioreactors in the presence of cell-protecting additives, Biotechnol Bioeng, 47: 407.

[493] Michele, J. and Michele, V. (2002), "The free jet as a means to improve water quality: Destratification and oxygen enrichment", Limnologica, vol. 32, no. 4, pp. 329-337.

[494] Miles J. W. 1967. Surface-Wave Damping in Closed Basins. Proc. R. Soc. Lond. A. 297, 459-475.

[495] Milgram, J. H. 1983 Mean flow in round bubble plumes. J. Fluid Mech. 133, 345–376.

[496] Ming-yan Liu, Juan-ping Xue, Ai-hong Qiang, M. Chaotic forecasting of time series of heat-transfer coefficient for an evaporator with a two-phase flow. Chemical Engineering Science, Vol. 60, 883-895 (2005).

[497] Miyahara, T., Matsuba, Y., and Takahashi, T. (1983). The size of bubbles generated from perforated plates. International Chemical Engineering, 23(3), 517–602.

[498] Miyahara, T., and Takahashi, T. (1984). Bubble volume in single bubbling regime with weeping at a submerged orifice. Journal of Chemical Engineering of Japan, 17(6), 597-602.

[499] M. Kameda and Y. Matsumoto, “Shock waves in a liquid containing small gas bubbles,” Phys. Fluids 8, 322 (1996).

[500] Mobley, M. H. (1997), TVA reservoir aeration diffuser system, TVA technical paper 97–3 presented at ASCE Waterpower ’97, Am. Soc. of Civ. Eng., Atlanta, Ga., 5 – 8 Aug.

[501] Monji, H., and Matsui, G., Two-Phase Flow Modelling and Experimentation 1995, (1995), 367.

[502] Moraga, F. J., Carrica, P. M., Drew, D. A. and Lahey Jr., R. T. (2008), "A sub-grid air entrainment model for breaking bow waves and naval surface ships", Computers and Fluids, vol. 37, no. 3, pp. 281-298.

[503] Moran J. Michael and Shapiro N. Howard. A review of “Fundamental of Engineering Thermodynamics” Third Edition, 1996 New York, Wiley ISBN 0471076813 £23.50. European Journal of Engineering Education. Volume 21, 1996 - Issue 4.

[504] Morgenstern, I. B., and Mersmann, A. (1982). Aeration of highly viscous liquids. German Chemical Engineering, 5, 374-379.

[505] Moran, Robert P. and Houston, Janice D. Infrared Imagery of Solid Rocket Exhaust Plumes. JANNAF 8th Modeling and Simulation Subcommittee Meeting. Worldwidescience. org. 2011. https://worldwidescience.org/topicpages/s/solid+rocket+plume.html.

[506] Mori, Y., Hijikata, K., and Komine, A. (1975). “Propagation of pressure waves in two-phase flow.” Int. J. Multiphase Flow, 2(2), 139–152.

[507] Mortimer, C. H. (1941). "The exchange of dissolved substances between mud and water in lakes (Parts I and II)." J. Ecol., 29,280-329.

[508] Mortimer, C. H. (1942). "The exchange of dissolved substances between mud and water in lakes (Parts III and IV)." J. Ecol., 30, 147-201.

[509] Morton, B. R., Taylor, G. I., and Turner, J. S. (1956). "Turbulent gravitational convection from maintained and instantaneous sources." Proc. Roy. Soc. A, 234,1-23.

[510] Mory, K., Sano, M., 1981. Process kinetic in injection metallurgy. Tetsu-to-Hagan 67, 672–695.

[511] Motarjemi, M., and G. J. Jameson (1978), Mass transfer from very small bubbles - The optimum bubble size for aeration, Chemical Engineering Science, 33, 1415-1423.

[512] Moursali, E., Mari_e, J.L., Bataille, J., 1995. An upward turbulent bubbly layer along a vertical flat plate. Int. J. Multiphase Flow 21, 107–117.

[513] M. Sussman, E. Puckett, A coupled level set and volume-of-fluid method for computing 3d and axisymmetric incompressible two-phase flows, J. Comput. Phys. 162 (2) (2000) 301–337.

[514] M. Sussman, K.M. Smith, M.Y. Hussaini, M. Ohta, R. Zhi-Wei, A sharp interface method for incompressible two-phase flows, J. Comput. Phys. 221 (2) (2007) 469–505.

[515] Mudde, R.F., Simonin, O., 1999. Two- and three-dimensional simulations of a bubble plume using a two-fluid model. Chemical Engineering Science 54, 5061-5069.

[516] R. Mudde and O. Simonin. Two- and three-dimensional simulations of a bubble plume using a two-fluid model. Chem. Eng. Sci., 54, 5061–5069 (1999).

[517] Mudde, Robert F. and Saito Takayuki, 2001, Hydrodynamical similarities between bubble column and bubbly pipe flow, J. Fluid Mech, 437, 203-228.

[518] Mudde, R. F. (2005). “Gravity-driven bubbly flows.” Annu. Rev. Fluid Mech., 37, 393–423.

[519] Murai Yuichi, Ohno Yasushi, Abdulmouti Hassan, Ohata Junichi, Yamamoto Fujio 1999. Numerical Prediction of a Horizontal Surface Flow Generated by Bubbles. The Asian Symposium on Multiphase Flow 1999 (ASMF’99) Osaka, Japan. Pp. 45-50.

[520] Murai, Yuichi, Abdulmouti Hassan, Ohno Yasushi, Ohta Junichi, Yamamoto Fujio 2000. Two-Phase Flow Induced by a Bubble Plume in the Vicinity of a Free Surface. Proceeding of ASME FEDSM 2000. ASME 2000 Fluid Engineering Division Summer Meeting. June 11-15, 2000, Boston, Massachusetts. FEDSM-11275, pp.1-6.

[521] Murai Yuichi, Ohno Yasushi, Abdulmouti Hassan, Yamamoto Fujio 2000. Article of Fluid Dynamic characteristics of oil fence using air bubbles “In order to reduce the damage of heavy oil leakage at sea”. Nature and Environment of The Sea of Japan Districts. The Memoirs of the Research and Education Center for Regional Environment, Fukui University. No. 7, pp. 63-68.

[522] Murai Yuichi, Ohno Yasushi, Bae Dae Seeok, Abdulmouti Hassan, Yamamoto Fujio 2001. Bubble-Generated Convection in Immiscible Two-phase Stratified Liquids. Proceeding of ASME FEDSM 2001, May 29- June 1-18180. New Orleans U.S.A.

[523] Murai Yuichi, Ohno Yasushi, Abdulmouti Hassan, Yamamoto Fujio 2001. Flow in the Vicinity of Free Surface Induced By a Bubble Plume. JSME. 067, 657, B.

[524] Murai Y. and Matsumoto Y. 1998. Numerical Analysis of Detailed Flow Structures of a Bubble Plume. JSME International Journal, Series B, Vol. 41, No. 3, 1998. Pp.568-575.

[525] Murai, Y., Matsumoto, Y., Yamamoto, F., Qualitative and quantitative flow visualization of bubble motions in a plane bubble plume [J]. J. Visualization. 2000, 3, 27-35.

[526] MURAI, Y.,MATSUMOTO, Y., SONG, X. and YAMAMOTO, F. 2000b Numerical analysis of turbulence structures induced by bubble buoyancy. JSME, Int. J., Serie B 43, 180–187.

[527] Murakami, A. et al., Numerical Simulation of Flow around a Full-Scale Ship Equipped with Bubble Generators, Conference Proceedings, the Japan Society of Naval Architects and Ocean Engineers, Vol.6 (2008) p.153.

[528] Murray, K.R, 1980, "The Design and Performance of Airlift Pumps in a Closed Marine Recirculation system," Proceedings of the World Symposium of Aguaculture in Heated Effluents and Recirculation Systems, 28-30 May, Vol 1.

[529] Nader, M., Kermani, M. and Barani, G., 2021. *Application of bubble curtain system for prevention of seawater intrusion inestuary of tidal rivers*. [online] Scholarsresearchlibrary.com. Available at: <https://www.scholarsresearchlibrary.com/abstract/application-of-bubble-curtain-system-for-prevention-of-seawater-intrusion-inrnestuary-of-tidal-rivers-7867.html>.

[530] Nagy, Z., 1979, "The Airlift Aerator and its Application in Sewage Treatment," Progressive Water Technology, Vol. 11, No.3, pp. 101-109.

[531] Nakamura, Y., and T. Inoue (1996), A theoretical study on operation condition of hypolimnetic aerators, Water Sci. Technol., 34(7–8), 211 –218.

[532] Nakoryakov, V.E., and O.N. Kashinsky, 1982, "Local Characteristics of Upward Gas-Liquid Flow," International Journal of Multiphase Flow, Vol. 7, pp 63-81.

[533] Nakoryakov, V.E., O.N. Kashinsky, and B.K. Kozmenko, 1986, "Experimental study of Gas-Liquid Slug Flow in a Small Diameter vertical Pipe," International Journal of Multiphase Flow, Vol. 12, No.3, pp. 337-355.

[534] Natalia Melnichanskaya and Alexander Gelfgat. CFD simulations of single Taylor bubbles in vertical pipes using a variety of numerical approaches. International Conference on Multiphase Flow, ICMF 2007, Leipzig, Germany, July 9 – 13, 2007.

[535] Nicklin, D.J. and Davidson, J.F. 1962. The onset of instability in two-phase slug flow. Presented at a Symp. on Two-phase flow, Inst. Mech. Engrs, London, paper No 4.

[536] Nicklin, D.J.; Wilkes, M.A. and Davidson, M.A. 1962. Two-phase flow in vertical tubes. Trans. Instn. Chem. Engrs., Vol. 40, pp. 61-68.

[537] Nicklin, D.J., 1963, "The Air-Lift Pump: Theory and Optimization," Transactions of the Institution of Chemical Engineers, Vol. 41, pp. 29-39.

[538] Nickens, H.V., and D.W. Yannitell, 1987, "The Effects of Surface Tension and Viscosity on the Rise Velocity of a Large Gas Bubble in a Closed, vertical LiquidFilled Tube," International Journal of Multiphase Flow, Vol. 13, No. I, pp. 57-69.

[539] Nienow, A.W. and Bujalski, W. The versatility of up-pumping hydrofoil agitators. Chem Eng Res Des, Vol. A9, 1073-1081 (2004)

[540] Nikolov, L., Karamanev, D. and Elenkov, D. G., 1982, Bulgarian Patent, 53798.

[541] Nikolov, L. and Karamanev, D., 1987, Experimental study of inverse fluidized bed bio. lm reactor, Can J Chem Eng, 65: 214.

[542] Nikolov, L. and Karamanev, D., 1990, The inverse fluidized bed bio. Lm reactor: a new laboratory scale apparatus for bio. lm research, J Ferm Bioeng, 69: 265.

[543] Niwa, Y., Kamiya, Y., Kawaguchi, T., and Maeda, M. (2000). Bubble sizing by interferometric laser imaging. In 10th International Symposium on Application of Laser Techniques to Fluid Mechanics, Lisbon.

[544] Nogueira, S., M.L. Riethmuller, J.B.L.M. Campos and A.M.F.R. Pinto (2006). Flow in the nose region and annular film around a Taylor bubble rising through vertical columns of stagnant and flowing Newtonian liquids. Chemical Eng. Sci. 61, 845- 857.

[545] Nordin, R., et al. (1995), Hypolimnetic aeration of St Mary Lake, British Columbia, Canada, Lake Reservoir Manage., 11(2), 176.

[546] NRC (2002) Oil in the sea III: inputs, fates, and effects. National Research Council, National Academy Press.

[547] Ohkawa, A., Kusabiraki, D., Kawai, Y., Sakai, N. and Endoh, K. (1986), "Some flow characteristics of a vertical liquid jet system having downcomers", Chemical Engineering Science, vol. 41, no. 9, pp. 2347-2361.

[548] Ohno Yasushi, Murai Yuichi, Hassan Abdulmouti, Ohta Junichi, Yamamoto Fujio Numerical Analysis of the Surface Flow Induced by a Bubble Curtain. CFD symposium`98. Tokyo. Pp. 235 ~236. 1998.

[549] Ohnuki, A., and Akimoto, H., 2000, "Experimental Study on Transition of Flow Pattern and Phase Distribution in Upward Air-Water Two-Phase Flow Along a Large Vertical Pipe," Int. J. Multiphase Flow, 26, pp. 367–386.

[550] Orell, A. and R. Rembrand (1986). A model for gasliquid slug flow in vertical tube. Ind. Eng. Chem. Fundam. 25(2), 196-206.

[551] Osamasali, S.I., Chang, J.S., 1988. Two-phase flow regime transition in a horizontal pipe and annulus flow under gas-liquid two-phase flow. ASME Fluid Engineering Division 72, 63–69.

[552] Padmanabhan, M., Ames, W. F., and Martin, C. S. (1978a).

"Numerical analysis of pressure transients in bubbly two-phase mixtures by explicit-implicit methods." J. Eng. Math., 12(1), 83–93.

[553] Padmanabhan, M., and Martin, C. S. (1978b). "Shock-wave formation in flowing bubbly mixtures by steepening of compression waves." Int. J. Multiphase Flow, 4(1), 81–88.

[554] Page, R. E., 1970, Some Aspects of Three-Phase Fluidization, PhD Thesis (University of Cambridge, Cambridge, UK).

[555] Pal, R. and Masliyah, J., 1989. Flow characterization of a rotation column. Can. J. Chem. Eng., 67, pp. 916-923.

[556] Pastorok, R. A., Ginn, TC., Lorenzen MW., (1981), Evaluation of Aeration/Circulation as a Lake Restoration Technique, Report, U. S. Environ. Protect. Agency, Off. Res. and Devel., Corvalis, OR.

[557] Pastorok, R. A., Lorenzen, MW., Ginn TC., (1982), Environmental Aspects of Artificial Aeration and Oxygenation of Reservoirs: A review of Theory, Techniques, and Experiences, Report, 192 pp, U.S.

[558] Peterson, M. J., G. F. Cada, M. J. Sale, and G. K. Eddlemon (2003), Regulatory Approaches for Addressing Dissolved Oxygen Concerns at Hydropower Facilities, 38 pp, U.S. Department of Energy, Energy Efficiency and Renewable Energy, Wind and Hydropower Technologies

[559] Phu D. Tran. Propagation of Pressure Waves in Two-Component Bubbly Flow in Horizontal Pipes. JOURNAL OF HYDRAULIC ENGINEERING. ASCE. Pp 668-678. JUNE 2011.

[560] Pickert, F. 1932. The theory of the air-lift pump. Engineering, Vol. 34, pp. 19-20.

[561] Pinto, A.M.F.R. and Campos J.B.L.M. (1996). Coalescence of two gas slugs rising in vertical column of liquid. Chem. Eng. Sci. 1(1), 45-54.

[562] Pfleger, D., Gomes, S., Gilbert, N., Wagner, H.G., 1999. Hydrodynamic simulation of laboratory scale bubble columns: Fundamental studies of Eulerian-Eulerian modelling approach, Chemical Engineering Science, 54, 5091-5099

[563] Pfleger, D., and S. Becker, "Modelling and Simulation of the Dynamic Flow Behavior in a Bubble Column," Chemical Engineering Science. 56, 1737-1747 (2001).

[564] Von Platen, B.C. and Munters, C.G., 1928. "Refrigerator", U.S. Patent 1,685,764.

[565] Polonsky S, Barnea D, Shemer L (1999a). Average and time-dependent characteristics of the motion of an elongated bubble in vertical pipe. Int J Multiphase Flow 25:795–812.

[566] Polonsky S, Shemer L, Barnea D (1999b). The relation between the Taylor bubble motion and the velocity field ahead of it. Int J Multiphase Flow 25:957–975

[567] Poullikkas, A., 2003. Efiects of two-phase liquid-gas flow on the performance of nuclear reactor cooling pumps. Prog. Nucl. Energ., 42, pp. 3 - 10.

[568] Price, R. E. (1988). "Applications of mechanical pumps and mixers to improve water quality," Water Operations Technical Support Bulletin E-88-3, 6-9.

[569] P. Tirto, T. Koichi and T. Hideki, Effect of Operating Conditions on Two-Phase Bubble Formation Behavior at Single Nozzle Submerged in Water, Journal of Chemical Engineering, 34 (2) (2001) 114-120.

[570] Punnet, R. E. (1991). "Design and operation of axial flow pumps for reservoir destratification," Instruction Report W-9 1 -I, U.S. Army Engineer Waterways Experiment Station, Vicksburg, MS.

[571] Rajaratnam, N. (1976). Turbulent jets, Elsevier Scientific, Amsterdam. The Netherlands.

[572] Rampure, M. R., Kulkarni, A. A. and Ranade, V. V. (2007), "Hydrodynamics of bubble column reactors at high gas velocity: Experiments and computational fluid dynamics CFD simulations", Industrial and Engineering Chemistry Research, vol. 46, no. 25, pp. 8431-8447.

[573] Ranade, V. V. and Tayalia, Y. (2001), "Modelling of fluid dynamics and mixing in shallow bubble column reactors: Influence of sparger design", Chemical Engineering Science, vol. 56, no. 4, pp. 1667-1675.

[574] Rayyan, F., and R. E. Speece (1977), Hydrodynamics of bubble plumes and oxygen absorption in stratified impoundments, Prog. Water Technol., 9, 129-142.

[575] R. B. H. Tan and W. B. Chen, K. H. Tan. A non-spherical model for bubble formation with liquid cross-flow. Chemical Engineering Science 55 (2000) 6259-6267.

[576] Reinemann, D.J., and M.B. Timmons, 1987, An Interactive Program for the Design of Airlift Pumping and Aeration Systems, Department of Agricultural Engineering, Internal Report, Cornell University, Ithaca, NY.

[577] Reinemann, D.J., J.Y. Parlange, and M.B. Timmons, 1987, "Theory of Small Diameter Airlift Pumps," International Journal of Multiphase Flow.

[578] Rensen, J., and Roig, V. (2001). "Experimental study of the unsteady structure of a confined bubble plume." Int. J. Multiphase Flow, 27(8), 1431–1449.

[579] Richardson, J.F. and D.J. Higson, 1962, "A Study of the Energy Losses Associated with the Operation of an Air-Lift Pump," Transactions of the Institution of Chemical Engineers, Vol. 40, pp. 169-182.

[580] Riemer, B., et al., 2002, "Status Report on Mercury Target Related Issues," Technical Report No. SNS-101060100-TR 0006-R00, Oak Ridge National Laboratory, TN.

[581] Riess, I. R., and Fanneløp, T. K. (1998). "Recirculation flow generated by line-source bubble plumes." J. Hydraul. Eng., 124(9), 932–940.

[582] R. Krishna, P. M. Wilkinson, and L. L. van Dierendonck, A model for gas holdup in bubble columns incorporating the influence of gas density on flow regime transitions, Chem. Eng. Sci. 46, 2491 (1991).

[583] Robert S. Bernard, Robert S. Maier, Henry T. Falvey, A simple computational model for bubble plumes, Applied Mathematical Modelling, Volume 24, Issue 3, 2000, Pages 215-233, ISSN 0307-904X,

[584] Rode, S., Altmeyer, S. and Matlosz M. Segmented thin-gap flow cells for process intensification in electrosynthesis. Journal of Applied Electrochemistry, Volume 34, 674 – 680

(2004).

[585] Rocheleau, J., 2021. *Bubble Plumes – Ven Te Chow Hydrosystems Lab*. [online] Vtchl.illinois.edu. Available at: https://vtchl.illinois.edu/bubble-plumes/.

[586] R. Riess and T. K. Fanneløp. Recirculating Flow Generated by Line-Source Bubble Plumes. https://doi.org/10.1061/(ASCE)0733-9429(1998)124:9(932). Published online: September 01, 1998. Journal of Hydraulic Engineering. Vol. 124, Issue 9 (September 1998). Copyright © 1998 American Society of Civil Engineers

[587] R. Singh, W. Shyy, Three-dimensional adaptive cartesian grid method with conservative interface restructuring and reconstruction, J. Comput. Phys. 224 (1) (2007) 150–167.

[588] Ruzicka, M., Drahos, J., Zahradnik, J., and Thomas, N. H. (1999). Natural modes of multi-orifice bubbling from a common plenum. Chemical Engineering Science, 54, 5223–5229.

[589] Ruzicka, M., Drahos, J., Zahradnik, J., and Thomas, N. H. (2000). Structure of gas pressure signal at two-orifice bubbling from a common plenum. Chemical Engineering Science, 55, 421–429.

[590] Ruzicka, M.C. On bubbles rising in line. Int. J. Multiphase Flow, Vol. 26, 1141-1181 (2000).

[591] Sadatomi, M., Sato, Y., Saruwatari, S., 1982. Two-phase flow in vertical noncircular channels. International Journal of Multiphase Flow 8 (6), 641–655.

[592] Sahoo, G. B., and Luketina, D. (2003). "Modeling of bubble plume design and oxygen transfer for reservoir restoration." Water Res., 37(2), 393–401.

[593] Sahoo, G. B., and Luketina, D. (2005). "Gas transfer during bubbler destratification of reservoir." J. Environ. Eng., 131(5), 702–715.

[594] Sangani, A. S. 1988 Sedimentation in ordered emulsions of drops at low Reynolds number. Z. Angew. Maths Phys. 38, 542-555.

[595] Sangani, A. S. "A pairwise interaction theory determining the linear acoustic properties for dilute bubbly liquids," J. Fluid Mech. 232, 221 (1991).

[596] Sani Basic and Leopold Skerget. Drift Flow Convection in Partial Nucleate Boiling Regime. International Conference on Multiphase Flow, ICMF 2007, Leipzig, Germany, July 9 – 13, 2007.

[597] Sanyal, J., Vásquez, S., Roy, S. and Dudukovic, M. P. (1999), "Numerical simulation of gas-liquid dynamics in cylindrical bubble column reactors", Chemical Engineering Science, vol. 54, no. 21, pp. 5071-5083.

[598] Sassen R, Joye S, Sweet ST, DeFreitas DA, Milkov AV, Mac- Donald IR (1999) Thermogenic gas hydrates and hydrocarbon gases in complex chemosynthetic communities, Gulf of Mexico continental slope. Org Geochem 30: 485–497.

[599] Sathe, A. 2001. Experimental and theoretical studies on a bubble pump for a diffusion absorption refrigeration system. Master of Technology Project Report, Universitat Stuttgart. (http://www.geocities.com/abhijitsathe/project/project.html).

[600] Saunder, E., Ledakdwicz, S. and Decker, W. D., 1986, Fisher-Tropsch synthesis in bubble column slurry reactors on Fe/K-catalyst, Can J Chem Eng 64: 133.

[601] Saxena, S.C., Patel, D., Smith, D.N. and Ruether, J.A., 1988. An assessment of experimental techniques for the measurement of bubble size in a bubble slurry reactor as applied to indirect coal liquefaction. Chem. Eng. Comm., 63, pp. 87-127.

[602] S. Benattalah, F. Aloui and M. Souhar. Experimental Analysis on the Counter-Current Dumitrescu- Taylor Bubble Flow in a Smooth Vertical Conduct of Small Diameter. Journal of Applied Fluid Mechanics, Vol. 4, No. 4, pp. 1-14, 2011.

[603] Schaefer, L. A. 2000. Single Pressure Absorption Heat Pump Analysis, PhD Dissertation, Georgia Institute of Technology.

[604] Schladow, S.G. "Bubble Plume Dynamics in a Stratified Medium and the Implications for Water Quality Amelioration in Lakes." Water Resources Research, Vol. 28, No. 2, pp.313-321, February 1992.

[605] Schladow S. Geofirey. Observations of artificial destratification. In H. W. Shen, S. T. Su, and

[606] F. Wen, editors, Hydraulic Engineering. ASCE, 1993a.

[607] Schladow S. Geoffrey. Lake Destratification by Bubble-Plume Systems: Design Methodology. ASCE. Journal of Hydraulic Engineering, Vol. 119, No. 3, 350-368 paper No. 3152. March, 1993b.

[608] Schladow S. Geofirey. A design methodology for bubble plume destratification systems. In Lee and Cheung, editors, Environmental Hydraulics, Rotterdam, 1991. Balkema.

[609] Schmidtke, M., Danciu, D. and Lucas, D. (2009), "Air entrainment by impinging jets: Experimental identification of the key phenomena and approaches for their simulation in CFD", International Conference on Nuclear Engineering, Proceedings, ICONE, Vol. 3, pp. 297.

[610] Scott A. Socolofsky, Brian C. Crounse and E. Eric Adams. Studies of two-phase plumes in stratified environments. Massachusetts Institute of Technology. February 24, 1999

[611] S. Dehaeck · J.P.A.J. van Beeck · M.L. Riethmuller. Extended Glare Point Velocimetry and Sizing for Bubbly Flows. Experiments in Fluids (2005) 39: 407-419.

[612] Sekoguchi, K., K. Matsumura, and T. Fukano, 1981, "Characteristics of Flow Fluctuation in Natural Circulation Air-Lift Pump," Bulletin JSME, Vol. 24, No. 197, pp. 1960-1966.

[613] Serizawa, A., I. Katocoka, and I. Michiyoshi, 1975, "Turbulence Structures of Air-water Bubbly Flow," International Journal of MUltiphase Flow, Vol. 2, pp. 221-246 .

[614] Serizawa A., Kataoka I. and Michiyoshi I. 1975 a Turbulence Structure of Air-Bubbly Flow-I. Measurements Techniques. Int. J. Multiphase Flow 2, pp. 221-233.

[615] Serizawa A., Kataoka I. and Michiyoshi I. 1975 b Turbulence Structure of Air-Bubbly Flow-II. Local Properties. Int. J. Multiphase Flow 2, pp. 235-246.

[616] Serizawa A., Kataoka I. and Michiyoshi I. 1975 c Turbulence Structure of Air-Bubbly Flow-III. Transport Properties. Int. J. Multiphase Flow 2, pp. 247-259.

[617] Serizawa, A. and Kataoka, I. (1988) Phase Distribution in Two-Phase Flow: Transient Phenomena in Multiphase Flow (Ed. N. H. Afghan). Hemisphere Publishing Corporation, New York pp. 179–224.

[618] Serizawa, A., and Kataoka, I., 1990, "Turbulence Suppression in Bubbly Two- Phase Flow," Nucl. Eng. Des., 122, pp. 1–16.

[619] Serizawa, A. and Kataoka, I. (1992). *Dispersed Flow*, Proc. of the 3rd Int. Workshop on Two-Phase Flow Fundamentals, June 15–19, 1992, London, UK.

[620] Serizawa, A., Kataoka, I., Michiyoshi, I., 1992. Phase distribution in bubbly flow. In: Hewitt, G.F., Delhaye, J.M., Zuber, N. (Eds.), Multiphase Science And Technology, vol. 6. Hemisphere Publishing Corporation, New York, pp. 257–301.

[621] Serizawa, A., Feng, Z., Kawara, Z., 2002. "Two-phase flow in microchannels." Experimental Thermal and Fluid Science (26), 703_714.

[622] Serizawa Akimi, Tomohiko Inui, Toshihiko Yahiro, Zensaku Kawara. Laminarization of Micro-Bubble Containing Milky Bubbly Flow in A Pipe. 3rd European-Japanese Two-Phase Flow Group Meeting Certosa di Pontignano, 21-27 September 2003.

[623] S. Hara, M. Ikai, and S. Namie Fundamental Study on an Air Bubble Type of Oil Boom, Trans. Ship-Making Society of Kansai-Japan, 194 (1984).

[624] Singleton, V. L., and J. C. Little (2006), Designing hypolimnetic aeration and oxygenation systems - A review, Environ. Sci. Technol., 40, 7512-7520.

[625] Singleton, V. L., and J. C. Little (2005), Linear bubble plume model for hypolimnetic oxygenation: Full-scale evaluation and sensitivity analysis, paper presented at 9th 96 Workshop on Physical Processes in Natural Waters, Lancaster University, Lancaster, United Kingdom, 4-6 September.

[626] V. L. Singleton, F. J. Rued, D. F. McGinnis and J. C. Little. Coupled Bubble Plume/Reservoir Models For Hypolimnetic Oxygenation. Surface Waters - Research and Management, Federal Institute for Environmental Science and Technology (Eawag), Kastanienbaum, CH-6047, Switzerland. Water Resources Research. 2008.

[627] Vickie L. Singleton. Hypolimnetic Oxygenation: Coupling Bubble-Plume and Reservoir Models. Ph. d. thesis. Virginia Polytechnic Institute and State University. March 26, 2008.

[628] S. Guet, G. Ooms, R.V.A. Oliemans. Influence of bubble size on the transition from low-Re bubbly flow to slug flow in a vertical pipe. Experimental Thermal and Fluid Science 26 (2002) 635–641.

[629] Shah, Y. T., Kelkar, B. G., Gobole, S. P., Deckwer, W. D., 1982. Design parameter estimation for bubble column reactors. AIChE Journal 28 (3), 353–379.

[630] Shang, E. H. H., R. M. K. Yu, and R. S. S. Wu (2006), Hypoxia Affects Sex Differentiation and Development, Leading to a Male-Dominated Population in Zebrafish (Danio rerio), Environ. Sci.Tech., 40, 3118-3122.

[631] Shelton, S.; Delano, A. and Schaefer, L. 1999. Second Law Study of the Einstein Refrigeration Cycle, Proceedings of the Renewable and Advanced Energy Systems for the 21st Century, April 1999.

[632] Sheng, Y.Y., Irons, G.A., 1992. Measurements of The Internal Structure of Gas- Liquid Plumes. Metallurgical and Materials Transactions Vol. 23-B, 779-788.

[633] Sheng, Y. Y. and Irons, G. A. (1995) The Impact of Bubble Dynamics on the Flow in Plumes of Ladle Water Models., Metallurgical Trans. B, 26B, 625-635, 1995.

[634] Shi, F., J. T. Kirby, and G. Ma (2010), Modeling quiescent phase transport of air bubbles induced by breaking waves, Ocean Modell., 35, 105–117.

[635] Shimodaira, C., Yushina, Y., Kamata, H., Komatsu, H., Kurima, A., Mabu, O. and Tanaka, Y., 1981, US Patent, 4, 256573.

[636] Shipley, D.G., 1984, "Two-phase Flow in Large Diameter Pipes," Chemical Engineering Science, Vol. 39, No. 1, pp. 163-165.

[637] Shiro Matsunashi and Yoichi Miyanaga. A field study on the characteristics of air bubble plume in a reservoir. Journal of Hydroscience and Hydraulic Engineering, 8(2):65-77, 1990.

[638] Shoichi Hara, Michiaki Ikai, Sadahiro Namie 1982. Fundamental Study on an Air Bubble Type of Oil Boom. Trans. Ship-making Society of Kansai-Japan 1982.

[639] Shoichi Hara, Michiaki Ikai, Sadahiro Namie 1984. Two-Dimensional Plume Induced by Air Bubbles in Water (Fundamental Study on an Air Bubble Type of Oil Boom. Trans. Ship-making Society of Kansai-Japan 1984.

[640] Shoichi Hara, Michiaki Ikai, Sadahiro Namie 1985. Two-Dimensional Plume Induced by Air Bubbles in Water (Fundamental Study on an Air Bubble Type of Oil Boom. Trans. Ship-Technology Instituted Reports Vol.22. No. 3. 1985. pp. 261-285.

[641] Shuyi Xie, Reginald B. H. Tan. Bubble formation at multiple orifices-bubbling synchronicity and frequency. Chemical Engineering Science 58 (2003) 4639 – 4647.

[642] Siegel, M. H. and Robinson, C. W., 1992, Applications of airlift gasliquid- solid reactors in biotechnology, Chem Eng Sci, 47: 3215.

[643] Sjoberg, A. Stromningshastigheter kring luft-bubbelridat athetshomogentoch stillastaendevatten. (In Swedish), Chalmers Institute of Technology, Hydraulics Division. Report No. 39, (1967).

[644] S. J. HAN, R. B. H. TAN and K. C. LOH. Hydrodynamic Behaviour in A New Gas-Liquid solid Inverse Fluidization Airlift Bioreactor. Institution of Chemical Engineers Trans IChemE, Vol 78, Part C, December 2000.

[645] Singh, P. and Joseph, D. D. 1995 Dynamics of fluidized suspension of spheres of finite size. Intl J. Multiphase Flow 21, 1-26.

[646] C. Jones and R. T. Lahey, Turbulence Structure and Phase Distribution Measurements in Bubbly Two-phase Flows, International Journal of Multiphase Flow, 13 (1987)

327-343.

[647] Slotboom, J.G., 1957, "The Behavior of a Gaslift Pump for Liquids," Transactions of the 9th Int. Congress of Applied Mechanics, Vol. II, pp. 371-383. (Brussels: the University)

[648] Smith, J. A. (1998), Evolution of Langmuir circulation during a storm, J. Geophys. Res., 103(C6), 12,649–12,668, doi:10.1029/97JC03611.

[649] Smith, B.L., 1998. On the modelling of bubble plumes in a liquid pool. Applied Mathematical Modelling 22, 773e797.

[650] Snape, J. B., Zahradnik, J., Fialova, M. and Thomas, N. H., 1995, Liquid-phase properties and sparger design effects in an external-loop airlift reactor, Chem Eng Sci, 50: 3175.

[651] Socolofsky, S. A. (2001). "Laboratory experiments of multiphase plumes in stratification and crossflow." Ph.D. thesis, MIT, Cambridge, Mass.

[652] Socolofsky, S. A., and Adams, E. E. (2003). "Liquid volume fluxes in stratified multiphase plumes." J. Hydraul. Eng., 129(11), 905–914.

[653] Socolofsky, S. A., and Adams, E. E. (2005). "Role of slip velocity in the behavior of stratified multiphase plumes." J. Hydraul. Eng., 131(4), 273–282.

[654] Socolofsky, S. A., Bhaumik, T., and Seol, D. G. (2008). "Double-plume integral models for near-field mixing in multiphase plumes." J. Hydraul. Eng., 134(6), 772–783. 2001.

[655] Sokolichin, A. and Eigenberger, G. (1994), "Gas-liquid flow in bubble columns and loop reactors: Part I. Detailed modelling and numerical simulation", Chemical Engineering Science, vol. 49, (24B) no. 24, pp. 5735-5746.

[656] Sokolichin, A., Eigenberger, G., 1995. Gas-liquid flow in bubble columns and loop reactors: part I. Detailed modeling and numerical simulation. Chemical Engineering Science 49 (24B), 5735e5746.

[657] Sokolichin, A., Eigenberger, G., Lapin, A., and Lubbert, A., 1997. Dynamics numerical simulation of gas-liquid two-phase flows Euler/Euler versus Euler/Lagrange, Chemical Engineering Science, 52(4), 611-626.

[658] Sokolichin, A. and Eigenberger, G. (1999) Applicability of the standard k-ε turbulence model to the dynamic simulation of bubble columns: Part I. Detailed numerical simulations, Chemical Engineering Science 54, 2273-2284. pp.2273-2284.

[659] Sokolichin, A., Eigenberger, G., and Lapin, A., 2004. Simulation of buoyancy driven bubbly flow: Established simplifications and open questions, AIChE Journal, 50(1), 24-45.

[660] Sokolichin, A., Mathematische Modellbildung und numeris che Simulation von Gas-Fl¨ussigkeits- Blasenstr¨omungen. Habilitationsschrift, Universit¨at Stuttgart, 2004.

[661] Sokolichin, A., G. Eigenberger and A. Lapin. Simulation of Buoyancy Driven Bubbly Flow: Established Simplifications and Open Questions. Journal Review. 2004 American Institute of Chemical Engineers AIChE J, 50: 24–45. AIChE Journal 2004 Vol. 50, No. 1

[662] Soltero, R. A., et al. (1994), Partial and full lift hypolimnetic aeration of Medical Lake, WA to improve water quality, Water Res., 28(11), 2297-2308.

[663] Son, G., Dhir, V.K. and Ramanujapu, N. Dynamics and heat transfer associated with a single bubble during nucleate boiling on a horizontal surface. J. Heat Transfer, Volume 121, 623 – 631 (1999)

[664] Sondergaard, M., et al. (2000), Lake restoration in Denmark, Lakes and Reservoirs: Research and Management, 5(3), 151-159.

[665] Speece, R. E., and J. L. Adams (1968), U-tube oxygenation operating characteristics, paper presented at Proceedings of the Industrial Waste Conference, May.

[666] Speece, R. E., and G. Murfee (1973), Hypolimnetic Aeration with Commercial Oxygen -Volume 2: Bubble Plume Gas Transfer, US Environmental Protection Agency, Washington, DC. 42

[667] Speece, R. E., and F. Rayyan (1973), Hypolimnetic Aeration with Commercial Oxygen -Volume I: Dynamics of Bubble Plume, US Environmental Protection Agency, Washington, DC.

[668] Speece, R. E., et al. (1973), Alternative considerations in the oxygenation of reservoir discharges and rivers, in Applications of Commercial Oxygen to Water and Wastewater Systems, edited by R. E. Speece and J. F. Malina, pp. 342-361, Center for Research in Water Resources, Austin, TX.

[669] S.P. MacLachlan, J.M. Tang, C. Vuik. Fast and Robust Solvers for Pressure Correction in Bubbly Flow Problems. Journal of Computational Physics 227 (2008) 9742–9761.

[670] S.P. van der Pijl, A. Segal, C. Vuik, P. Wesseling, A mass-conserving level-set method for modelling of multi-phase flows, Int. J. Numer. Meth. Fluids 47 (2005) 339–361.

[671] S.P. van der Pijl, A. Segal, C. Vuik, P. Wesseling, Computing three-dimensional two-phase flows with a mass-conserving level set method, Comput. Vis. Sci. 11 (2008) 221–235.

[672] Sreedhar, N., 2021. *Can we resist our plastic temptation?*. [online] mint. Available at: https://www.livemint.com/mint-lounge/features/can-we-resist-our-plastic-temptation-11573827512729.html.

[673] S. Sarı, S. Ergün, M. Barık, C. Kocar, C. N. Sökmen, "Modeling of isothermal bubbly flow with ınterfacial area transport equation and bubble number density approach," Annals of Nuclear Energy, vol. 36, pp. 222-232, 2009.

[674] Steffen Richter and Masanori Aritomi. A New Electrode-Mesh Tomograph for Advanced Studies on Bubbly Flow Characteristics. JSME International Journal Series B. Volume 45, No.3 August 2002. pp.565-576.

[675] Stenning, A.H., and C.B. Martin, 1968, "An Analytical and Experimental study of Air-lift Pump Performance," Journal of Engineering for Power Transmission ASME, Apr 1968, pp. 106-110.

[676] Stepanoff, A.J. 1929. Thermodynamic theory of the air lift pump. ASME Transactions, Vol. 51, pp.49-55.

[677] Steven C. Wilhelms and Sandra K. Martin. Gas Transfer in

Diffused Bubble Plumes. Proceedings of the Hydraulic Engineering sessions at Water Forum '1992.

[678] Stevenson, P., Fennell, P.S. and Galvin, K.P., 2008. On the drift-flux analysis of otation and foam fractionation processes. Can. J. Chem. Eng., 86, pp. 635-642.

[679] Sullivan, P. P., J. C. McWilliams, and W. K. Melville (2004), The oceanic boundary layer driven by wave breaking with stochastic variability. Part 1. Direct numerical simulations, J. Fluid Mech., 507, 143–174.

[680] Sullivan, P. P., and J. C. McWilliams (2010), Dynamics of winds and currents coupled to surface waves, Annu. Rev. Fluid Mech., 42, 19–42.

[681] Sung Hoon Kim; Jae-yun Kim; Heekyung Park; and No-Suk Park. Effects of Bubble Size and Diffusing Area on Destratification Efficiency in Bubble Plumes of Two-Layer Stratification. DOI:10.1061/(ASCE)HY.1943-7900.0000152. Journal of Hydraulic Engineering. ASCE / February 2010.

[682] Sun T. Y. and Faeth G. M. 1986 a. Structure of Turbulent Bubbly Jets-I. Methods and Centerline properties. Int. J. Multiphase Flow 12, pp. 99-114.

[683] Sun T. Y. and Faeth G. M. 1986 b. Structure of Turbulent Bubbly Jets-II. Phase Property profiles. Int. J. Multiphase Flow 12, pp. 115-126.

[684] Sun, X., Kuran, S., Ishii, M., 2004. Cap bubbly-to-slug flow regime transition in a vertical annulus. Experiments in Fluids 37, 458–464.

[685] Sun, X., S. Paranjape, S. Kim, B. Ozar, and M. Ishii, "Liquid velocity in upward and downward air-water flows," Ann. Nucl. Energy 31, 357 (2004).

[686] Sun, X., S. Paranjape, S. Kim, H. Goda, M. Ishii, and J. M. Kelly, "Local liquid velocity in vertical air-water downward flow," ASME Trans. J. Fluids Eng. 126, 539 (2004).

[687] Susan Jennifer White. Bubble Pump Design and Performance. Ph. d. Thesis. Georgia Institute of Technology. August 2001.

[688] Szekely, J., Carlson, G. and Helle L. 1988. Ladel Metallurgy. Springer. Berlin.

[689] Szilas, A.P., 1975. Production and transport of oil and gas. Akademiai Kiado, Budapest.

[690] Tacke, K. H., Schubert, H. G., Weber, D. J. and Schwerdtfeger, K. 1985 Characteristic of round vertical gas bubble jets. Metallurgical Transactions B, 16B(2): 263-275, June 1985.

[691] Taitel, Y., Bornea, D., Dukler, A.E., 1980. Modelling flow pattern transitions for steady upward gas–liquid flow in vertical tubes. AIChE Journal 26 (3), 345–354.

[692] Takano, S. et al., Experimental Investigation of the Bubble Diameter of Injected Air on the Ship Bottom and Its Influence on Propeller, Conference Proceedings, the Japan Society of Naval Architects and Ocean Engineers, Vol.10 (2010) p.455.

[693] Takashi Goshima and Koichi Terasaka. Behavior of bubble from a coaxial nozzle in capillary tube into flowing liquid. International Conference on Multiphase Flow, ICMF 2007, Leipzig, Germany, July 9 – 13, 2007.

[694] Takeda, Y., Development of Ultrasound Velocity Profile Monitor, Nucl. Engrg. Des., 126 (1990) 277.

[695] Taggart, C. T., and D. J. McQueen (1981), Hypolimnetic aeration of a small eutrophic kettle lake: Physical and chemical changes, Archiv fur Hydrobiologie, 91(2), 150-180.

[696] Taggart, C. T., and D. J. McQueen (1982), A model for the design of hypolimnetic aerators,

[697] Water Res., 16, 949-956.

[698] Tan, R. B. H., and Harris, I. J. (1986). A model for non-spherical bubble growth at a single oriandce. Chemical Engineering Science, 41, 3175–3182.

[699] Taşdemir, T., Öteyaka, B. and Taşdemir, A. (2007), "Air entrainment rate and holdup in the Jameson cell", Minerals Engineering, vol. 20, no. 8, pp. 761-765.

[700] Taylor Sir Geofffery. The action of a Surface Current Used as a Breakwater, Proc. Royal Society, A., Vol. 231, 1955, p. 466-478.

[701] T. Colonius, F. d'Auria, and C. E. Brennen, "Acoustic saturation in bubbly cavitating flow adjacent to an oscillating wall," Phys. Fluids 12, 2752 (2000).

[702] Terasaka, K., and Tsuge, H. (1990). Bubble formation at a single orifice in Non-Newtonian liquids. Chemical Engineering Science, 46, 85–93.

[703] Terrill, E. J., W. K. Melville, and D. Stramski (2001), Bubble entrainment by breaking waves and their influence on optical scattering in the upper ocean, J. Geophys. Res., 106, 16,815–16,823.

[704] Theofanous T. G. and Sallivar J. 1982. Turbulence in Two-Dispersed Flow. Journal of Fluid Mechanics. 116, pp. 343-362.

[705] The University of Cambridge. Ceb.cam.ac.uk. 2021. Bubble plumes | Department of Chemical Engineering and Biotechnology. [online] Available at: https://www.ceb.cam.ac.uk/research/groups/rg-feg/recent-projects-folder/bubble-plumes.

[706] Thomas, J. A., et al. (1994), Short term changes in Newman Lake following hypolimnetic aeration with the Speece Cone, Lake Reservoir Manage., 9(1), 111-113.

[707] Thorpe, S. A. (1982), On the clouds of bubbles formed by breaking windwaves in deep water, and their role in air-sea gas transfer, Philos. Trans. R. Soc. London, Ser. A, 304, 155–210.

[708] Thorpe, S. A., T. R. Osborn, D. M. Farmer, and S. Vagle (2003), Bubble clouds and Langmuir circulation: Observati ons and models, J. Phys. Oceanogr., 33, 2013–2031.

[709] Tianshi Lu, Roman Samulyak, James Glimm. Direct Numerical Simulation of Bubbly Flows and Application to Cavitation Mitigation. Journal of Fluids Engineering. Transactions of the ASME. MAY 2007, Vol. 129. 595-604.

[710] Titomanlio, G., Rizzo, G., and Acierno, D. (1976). Gas bubble formation from submerged oriandces — "simultaneous bubbling" from two orifices. Chemical Engineering Science, 31, 403–404.

[711] Todoroki, I., Y. Sato, and T. Honda, 1973, "Performance of Air-lift Pumps," Bulletin of JSME, Vol. 16, pp. 733-740.

[712] Topham, D. R. 1974. The Hydrodynamic Aspects of the Behavior of Oil Released Under Sea Ice. Int. Rep. Dept. Electrical Engng, Univ. Alberta.

[713] Tokuhiro, A., M. Maekawab K. Iizukab K. Hishidab M. Maedab. Turbulent flow past a bubble and an ellipsoid using shadow-image and PIV techniques. Int. Journal of Multiphase Flow, 24 (1998), 1383.

[714] Toné, Arthur & Pacheco, Carlos & Lima Neto, Iran. (2017). Circulation induced by diffused aeration in a shallow lake. Water S.A. 43. 10.4314/wsa.v43i1.06.

[715] Tomiyama,A., Uegomori,S., Minagawa,H., Fukuda,T. and Sakaguchi,T. Numerical Analysis of Bubble-Induced Natural Circulation based on Multidimensional Two-Fluid Model, Trans. JSME (Jpn. Soc. Mech. Eng.), 60-580, B, 1994, 9-14.

[716] Tomiyama, A., Sou, A., Z_ un, I. and Sakaguchi, T. 1994 Three-dimensional detailed numerical simulation of bubbly upflow in a vertical square duct. Proc. German-Japanese Symp. On Multiphase Flow KfK 5389, p. 487.

[717] Tomiyama, A., Zun, I., Higaki, H., Makino, Y. and Sakaguchi, T., "A Three- Dimensional Particle Tracking Method for Bubbly Flow Simulation", Nuclear Eng. Des., 175, pp.77-86 (1997).

[718] Tomiyama, A., "Struggle with Computational Bubble Dynamics", on CD-ROM Proc. of the Third International Conference on Multiphase Flow, ICMF' 98 Lyon. France, June 8-12, 1998, also in Multiphase Science and Technology, 10, 4 (1998).

[719] Tomiyama, A., Miyoshi, K., Tamai, H. Zun, I. and Sakaguchi, T., "A Bubble Tracking Method for the Prediction of Spatial-Evolution of Bubble Flow in a Vertical Pipe", on CD-ROM of 3rd Int. Conf. Multiphase Flow, ICMF'98-Lyon, pp.1-8 (1998).

[720] Tomiyama, A. and Shimada, N., "A Numerical Method for Bubbly Flow Simulation based on a Multi-Fluid Model", Trans. ASME, J. of Pressure Vessel Technology, 123, 4, pp.510-516 (2001).

[721] Tomiyama, A. and Shimada, N., "(N+2)-Field Modeling for Bubbly Flow Simulation", Computational Fluid Dynamics J., 9, 4, pp.418-426 (2001).

[722] Tomiyama, A., Tamai, H., and Hosokawa, S., "Velocity and Pressure Distributions around Large Bubbles rising through a Vertical Pipe", on CD-ROM of 4th Int. Conf. Multiphase Flow, New Orleans, USA, pp.1-12 (2001).

[723] Tomiyama, A., Celata, G. P., Hosokawa, S. and Yoshida, S., "Terminal Velocity of Single Bubbles in Surface Tension Force Dominant Regime", Int. J. Multiphase Flow, 28, 9, pp.1497-1519, (2002), also on CD-ROM of 39th European Two-Phase Flow Group Meeting, Aveiro, Portugal, F-2, pp.1-8 (2001).

[724] Tomiyama, A., Yoshida, S. and Hosokawa, S., "Surface Tension Force Dominant Regime of Single Bubbles rising through Stagnant Liquids", on CD-ROM of 4th UK-Japan Seminar on Multiphase Flow, Bury St. Edmunds, UK pp.1-6 (2001).

[725] Tomiyama, A., Nakahara, Y and Morita, G., "Rising Velocities and Shapes of Single Bubbles in Vertical Pipes", on CD-ROM of 4th Int. Conf. Multiphase Flow, New Orleans, Paper No. 492, pp.1-12 (2001).

[726] Tomiyama, A., Nakahara, Y., Adachi, Y. and Hosokawa, S., "Interface Tracking Simulation of Large Bubbles in Vertical Conduits", on CD-ROM of 5th JSME-KSME Fluids Eng. Conf., Nagoya, Japan, 1-6 (2002) to be published.

[727] Tomiyama, A., Adachi, Y., Nakahara, K. and Hosokawa, S., "Shapes and Rising Velocities of Single Bubbles rising through an Inner Subchannel", Proc. 3rd Korea-Japan Symposium on Nuclear Hydraulics and Safety, Kyeongju, Korea, pp.1-6 (2002).

[728] Tomiyama, A., Tamai, H., Zun, I. and Hosokawa, S., "Transverse Migration of Single Bubbles in Simple Shear Flows". Chemical Engineering Science, Vol. 57, 11, pp.1849-1858 (2002).

[729] Tomiyama, A., "Reconsideration of Three Fundamental Problems in Modeling Bubbly Flows", Proc. JSME-KSME Fluid Eng. Conf. Pre-Symposium, Nagoya, pp.47-53 (2002).

[730] A. Tomiyama. Report on Single Bubbles In Stagnant Liquids And In Linear Shear Flows (2002).

[731] Tomomi Uchiyama and Shoji Matsumura. Three-Dimensional Vortex Method for the Simulation of Bubbly Flow. Journal of Fluids Engineering. Transactions of the ASME. October 2010, Vol. 132 / 101402. (1-8) DOI: 10.1115/1.4002574.

[732] T. Oshinowo and M. E. Charles, "Vertical two-phase flow. II. Holdup and pressure drop," Can. J. Chem. Eng. 52, 438 (1974).

[733] Trevorrow, M. V. (2003), Measurements of near-surface bubble plumes in the open ocean, J. Acoust. Soc. Am., 114, 2672–2684.

[734] Trinh, K., Garcia-Briones, M., Hink, F. and Chalmers, J. J., 1994, Quanti. cation of damage to suspended insect cells as a result of bubble rupture, Biotechnol Bioeng, 43: 37.

[735] Tsang, G. (1990), Theoretical investigation of oxygenating bubble plumes, paper presented at Second International Symposium on Gas Transfer at Water Surfaces, Am. Soc. Civ. Engineers, Minneapolis, MN, 11-14 Sept.

[736] Tsuge, H., Hibino, S., and Nojima, U. (1981). Volume of a bubble formed at a single submerged ori"ce in a flowing liquid. International Chemical Engineering, 21(4), 630-636.

[737] Tung, K.W., and J.Y. Parlange, 1976, "Note on the Motion of Long Bubbles in Closed Tubes-Influence of Surface tension," Acta Mechanica, Vol. 24, pp. 313-317.

[738] Uchiyama, T., and Degawa, T., 2006, "Numerical Simulation for Gas-Liquid Two-Phase Free Turbulent Flow based on Vortex in Cell Method," JSME Int. J., Ser. B, 49, pp. 1008–1015.

[739] Uchiyama, T., and Naruse, M., 2006, "Three-Dimensional Vortex Simulation for Particulate Jet Generated by Free Falling Particles," Chem. Eng. Sci., 61, pp. 1913–1921.

[740] Unverdi, S. O. and Tryggvason, G. (1992). A front-tracking method for viscous, incompressible, multi-fluid flows, J. Comput. Phys., 100, 25–37.

[741] Vagle, S., C. McNeil, and N. Steiner (2010), Upper ocean bubble measurements from the NE Pacific and estimates of their role in air-sea gas transfer of the weakly soluble gases nitrogen and oxygen, J. Geophys. Res., 115, C12054, doi:10.1029/2009JC005990.

[742] Van De Sande, E. and Smith, J. M. (1976), "Jet break-up and air entrainment by low velocity turbulent water jets", Chemical Engineering Science, vol. 31, no. 3, pp. 219-224.

[743] Van Hout R., Gulitski A., Barnea D. Shemer L., 2002. Experimental investigation of the velocity field induced by a Taylor bubble rising in stagnant water. Int. J. of Multiphase Flow, 28, 4, 579-596.

[744] Vivek Buwa, Stefan Donath, Swapna Rabhaz, Ulrich Rude. Lattice Boltzmann simulation of bubbly Fows: First results of experimental verification and comparison with Volume of Fluid model. Technical Report 10-4. Lehrstuhl fur Informatik 10 (Systemsimulation). Friedrich-Alexander-Universit At Erlangen-Nurnberg Institut Fur Informatik (Mathematische Maschinen Und Datenverarbeitung). February 16, 2010.

[745] Wace, P. F., Morrell, M. S., and Woodrow, J. (1987). Bubble formation in a transverse horizontal liquid flow. Chemical Engineering Communications, 62, 93-106.

[746] Walsche, C. D., de Cachard, F., 2000. Experimental investigation of condensation and mixing during venting of a steam/non-condensable gas mixture into a pressure suppression pool. Proc. 98th International Conference on Nuclear Engineering (ICONE-8). Baltimore, Maryland, USA.

[747] Wang, S.K, Lahey Jr., R.T., Jones Jr., O.C., 1987. Three dimensional turbulence structure and phase distribution measurements in bubbly two-phase flows. Int. J. Multiphase Flow 13, 327–343.

[748] Wang, Ruo-Qian & Shao, Dongdong & Yin, Hailong. (2016). On the Efficiency of Lake Destratification by Bubble Plumes. The Second Conference of Global Chinese Scholars on Hydrodynamics. Wuxi, China. https://www.researchgate.net/publication/316412984.

[749] Wanninkhof, R., W. E. Asher, D. T. Ho, C. Sweeney, and W. R. McGillis (2009), Advances in quantifying air-sea gas exchange and environmental forcing, Annu. Rev. Mar. Sci., 1, 213–244.

[750] Wallis, G.B. (1969) One-Dimensional Two-Phase Flow. McGraw-Hill, New York, 243.

[751] Watanabe, W., and Prosperetti, A., 1994, "Shock Waves in Dilute Bubbly Liquids," J. Fluid Mech., 274, pp. 349–381.

[752] W. Bai, Niels G. Deen and J.A.M. Kuipers. Bubble Properties of Heterogeneous Bubbly Flows in A Square Bubble Column. CP1207, the 6th International Symposium on Multiphase Flow, Heat Mass Transfer and Energy Conversion, 2010 American Institute of Physics 987-07354-07440.

[753] W. B. Chen and Reginald B. H. Tan. Theoretical Analysis of Two-Phase Bubble Formation in an Immiscible Liquid. August 2003. Vol. 49, No. 8 AIChE Journal (1964-1971).

[754] Wei Chen, Tatsuya Hasegawa, Atsushi Tsutsumi, Man. Generalized dynamic modeling of local heat transfer in

[755] bubble columns. Chemical Engineering Journal, Vol. 96, 37-44 (2003).

[756] Welch, S. W., 1995, "Local Simulation of Two-Phase Flows Including Interface Tracking With Mass Transfer," J. Comput. Phys., 121, pp. 142–154.

[757] Wender, I., Reactions of Synthesis Gas, (1996) Fuel Processing Technology, 48, 189.

[758] Wenxing Zhang and R. B. H. Tan. A model for bubble formation and weeping at a submerged orifice. Chemical Engineering Science 55 (2000) 6243-6250.

[759] White, E.T., and R.H. Beardmore, 1962, "The Velocity of Rise of Single cylindrical Air Bubbles Through Liquids Contained in vertical Tubes," Chemical Engineering science, Vol. 17, pp. 351-361.

[760] W.H. Liu, T. Wan, W. Cheng, Yuichi Murai. Research on the Flow Pattern of Bubble Plume in an Aeration Tank. AIP Conf. Proc. CP1207. The International Symposium on Multiphase Flow, Heat Mass Transfer and Energy Coversion. American Institute of Physics. 646-652. (2010); doi: 10.1063/1.3366442.

[761] Wijn, E. F. (1998). On the lower operating range of sieve and valve trays. Chemical Engineering Journal, 70, 143–155.

[762] Wilkinson, D. L. (1979), Two-dimensional bubble plumes, J. Hydraulics Div., Proc. Am. Soc. Of Civil Engineers, 105(HY2), 139-154.

[763] W. K. Melville E. Lamarre, and M. R. Loewen. The dynamics and acoustics of breaking waves. 123rd Meeting: Acoustical Society of America. Vol. 91, No. 4, Pt. 2, April 1992.

[764] W. L. Haberman and R. K. Morton, An experimental investigation of the drag and shape of air bubbles rising in various liquids, David W. Taylor Model Basin Report 802, Navy Dept., Washington, D.C. (1953).

[765] W. Luewisutthichat, A. Tsutsumi and K. Yoshida, Chaotic Hydrodynamics of Continuous Single-Bubble Flow Systems, Chemical Engineering Science, 52 (1997) 3685-3691.

[766] Wongwises, S., Pipathattakul, M., 2006. Flow pattern, pressure drop and void fraction of two-phase gas–liquid flow in an inclined narrow annular channel. Experimental Thermal and Fluid Science 30, 345–354.

[767] Woolf, D. K., and S. A. Thorpe (1991), Bubbles and the air-sea exchange of gases in near-saturation conditions, J. Mar. Res., 49, 435–466.

[768] Woolf, D. K. (1997), Bubbles and their role in gas exchange, in The Sea Surface and Global Change, edited by P. S. Liss and R. A. Duce, pp. 173–205, Cambridge Univ. Press, New York.

[769] Woolf, D. K. (2005), Parametrization of gas transfer velocities and seastate- dependent wave breaking, Tellus B, 57, 87–94.

[770] Woorim Lee and Gihun Son. Numerical Simulation of Bubble Dynamics in a Microchannel. International Conference on Multiphase Flow, ICMF 2007, Leipzig, Germany, July 9–13, 2007.

[771] Wuest, A., Brooks, N.H., Imboden, D.M., 1992. Bubble plume modeling for lake restoration. Water Resources Research 28 (12), 3235-3250.

[772] Wu, Q., Kim, S., Ishii, M., Beus, S.G., 1998. One-group interfacial area transport in vertical bubbly flow. International Journal of Heat and Mass Transfer, Vol. 41, 1103– 1112.

[773] Wu, R. S. S., B. S. Zhou, D. J. Randall, N. Y. S. Woo, and P. K. S. Lam (2003), Aquatic hypoxia is an endocrine disruptor and impairs fish reproduction, Environ. Sci. Technol., 37(6), 1137– 1141.

[774] W. Warsito, L.-S. Fan, Dynamics of spiral bubble plume motion in the entrance region of bubble columns and three-phase fluidized beds using 3D ECT, Chemical Engineering Science, Volume 60, Issue 22, 2005, Pages 6073-6084, ISSN 0009-2509, https://www.sciencedirect.com/science/article/pii/S0009250905000965.

[775] Xiaobo Gong, Shu Takagi, Huaxiong Huang, Yoichiro Matsumoto. A numerical study of mass transfer of ozone dissolution in bubble plumes with an Euler-Lagrange Method. Chemical Engineering Science DOI:10.1016/j.ces.2006.11.015.

[776] X. Junli, Bubble Velocity, Size and Interfacial Area Measurements in Bubble Columns. Saint Louis, Missouri, Washington University (2004).

[777] X. Tu and C. Trägårdh, Methodology development for the analysis of velocity particle image velocimetry images of turbulent, bubbly gas-liquid flows, Measurement science and technology, 13 (7) (2002) 1079-1086.

[778] Yan Liu, Shao-feng Zhang, Ji-ping Liang and Jin-hong Li. Nonlinear Analysis on Pressure Fluctuation Phenomena of Boiling Two-Phase Flow. International Conference on Multiphase Flow, ICMF 2007, Leipzig, Germany, July 9 – 13, 2007.

[779] Yassin A. Hassan. Dancing Bubbles in Turbulent Flows: PIV Measurements and Analysis. Experiments in Fluids, 35(1), pp. 112-115. 2003.

[780] Y. Chen and S. D. Heister, “Modeling hydrodynamic nonequilibrium in cavitating flows,” ASME J. Fluids Eng. 118, 172 (1996).

[781] Y. C. Wang and C. E. Brennen, “Numerical computation of shock waves in spherical cloud of cavitation bubbles,” ASME J. Fluids Eng. 121, 872 (1999).

[782] Yeoh, G.H., Tu, J.Y., 2004. Population balance modelling for bubbly flows with heat and mass transfer. Chemical Engineering Science 59, 3125–3139.

[783] Yeoh, G.H., Tu, J.Y., 2006. Two-fluid and population balance models for subcooled boiling flow. Applied Mathematical Modelling 30, 1370–1391.

[784] Yoshihito Sasada and Koichi Terasaka. Submilli-bubble dispersion from a novel gas distributor into water. International Conference on Multiphase Flow, ICMF 2007, Leipzig, Germany, July 9 – 13, 2007.

[785] Yum, K., Ahn, J., Park, H., and Ko, I. H. (2005). “Two-phase computational fluid dynamics assessment of bubble plume in air-diffuser destratification.” Environ. Technol., 26(9), 1043–1054.

[786] W¨uest Alfred, Norman H. Brooks, and Dieter M. Imboden. Bubble plume modeling for lake restoration. Water Resources Research, 28(12):3235-3250, 1992.

[787] Zedel, L., and D. Farmer (1991), Organized structures in subsurface bubble clouds: Langmuir circulation in the open ocean, J. Geophys. Res., 96(C5), 8889–8900, doi:10.1029/91JC00189.

[788] Zielinski, P., Castro, W.E., and P.A. Sandifer, 1978, "Engineering Considerations in the Aquaculture of 'Macrobium Rosenbergi' In South Carolina," Transactions of the ASAE, Vol. 21, No.2, pp. 391 -394,398.

[789] Zic, K., Stefan, H. G., and Ellis, C. (1992). “Laboratory study of water destratification by a bubble plume.” J. Hydraul. Res., 30(1), 7–27.

[790] Zhang, X., M. Lewis, and B. Johnson (1998), Influence of bubbles on scattering of light in the ocean, Appl. Opt., 37, 6525–6536.

[791] Zheng, L., Poojitha D. Yapa &Fanghui Chen (2002), A model for simulating deepwater oil and gas blowouts–Part I: theory and model formulation Journal of Hydraulic Research, 41, 339-351. Received 20 Mar 2002, Published online: 01 Feb 2010.

[792] Zongyuan Xiao and Reginald B.H. Tan. An improved model for bubble formation using the boundary-integral method. Chemical Engineering Science (2004). www.elsevier.com/locate/ces.

[793] Zuber, N., Findlay, J., 1969. Average volumetric concentration in two-phase flow systems. Transactions on ASME Journal of Heat Transfer 87, 453–468.

[794] Zuiderweg, F. J. (1982). Sieve trays—a view on the state of the art. Chemical Engineering Science, 37, 1441–1461.

[795] Zukoski, E.E., 1966, "Influence of Viscosity, Surface Tension, and Inclination Angle on Motion of Long Bubbles in Closed Tubes. Journal of Fluid Mechanics, Vol. 20, pp. 821-832.

[796] Zun, I., 1990. The mechanism of bubble non-homogeneous distribution in two phase shear flow. Nuclear Engineering and Design 118, 155–162.